Feasibility Study on Heavy-Traffic FRP Bascule Bridges

J.C. Moen

Delft University of Technology

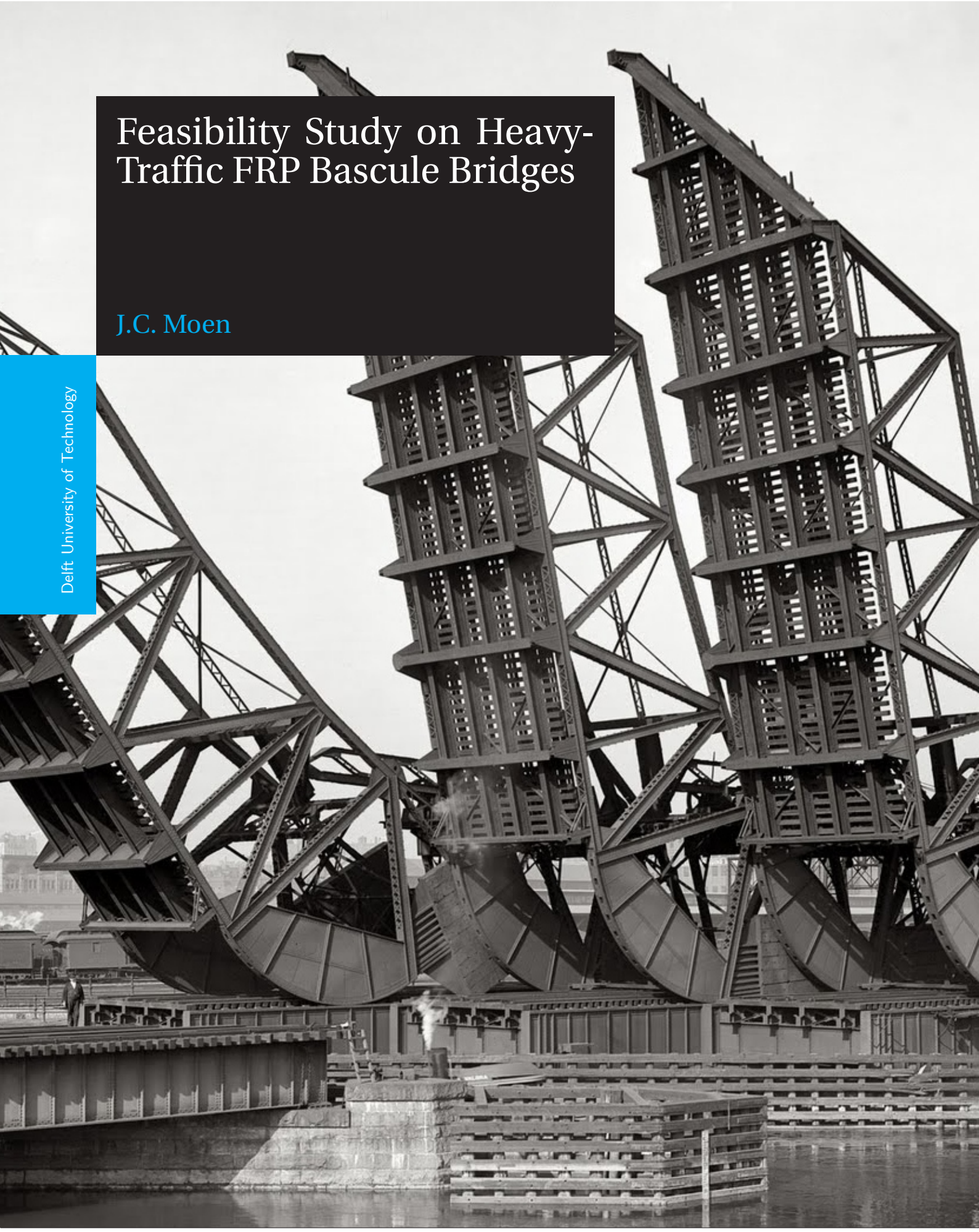

TU Delft Delft University of Technology

Challenge the future

Cover photo:
Three of the very first cast iron rolling bascule bridges, in service from 1900-1980 in Boston, designed by 'Scherzer Rolling Lift Bridge Co.' [Detroit Publishing Company, 1904]

FEASIBILITY STUDY ON HEAVY-TRAFFIC FRP BASCULE BRIDGES

by

J.C. Moen

in partial fulfillment of the requirements for the degree of

Master of Science
in Civil Engineering

at the Delft University of Technology,
to be defended publicly on Tuesday July 29, 2014 at 15:45.

Thesis committee:	Prof. ir. R. Nijsse	TU Delft
	Dr. M.H. Kolstein	TU Delft
	Ir. J.E.P. Smits	TU Delft
	Ir. H. de Waardt	Witteveen+Bos

TU Delft Delft University of Technology

Preface

This thesis was written as part of the Civil Engineering master curriculum at the Delft University of Technology. The research was carried out in cooperation with the the Faculty of Civil Engineering & Geosciences and the Dutch engineering and consulting company 'Witteveen+Bos'.

I would like to express my gratitude to all of those who have helped me in completing my engineering studies and master thesis in particular.

First of all, i would like to thank Huig de Waardt, my supervisor at Witteveen+Bos, for the time and energy he dedicated to my work. His engineering experience and genuine interest in the topic proved to be a source of inspiration, and helped me find my way though the overload of information and ideas.

I would also like to express my appreciation to the other committee members. Prof.ir. Rob Nijsse; for keeping an eye on the general organisation, ir. Joris Smits; for his critical view and original ideas, and dr. Henk Kolstein for sharing his knowledge on composite material and reference projects.

My appreciation goes out to 'Witteveen+Bos' for providing me with the resources to work on my thesis. A special thanks to ir. Hans van Daelen, for involving me in the case study and connecting me to the company.

Furthermore, i would like to acknowledge the help of Markku Palantera, general manager at Componeering Inc., for providing me a licence for the ESAComp software package.

On a personal note, I would like to share my gratitude towards my parents, family and girlfriend for their support and motivation.

Joris Moen

Den Haag, July 2014

Abstract

Fibre reinforced polymer (FRP) composites have emerged from niche markets to become a common material in the construction industry. The adaption was driven by the material's high specific strength and stiffness, and excellent fatigue and corrosion resistance compared to common metallic alloys.

The material characteristics of composites fundamentally differ from those of construction steel; composites are less stiff, brittle, anisotropic and more expensive. Composite structures must be designed with these differences in mind, in order to capitalise the full potential of the material. Simple substitution of steel elements by composite counterparts will inevitably result in inefficient structures. When the material's characteristics are however respected in the design, one can create extremely lightweight, durable and practically maintenance-free structures at a competitive price.

The ability to create lightweight structures is especially beneficial in the field of movable bridges. Many of these bridges originate from the 60's and 70's of the last century, and require imminent rehabilitation. Replacing a steel superstructure by one composed of lightweight composites allows to reuse the concrete substructure without further strengthening. Next to that, the replacement operating system can be much simpler and thus cheaper in purchase and use.

Some examples of heavy-traffic movable composite bridges exist, however none of these is based on the bascule principle. The use of composite material imposes additional challenges on the design of bascule bridges, which concentrate around pivot system of the structure.

In this thesis, the material-specific challenges regarding the design and production of composite bascule bridge superstructures are investigated. Subsequently, the influence of several design parameters on the efficiency of the structure is analysed. Based on the drawn conclusions, different alternatives for the geometry and pivot system of the superstructure are evaluated based on their respective compatibility with composite material. Finally, the technical- and economical feasibility of the conceptual design is assessed. The results of this research show that there may be a promising future for composites in the (bridge) construction industry, as long as material-adapted design and optimisation techniques are embraced.

In order to quantify the boundary conditions during the design study, the Julianabrug in Alphen aan den Rijn (Netherlands) is used as a case study. The study has however been carried out in such a way that the conclusions can also be applied to other bascule bridge replacement projects.

Acronyms

AASHTO	American Association of State Highway and Transportation Officials
ASCE	American Society of Civil Engineers
CLD	Constant Life Diagram
CLT	Classical Laminate Theory
FHWA	Federal Highway Administration
FLM	Fatigue Load Model
FOS	Fibre Optic Sensing
FPF	First Ply Failure
FRP	Fiber-Reinforced Polymers
LCC	Life Cycle Cost
LM	Load Model
LPF	Last Ply Failure
SLS	Serviceability Limit State
ULS	Ultimate Limit State
VOBB	Voorschriften voor het Ontwerpen van Beweegbare Bruggen

Contents

1 Introduction

1.1 Problem definition

In the Netherlands, as in most countries of the Western world, motorised transportation became available to the masses after the Second World War. The amount of motorised vehicles increased from half a million to seven million within a decade after 1960, after which the growth stabilised towards ten million vehicles nowadays [Centraal Bureau voor de Statistiek, 2013]. This rapid increase of vehicles instigated the expansion the Dutch road network and as a result, a substantial amount of currently existing bridge structures originate from the 60's and 70's of the last century. These structures were designed according to knowledge and forecasts at the time, aiming at a design service life of around sixty to eighty years [Rijkswaterstaat, 2007].

Due to the fast rise in economic prosperity, the number of vehicles and their axle loads have however grown more substantially than anticipated for. The strength of bridge structures, on the other hand, was often overestimated; the shear capacity of the concrete substructures and the fatigue strength of steel superstructures have frequently proven to be insufficient. In other cases de-icing agents and poor water tightness of expansion joints, together with the lack of frequent maintenance, has caused severe corrosion of the steel elements.

As a result of the underestimation of loads and the overestimation of capacities, many (movable) steel bridges have been classified as structurally deficient and require attention. This classification does not mean the structures are unsafe, however they require major rehabilitation to restore their load carrying capacity to comply with regulations [Tang and Hooks, 2001]. The rehabilitation of these bridges can be addressed by either repairing and strengthening the existing structure, or by (partial) replacement. The first method usually involves the replacement of asphalt by a layer of high-strength concrete and maintenance to the steel elements. The latter method involves replacing either the deck or the complete superstructure of the bridge by new components to achieve sufficient capacity to comply with the current standards. In either way, the service life of the structure can be extended by at least a decade for a relatively small investment.

For moveable bridges however, such rehabilitations can be problematic. Strengthening or replacing parts of the bridge normally entails an increase of the structure's weight. After the rehabilitation, the balance of the movable structure has to be restored. Since the weight at the span-side of the pivot axis has increased, the counterweight must be increased as well. The recalibration capacity is however bound to the availability of weight expansion slots, which is normally limited to around 5% of the initial counterweight. Secondly, the operating mechanism needs to be adapted to cope with the higher rotational inertia and friction of the heavier structure. Lastly, the substructure will also be subjected to higher loads, and therefore requires structural analysis and possibly strengthening as well.

1.2 Scope

The challenges with movable bridge rehabilitation derive from the often associated increase in weight. To avoid these challenges, one should seek for ways to increase the strength of the structure while maintaining the current weight. This requires a material that exhibits a higher strength-to-weight ratio than conventional construction materials. Fibre reinforces polymers composites is such a material group, offering an ultimate strength comparable to steel at only a fifth of the weight.

1.2.1 Choice of material

Composite material is defined as "structural material that consists of two or more constituents that are combined at a macroscopic level and are not soluble in each other" [Kaw, 2006]. Based on this definition, concrete and wood composites as well. In the context of this thesis however, composite materials are those composed of synthetic fibres and a polymer resin; sometimes referred to as 'high-performance' composites.

Composites consist of reinforcement and matrix material, which strongly differ in physical and chemical properties. When combined, they result in a material that has superior properties compared to the individual components alone [Campbell, 2010]. The material has become increasingly important over the past fifty years, and is commonly used for high-tech products in for example the automotive, aerospace and wind-energy industries. The bridge construction industry started adopting the material about twenty years ago, and nowadays one can claim that it is a viable alternative for conventional materials for application in cycle- and pedestrian bridges. The same cannot yet be said about heavy-traffic bridges, but also in that sector the use of composites is rising.

The high strength-to-weight ratio of the material allows to design extremely lightweight structures. Especially for movable bridges this has multiple advantages; structures are easier to transport and assemble, the counterweight will be smaller, the substructure can be simpler, the operational mechanism may be less robust, and the opening/closing cycles require less energy. But the high strength-to-weight ratio is not the only driver for the material's selection; composites also often outperform conventional materials because of other mechanical, physical or chemical properties. For the construction industry, the geometrical freedom, the high fatigue strength and the resistance to corrosion are the main benefits. The latter two ensure a very long service life for composite bridge structures, while at the same time reducing the need for inspection and maintenance. While composite material is relatively expensive, all these beneficial characteristics could lead to a cost-efficient structure in the long run.

(a) Geometrical freedom in design

(b) Ease of transportation and assembly

Figure 1.1: *Advantages of fibre reinforced composites over conventional materials*

1.2.2 Choice of structure

1.2.2.1 Bridge rehabilitation/replacement

As indicated, the majority of all Dutch movable bridges is constructed between the 60's and 70's of last century. Mainly as a result of underestimated loads and deterioration by corrosion, a substantial number of these bridges require imminent rehabilitation or replacement of the superstructure. The concrete substructure is however mostly still in reasonable shape, and could service for another period as long as the subjected loads do not increase too much.

These bridge rehabilitation/replacement contracts are nowadays an important source of income for the construction industry, and thus become an interesting topic of study.

1.2.2.2 Bascule bridge

The lightweight character of composite structures is more beneficial for movable bridges than for static bridges, since a lower weight of the span results in a less complex operational mechanism and a lower energy consumption during the opening/closing cycle.

Some full-composite movable bridges for heavy-traffic purposes have been constructed. Bascule bridges, however, remain very challenging. This is mainly caused by the fact that the full span of the bridge acts as a cantilever in the opened position, which makes the structure susceptible to wind loads. The combination of self-weight and wind loads results in high localised stresses in the vicinity of the supports, which furthermore change in direction during the opening/closing cycle. Steel has the capacity to plastically deform, and is therefore capable of redistributing such localised loads over a larger area. Fibre-reinforced composites, on the other hand, do not possess the ability to plastically deform. Furthermore, the anisotropic nature of composite material is not ideal for changing load directions. Although some attempts have been made, so far no heavy-traffic bascule bridge has made it to construction (see section 2.5.3).

1.3 Research objective

As discussed, there is a need for an effective solution for structurally deficient movable bridges. Fibre reinforced composites seem to be a very promising construction material for such purposes, and has already proven to be successful in some heavy-traffic bridges. There are however still challenges regarding the design of composite bascule bridges that remain unsolved. The objective of this research is to address some of these challenges, and to evaluate the feasibility of a heavy-traffic composite bascule bridge.

To fulfil this objective, the technical challenges regarding the design, production and exploitation of composite structures will be investigated. For this purpose, the Julianabrug in Alphen aan den Rijn will act as a case study. The engineering and consulting company 'Witteveen+Bos' has made a design for the replacement of this bascule bridge, and has shown interest for composite material in the process. The final design of this bridge does indeed feature a composite bridge deck, but the load-carrying structure is conventional. The objective of this thesis is to take the integration of composite material a step further.

1.4 Research questions

1.4.1 Main question

The research objective can be translated into the the following main research question:

"Can fibre reinforced polymer composites be used to develop technically and economically feasible alternatives for the rehabilitation or replacement of existing, heavy-traffic, bascule bridges?"

1.4.2 Sub-questions

The following set up sub-questions focus on different aspects of the research question. The chapter(s) in which the question is addressed is indicated in parentheses.

1. What is the state-of-the-art in the composite movable bridge industry? (Ch. 2 & 3)
2. What are the material-specific challenges regarding the design and production of composite structures, and how are they addressed in practice? (Ch. 3)
3. What are the requirements for a heavy-traffic bascule bridge? (Ch. 4 & 5)
4. What are the boundary conditions of the case study bridge? (Ch. 5)
5. What is good design practice when working with composites, and how can the design parameters be analysed and optimised by simple hand-calculations? (Ch. 6)
6. Which design principles can contribute to solving the material-specific challenges in the design of composite bascule bridges? (Ch. 7)
7. How can the configuration of a composite structure be analysed and optimised with the help of computational models? (Ch. 8)

1.5 Reading guide

This section describes the subjects that are being addressed in the respective chapters of the report. The report is composed of two main parts, which include a total of seven chapters.

1.5.1 Literature study

Chapter 2: Bascule bridges
The different types of bascule bridges and their components are discussed, in which most attention is paid to the balance of the structure. Subsequently, the role of composite material in the rehabilitation or replacement of structurally deficient bridges is discussed. Lastly, a couple of relevant reference projects is presented.

Chapter 3: Fibre reinforced polymers
Chapter three introduces the reader to fibre reinforced polymer composites, discussing properties of the constituents and final products. After a brief introduction, the subject will become more technical as the micro- and macromechanics of laminates and sandwich panels are discussed on the basis of established models and theories. Lastly, the material-specific design practice with respect to fatigue, creep, impacts and joints are discussed.

Chapter 4: Design input
This chapter enumerates and clarifies the most relevant parts of the design codes for bascule bridges, and recommendations for the design of composite structures. The conditions and requirement of the composite bascule bridge design are drafted. Subsequently, a brief introduction is given to material-specific design tools for the different stages of the design phase.

1.5.2 Design study

Chapter 5: Quantification of design input

In order to define the context of the design study, the boundary conditions and functional requirements of the case study bridge are quantified. Subsequently, the material set and production technique for the composite structure are defined, and the associated material properties are quantified.

Chapter 6: Parametric analysis of sandwich plate

In order to get a feeling for dimensions and the sensitivity of model parameters, the problem is heavily simplified so that the span can be modelled by a simple sandwich panel. The panel is subjected to realistic traffic loads, and the response is analysed by simple hand-calculations. The influence of several model parameters on the strength and stiffness of the span are subsequently analysed and optimised with respect to self-weight and material-cost. The results give insight in good design practice of composite sandwich panels.

Chapter 7: Bascule design

Material-specific challenges regarding the design of bascule bridges are addressed in this chapter. Solutions to these challenges are proposed and evaluated based on their compatibility with the composite material. The result is a bascule design that is most likely to prove technically feasible in the modelling phase. The main focus is on the tail-section of the bridge, including the pivot-, operating- and stabilising systems.

Chapter 8: Finite element analysis

Based on the conclusions from chapter 6 and 7, a first global configuration of the composite bridge structure is modelled in a finite element software package. The structural optimisation process is demonstrated by discussing a single iteration step in detail. Subsequently, the final result after a number of iterations is presented, and the response to the different load combinations is compared to the defined limit states. Lastly, some recommendations for further analysis and optimisation are given.

Part I

Literature study

2 Bascule bridges

By definition, bascule bridges are only those bridges that consist of a single moving element, which pivots about a horizontal line near its centre of gravity so that the weight on one side of the pivot axis nearly balances the weight on the other side [Koglin, 2003]. One can easily make the analogy with a seesaw, which is called a 'bascule' in French. Bascule bridges are modern versions of medieval draw bridges, as were often applied in fortifications and castles as part of their defence system. Modern long-span bascule bridge design can be traced back to the late nineteenth century, with the construction of rolling lift bascules in Chicago and the roller-bearing trunnion bascule in the London Tower Bridge.

Bascules are often selected for narrow to moderately wide channels where unlimited vertical clearance is required for navigation. In the United States, about forty percent of the operable movable bridges is classified as a bascule. This type is nowadays the most popular for newly constructed movable bridges, accounting for about sixty percent over the last two decades.

A bascule bridge is generally the quickest as it comes to clearing the navigational waterway, both because it opens quickly and because vessels can relatively easily pass a partially opened bascule. Bascule bridges are less invasive for the surroundings compared to other alternatives, having large machines that are difficult to disguise [Ryan et al., 2006].

2.1 Types

Quite some variations to the bascule concept were developed at the end of the nineteenth and beginning of the twentieth century. All of these types can be executed in both a single-leaf or double-leaf manner, spanning the waterway with respectively one or two continuous load-bearing structures. Double-leaf bascules are worldwide most commonly applied, but are however very rare in the Netherlands. Double-leaf bascules allow for larger total horizontal channel clearances. For unchanged channel spans they offer smaller cantilevers that allows for more a lightweight structure and thus smaller counterweights, faster opening and smaller operating systems. On the other hand they require twice as many components, increasing construction and maintenance costs.

In closed state, single-leaf bascules transfer dead load as a cantilever to the bascule pier, whereas live loads (and the intended span-heavy imbalance) are simply supported at both abutments. At double-leaf bascules, each leaf supports its own dead load. Live loads are transferred by both leaves together, as the lock systems are capable of transferring shear loads so that passing vehicles do not experience a vertical dislocation as they pass from one leaf to the other [Coates and Bluni, 2004].

(a) Erasmusbrug (Rotterdam) (b) Tower Bridge (London)

Figure 2.1: *Well-known single- and double leaf bascule bridges [Wikipedia, 2014]*

2.1.1 Trunnion bascule

This type is by many experts considered to be the only true bascule bridge, consisting of a rigid displaceable structure supported on a horizontal pivot. Typically the trunnion shafts are fixed to the main girders of the bridge span and the shaft ends rotate within anti-friction bearings supported on the abutment. However, an alternate arrangement keeps the trunnions stationary while the span pivots around them.

The counterbalance is located underneath the approach deck, and rotates in a downward direction as the bridge is opened. Dipping the counterweight into the water would introduce a buoyancy force that would disturb the balance during opening. In order to prevent this contact, the bridge should either be positioned at a sufficient height above the water level, or the counterweight should be sealed in a watertight bascule chamber.

2.1.2 Rolling bascule

The rolling bascule type rides on a curved treaded track as it opens and closes, translating away from the channel as it rotates. This characteristic makes that this type of bascule does not require such a big opening angle of the leaf as other types to provide the same clearance over the waterway, making it generally the quickest opening bascule bridge.

The curved tread plate fixed to the bottom of each main girders, on which the bridge rocks backwards as it opens, has found to be prone to wear and tear. Furthermore, this type of mechanism is hard to inspect and maintain.

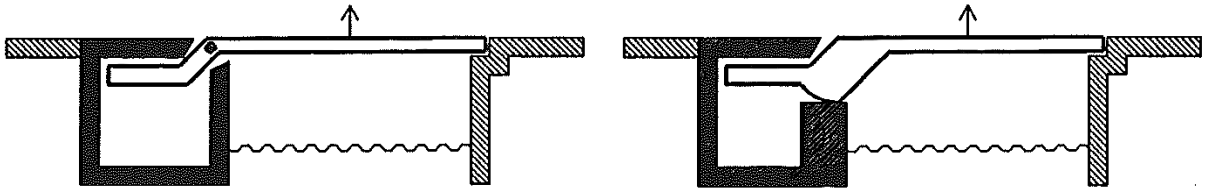

(a) Trunnion bascule (b) Rolling bascule

Figure 2.2: *Two most common bascule bridge types [Oosterhoff and Coelman, 1999]*

2.2 Components

Generally, a bascule bridge consists of a deck on main supporting members with a counterweight rigidly attached to the rear portion, supported near its centre of gravity on a heavy shaft that rest on bearings. This shaft is referred to as the 'trunnion', a word that originates from the supporting mechanism of medieval cannons that allowed for the adjustment of the projection angle. The upward moving deck section of a bascule bridge is referred to as a the 'leaf', like the pages of a book. The outer end of the leaf, furthest away from the pivot point, is referred to as 'toe'. In the closed position of the bridge the toe is supported on the 'rest pier' in case of single-leaf bascules, or connected to the mating leave with a shear lock in case of double-leaf bascules. The inner end of the leaf is referred to as 'heel' or 'tail' and is supported on the 'bascule pier'. Generally, the counterweight is located in a 'bascule chamber' for preservation and safety reasons, located under the approach span in the bascule pier. Other configurations are also accustomed, having the counterweight located freely under the approach deck, or even hanging above it.

2.2.1 Trunnions

The bascule's trunnions act as the hinge pins for the pivoting leaf and other components, and are machined to fit precisely and very tightly into a collar or hub attached to the main bascule girders. The full dead weight of the span and counterweight, as well as wind loads, are supported by the trunnions during operation. Depending on the bridge size, the diameter of the solid alloy steel shaft can range up to half a meter. For the purpose of quality control, holes are bored through the longitudinal axis, so that flaws can be detected prior to installation. Proper fabrication and installation of the element requires special skills, and is known to lead to difficulties. Also, due to the difficult to reach position of the trunnion, maintenance issues frequently arrive during exploitation.

As mentioned, typically the trunnion shafts are fixed into a collar or hub, which is subsequently attached to the main girders. To assure a very tight interference fit, the slightly oversized outer diameter of the trunnion is mechanically fastened to the inner diameter of the hub by means of either force- or shrink fitting. The latter method involves assembling the trunnion into position, after the internal diameter of the hub was expanded by heating it up.

(a) Trunnion shaft (b) Trunnion girder connection (c) Trunnion bearing assembly

Figure 2.3: *Assembly of trunnion pivot system [University of South Florida, 2001]*

2.2.2 Trunnion bearings

In small sized bascule bridges, the trunnion can be supported by a single bearing on each outboard side of the main bascule girders. A compressive strut, called the trunnion girder, between the inboard sides of the main bascule girders provides the force equilibrium in the support. Heavy trunnion bascule bridges, in excess of 1000 tons, are usually equipped with two bearings per support to distribute the frictional stresses during operation.

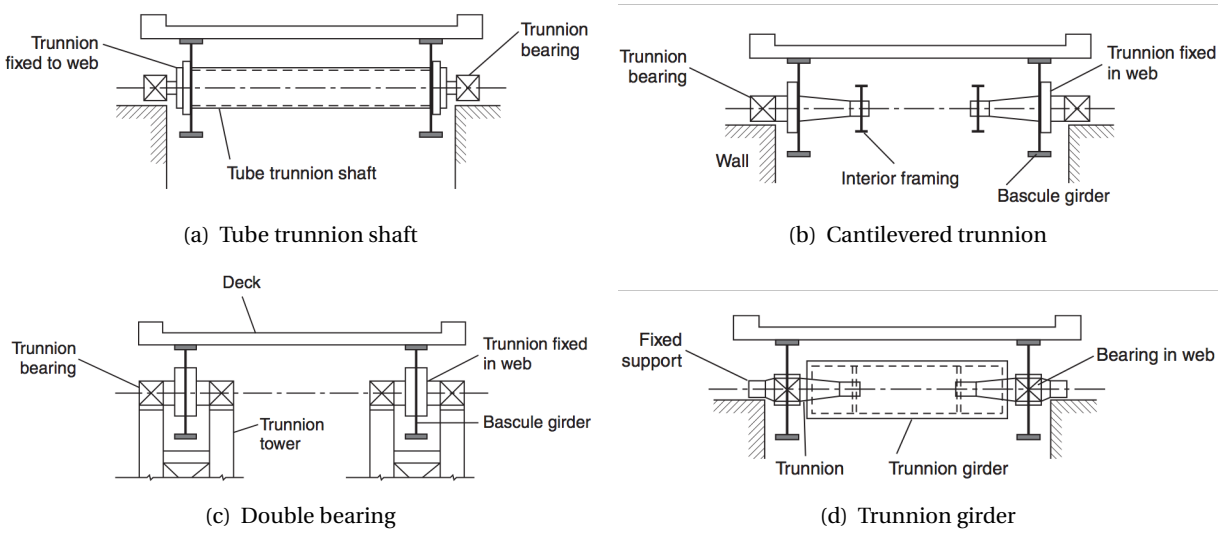

(a) Tube trunnion shaft

(b) Cantilevered trunnion

(c) Double bearing

(d) Trunnion girder

Figure 2.4: *Trunnion bearing configurations [Parke and Hewson, 2008]*

A perfect relative alignment of the trunnions is essential for the durability of the bearings and trunnions itself. Good alignment manifests itself in a smoothly running bridge, whereas misalignment results in excessive friction and serious wear at the contact area. During inspection and erection of the bridge, the axial holes though the trunnions are sometimes used to check the alignment. The required precision of alignment can be reduced by making use of spherical housings for the trunnion bearings, enabling a degree of self-alignment. The application of spherical roller bearings can also eliminate misalignment as a result of consolidation.

Most older bascule bridges make use of bronze friction bearings, which are generally quite durable but fairly large and difficult to lubricate. Improper lubrication increases friction during operation, accelerating the deterioration. A more recent development is anti-friction bearings, commonly applied in new bridges. These bearings eliminate wear and offer reduced maintenance requirements. They may however not be suitable for heavy bascules with a limited rotation angle.

As mentioned before, an alternative supporting mechanism makes use of stationary trunnions. The span pivots around the fixed trunnion, so that frictional stresses occur between the trunnion and the hub. Since the span is supported on the trunnion these stresses occur at the top of the shaft, making it difficult to provide proper lubrication. The anti-friction bearing of these configurations should therefore be designed to be larger in order to reduce frictional stresses.

2.2.3 Counterweight

Counterweights are applied at the tail-side of the structure in order to counterbalance the weight of the span-side. The idea is to shift the gravitational centre of the structure towards the pivot axis, so that the required amount of energy during the opening/closing cycles is minimised. Theoretically, a friction-free bascule of which the centre of gravity coincides with the pivot point would only require a small impulse to open and close. In practice however, the gravitational centre is located at some distance from the pivot axis, so that the bridge is stable under the influence of loads that induce a opening/closing momentum. The position of the gravitational centre with respect to the pivot axis determines the behaviour of the bridge, and should thus be well considered (see section 2.3).

Counterweights are usually designed to be as cheap as possible in construction and maintenance. Most bascule counterweights are largely composed of concrete, as the material is dense, easy to install and maintenance free. The dimensions of the counterweight must be carefully detailed not to interfere with fixed structural members, and to fit within the confined bascule chamber. High-density aggregate can be applied to reduce their overall size. In special cases, steel, cast iron and even lead can be used. The cheapest solution for counterweights is a cast concrete block, attached to the main bascule girders. Gravity introduces tensile stresses in the hanging concrete block, which should be transferred to the girders by a framework of steel. Especially in case the counterweight is positioned underneath the deck, durability of this type of construction is a problem as de-icing salts induce corrosion resulting in spalling of the concrete.

A more practical and durable solution is a steel box filled with concrete, creating a fully supported situation without the need of reinforcement inside the block. The thickness of the steel enclosure is usually about one centimetre, dependent on the dimensions and density of the block.

The counterweight should offer pockets to hold adjustment blocks, so that the balance of the structure can be recalibrated during its service life. These portable weights are usually made of iron or steel, and weight no more than a single person is allowed to lift; around 35 kilos. At commissioning of the bridge, one should aim at having half of the pockets filled with adjustment blocks so that they can both be added or removed if needed. A major shift in the position of the gravitational centre is however not possible. This should be kept in mind before executing renovation works to the bridge deck.

2.2.4 Operating system

A major advantage of bascule bridges is their relatively modest and simple machinery. Because of the balanced weight, a bascule would only require approximately a thirtieth of the energy per operation compared to an equivalent sized vertical lifting bridge [Parke and Hewson, 2008, p. 468].

On the other hand, the equipment of bascules has to cope with much higher live loads in the opened position as the wind impacts perpendicular to the deck. As a result, the size of the operating system is almost entirely determined by the highest wind loads at which the bridge should still remain functional. In hurricane sensitive regions, bascules may be equipped with span locks to hold the bridge in the open position without exposing the machinery to excessive stresses.

Span drives may be assembled from many combinations of equipment. Modern configurations are composed of an electric motor driving the gears directly, or distribute the power hydraulically to drive a radial piston or hydraulic cylinders. The purpose of these systems is to convert the low-torque high-speed output from the prime mover to a high-torque low-speed rotation needed to move the span.

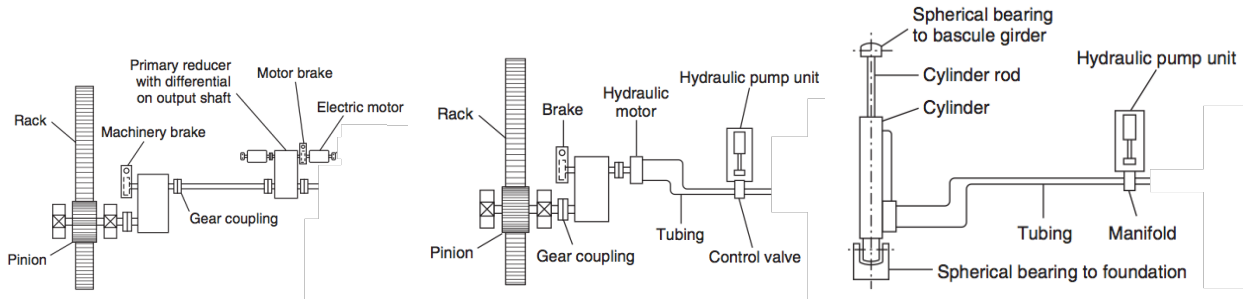

(a) Mechanical (b) Hydraulic motor (c) Hydraulic cylinder

Figure 2.5: *Types of operating systems [Parke and Hewson, 2008]*

Most typical trunnion bascules are equipped with two drive machineries attached to both main girders, at the location of the bascule pier. In case of an electromechanical system, circular rack segments are fixed to the main girders that are driven by the pinions. To equalise the applied torque at both main girders, differential gearings are applied between the two systems. Omitting the differential would eventually lead to an unequal driving load distribution and breaking torque, introducing additional stresses on the rack and pinions and thus inciting deterioration. Hydraulic systems have the advantage of being self-equalising, as the torque is levelled at the pressure source.

Considering hydraulic systems, equal distribution of the torque is not the only advantage. Modern hydraulic systems are relatively easy to design, install and maintain. Furthermore they are quiet in operation, small, energy efficient and offer superior service life over mechanical drives. Engineers are however reluctant as it comes to applying hydraulic systems, due to a poor image of reliability that has developed over the years [Adams, 1987].

The racks and pinions tend to wear most heavily at the contact area of the teeth in the closed position of the bridge. The teeth suffer from the impacts caused by the movement of the bridge span under the influence of live loads. Stabilising systems are used to mitigate this movement, as well as to prevent dangerous situations in case of failure of the operating system.

2.2.5 Stabilising system

Live loads can do great damage to the machinery, often more severe and destructive than the effects of normal operation. The 'stabilising system' is the collective term of elements that secure the span in the closed position, and comprises live load shoes, span/tail locks, anchorage, machinery brakes, buffering cylinders and bumper blocks. Centring devices to retain the bridge's alignment during its service life are not required for the simple trunnion type, as the rigid connections of the pivot to the support provide adequate stabilisation. Ultimate consequences of inadequate or improperly adjusted stabilising systems are the cracking of concrete piers, fracture of gear teeth and failure of the trunnion bearings [Cragg, 1987].

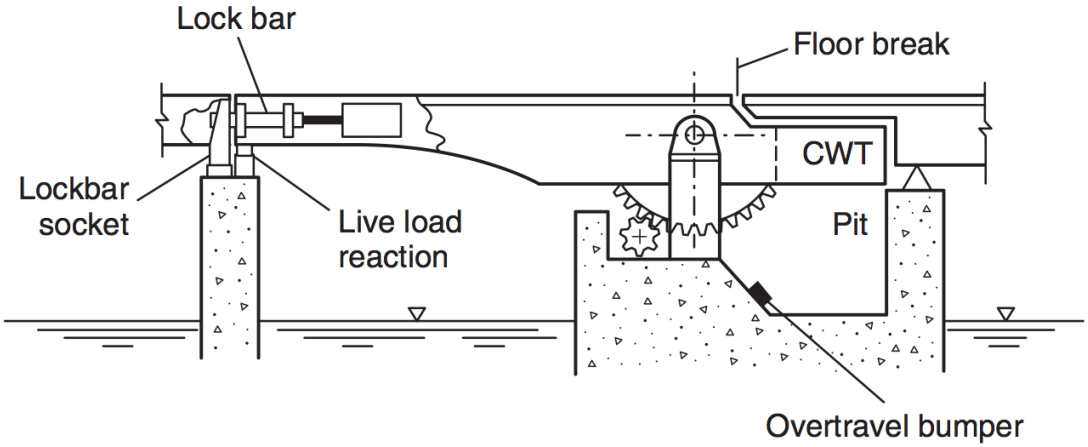

Figure 2.6: *Stabilising systems in bascule bridge structures [Parke and Hewson, 2008]*

2.2.5.1 Live load shoes

As mentioned before; in the closed position, the span's dead weight is supported as a cantilever, whereas the live load is simply supported to both abutments. At the heel of the bridge, the main trunnions carry these live loads to the bascule pier. At the toe ends of the main girders, live load shoes perform this task. These supports are elementary devices consisting of a steel shoe attached to the bascule girder, and a strike plate fixed to the rest pier. In order for live load shoes to work properly, the shoe and strike plate must be in firm contact when the leaf is in the closed position. Without this firm contact, frequent high impact loads from traffic can eventually cause concrete cracks in the support [Cragg, 2004].

2.2.5.2 Locks and anchorage

Bascule bridges can be fitted with locks or anchorages in order to assure firm contact at the life load shoes and prevent accidental opening of the bridge. Most commonly the locks are situated at the tips of the bascule leaf (span locks), but also positioning them right behind (tail locks) or above (anchorages) the counterweight is possible.

2.2.5.3 Machinery breaks

Bascules are equipped with mechanical breaks for two purposes: to be able to arrest movement of the span within a specified period of time, and to hold the span stationary against a specified wind pressure. The brakes must be set automatically when the driving motor is de-energized, whether by accidental or intentional power interruption.

2.2.5.4 Buffering cylinders

Many bascule bridges are equipped with buffer cylinders which act as a backup mechanism in case of a failing control system, preventing the leaf to impact on the restpier. Heavy impacts can happen as a result of brake failure, coupling failure, operator error or an excessive imbalance of the structure. In such instances the buffer cylinders absorb part of the kinetic energy, reducing the maximum stress in the affected components of the bridge. Equally adjusting the buffer cylinders is of vital importance, as unevenly distributed forces may cause warping of the leaf. The cylinders are equipped with pressure gauges to check if they develop the same maximum pressure during seating of the bridge.

2.2.5.5 Bumper blocks

A fairly cheap safety mechanism that is commonly applied is bumper blocks. In case of over-travelling of the leaf during opening, the movement is arrested by means of a physical block at the bottom of the bascule chamber. In case of heavy wind loads and failing breaks, the blocks could save the bridge from severe damage.

2.3 Balance

The balance of the bascule bridge is an important consideration, as it has a major effect on the behaviour of the bridge. The desired behaviour may vary for different structures, depending on the conditions of the location. The most important aspects in the determination of the right balance are discussed in this section.

2.3.1 Location of gravitational centre

By positioning the gravitational centre at some distance from the pivot axis, one creates an intentional imbalance. The magnitude and direction of this imbalance may depend on the opening angle of the bridge. Based on the desired behaviour of the bridge, a location for the gravitational centre is chosen. The four principle locations of the gravitational centre with respect to the pivot axis are displayed in fig. 2.7. These figures represent the area around the pivot axis, where the counterweight is on the lefthand-side and the span is on the righthand-side of the circle. The midpoint of the circle represents the pivot axis. The dot at some distance from the midpoint represents the location of the gravitational centre. A counterclockwise rotation resembles the opening of the bridge, whereas a clockwise rotation resembles closure.

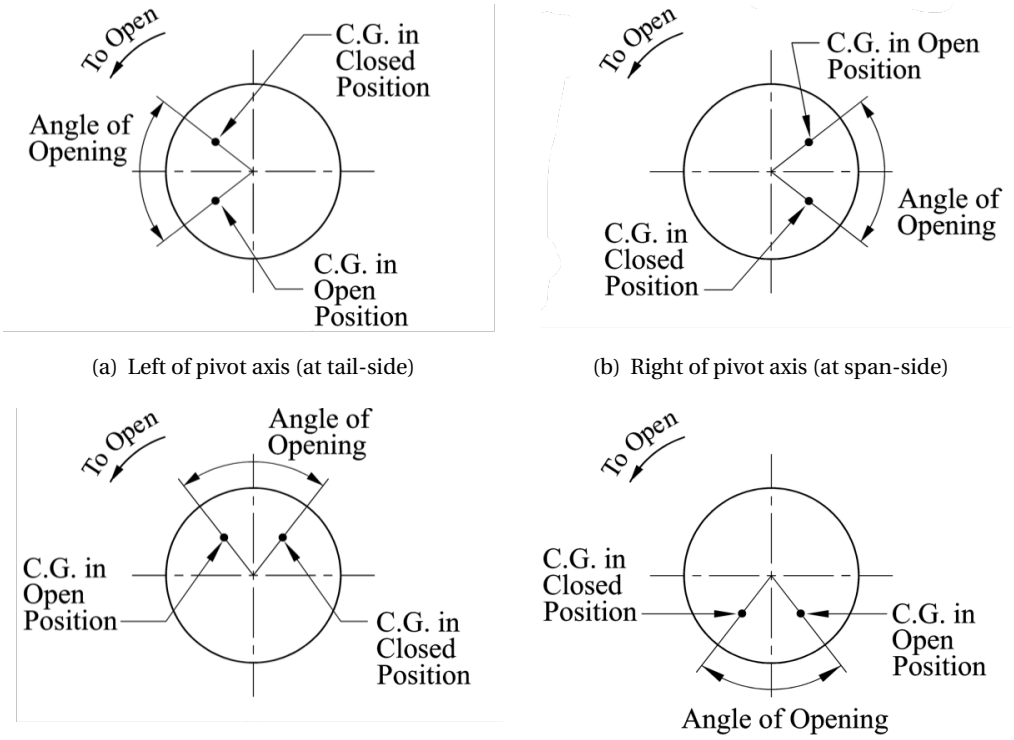

(a) Left of pivot axis (at tail-side)

(b) Right of pivot axis (at span-side)

(c) Above pivot axis

(d) Below pivot axis

Figure 2.7: *Positions of gravitational centre with respect to pivot axis [Koglin, 2003]*

2.3.1.1 Energy efficiency

The location of the gravitational centre has a very significant influence on the energy efficiency during the opening/closing cycles of the bridge. Obviously, the closer the gravitational centre is to the pivot axis, the less energy is required for the cycle. But apart from the actual distance, also the location with respect to the pivot axis determines the energy efficiency.

Considering the four principle locations from fig. 2.7, it is clear that the travelled vertical distance of the gravitational centre during a cycle is much bigger for configurations (a) and (b) than for (c) and (d). Provided that the potential energy of the bridge is not recovered during the cycle, this implies that configurations (a) and (b) require much more energy during a cycle than configurations (c) and (d). The higher demand for energy also translates into the size and cost of the operating mechanism itself.

2.3.1.2 Stabilising systems

The four principle locations all result in different opening angles in which the bridge is stable. Therefore, all four configurations require a different set of locking systems in order to assure stability in all opening angles. Next to that, different buffer cylinders are required to dissipate the kinematic energy at the end of the opening/closing cycle, in order to allow for a controlled stop. The following stabilising systems are required for the four principle locations as displayed in fig. 2.7:

(a) The stable position for this configuration is in the opened position. In the closed position, the bridge has a tendency to open. This has to be prevented by a span lock at the abutment pier. The opening movement of the bridge has to be controlled by a buffer cylinder.

(b) The stable position for this configuration is in the closed position. In the opened position, the bridge has a tendency to close. This has to be prevented by a span lock at the bascule pier, or a mechanical break on the operating mechanism. The closing movement of the bridge has to be controlled by a buffer cylinder.

(c) The stable position for this configuration is in both the opened and closed position. Therefore no stabilising mechanisms are required, provided that the magnitude of the imbalance is adequate. A buffer cylinder is however required to control both the opening- and closing movement of the span.

(d) The stable position for this configuration is in the half-opened position. Therefore, span locks are required to maintain both the opened- and closed position of the bridge. Both the opening- and closing movement of the span are controlled, thus no buffering mechanism is required.

2.3.1.3 Traffic- and vessel safety

Depending on the location of the gravitational centre, the stability of the bridge in its different positions either relies on gravity or on the stabilising system. In the latter case, one should consider the safety risk that a potential failure of this stabilising system poses to the users of the bridge.

(a) In case of a locking failure, the closed bridge will swing open. This poses a risk to the traffic on the bridge.

(b) In case of a locking failure, the opened bridge will fall down. This poses a risk to the vessels passing the bridge.

(c) The stability of this configuration relies on gravity. Provided that the magnitude of the imbalance is adequate, there is no risk for either traffic or vessels.

(d) The stability in both opened- and closed position relies on a locking mechanism. Therefore, there is a risk for both traffic and vessels.

2.3.1.4 Service during failure of operating mechanism

Another consideration for the positioning for the gravitational centre is the serviceability during a failure of the operating mechanism, for example during a power outage. Only when the gravitational centre is located towards the leaf (configuration b), one can guarantee that traffic can safely continue to use the bridge. In configuration (a) however, one can guarantee the safe passage of vessels. The choice for either of these depends on the importance of the considered road- and shipping infrastructure.

2.3.1.5 Sensitivity to changing balance

Setting and maintaining the balance of the bascule is of vital importance for the durability of the bridge. A mismatch between the intended balance and the actual balance may result in the accelerated deterioration of elements and mechanical systems, and may ultimately lead to dangerous situations. A shift in the location of the gravitational centre may for example result from maintenance operations [Oosterhoff and Coelman, 1999].

When looking at the different options in fig. 2.7, it becomes apparent that configuration (c) and (d) are very sensitive to changes in the location of the gravitational centre. A slight shift to the left or right results in a drastic change in the balance of the bridge, so that the bridge might become inoperable. Configurations (a) and (b) on the other hand are much more robust in this regard.

2.3.2 Magnitude of imbalance

Uplifting effects in the closed state of the bridge are mainly caused by wind loads. At the right angle, wind can create pressure on the bottom and suction on the top of the bridge deck, resulting in an upward force acting on the span-side of the bascule. Traffic can also introduce uplifting effects on the bascule, caused by the dynamic response of the bridge as vehicles pass.

Unintentional opening of the bridge can be avoided by, under any circumstance, ensuring a positive support reaction at all liveload supports. This can be achieved by a establishing a pre-pressure at the supports. The pre-pressure can be introduced by a combination of an intentional imbalance and a setting force. This setting force is usually applied at the tail-side of the bascule, resulting in an additional pressure at the supports after closing the bridge.

The Dutch regulations for the design of movable bridges (VOBB) requires a minimum total pre-pressure at the supports of 20 kN for movable traffic bridges. Obviously, the pre-pressure must be larger if the uplifting effects at the supports surpass this value [NEN 6786, 2001, section 9.9].

2.4 Rehabilitation and replacement

The substructures of movable bridges have proven to be more resistant to damage and deterioration than the superstructure. The remaining service life is thus generally determined by the condition of the superstructure, while the substructure might only require minor maintenance. If the bridge still meets the functional requirements in terms of geometry, rehabilitation or replacement of just the superstructure could well be a cost-effective solution.

Rehabilitation or replacement of a bridge is required if the structure is either structurally deficient or functionally obsolete. A structurally deficient bridge is one whose components have deteriorated or have been damages to such extend that its use is restricted. A functionally obsolete bridge might be in good structural condition, however it does not satisfy the current functional requirements in terms of load levels, traffic volume or under/over-clearance. The FHWA[1] has estimated that forty percent of the bridges in the United States is classified as such [Parke and Hewson, 2008, p. 509].

Considering the condition of the structure, its desired remaining service life, likelihood of failure and legal considerations of liability, the following options should be considered [Koglin, 2003]:

- Do nothing: Structures are often over-dimensioned, and this extra strength can be utilised as long as adequate safety can be proven. The probability and financial effects of a catastrophic failure should be considered.
- Repairs: Repairs can usually be done while maintaining the bridge in operable condition, but only postpones the need for major rehabilitation.
- Rehabilitate: Rehabilitation is can be done by reinforcing members or replacing them by stronger ones. These measures increase the deadweight of the span, which is limited by the possibility to increase the counterweight.
- Replace: Replacement of the bridge causes major nuisance for traffic for a longer period, but future hindrance is minimised. Constructing a replacement bridge alongside to the existing bridge may be a consideration.
- Change loading on the bridge: By imposing restrictions to the traffic loads on the bridge, by limiting axle loads or closing lanes, the structure's remaining service life can be extended. Furthermore, one can decide not to open and close the bridge any longer in order to relieve the bridge from accompanying stresses.
- Take bridge out of service: In exceptional cases, it is decided to simply take the bridge out of service. The investments don't weigh up to the benefits of a new bridge.

In the scope of this thesis, the focus will be on the third and fourth option: rehabilitation and replacement of existing bascule bridges.

[1] Federal Highway Administation

2.4.1 Triggers

Rehabilitation or replacement can triggered from both safety and usability considerations. Structural deterioration is generally instigated by corrosion or fatigue. Not being able to fulfil the functional requirements is mostly a result of an increased traffic intensity.

2.4.1.1 Corrosion

In the manufacturing of construction steel, much energy is used to convert iron ore into pure iron. During the service life of a steel structure, the natural tendency of the metal is to revert to their natural state; iron oxide. The total annual costs due to the effects of corrosion in the United States are estimated at approximately three to five percent of the gross national product [Aseff, 1987].

For corrosion to occur, the following four elements must be present: an anode, a cathode, a conductor and a continuous conductive path (electrolyte). The first three elements are formed by the metal structure itself, and the electrolyte is generally water. The presence of chloride ions in this water accelerates the corrosion process, as it makes the electrolyte more conductive. Anti-corrosion measurements eliminate one of the four required elements, thereby stopping the corrosion process.

To prevent steel bridge elements from corroding, usually a coating is applied. The most common one, paint, acts as a physical barrier to prevent direct contact of water with the steel. A somewhat different type of coating acts as a sacrificial or galvanic protection coating, changing the anode from the construction steel to the zinc in the coating itself. A more drastic method would be the use of cathodic protection, in which a sacrificial anode is connected to the steel.

In course of time, most coatings permit moisture and oxygen to permeate the system and attack the steel. In the first stages, rust develops underneath the coating layer and forms blisters. In progressive stages, the coating will debond from the steel which further accelerates the oxidation process. Pitting and flaking of the steel exposes the interior or the elements to the environment. In final stages significant parts of the cross-section may have corroded resulting in structural loss.

Elements are treated differently, depending on the severity of the corrosion. If early-stage local corrosion is spotted, the spots can be sanded and repainted. If larger areas are affected, whole structures can be sandblasted and spray painted. Severely corroded elements that suffer from structural loss might have to be replaced [National Association of Corrosion Engineers, 1994].

Corrosion is a typical problem for bascule bridges due to the inaccessibility of steel elements in need of recurring maintenance. The parts around the trunnion can not be maintained without taking the bridge out of service, as they are enclosed by the concrete bascule pier. Rainwater however has free access to these steel elements. De-icing salts can descent into the bascule chamber and settle on these elements, accelerating the deterioration.

2.4.1.2 Fatigue

Fatigue is the mechanism whereby cracks initiate and grow under fluctuating stresses. Due to the nature of the structure, bascule bridges are subject to severe fatigue loading in the superstructure under the influence of live loads. In the closed state, the deadweight of the bridge is supported as a cantilever from the bascule pier side. This loading introduces tensile stresses in the top flange of the main girders, or the top plate of the orthotropic deck. Live loads are however transferred to both abutments, and superimpose compressive stresses in the top fibres. The passage of heavy vehicles therefore cause high stress ranges in relation to the mean stress. This effect is further enhanced as the superstructure becomes more material efficient; having a higher ratio between live- and dead loads.

Bascule bridges constructed after the Second World War are often equipped with orthotropic steel decks. These consist of a deck plate supported in two mutually perpendicular directions by transverse diaphragms (crossbeams) and longitudinal stiffeners (ribs), creating a very material efficient superstructure. Orthotropic plates also have large numbers of welded connections. Stress concentrations at these welds, together with residual stresses, make them potentially liable for the initiation of fatigue cracks [Qian and Abruzzese, 2009].

There is indeed a number of bascule bridges equipped with orthotropic decks that have failed prematurely due to fatigue. The best known example in Holland is the 'Van Brienenoordbrug' bascule bridge, which had developed severe cracks at the location of the heavy truck lane. This occurred only seven years after commissioning, long before its designed service life [Romeijn, 2006].

Next to traffic, the opening/closing cycles impose a fatigue load on the structure. Both the leaf as well as the counterweight support frame are subjected to a complete stress reversal during the opening and closing cycles. The stress range during these events is higher compared to live loads, however the number of cycles is much lower. Nonetheless, as fatigue damage is cumulative, they contribute to the degradation of the structure [Koglin, 2003].

2.4.1.3 Increased traffic intensity

Motorised transportation became available to the masses after the Second World War. Within ten years from 1960, the total number of motorised vehicles had increased from half a million towards seven million. Nowadays, this number is stabilising at around ten million vehicles. This rapid increase of vehicles instigated the expansion of the Dutch road networks and as a result, the majority of the infrastructural system originates from the 60's and 70's of the last century. The bridge structures within this system were designed according to at the time applicable standards of traffic intensity and service life.

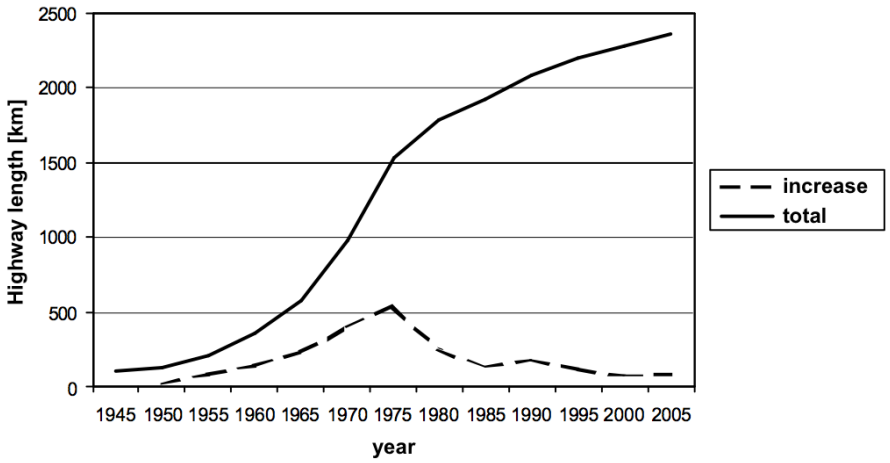

Figure 2.8: *Growth of highway infrastructure in the Netherlands [Rijkswaterstaat, 2007]*

Over the years, the traffic intensity has changed. Not only do roads accommodate more, but also more heavy traffic. As a result regulations have repeatedly changed to be more stringent, adjusting the design loads to better reflect actual loading. All newly constructed structures have to comply with prevailing regulations. For existing structures structures it holds that they should comply with partial safety levels under influence of the actual loads on the structure, which is less stringent. Rehabilitated structures have to comply with prevailing regulations for new structures, unless it can be proven that this would require disproportional efforts [Rijkswaterstaat, 2013a].

Next to compliance with regulations, there may also be a demand for increased traffic capacity for particular constructions. This capacity can for instance be provided by a more efficient layout of the road's cross sectional profile. Usually the associated increased live loads will require strengthening of the existing structure. Replacement is sometimes considered a more feasible solution.

2.4.2 Use of fibre reinforced polymer composites

The goal of bridge rehabilitation or replacement is upgrade the structure to comply with current functional requirements and modern safety standards. In case of movable bridges, and bascule bridges in particular, there must be special attention to retaining the balance of the structure. Many conventional strengthening methods would shift the gravitational centre of the span to such an extent that this can not be compensated for. This can be avoided by making use of fibre reinforced polymers (composites) as a construction material, which feature excellent strength-to-weight ratios. By making use of composite elements structures can be strengthened while retaining or even reducing their weigh, resulting in a well-adjusted balance and improved live load capacity.

In the rehabilitation of movable bridges, composites can be used to replace deteriorated elements or to strengthen the structure. Successful results have been achieved in the application of composite bridge decks, the strengthening of beams and columns by means of externally bonded sheets and the installation of external post-tensioning tendons. Replacement is a more radical solution, for which composites can be used for several bridge elements or even the entire structure. Rapid installation and the reduced need for maintenance are the main incentives to choose for composites.

The material properties of composites highly depend on the type and volume percentage of fibres, resin type, additives, fibre orientation and manufacturing method. The following overview of advantages and disadvantages is applicable to all types of fibre composites, to a greater or lesser extent. Please note that the disadvantages have a practical character, and can be overcome taking these material characteristic into consideration in the initial design phase [O'Connor, 2013].

2.4.2.1 Advantages

- Weight: the high strength-to-weight of composite elements allows for bridge renovations without alterations of the substructure, rapid installation with simple equipment, decreased hindrance for traffic and higher live load capacity
- Life Cycle Cost: composite elements are generally maintenance free and offer a long service life, reducing the cost over the service life of the structure
- Durability: composites do not suffer from corrosion and offer much better resistance to freeze-thaw cycles than traditional materials, elongating the service life of structures up to an estimated 75 years
- Sustainability: extending the service life of structures delays the need of a completely new structure, reducing associated waste and pollution

2.4.2.2 Disadvantages

- Initial costs: traditional engineering- and construction companies are not using LCC[2] models, but focus on initial investments
- Stiffness: the low modulus of elasticity of glass reinforced composites results in over-dimensioned structures from a strength perspective, reducing material efficiency
- Creep: under the influence of prolonged loading, composites tend to deform more than traditional materials
- Degradation: improper addition of additives can result in poor durability of elements under the influence of moisture and UV radiation
- Ductility: composites exhibit brittle failure, so there is no indication that a structure is in potential danger
- Connections: applicability of connections is dependent on composites, and traditional connection techniques may not be effective
- Standardisation: design and manufacturing standards as well as long-term performance data are non-existent, causing reluctance towards the material

[2]Life Cycle Cost

2.5 Reference projects

In this section, three reference projects are reviewed, two of which have actually been built. All three bridges use fibre composite material in the main loadbearing structure, have a material-adapted design and can support heavy-traffic. The third case (Andelbrug) has not made it to actual construction, but is still reviewed as the boundary conditions of the problem are very similar to the case study of this thesis.

2.5.1 Hoofdbrug Oosterwolde

The Hoofdbrug (Oosterwolde, the Netherlands) bridge is reportedly the first heavy-traffic vertical lifting bridge composed entirely of composite material. The bridge spans a total of 12 meters, and weighs around 65 tons. The pylon is equipped with a hydraulic riser to lift the bridge. The cable stays do not offer any structural support, but are merely there for aesthetic reasons. Due to the eccentrical positioning of the pylon, the shorter end of the bridge is balanced by a lead core. The bridge has been in service since June 2010, and was established by engineering firm 'Witteveen+Bos', manufacturer 'Fibercore Europe' and main contractor 'Knol Akkrum'.

(a) Hoisting (b) After installation (c) Final state

Figure 2.9: *Hoofdbrug Oosterwolde, the Netherlands [Provinsje Fryslan, 2010]*

Structure The load bearing structure is of the bridge is composed of a unitised glass-fibre sandwich panel, produced by the VARTM technique, as discussed in section 3.2.3.2. The 12 meter width of the bridge is made up of two parts which have been adhesively bonded at the construction site. At the location of the supports the cross-section contains four embedded solid composite beams in the spanning direction. These beams are composed of 50% fibres in the horizontal and 50% in the vertical direction, allowing the beam to transfer the vertical loads to the abutments. The beams are mainly there in order to help comply with stiffness criteria of the bridge, as merely low-modulus glass-fibres are used. The sandwich faces are composed of glass-fibre laminates, having 75% of the fibres in the bridge's spanning direction and 25% perpendicularly oriented.

Coupons of the construction material have been extensively tested for static and fatigue loading, executed at the Civil Engineering faculty of the Technical University of Delft.

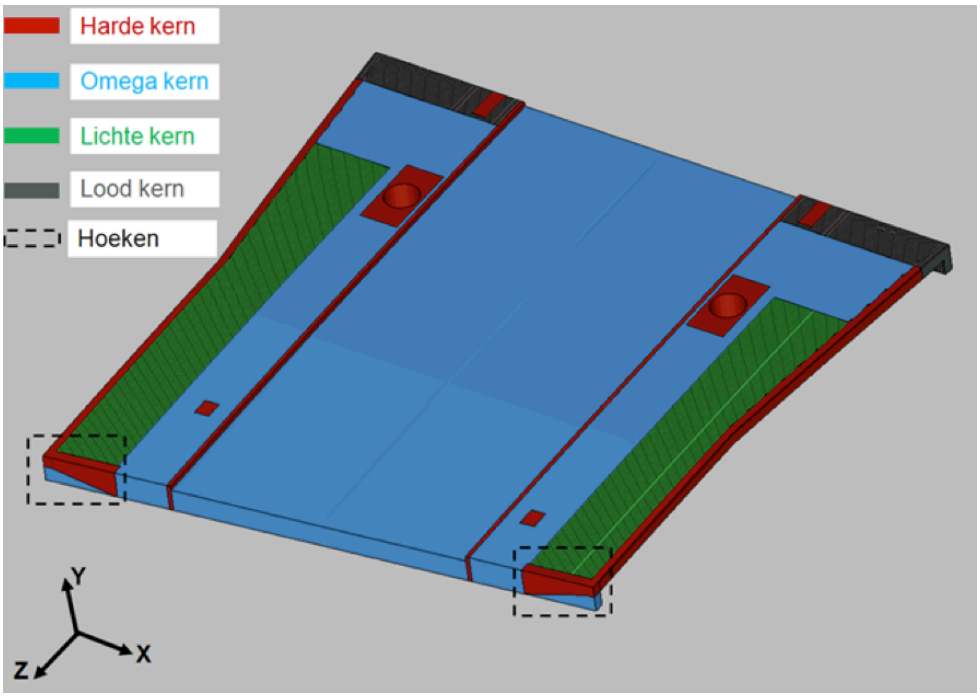

Figure 2.10: *Core material distribution in sandwich deck - courtesy of Witteveen+Bos*

2.5.2 Chamberlain drawbridge

The island of Barbados, a British colony, decided in 1990 to replace a heavily corroded bascule bridge by a composite structure. The new structure was formed using Strongwell's trademarked COMPOSOLITE pultruded modular panel system (see section 3.2.3.2). The bridge measures 8.9 meter wide, 11.7 meter long and about 1 meter deep. It mainly supports pedestrians, although it was designed to support vehicles. Due to the reduced weight of the structure, the bascule lifting system could be replaced by an electrically driven hydraulic system consisting of two large rams.

(a) Checking tolerances (b) Shipping (c) Final state

Figure 2.11: *Chamberlain drawbridge, Barbados [Barefoot, 2007]*

Structure The bridge structure is composed of glass-fibre pultruded hollow deck panels, which have been connected to form a box structure. One set of panels runs longitudinally, and a second set runs transversely above the first to form the deck. Vertical panels between the two panel layers transfer the shear forces and serve as spreaders to obtain sufficient bending stiffness. The panels are joined by three-way toggles that are adhesively bonded and provide mechanical interlocking between the panels (see fig. 3.14).

Prior to its shipment to Barbados, Strongwell assembled the entire bridge in its factory in order to check tolerances. The structure was subsequently broken down into four sections, and shipped in two ocean containers in late January 2006. The four sections were assembled onsite and inserted into a large clamp that is connected to the hydraulic lifting system [Barefoot, 2007].

2.5.3 Andel basculebridge

In 1999, a combined team of experts composed of members from the Dutch organisations 'Rijkswaterstaat', 'Centrum voor Lichtgewicht Constructies' and 'TNO Bouw' undertook a feasibility study for a heavy-traffic composite bascule bridge in Andel, the Netherlands. The team went through a design process to generate alternatives, design joint details, investigate the manufacturability and finally test specimens in the lab. The design did not make it to actual construction due to a lack of funds. The study is however very similar to the case study of this thesis, and will therefore be discussed in this section.

Please note that the production techniques have considerably advanced in the past two decades since this feasibility study was performed. The team had no access to modern-day pultrusion techniques that can achieve high fibre volume fractions of up to 70%. Instead, they were limited to hand lay-up techniques offering a maximum fibre fraction of 35%.

2.5.3.1 Requirements and conditions

A major requirement was the exchangeability with a steel bascule bridge, i.e. the geometry of the composite variant had to fit within the steel variant. This determined the characteristic dimensions of the bridge:

- Width: 15.15 meter
- Length: 14.6 meter
- Structural height: max. 1.65 meter
- Span (rotational point to abutment): 16.8 meter
- Transverse distance between supports: 10 meter

Load models The load models were of the traffic category 600, according to the VOSB 1995 regulations; one 600 kN truck or two 600 kN truck at 80% in addition of a distributed load between 2 and 4 kN/m^2.

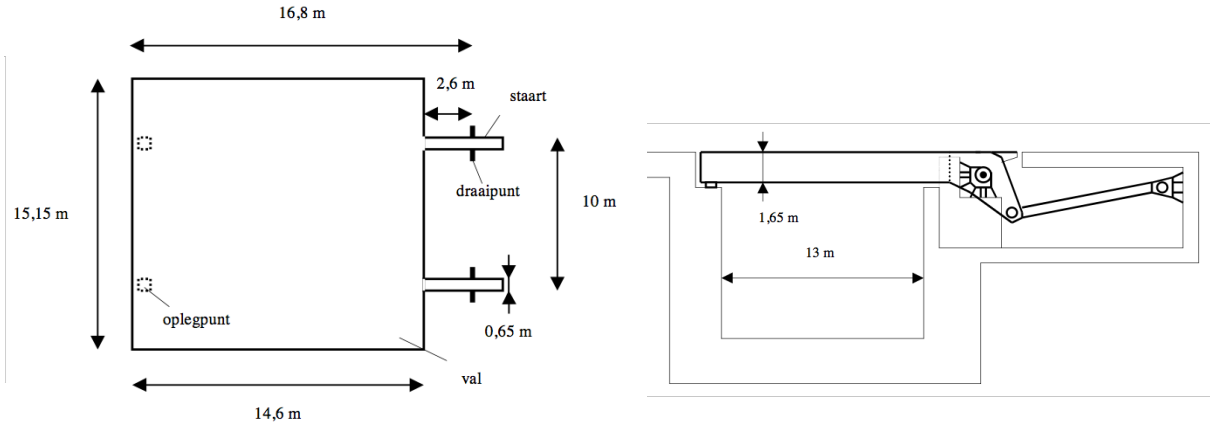

(a) Top view (b) Side view

Figure 2.12: *Geometry and configuration of the steel variant [Souren, 1999]*

The fatigue load models accounted for 50 years of traffic, and a number of 100.000 opening/closing cycles.

Stiffness Based on considerations with respect to comfort, a serviceability limit state deflection of 0.003 times the bridge span was maintained as a requirement. In addition to this static dispacement, the vibrational behaviour of the bridge was verified to be acceptable for pedestrians.

In the transverse direction, the stiffness requirement was dominated by the maximum allowed vertical gap (max. 6 mm) between the bridge deck and the abutments. To avoid flapping of the bridge, it was decided to have a statically determined structure; i.e. just two supports at either side of the bridge. As a result of this, the transverse stiffness of the leaf became a decisive requirement.

2.5.3.2 Concepts

The main loadbearing structure and the bridge deck were initially considered separately.

Main loadbearing structure The team had extracted six usable alternatives from a brainstorm session. A distinction was made between alternatives consisting of one and two loadbearing plates, as can be seen in fig. 2.13. A selection procedure was based on considerations such as stiffness, manufacturability, assembling method, safety, inspectability, maintainability, weight and cost.

Based on these considerations, the sandwich frame structure (1) was chosen to be further developed. In order to comply with the stiffness and height requirements, it was decided to use carbon fibres in the main loadbearing structure.

Bridge deck Based on the availability of composite bridge decks at the time, a simple plate structure composed of rectangular boxes was selected (1).

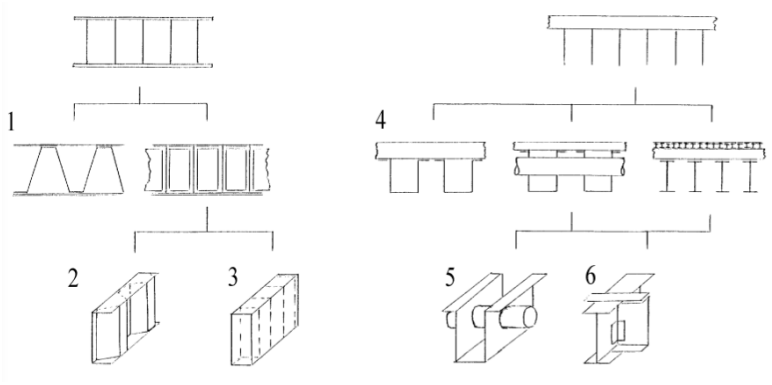

(a) Double faced (sandwich) (b) Single faced

Figure 2.13: *Main loadbearing structure concepts [Souren, 1999]*

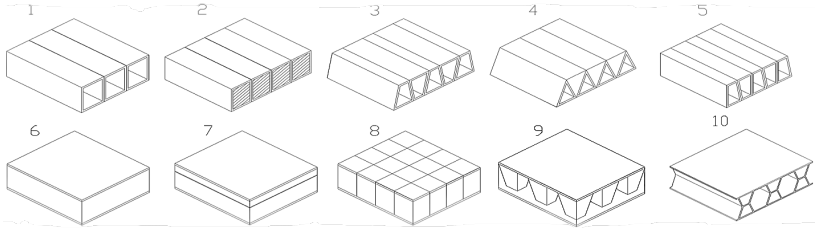

Figure 2.14: *Commercially available bridge deck types [Souren, 1999]*

Leaf-tail connection Two concepts were considered to connect the main loadbearing system to the operating system in the bascule chamber; a fully composite structure and a traditional steel structure. The principle of the feasibility study was to apply composites wherever possible. It however appeared to be too complicated to produce the tail of the bascule structure out of composite material. Furthermore, the weight and cost of the composite alternative proved to be disappointing.

It was finally decided to go for a traditional steel tail structure, and to connect it to the composite leaf, as shown in fig. 2.16(a).

2.5.3.3 Preliminary design

The 1575 millimetre height of the leaf's cross-section is composed of (top to bottom):

- Sacrificial layer: 6 mm thick (glass-fibre)
- Structural laminate: 4 mm thick (glass-fibre)
- Bridge deck: 169 mm high, 50 mm wide hollow tubes spanning in transverse direction (glass-fibre)
- Structural laminate: 8 mm thick, transverse fibre orientation (carbon-fibre)
- Z-beams: 1380 mm high, 505 mm wide, 17 mm flange and 13 mm web thickness (carbon-fibre)
- Structural laminate: 8 mm thick, transverse fibre orientation (carbon-fibre)

The main loadbearing elements are composed of carbon-fibre reinforced epoxies, in order to obtain a high degree of stiffness. For the sacrificial layer and bridge deck it was decided to apply glass-fibre reinforcement, because of the superior resistance to impact. Furthermore, as the stiffness of the glass-fibre bridge deck is relatively low, the shear stresses in the adhesive between the Z-beams and hollow tubes is limited.

The weight of the bridge deck, including sacrificial and structural layers, comes down to 99 kg/m^2. The main bearing structure totals a weight of 173 kg/m^2.

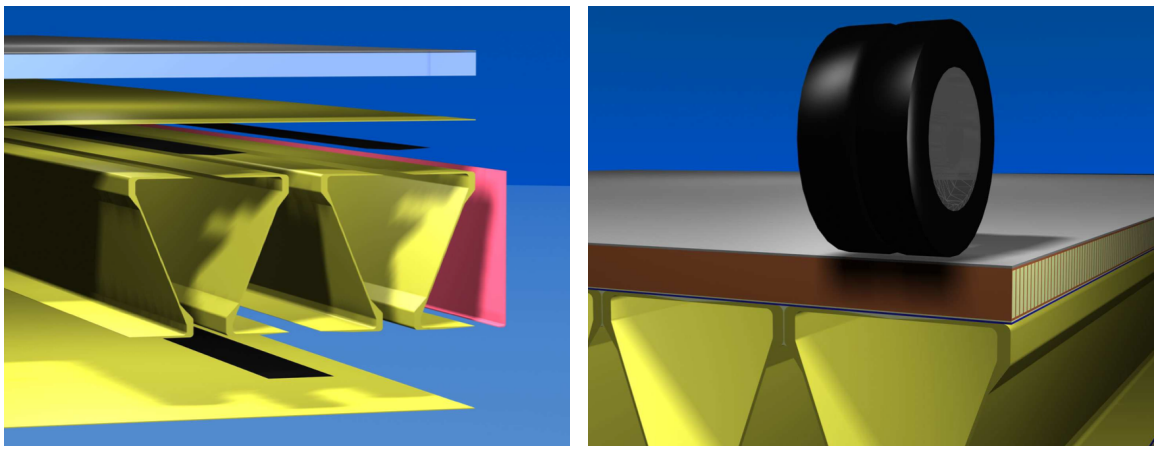

(a) Exploded view (b) 3-dimensional view

Figure 2.15: *Assembly of bridge structure [Souren, 1999]*

Joints In order to comply with the stiffness requirements it was necessary to structurally bond the bridge deck to the main loadbearing structure, thereby increasing the bending stiffness of the structure. This was done by an adhesive bond between the structural laminates, the Z-beams and the bridge deck tubes.

The Z-shaped beams were interconnected by a combined joint of adhesives and mechanical fasteners. Both joint types are able to bear the full load. A higher safety-factor is achieved by combining both, introducing ductility in the structure (see section 3.4.3.3).

The connection between the steel tail and the composite leaf is subject to high (fatigue)loads, imposed by traffic and opening/closing cycles. The magnitude of the maximum bending moment and shear force were computed to be respectively 5754 kNm and 2131 kN. In the combined double-lap joint design from fig. 2.16(c), 90% of the bending moment would be transferred through the coupling plates at the flanges, while the remaining 10% is transferred through the webs. The shear force is transferred fully through the webs. Compressive forces, primarily exerted in the opened state of the bridge, are transferred through the endplate between the tail and leaf.

The coupling plates are connected to the steel tail by means of prestressed bolts. The connection to the composite leaf is provided by an adhesive bond. Note that the coupling plates are tapered in order to reduce peak stresses at the edge of the connection. Once again, mechanical fasteners are merely installed to obtain additional safety and ductility.

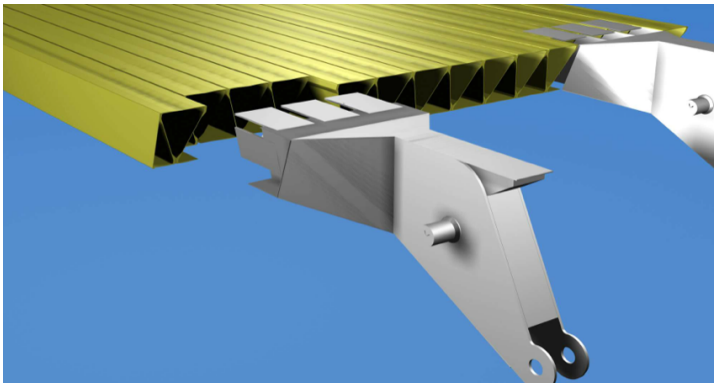

(a) Leaf-tail connection

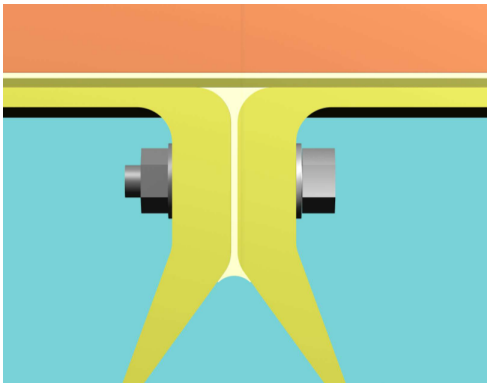

(b) Z-shaped beams

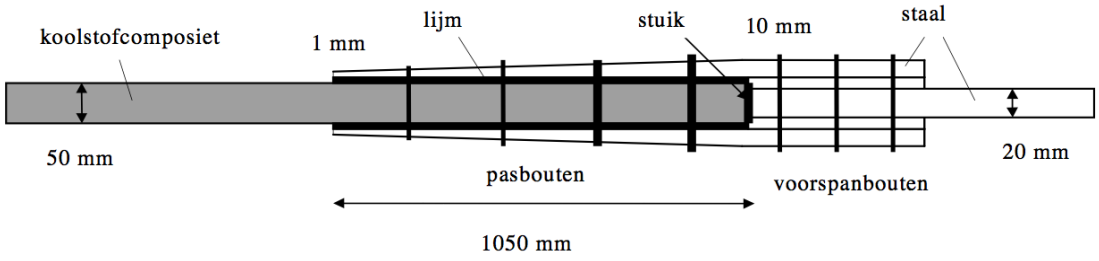

(c) Composite-steel conneciton

Figure 2.16: *Joint design [Souren, 1999]*

3 Fibre reinforced polymers

In the broad sense, composites are solid materials composed of more than one component which are in separate phases. Fibre reinforced polymers is the collective term for a subsection of composite materials made up of a polymer resin and fibre shaped reinforcement, covering over 90% of the modern composite market. The polymer-based matrix and reinforcement have complementary properties, which is what makes them efficient and commercially interesting. A variety of different material parameters, such as compound types, fractions and orientations, allow the engineer to design highly efficient purpose-made applications [Strong, 2008].

3.1 Material

3.1.1 Fibres

Fibres are materials that have a high aspect ratio, i.e. one long axis compared to the other dimensions. This means that loads can be transferred into the fibres along the long axis, making them suitable for reinforcement. In addition to this, the molecular structure of fibres is often oriented in the long direction as well. This is the result of the manufacturing process, in which the solid but pliable fibre is physically pulled in the long direction. This pulling force stretches the polymeric backbone, aligning the molecules in the longitudinal direction.

The slenderness of fibres is an important parameter for the mechanical properties of composites. Fibres exhibit a size effect; an increase in actual strength is gained at a decreased diameter. The actual strength of materials is lower than the theoretical strength, due to inherent flaws. As the fibre diameter becomes smaller, the chance of inherent flaws is reduced, thus the actual strength is increased. Furthermore, at a constant fibre fraction, the fibre-matrix interface is increased which results in higher ductility and more gradual transfer of loads from matrix to fibre.

The principal role of the reinforcement fibres is to provide the mechanical properties to the composite. Material properties such as strength, stiffness, thermal expansion and conductivity, are dominated in the direction of the fibre orientation. High fibre percentages results in composites having increased strength and stiffness properties. A 60-70% fraction of fibres has been found to be the upper limit, above which there is insufficient resin available to fully wet the fibres.

A range of materials can be used as reinforcement. From mechanical and economical considerations, the focus will be on the fibre materials that dominate the modern composite market; glass, carbon and aramid [Strong, 2008].

3.1.1.1 Glass fibres

Fibreglass is by far the most dominant reinforcement material for composites in terms of usage, due to the combination of its low price and excellent properties for normal use. Glass fibres have a relatively high toughness; having the ability to absorb energy without fracturing. The raw materials of glass fibres are silica sand and various subcomponents.

At a temperature of 1250 °C the molten glass flows through bushing holes and forms continuous strands, called filaments. The hot filaments are being sprayed with water to cool below the transition temperature. After the application of a protective coating, the fibres are drawn (mechanically elongated) and then wound up on rolls. After a curing phase, they are used as a basis of a range of fibreglass products such as yarns, roving, woven fabrics and mats.

Several types of glass fibres are manufactured, each having different oxide components attached to the silica (SiO_2) backbone resulting in specific properties. The four most common types are E-glass, C-glass and S-glass. The letters are indicators for the specific properties the glass types are known for; respectively their low electrical conductivity (E), high resistance to chemical environments (C) and the superior strength properties (S) [Strong, 2008].

3.1.1.2 Carbon fibres

Carbon fibres are nowadays among the highest specific strength and modulus of any material. Quality does however come at a price, with ranges up to 5 to 10 times that of glass fibres (per unit mass). Carbon fibres are furthermore chemically inert, exhibit outstanding resistance to creep and fatigue and have high damping characteristics. On the other hand, they have a low impact resistance, compressive strength and elongation to fracture.

Different production techniques come down to the same principle; high free-carbon material is stabilised by thermosetting, in which the molecules are crosslinked and rearranged. Subsequently the fibres are carbonised in a high temperature nitrogen atmosphere, removing the hydrogen molecules and interconnecting the carbon rings. The carbon content after this process is around 80-95%. Further heat treatment, called graphitization, results in high performance fibres having a carbon content of above 99% [Strong, 2008].

3.1.1.3 Aramid fibres

Aramid fibres, better known under the brand name Kevlar, provide the highest tensile strength-to-weight ratio among reinforcement fibres. Furthermore, they provide high energy absorption and impact resistance. Unlike glass and carbon fibres, aramid fibres fracture in a ductile manner, inducing fibrillation of the fibres. These combined characteristics make that aramid fibres are the preferred choice for application in ballistic protection and protective clothing and gloves. As a construction material aramid fibres may not be very useful, as they are relatively prone to fatigue and creep. In addition, they exhibit a low compressive strength [Strong, 2008].

Aramid filaments are produced by drawing an extruded acidic solution through a spinneret. During this operation, the molecules become highly oriented in the longitudinal direction [Mazumdar, 2002].

3.1.1.4 Comparison

Quantitative The reviewed literature shows quite some spread in specified mechanical properties of fibres. The following table presents an overview of representative values for bare fibres[1].

Table 3.1: *Representative fibre properties [Campbell, 2010; Kolstein, 2008; Strong, 2008]*

	Density $[kg/m^3]$	Tensile modulus *[GPa]*	Tensile strength *[MPa]*	Elongation to break *[%]*	Thermal expansion $[10^{-6}\ ^oC]$
E-glass	**2500**	**69**	**3400**	**4.9**	**5.2**
C-glass	**2500**	**72**	**3450**	**5.0**	**7.3**
S-glass	**2500**	**83**	**4600**	**5.7**	**5.7**
Carbon HM	**1900**	**440**	**3450**	**0.5**	**-0.75**
Carbon HS	**1800**	**270**	**5300**	**1.8**	**-0.6**
Aramid HM	**1450**	**180**	**3400**	**2.0**	**-2.0**
Aramid HS	**1450**	**130**	**4000**	**2.8**	**-2.0**

Qualitative As mentioned before, the characteristics of fibres depend on the ingredients, production method, curing treatment and fibre diameter. Properties can however be compared in a relative manner, as indicated in the following table as subtracted from different literature sources.

[1] HM: High Modulus, HS: High Strength

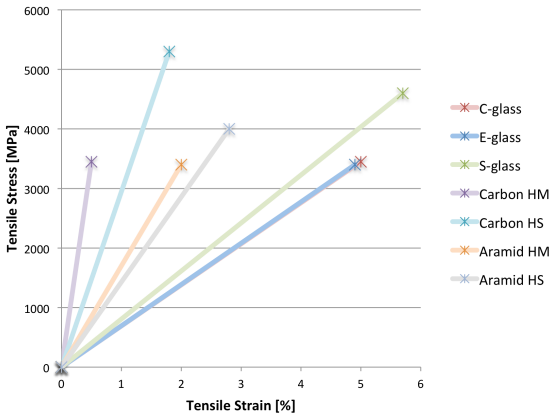

Figure 3.1: *Stress-strain diagrams fibre types*

	Fibre types		
	Glass	Carbon	Aramid
Specific strength			
Strength-to-weight			
Specific stiffness			
Stiffness-to-weight			
Density			
Toughness			
Creep / fatigue			
Cost			

Figure 3.2: *Qualitative comparison fibre types*

Hybrids The superior properties of various reinforcement types can be utilised by making combinations of fibres. A practical application is in elements that require high strength and should be able to cope with impact loads. This can be achieved by a selective placement of carbon and aramid fibres, as illustrated in fig. 3.3. This principle is often applied in the construction of composite bridge decks.

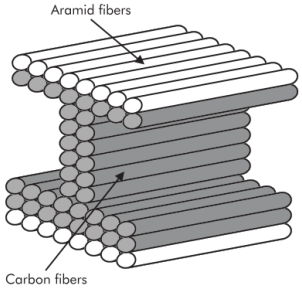

Figure 3.3: *Hybrid section model [Strong, 2008]*

3.1.2 Reinforcement forms

Depending on the production method, desired fibre fraction and fibre orientation a suitable reinforcement is chosen. The reinforcement is supplied in different physical forms, composed of either chopped strands or continuous filaments. Continuous-fibre composites normally have a preferred fibre orientation, while discontinuous fibres are generally randomly oriented. This dramatically reduces their strength and modulus of discontinuous-fibre composites, however the product is generally much less costly.

3.1.2.1 Continuous fibres

Continuous fibres are generally wound in parallel onto a spool, creating a roving. It can be processed into elements using the filament winding production method. Alternatively, roving goes through a weaving process to form woven fabrics. By applying different weaving techniques, one can create woven fabrics that possess special properties (strength, drapability, distortion resistance, thermal expansion) in the principle directions. Continuous-fibre composites are often made into laminates by stacking single sheets of continuous fibres in different orientations to obtain the desired strength and stiffness properties with fibre fractions up to 60 to 70 percent. Another option is to treat the fabrics with matrix material, such as epoxy, to create 'prepregs'. The product is only partially cured to allow for easy handling. The curing is completed in the final production step which usually involves hot moulding or an autoclave [Mazumdar, 2002].

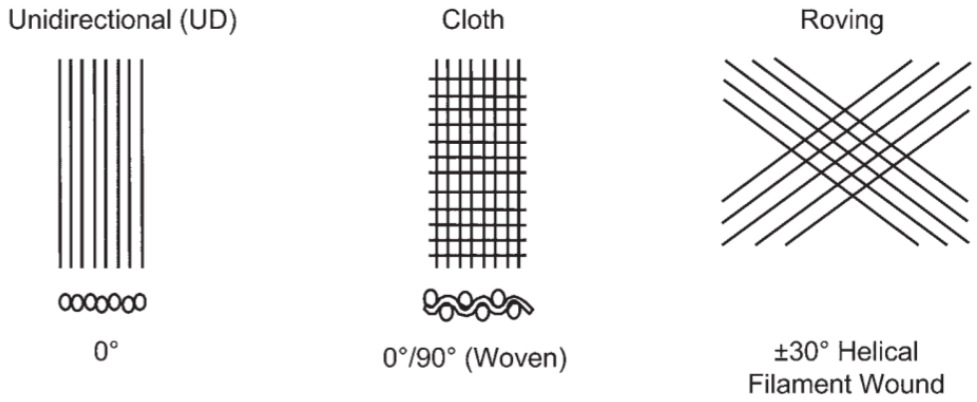

Figure 3.4: *Continuous fibre types [Campbell, 2010]*

3.1.2.2 Discontinuous fibres

Short fibres can be processed in chopped stand mats or mixed with resin as a moulded compound. Chopped stand mats are the default choice for hand moulding processes, in which the several mats are stacked and wetted with resin. Moulding compounds are shaped in their final form in a mould under pressure and heat.

Figure 3.5: *Discontinuous fibre types [Campbell, 2010]*

3.1.3 Matrix

The principle role of the matrix is binding the fibres together in a determined array and protecting them from environmental influences such as temperature, moisture and UV radiation. The matrix transfers the applied loads to the fibres, carry interlaminar shear and prevent premature failure in compression due to microbuckling of fibres. Furthermore, the matrix provides the composite with toughness, damage tolerance, and impact and abrasion resistance [Campbell, 2010].

The matrix of fibre reinforced composites can be polymeric, metallic or ceramic. In the scope of this thesis, only polymeric based matrices are considered. The polymeric matrix consists for the majority of a resin of polymers and might contain some additives to enhance the material properties. The term 'polymer' refers to individual molecular units (monomer) which are joined together into a chain-like structure [Strong, 2008].

A clear distinction is made between thermoplastics and thermosets. The choice between either of these as matrix material highly influences the mechanical properties of the final product. The chemical difference is in the creation of crosslinks between polymers during the curing of the material.

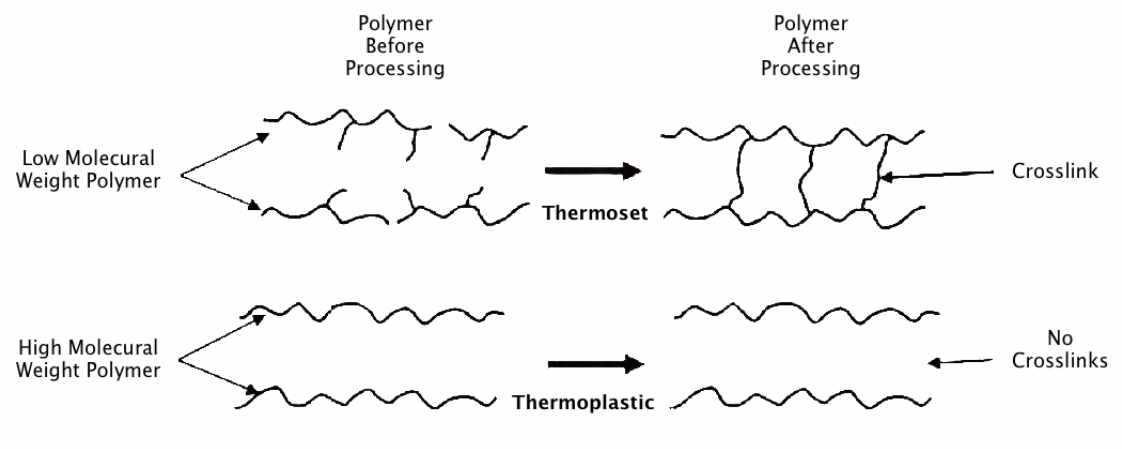

Figure 3.6: *Comparison of thermoset and thermoplastic polymers [Campbell, 2010]*

3.1.3.1 Thermosets

The polymer molecules of thermosets are relatively short, which causes the resin to generally be liquid at room temperature. This property makes thermosets easy to process and to provide excellent fibre impregnation. In the curing process, under the influence of heat or a catalyst and accelerator, the short polymers form three-dimensional molecular chains [Strong, 2008].

Due to this crosslinking fully cured thermosets cannot be remelted, however some may soften at elevated temperatures allowing for curving the structure. Instead of melting, thermosets decompose at a certain temperature; a process which is irreversible and results in the formation of char. The higher the number of crosslinks, the more rigid and thermally stable the material will be. This can partly be controlled by the temperature and duration of the curing and post-curing processes. The most common resin materials used in thermoset composites are polyesters, epoxies, polyimides and phenolics [Mazumdar, 2002].

3.1.3.2 Thermoplastics

Thermoplastics are resins that are solid at room temperature, consisting of long polymer chains. This solidity requires the resin to be injected under pressure or at an elevated temperature. After cooling down the thermoplastic will harden in the shape of the mould, confining the reinforcement fibres. There is no chemical curing; the changes are purely physical and reversible.

The absence of crosslinks has both advantages and disadvantages. Excellent toughness and resistance to impact damage is considered the most important advantage. Furthermore, the reversibility of the moulding process makes thermoplastics highly recyclable, in contrast to thermosets. On the downside, there are lower strength and stiffness properties as well as poor creep resistance, especially at elevated temperatures. Furthermore, the solid material state at room temperature complicates the production process, which drives the cost [Mazumdar, 2002].

3.1.3.3 Comparison

Most composite properties depend on the combination of the matrix and reinforcement acting together, however for some are dominated by the matrix. As mentioned before, the principle role of the matrix as a component of the composite is to bind and protect the reinforcement. These properties are furthermore strongly affected by the applied additives. Nonetheless, understanding the properties of the non-reinforced matrix can be useful and are therefore presented[2] [Campbell, 2010].

Table 3.2: *Representive physical and mechanical properties of several resins [Campbell, 2010]*

	Density $[kg/m^3]$	Tensile modulus *[GPa]*	Tensile strength *[MPa]*	Maximum use temperature $[^oC]$
Polyesters	**1100-1200**	**200-400**	**20-90**	**80-140**
Epoxies	**1200-1250**	**400-500**	**35-105**	**90-180**
Polyimides	**1300-1400**	**300-400**	**40-90**	**200-320**
Phenolics	**1300-1400**	**600-1200**	**35-60**	**150-200**
'Thermoplastics'	**1100-1200**	**200-500**	**35-140**	**170-230**

3.1.3.4 Additives

Additives can be added to the composite to improve specific material characteristics. Improvements can be made to physical, mechanical, electrical and thermal properties, as well as to improve resistance chemical and environmental resistance, or to reduce cost.

Additives that improve the mechanical properties generally aim at decreasing the release of heat and shrinkage during curing. The result is a stronger and stiffer, yet more brittle, composite. Another common method is to apply a surface finish to the fibres, called sizing, which improves the fibre-matrix bond and protects the individual fibres.

Fillers can be added to help reduce cost by diluting the more expensive resin. It is generally assumed that their use negatively affects the composite properties, but this is not always the case. By application of the right filler in the right quantity, one can tailor composites that exhibit better properties for its purpose at a lower price. Fillers can for example be beneficial for the impact resistance and toughness, as well as the fire resistance [Campbell, 2010].

[2] Properties of several thermoplastics are combined within one row

3.1.4 Sandwich cores

A structural composite sandwich typically consists of two face laminates, bonded to a thick lightweight core. An adequate core materials should selected by a trade-off between mechanical properties, weight and price. Generally, three types of cores are distinguished; solid cores, foam cores and honeycomb cores.

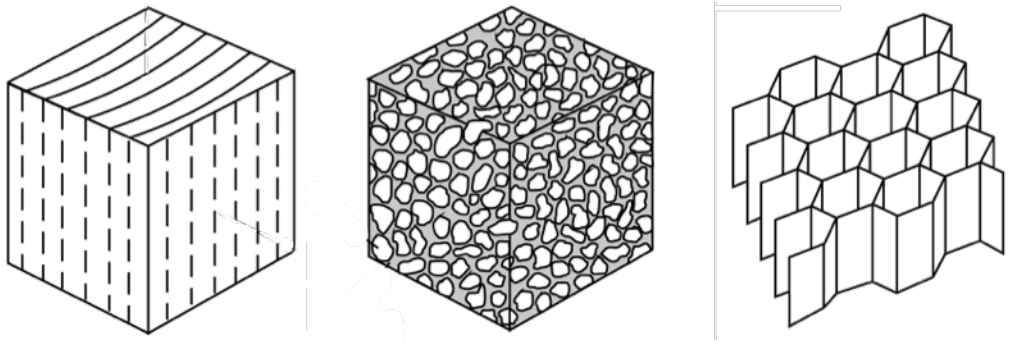

(a) Solid (b) Foam (c) Honeycomb

Figure 3.7: *Common types of sandwich cores [Carlsson and Kardomateas, 2011]*

3.1.4.1 Solids

Wood is commonly applied as solid sandwich core material in products such as doors and partitions. Balsa wood is can be used for lightweight applications, although the use of solid cores is being superseded by synthetic foam materials.

3.1.4.2 Foam

Foams are dominating in the manufacturing of structural sandwiches as a result of their favourable strength and stiffness-to-weight ratios and their relatively low price. Depending on the requirements of the panel, one could choose to apply structural or non-structural foam. The latter is low density foam, which merely acts as formwork during the production of the sandwich, and contributes only to a small extend to the bearing capacity of the panel. Higher density foams, exhibiting good compression and shear rigidity, can be applied as structural foams for high performance panels.

3.1.4.3 Honeycomb

Honeycomb cores are used in high performance applications, exhibiting excellent compression and shear rigidity as a result of their directionality and shape. Any thin-sheet material, mainly impregnated fibreglass or aluminium, can be shaped and connected to the face sheets. The performance under compression, as well as the core's density, is largely determined by the wall thickness of the core material. Due to the use of high-quality material and the complexity of the production process, honeycombs are expensive compared to solid and foam cores.

3.2 Applications in bridge construction

The first composite products to show up in bridge construction were aimed at strengthening existing structures by taking advantage of the directionality of the composite material. Later, composite deck elements were combined with a main load-bearing system composed of conventional materials into hybrid structures. As the technique advanced, full-composite bridges made their way into the construction industry as pedestrian bridges and later as heavy-traffic bridges. This chapter briefly introduces several composite products and accompanying production techniques, in which the main focus is on those products that are considered suitable for the design of a full-composite bascule bridge; pultrusion profiles and structural sandwiches.

3.2.1 Repair and retrofitting

Depending on the application, composite strips or sheets can be applied for the strengthening of structural bridge elements. The methods are generally simple, rapid and effective.

3.2.1.1 Strips

Steel plates are often used to increase the flexural or shear strength, by mechanically bonding them to the structure. Composites have proven to be more cost-effective for this application, as they are much more durable and easier to install due to their light weight. Before application of the prepreg laminate strips, the structure has to be pre-treated to assure a durable bond. Concrete substrates are prepared by grit blasting to expose the aggregate. Steel substrates are solvent degreased and treated with chemicals. Depending on the required properties of the bond different adhesives can be applied; generally epoxies and their hybrids. The wet lay-up method, where the matrix material component of the composite also acts as the adhesive material, is an alternative to bonding pre-cured strips. The method is less effective, but a lot more flexible and thus useful for curved and uneven surfaces.

In order for the strips to be effective their stiffness should be of the same order as the structure itself, which is why generally only carbon fibre reinforced composites are being used. An increase in flexural strength of as much as 20% can be achieved, which beneficially affects the remaining fatigue life of the structure [Teng, 2001].

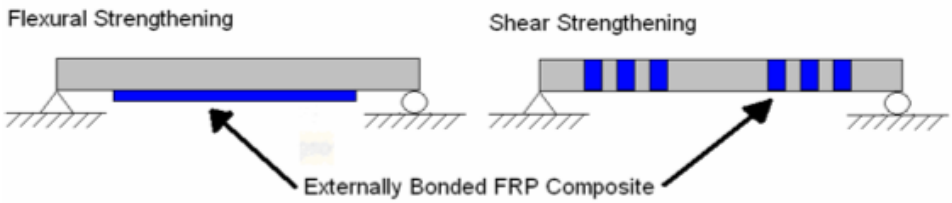

Figure 3.8: *Flexural and shear strengthening using externally bonded strips [Douglas, 2006]*

3.2.1.2 Sheets

Unidirectional prepreg sheets have demonstrated to be effective for the seismic retrofit of bridge columns. The lateral confinement strengthens the column to an extent that they comply with seismic design codes, providing adequate shear capacity, ductility and confinement in plastic hinges. By using unidirectional sheets, only hoop stresses are supported so that the bending stiffness of the column does not change. Conventional methods, which involve wrapping with steel sheets or cables, added stiffness which caused the seismic forces to be transmitted to adjacent elements. A beneficial side effect is the environmental protection of the column provided by the sheet [Teng, 2001].

3.2.2 Hybrid structures

In the context of this section, hybrid bridges are those composed of traditional materials (usually girders and columns) in combination with composite elements (decks, cables or tendons). As contractors are generally somewhat reluctant towards new materials due to the associated risks, hybrid structures provide a good opportunity to explore new grounds. The potential of composites is however not fully utilised.

3.2.2.1 Cables and tendons

As mentioned, the effectiveness of composites is maximised in the application of one-dimensional elements. Several types of tendons (for prestressing and cable-stayed bridges) and concrete reinforcement products are commercially fabricated. Their widespread acceptance in the construction industry is however retarded by a lack of initial economic incentive to use them.

Composite-reinforced concrete is mainly interesting to overcome corrosion problems in aggressive environments with combinations of moisture, temperature and chlorides. Practical examples are bridges in a marine environment, and buried concrete chambers. Another application is in structures supporting maglev trains and structures housing MRI equipment, as they do not respond to the flux due to their low electric conductivity [Transportation Research Board, 2006].

Prestressing tendons composed of carbon- and aramid fibres have been applied for nearly 30 years, both internally and externally. The performance of tendons is determined by strength, stiffness, creep and fatigue properties. Composites show superior performance to that of steel in both strength and fatigue, and stiffness is comparable. Creep however should be prevented by limiting the tendon stress to values no larger than 20% of the ultimate strength [Parke and Hewson, 2008].

3.2.2.2 Bridge decks

Bridge decks are generally the least durable part of bridges. Poor initial construction, the lack of proper maintenance and environmental conditions reduce the service life of bridge decks to an estimated average of ten to fifteen years. With the exclusion of painting, bridge deck repair and replacement can account for between 75 and 90 percent of the annual maintenance costs [Karbhari et al., 2001]. Next to using composites to replace deteriorated steel or concrete decks, they can also be applied to widen existing structures without significantly adding deadloads for piers and abutments.

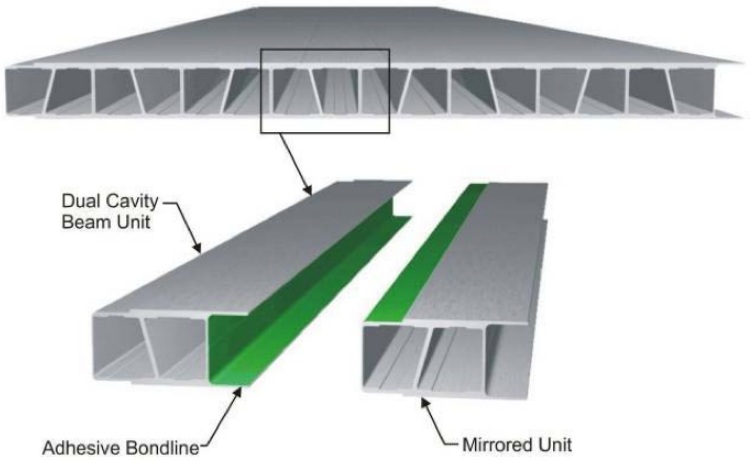

Figure 3.9: *Pultruded bridge deck panels [Transportation Research Board, 2006]*

Performance A composite bridge deck weighs roughly only 20% of a comparable concrete bridge deck, offering significant deadweight reduction of the global structure. Weight reductions compared to orthotropic steel decks are obviously more conservative, but still significant. This weight reduction can be utilised to partially cover for increased live loads, improving the material efficiency of the structure.

The efficiency can further be improved by utilising the composite action between the deck and the superstructure. By adhesively bonding the deck to the main girders, the deck can contribute to the load-carrying capacity of the top chords of the main girder. Mechanical fastening by means of shear studs is also possible, but less effective and more challenging due to localised introduction of stresses. Experiments have showed that full composite action can be achieved with adhesively-bonded joints. Ductile failure modes could be achieved by assuring the steel girders to yield prior to the brittle failure of the deck under compression [Gürtler, 2004].

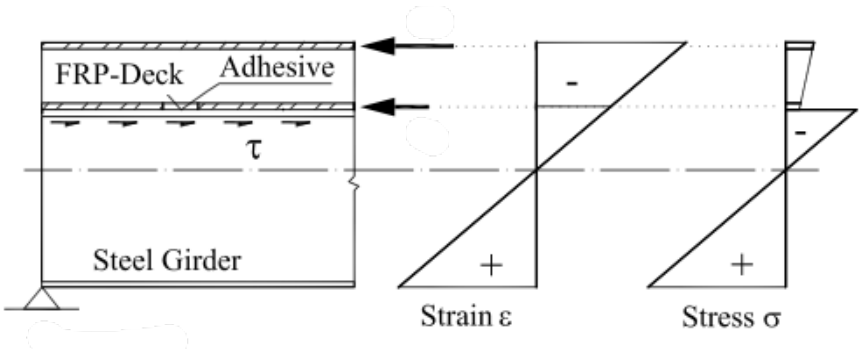

Figure 3.10: *Principle of composite action between girder and bridge deck [Gürtler, 2004]*

Durability There is few data available to quantify the long-term durability of composite bridge decks, as these systems have only been in service for about twenty years. Available studies were based on simulated laboratory testing in which time-dependent effects were accelerated. The results suggest a significant reduction of the deck's performance under long-term combination of mechanical and environmental loading, which should be taken into account in the initial design. Manufacturers claim an achievable service life of 75 years as a result of improved manufacturing methods, matrix additives and quality assurance [O'Connor and Hooks, 2006]. Studies however indicate to require further validation of data in order to propose a durability model [Wu and Yan, 2013].

Cost Although the initial investment of a composite deck system is roughly a factor five higher compared to conventional methods, the longer service life and elimination of need for maintenance make them economically competitive. Apart from financial consequences associated with maintenance and repair of bridge decks, there are the losses in productivity caused by delays and detours. The choice for quickly installable modular composite decks will reduce these side-effects. If it proves achievable to stretch the service life of composite bridge decks to 75 years, the total lifecycle cost over this period is estimated to be reduced by 80% [Karbhari et al., 2001].

3.2.2.3 Hybrid beams

Much like the seismic retrofitting as discussed in section 3.2.1.2, elements can be wrapped with composites from the initial construction. For beams however, a much more efficient design can be obtained by using the materials at the position where their advantages can be best utilised; concrete in the compressive zone and fibre composites in the tension zone.

Hybrid beams combine the durability and rapid installation of composites with the strength and stiffness of traditional materials, as fig. 3.11 illustrates. This hybrid beam design, by HC Bridge, consists of a concrete compression arch combined with tension reinforcement at the bottom of the cross-section. The low density foam acts as formwork for the shaping of the concrete, while the composite shell protects the beam from environmental loads. Shear connectors are provided to connect bridge deck elements [HCB Company, 2013].

(a) Concept (b) Easy installation (c) High capacity

Figure 3.11: *Hybrid composite beam [HCB Company, 2013]*

3.2.3 All-composite structures

In the context of this thesis, all-composite bridges are those of which the superstructure (beams and deck) is made exclusively of composite material. The abutment and piers are outside of this scope, and can thus be composed of traditional materials.

Two categories can be differentiated within all-composite structures; material substitution concepts and material-adapted concepts. The majority of today's new composite structures fall within the substitution category. The tendency is however to move away from linear components and adopt surface structures that are more suitable to fully utilise the potential of composites [Keller, 2003].

3.2.3.1 Material substitution

Most composite bridge concepts utilise the material as a replacement to and in the shape of traditional materials. The elements are to some extend standardised and the engineering methodology is analogue to that of steel or wood, which makes composites more accessible. The concepts are generally straightforward and do not require much additional specialist skills.

The design of traditional bridges is generally governed by strength limit states. When substituting elements with (fibreglass) composite equivalents in terms of strength, it is likely that deflection will become governing due to the low stiffness properties. A higher area moment of inertia is required in order to obtain the same bending stiffness. This can be achieved by either increasing the cross-sectional area or increasing the height of the structure. The first method results in more material, which strength is only being partially utilised. The latter method, using linear elements, can be achieved by creating trusses or frameworks, which results in an increase in number of joints.

An array of structural profiles and bridge decks is commercially available from numerous suppliers. Generally, manufacturers supply a design manual containing section properties, connection methods and material specific calculation methods. Three of the major manufacturers include Fiberline, Strongwell and Creative Pultrusions. The bridges that are produced following the substitution concept are limited to support pedestrian and lightweight vehicle traffic [Parke and Hewson, 2008].

Pultrusion production process Pultrusion is a continuous automated process to produce large quantities of identical parts, which translates into relatively low priced elements of consistent quality. Large initial investments are however required for the purchase of production machinery, which is why elements are generally ordered at large manufacturers instead of having own production lines.

Complex cross-sectional shapes and high fibre fractions can be achieved with the pultrusion process. Reinforcement is pulled through a resin bath and subsequently through a heated die. The die tapers into the final profile shape along its length, and the continuous profile emerges fully cured to be cut to length. A wide range of solid and hollow structures with constant cross-section can be produced that can be applied as bridge beams, deck panels, grating systems, handrails etc.

Pultrusion profiles can contain fibre fractions of up to 65 percent. These can however not be oriented with respect to the longitudinal axis, resulting in dominating mechanical properties in the axial direction. To obtain some degree of bidirectional properties woven fabrics or mats can be fed to the die to be integrated in laminate, but transverse properties remain limited [Mazumdar, 2002].

(a) Pontresina, Switzerland (b) Lleida, Spain (c) Kolding, Denmark

Figure 3.12: *Bridge structures from pultruded profiles - material substitution [Fiberline, 2013]*

3.2.3.2 Material-adapted

Material-adapted concepts are the result of form-finding processes, in which structural and non-structural considerations evolve to a more efficient use of material. Non-structural aspects for example include ease of manufacturing, assembly, maintenance and cost. As composite material is relatively expensive, composite-adapted concepts are generally aimed at minimising the use of high grade material in sections where it is not strictly required, for example by substitution of low grade material. Secondly, one aims at reducing the structure's complexity by minimising the number of joints. Hence the tendency to move away from linear elements and adapt surface elements and boxes [Dooley, 2004].

It is not a coincidence that one the first material-adapted bridge concepts (in 1994) resided from the aircraft manufacturer Lockheed-Martin, as the defence and aerospace industry had embraced fibre composites some 20 years before the bridge industry did. The bridge was composed of U-shaped hand-laminated GFRP girders connected to pultruded deck panels. The concept was further developed by integration of the deck, resulting in box girder bridges. As hand-lamination offers lower fibre fractions and less consistent quality, the development moved on toward using modular pultruded elements, sandwich panels and cocured sections.

(a) Lockheed Martin concept (1994) (b) Smith Road Bridge (1997)

Figure 3.13: *First material-adapted composite bridges [Keller, 2003]*

Modular pultruded elements Creating material-adapted structures while utilising the advantages of pultrusion can be done by assembling box-shaped sections from pultruded plate elements. One of the patented systems is ACCS[1] by Maunsell Structural Plastics (now part of AECOM). The manufacturing licence is in hands of Strongwell, which produce panels under the name COMPOSOLITE. The panels are combined to form the desired box shape by adhesively bonding the individual panels with cold-curing epoxy and application of mechanical toggles. The compressive flanges and webs of the multicell beams can be filled with foaming epoxy to provide the thin walls with support against local buckling. Two examples of movable bridges relying on this technique are the Bonds Mill bridge and the Chamberlain Bridge, as discussed in section 2.5.3 [Parke and Hewson, 2008].

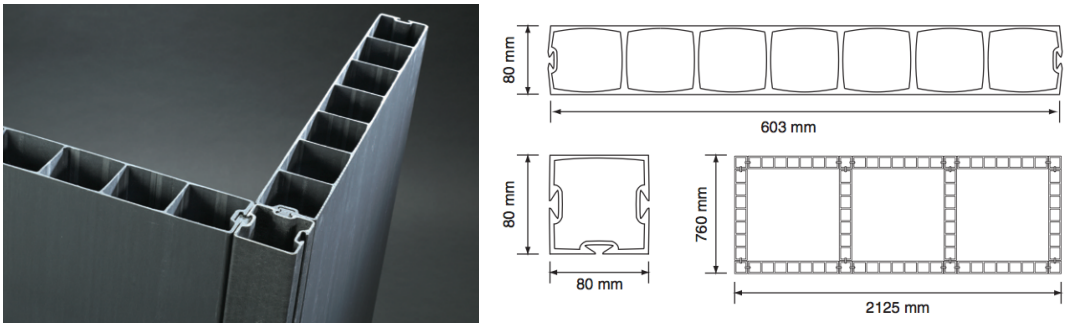

(a) Panel connection system (b) Assembled box-shaped section

Figure 3.14: *Modular pultruded panel system - COMPOSOLITE [Strongwell, 2013]*

[1]Advanced Composite Construction System

Sandwich elements Much like I-shaped beams, the concept of sandwich panels is that the facings (flanges) carry the bending loads in tension and compression, while the interior core carries the shear loads. Due to the low density of the core, one can achieve very stiff structures with only a minor increase of weight.

The face sheets sandwich elements are generally produced by a continuous laminating process. Fibre reinforcement is guided by a conveyor belt through a resin bath and subsequently a curing oven, after which the continuous laminate is cut to size. Honeycomb cores are made following the same procedure, but undergo a forming process resulting in corrugated sheets. The facings are fabricated separately from each other and from the core material. During the assembling of the sandwich panel, the facings are adhesively bonded to the core. The adhesive layer should be thick enough to provide a good bond over the entire surface, but not so thick that it becomes a point of failure.

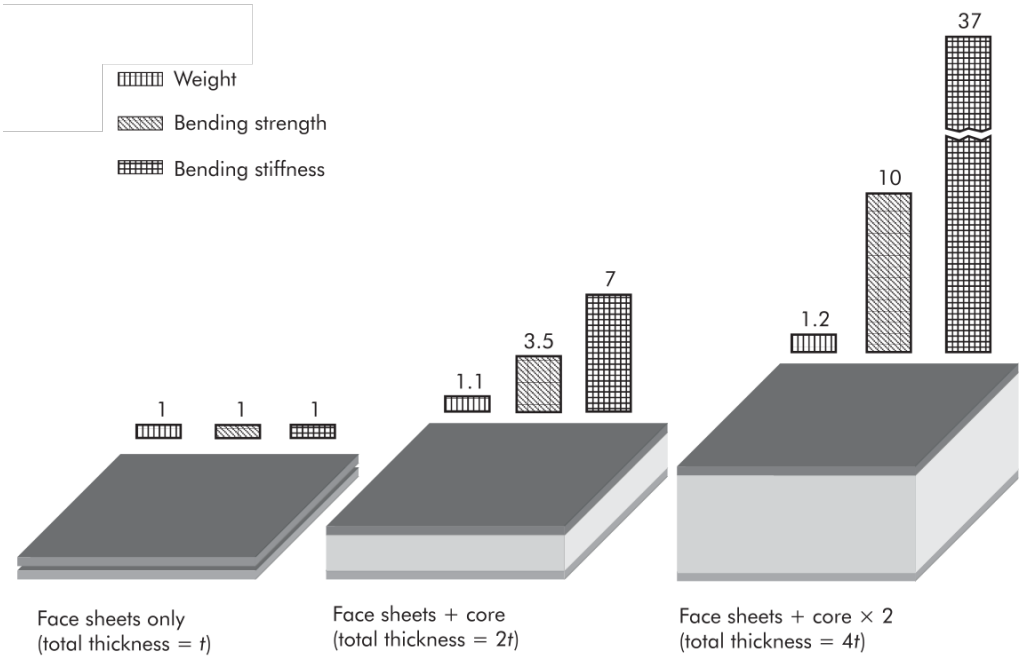

Figure 3.15: *Core thickness effect in sandwich elements [Strong, 2008]*

Unitised structures Cocuring is a method in which composite plies are cured while simultaneously being bonded to other composite parts or to core materials, creating unitised structures. The production method allows for more complex cross-sectional shapes and results in a unitised structure without resin-dominated joints. Unlike sandwich panels, unitised structures can have continuous fibres between the facings running through the webs. These continuous fibres increase the resistance to resin-dominated cracks at the stiffener toes. [Campbell, 2010].

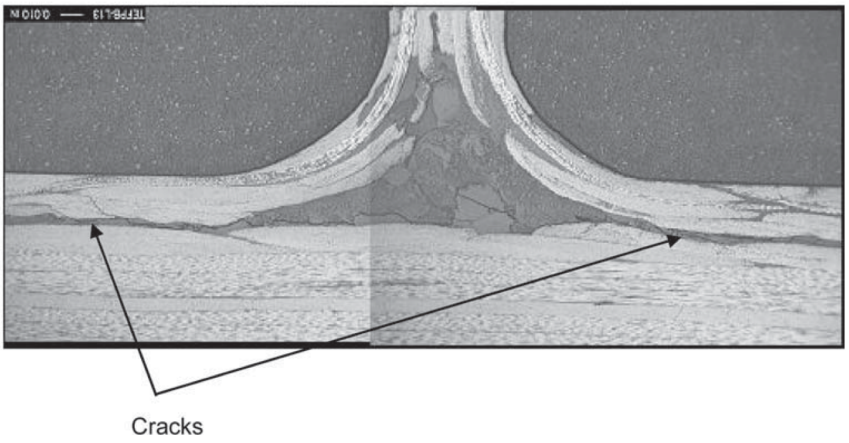

Figure 3.16: *Resin-dominated cracks at stiffener toe [Campbell, 2010]*

A production process patented by the Dutch company Fibercore comprises a series of parallel positioned core elements, which are wrapped in continuous woven fabrics. The reinforcement continuously runs from the element's horizontal face planes through the webs and the facings of adjacent core elements. The elements are positioned on a deformable mould plate. Subsequently the structure is sealed and resin is drawn into the reinforcement by a vacuum technique (VARTM[2]). Dependent of the equipment used, the web and flange thickness can be up to tens of centimetres, having fibre fractions of up to 70 percent. The core material generally does not fulfil a structural role in the final product, but is merely used as formwork in the production process. The foam should be able to resist the vacuum pressure during the impregnation process, and should furthermore be lightweight and cheap [Peeters, 2011].

By using continuous fibres between the face sheet and the webs, the element obtains a higher resistance against crack initiation as a result of localised loads and impacts. Initiated cracks are known to progress under the influence of passing traffic, which is why impact resistance is vital for the structure's durability.

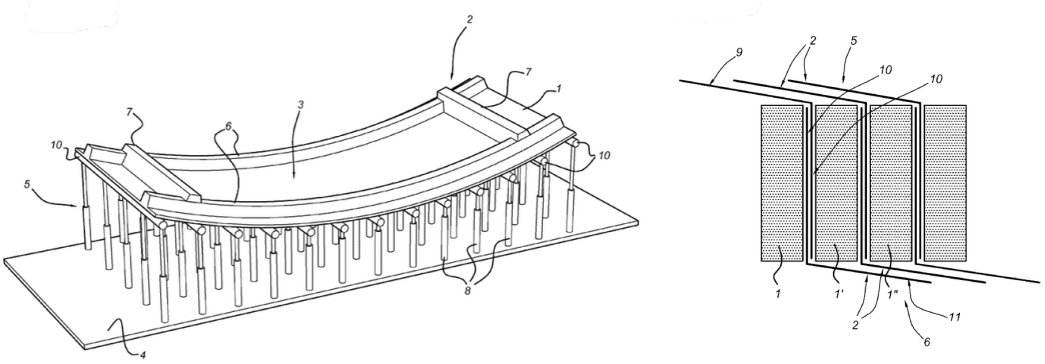

(a) Flexible mould system

(b) Continuous face-web fibres

Figure 3.17: *Fibercore technique for creating unitised structures [Peeters, 2011]*

[2]Vacuum Assisted Resin Transfer Moulding

3.3 Mechanical analysis

As composite materials inherently have a more complex structure than conventional materials, such as metals, the analysis and design of such materials is more complicated. As composites are composed of a matrix and fibres that are not equally oriented in all directions, the material is both inhomogeneous and anisotropic. This means that the material properties are, in contrast to metals, both dependent of location and orientation.

Composite structures are generally composed by stacking a number of laminae (plies) to from a laminate. As the laminae are the building blocks of the laminate, the first step in analysing the mechanical behaviour of a laminated structure is finding the average properties of the individual plies. This step involves using the properties of the constituents (matrix and reinforcement) to model the ply as being unidirectional and homogeneous. The second step is developing the stress-strain relationship of the individual plies. The third step is using the determined ply properties to assemble the stress-strain relationship of a laminate. The laminate failure theories are based on the stresses and strength properties in each ply of the laminate. This knowledge can eventually be used in the structural design of the composite structure. [Kaw, 2006]

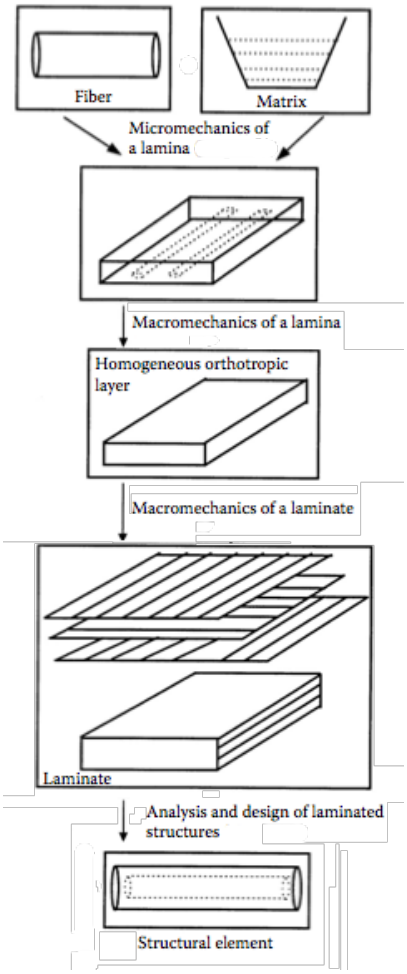

Figure 3.18: *Schematic of laminated element analysis [Kaw, 2006]*

3.3.1 Mechanics of lamina

A lamina is a thin layer of composite material, having a thickness of about 0.125 millimetres. The properties within the lamina vary from point to point, based on whether the point is in the fibre, the matrix, or at the fibre-matrix interface. Accounting for these variations would make any kind of mechanical analysis extremely complicated. To simplify the analysis, one can assume the lamina to be homogeneous by focusing on the average response of the lamina to applied loads. The lamina is modelled as a material whose properties are different in various directions (anisotropic), but not different from one location to another (homogeneous).

This section focuses on unidirectional continuous fibre-reinforced laminae, which are the basic building blocks of a composite structure. Such laminae behave in an orthogonal manner if the principal loading direction is aligned to the lamina fibre direction. The ply behaves anisotropically if the ply axis is not aligned to the loading axis, resulting in twisting and bending.

3.3.1.1 Coordinate systems

To simplify the notations, a local coordinate system is introduced which is aligned with the fibre direction of the ply. The direction of the 1-axis is parallel to the fibres, whereas direction of the 2-axis is perpendicular to the fibres. The global x-y coordinate system is generally aligned with the physical shape of the structural element. The global and local stresses in an angled lamina are related to each other through the angle θ in a transformation matrix $[T]$.

$$\begin{bmatrix} \sigma_1 \\ \sigma_2 \\ \tau_{12} \end{bmatrix} = \begin{bmatrix} \cos^2(\theta) & \sin^2(\theta) & 2{\cdot}\sin(\theta){\cdot}\cos(\theta) \\ \sin^2(\theta) & \cos^2(\theta) & -2{\cdot}\sin(\theta){\cdot}\cos(\theta) \\ -\sin(\theta){\cdot}\cos(\theta) & \sin(\theta){\cdot}\cos(\theta) & \cos^2(\theta){-}\sin^2(\theta) \end{bmatrix} \begin{bmatrix} \sigma_1 \\ \sigma_2 \\ \tau_{12} \end{bmatrix} \tag{3.1}$$

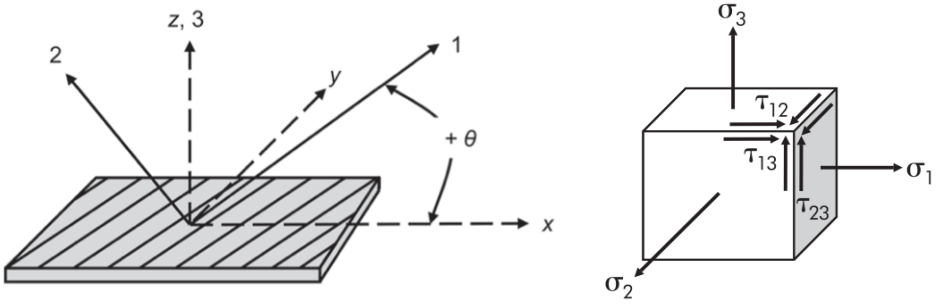

(a) Coordinate systems (b) Stress convention

Figure 3.19: *Sign conventions of stresses in the local and global coordinate systems [Strong, 2008]*

3.3.1.2 Stress-strain relation

The anisotropic form of Hooke's law for three-dimensional bodies relates applied stresses to strains through a square six-by-six symmetric stiffness matrix. Analysis would require 21 tests to be performed to provide the constants of proportionality. However, when a plane of symmetry is assumed through the thickness of the ply (in the 1-2 plane), the out-of-plane shear behaviour is decoupled from the in-plane behaviour. This assumption simplifies the stiffness matrix to have 14 independent constants. By only considering orthotropic laminae, having unidirectional or perpendicular arranged fibres, there are three orthogonal planes of symmetry. The shearing behaviour is fully decoupled from the normal stresses. This further simplifies the stiffness matrix to just nine independent constants. When considering only the in-plane behaviour of the ply, Hooke's law can be represented as:

$$\begin{bmatrix} \sigma_1 \\ \sigma_2 \\ \tau_{12} \end{bmatrix} = \begin{bmatrix} Q_{11} & Q_{12} & 0 \\ Q_{21} & Q_{22} & 0 \\ 0 & 0 & Q_{66} \end{bmatrix} \begin{bmatrix} \epsilon_1 \\ \epsilon_2 \\ \gamma_{12} \end{bmatrix} \tag{3.2}$$

In which:

σ_1	*stress in 1-direction*
σ_2	*stress in 2-direction*
τ_{12}	*in-plane shear stress*
ϵ_1	*strain in 1-direction*
ϵ_2	*strain in 2-direction*
γ_{12}	*in-plane shear strain*
Q_{11}	*ply axial modulus, which is equivalent to the axial Young's modulus*
Q_{22}	*ply transverse modulus, which is equivalent to transverse Young's modulus*
$Q_{12} = Q_{22}$	*Poisson's ratio effect of transverse strain to axial stress and vice versa*
Q_{66}	*ply shear modulus*

The stiffness matrix entries can be expressed in engineering constants:

$$\begin{aligned} Q_{11} &= \frac{E_1}{1-\nu_{12}\cdot\nu_{21}} \\ Q_{22} &= \frac{E_2}{1-\nu_{12}\cdot\nu_{21}} \\ Q_{12} = Q_{21} &= \frac{\nu_{12}\cdot E_2}{1-\nu_{12}\cdot\nu_{21}} \\ Q_{66} &= G_{12} \end{aligned} \tag{3.3}$$

In which:

E_1	*longitudinal Young's modulus (in 1-direction)*
E_2	*transverse Young's modulus (in 2-direction)*
ν_{12}	*major Poisson's ratio*
$\nu_{21} = \frac{E_2}{E_1}\cdot\nu_{12}$	*minor Poisson's ratio*
G_{12}	*in-plane shear modulus (in plane 1-2)*

For orthogonal laminae, the stresses and strains seem to be related through the above four independent engineering elastic constants. These constants can be quantified by tests in which the deformations of the lamina are measured at the application of stresses in the principal directions. Alternatively, one can use models to approximate the properties. Some two most common models are discussed; the rule of mixtures and the Halpin-Tsai model.

3.3.1.3 Rule of mixtures

The rule of mixtures is the most basic method to determine the engineering and physical properties of plies. The approach is based on the knowledge of the properties and proportions of the composite's constituents. The following assumptions are made in the rule of mixtures model [Kaw, 2006]:

- The bond between fibres and matrix is perfect
- The elastic moduli, diameters and space between fibres are uniform
- The fibres are continuous and parallel
- The fibres and matrix follow Hooke's law (linearly elastic)
- The fibres possess uniform strength
- The composite is free of voids

Due to the absence of voids in the model, the volume consists entirely of fibre and matrix material. This can be described as:

$$V_f + V_m = 1 \tag{3.4}$$

In which:

V_f *fibre-volume ratio, which is the physical volume of the fibres to the total ply volume*
V_m *matrix-volume ratio*

Longitudinal Young's modulus The longitudinal Young's modulus as a weighed mean of the fibre and matrix modulus can be described by:

$$E_1 = E_f \cdot V_f + E_m \cdot V_m \tag{3.5}$$

In which:

E_1 *longitudinal Young's modulus*
E_f *modulus of fibres*
E_m *modulus of matrix*

Transverse Young's modulus The transverse Young's modulus can be described by:

$$\frac{1}{E_2} = \frac{V_f}{E_f} + \frac{V_m}{E_m} \tag{3.6}$$

Major Poisson's ratio The major Poisson's ratio is defined as the negative of the ratio of the normal strain in the transverse (2-axis) direction to the normal strain in the longitudinal (1-axis) direction, when a normal load is applied in the longitudinal direction. As a weighed mean of the fibre and matrix modulus can be described by:

$$\nu_{12} = \nu_f \cdot V_f + \nu_m \cdot V_m \tag{3.7}$$

In which:

ν_{12} *major Poisson's ratio*

ν_f *Poisson's ratio of fibres*

ν_m *Poisson's ratio of matrix*

In-plane shear modulus The in-plane shear modulus as a weighed mean of the fibre and matrix modulus can be described by:

$$\frac{1}{G_{12}} = \frac{V_f}{G_f} + \frac{V_m}{G_m} \tag{3.8}$$

In which:

$$G_f = \frac{E_f}{2 \cdot (1+\nu_f)} \qquad \textit{shear modulus of fibres}$$

$$G_m = \frac{E_m}{2 \cdot (1+\nu_m)} \qquad \textit{shear modulus of matrix}$$

Verification Experimental results have shown that the rule of mixtures is an accurate model in predicting the longitudinal modulus and the major Poisson's ratio. The transverse modulus and in-plane shear modulus however do not agree that well with experimental results, as shown in the figure below. The model is too conservative in predicting the latter material properties.

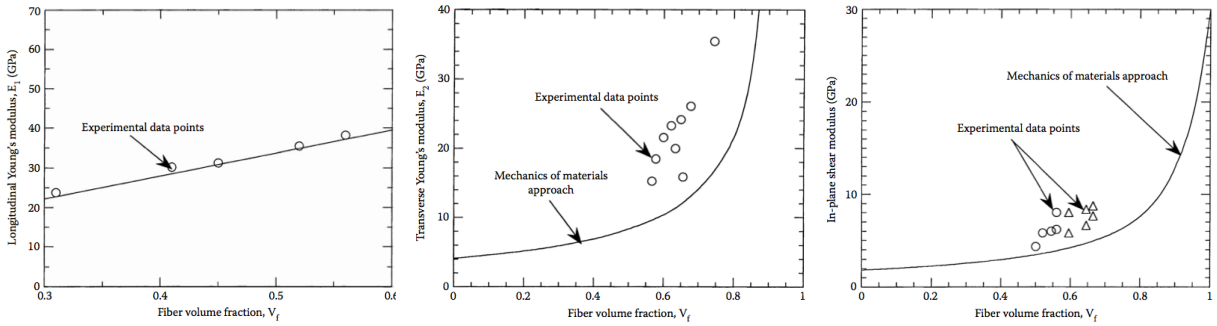

(a) Longitudinal Young's modulus (b) Transverse Young's modulus (c) In-plane shear modulus

Figure 3.20: *Comparison between rule of mixture model and experimental results [Kaw, 2006]*

3.3.1.4 Halpin-Tsai model

Several researchers have suggested improved models to more realistically predict the transverse modulus and in-plane shear modulus of laminas. Among the most well-known models is the semi-empirical approach of Halpin and Tsai, which can be used over a wide range of composites. The model is semi-empirical in nature, as the parameters in the curve-fitting equations have a physical meaning.

Transverse Young's modulus The Halpin-Tsai equation for the transverse Young's modulus is given by:

$$\frac{E_2}{E_m} = \frac{1+\xi\cdot\eta\cdot V_f}{1-\eta\cdot V_f} \tag{3.9}$$

In which:

$$\eta = \frac{\frac{E_f}{E_m}-1}{\frac{E_f}{E_m}+\xi} \tag{3.10}$$

The ξ-parameter is the so-called reinforcement factor, and depends on the geometry of the fibres, are geometric distribution of fibres within the matrix and the loading conditions. For the quantification of the reinforcement factors for different configurations is referred to [Halpin and Kardos, 1976].

In-plane shear modulus The Halpin-Tsai equation for the in-plane shear modulus is given by:

$$\frac{G_{12}}{G_m} = \frac{1+\xi\cdot\eta\cdot V_f}{1-\eta\cdot V_f} \tag{3.11}$$

In which:

$$\eta = \frac{\frac{G_f}{G_m}-1}{\frac{G_f}{G_m}+\xi} \tag{3.12}$$

Again, the reinforcement parameter depends on the material geometry and loading condition as specified in [Halpin and Kardos, 1976].

Verification As the Halpin-Tsai method is based on curve-fitting of actual experimental results, it predicts the material properties more accurately than the rule of mixtures.

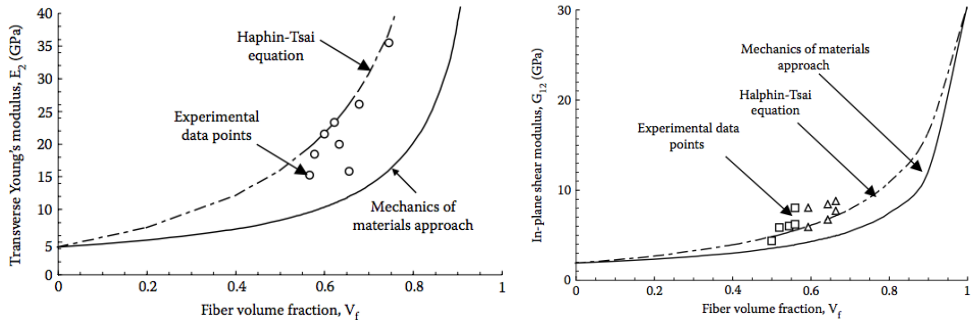

(a) Transverse Young's modulus (b) In-plane shear modulus

Figure 3.21: *Comparison between rule of mixture, Halphin-Tsai and experimental results [Kaw, 2006]*

3.3.2 Mechanics of laminate

Layers of plies are stacked to form a laminate. Dependent of the given loading and stiffness requirement of the structure, one can optimise the laminate by applying plies with various fibre material and angles. The mechanical properties of the final laminate can be assembles from the properties of the individual plies. The stress-strain relationship of the laminate is described by the classical laminate theory.

3.3.2.1 Classical laminate theory

The following assumptions are made to develop the relations of the classical laminate theory:

- Each lamina is orthotropic
- Each lamina is homogeneous
- Each lamina is elastic
- No slip occurs between the lamina interfaces
- A line straight and perpendicular to the middle surface remains straight and perpendicular to the middle surface during deformation ($\gamma_{xz} = \gamma_{yz} = 0$)
- The laminate is thin and is loaded only in its plane ($\sigma_z = \tau_{xz} = \tau_{yz} = 0$)
- Displacements are continuous and small throughout the laminate ($|w| << |h|$)

Kinematic relations According to the above assumptions, the strain at any point in the structure varies linearly along the thickness of the laminate. The strain can be expressed by a midplane strain component, plus an additional strain from the plate's curvature multiplied by the distance from the midplane (z).

$$\begin{Bmatrix} \epsilon_x \\ \epsilon_y \\ \gamma_{xy} \end{Bmatrix} = \begin{Bmatrix} \epsilon_x^0 \\ \epsilon_y^0 \\ \gamma_{xy}^0 \end{Bmatrix} + z \begin{Bmatrix} \kappa_x \\ \kappa_y \\ \kappa_{xy} \end{Bmatrix} \tag{3.13}$$

Constitutive relations If the strains are known at any point along the laminate, the stress-strain relation (eq. (3.3)) gives the global stresses in the plies. The reduced stiffness matrix corresponds to the ply located at the point along the thickness of the laminate [1].

$$\begin{bmatrix} \sigma_x \\ \sigma_y \\ \tau_{xy} \end{bmatrix} = \begin{bmatrix} \overline{Q_{11}} & \overline{Q_{12}} & \overline{Q_{16}} \\ \overline{Q_{21}} & \overline{Q_{22}} & \overline{Q_{26}} \\ \overline{Q_{16}} & \overline{Q_{26}} & \overline{Q_{66}} \end{bmatrix} \begin{bmatrix} \epsilon_x^0 \\ \epsilon_y^0 \\ \gamma_{xy}^0 \end{bmatrix} + z \begin{bmatrix} \overline{Q_{11}} & \overline{Q_{12}} & \overline{Q_{16}} \\ \overline{Q_{21}} & \overline{Q_{22}} & \overline{Q_{26}} \\ \overline{Q_{16}} & \overline{Q_{26}} & \overline{Q_{66}} \end{bmatrix} \begin{bmatrix} \kappa_x \\ \kappa_y \\ \kappa_{xy} \end{bmatrix} \tag{3.14}$$

[1] The overlining of the Q-elements indicates that the local stiffness matrix of the ply is rotated in the global element system

From the constitutive relations, the stresses vary linearly through the thickness of each of the plies. Jumps may however occur in the interface between two plies, as the reduced-stiffness matrix depends on the material and orientation.

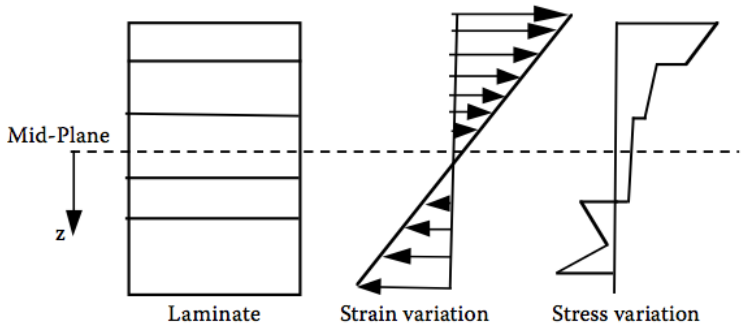

Figure 3.22: *Stress and strain variation through the thickness of the laminate [Kaw, 2006]*

Equilibrium relations The relation between the applied loads and the midplane strains and curvatures is derived by considering a laminate with n plies of thickness t_k, as depicted in fig. 3.23. Integration of the global stresses in each ply gives the resultant forces per unit length in the x-y plane through the laminate thickness as:

$$N_x = \int_{-h/2}^{h/2} \sigma_x \cdot dz \tag{3.15a}$$

$$N_y = \int_{-h/2}^{h/2} \sigma_y \cdot dz \tag{3.15b}$$

$$N_{xy} = \int_{-h/2}^{h/2} \tau_{xy} \cdot dz \tag{3.15c}$$

Similarly, integrating the global stresses the stresses gives the resultant moments per unit length in the x-y plane through the laminate thickness as:

$$M_x = \int_{-h/2}^{h/2} \sigma_x \cdot z \cdot dz \tag{3.16a}$$

$$M_y = \int_{-h/2}^{h/2} \sigma_y \cdot z \cdot dz \tag{3.16b}$$

$$M_{xy} = \int_{-h/2}^{h/2} \tau_{xy} \cdot z \cdot dz \tag{3.16c}$$

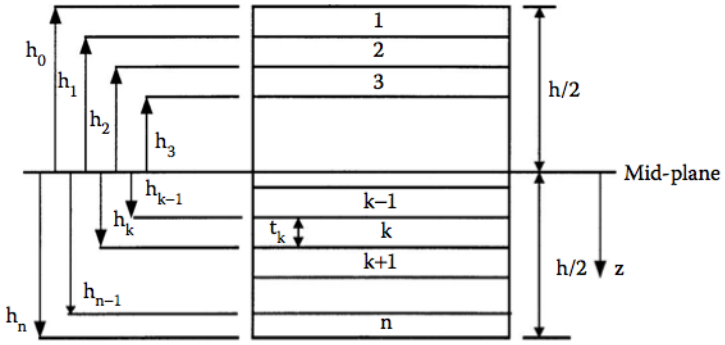

Figure 3.23: *Laminate composed of n plies [Kaw, 2006]*

By substitution of the equilibrium equations into eq. (3.14), one obtains six simultaneous linear equations and six unknowns than can be expressed in a so-called ABD-matrix:

$$\begin{bmatrix} N_x \\ N_y \\ N_{xy} \\ M_x \\ M_y \\ M_{xy} \end{bmatrix} = \begin{bmatrix} A_{11} & A_{12} & A_{16} & B_{11} & B_{12} & B_{16} \\ A_{12} & A_{22} & A_{26} & B_{12} & B_{22} & B_{26} \\ A_{16} & A_{26} & A_{66} & B_{16} & B_{26} & B_{66} \\ B_{11} & B_{12} & B_{16} & D_{11} & D_{12} & D_{16} \\ B_{12} & B_{22} & B_{26} & D_{12} & D_{22} & D_{26} \\ B_{16} & B_{26} & B_{66} & D_{16} & D_{26} & D_{66} \end{bmatrix} \begin{bmatrix} \epsilon_x^0 \\ \epsilon_y^0 \\ \gamma_{xy}^0 \\ \kappa_x \\ \kappa_y \\ \kappa_{xy} \end{bmatrix} \tag{3.17}$$

In which:

$$A_{ij} = \sum_{k=1}^{n} [(\overline{Q_{ij}})]_k \cdot (h_k - h_{k-1}) \qquad i = 1,2,6; \quad j = 1,2,6 \tag{3.18a}$$

$$B_{ij} = \frac{1}{2} \sum_{k=1}^{n} [(\overline{Q_{ij}})]_k \cdot (h_k^2 - h_{k-1}^2) \qquad i = 1,2,6; \quad j = 1,2,6 \tag{3.18b}$$

$$D_{ij} = \frac{1}{3} \sum_{k=1}^{n} [(\overline{Q_{ij}})]_k \cdot (h_k^3 - h_{k-1}^3) \qquad i = 1,2,6; \quad j = 1,2,6 \tag{3.18c}$$

The ABD-matrix is constructed of three matrices that relate the external to the internal forces. The extensional stiffness matrix $[A]$ relates the in-plane forces to the in-plane strains. The bending stiffness matrix $[D]$ relates the resultant bending moments to the plate curvatures. The coupling stiffness matrix $[B]$ couples the force and moment terms to the midplane strains and midplane curvatures.

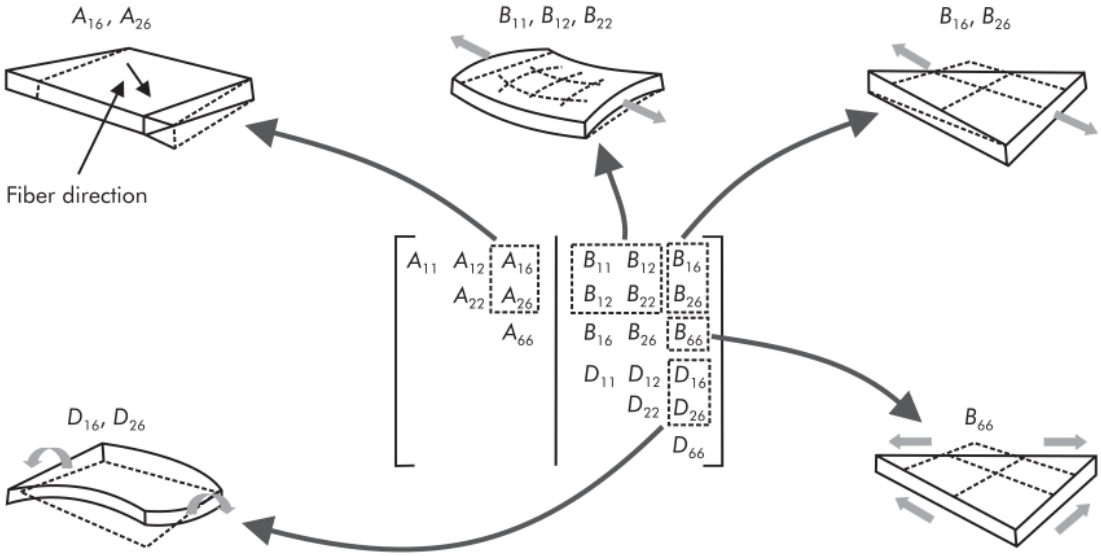

Figure 3.24: *Stiffness coupling phenomenon [Strong, 2008]*

3.3.2.2 Special laminates

By particular stacking of plies, one can obtain laminates that exhibit special structural behaviour. Based on the angle, material and thickness of the plies in a laminate, the symmetry or antisymmetry of a laminate may zero out some elements of the ABD-matrix. Special laminates simplify the mechanical analysis and may give desired mechanical performance for certain applications.

Symmetric laminates A laminate is symmetric if the material, angle and thickness of plies are mirrored about the structural midplane. Symmetric laminates do not possess coupling between in-plane (extorsional) and flexural behaviour, which results in a zero coupling matrix $[B] = 0$. Thus, eq. (3.17) can be decoupled to give:

$$\begin{bmatrix} N_x \\ N_y \\ N_{xy} \end{bmatrix} = \begin{bmatrix} A_{11} & A_{12} & A_{16} \\ A_{12} & A_{22} & A_{26} \\ A_{16} & A_{26} & A_{66} \end{bmatrix} \begin{bmatrix} \epsilon_x^0 \\ \epsilon_y^0 \\ \gamma_{xy}^0 \end{bmatrix} \tag{3.19}$$

and

$$\begin{bmatrix} M_x \\ M_y \\ M_{xy} \end{bmatrix} = \begin{bmatrix} D_{11} & D_{12} & D_{16} \\ D_{12} & D_{22} & D_{26} \\ D_{16} & D_{26} & D_{66} \end{bmatrix} \begin{bmatrix} \kappa_x \\ \kappa_y \\ \kappa_{xy} \end{bmatrix} \tag{3.20}$$

As the force and moment terms are uncoupled, a symmetric laminate subjected only to forces will have zero midplane curvature. Similarly, if it is subjected only to moments, it will have zero midplane strains. This behaviour is utilised in structures that are subject to thermal loading, as symmetric laminates will not twist as a result of temperature fluctuations.

Cross-ply laminates A cross-ply laminate consists only of 0 and 90° plies, having fibres parallel or perpendicular to the element axis. In such laminates, no coupling exists between normal and shear forces, as well as between bending and twisting moments. This results in the following ABD matrix:

$$\begin{bmatrix} N_x \\ N_y \\ N_{xy} \\ M_x \\ M_y \\ M_{xy} \end{bmatrix} = \begin{bmatrix} A_{11} & A_{12} & 0 & B_{11} & B_{12} & 0 \\ A_{12} & A_{22} & 0 & B_{12} & B_{22} & 0 \\ 0 & 0 & A_{66} & 0 & 0 & B_{66} \\ B_{11} & B_{12} & 0 & D_{11} & D_{12} & 0 \\ B_{12} & B_{22} & 0 & D_{12} & D_{22} & 0 \\ 0 & 0 & B_{66} & 0 & 0 & D_{66} \end{bmatrix} \begin{bmatrix} \epsilon_x^0 \\ \epsilon_y^0 \\ \gamma_{xy}^0 \\ \kappa_x \\ \kappa_y \\ \kappa_{xy} \end{bmatrix} \tag{3.21}$$

Angle-ply laminates An angle-ply laminate consists plies of the same thickness and material, and only oriented in the $+\theta$ and $-\theta$ directions. If such a laminate has and odd number of alternating $+\theta$ and $-\theta$ plies, then the laminate is symmetric. Furthermore, it the number of layers increases for the same laminate thickness, the A_{16}, A_{26}, D_{16} and D_{26} terms become small so that the behaviour is similar to a symmetric cross-ply laminate. However, these angle-ply laminates have higher higher shear stiffness and shear strength properties.

Antisymmetric laminates An antisymmetric laminate is a symmetric laminate in which the ply orientations at either side of the midplane are negative to each other. This lay-up results in a laminate that has in-plane balance and flexural balance; $A_{16} = A_{26} = 0$ and $D_{16} = D_{26} = 0$

Quasi-isotropic laminates A laminate is called quasi-isotropic if its extensional behaviour is independent of the angle of rotation of the laminate. In this case the extensional stiffness matrix $[A]$ is similar to that of an isotropic material, having $A_{11} = A_{22} = 0$, $A_{16} = A_{26} = 0$ and $A_{66} = \frac{A_{11} - A_{12}}{2}$. The $[B]$ and $[D]$ stiffness matrices may not be similar to isotropic materials. If the lay-up is also symmetric, the material behaves more isotropically, having no extensional and flexural coupling ($[B] = 0$). The use of quasi-isotropic laminate lowers the bar for engineers to adapt composites, however it is not generally the most optimal lay-up [Kaw, 2006].

3.3.3 Failure theories

Failure modes in composites are generally not catastrophic and may involve localised damage, such as fibre breakage, matrix cracking, debonding and fibre pull-out. These mechanisms can progress simultaneously and interactively, making failure prediction for composites complex.

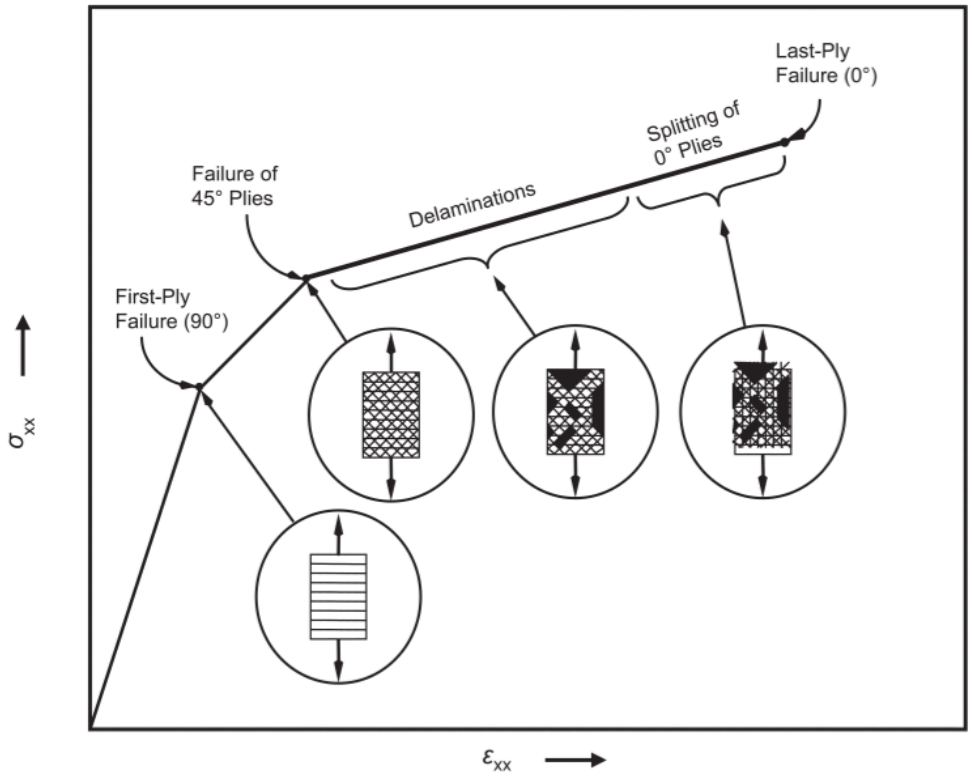

Figure 3.25: *Progressive ply failure [Campbell, 2010]*

Laminates fail in a progressive manner; not all plies fail simultaneously. Plies will fail successively in increasing order of strength in the loading direction, dependent of material properties and orientation. Generally, the plies with fibre directions transverse to the principle loading direction fail first, followed by the other off-angle plies. The failed plies start to debond from the remaining plies, a phenomenon called delamination. Finally, the strongest plies in the loading direction fail, resulting in catastrophic failure of the laminate. Although a laminate may have residual strength and stiffness properties after the initiation of failure, the typical design criterion is conservative; at the occurrence of first ply failure.

3.3.3.1 Strength parameters

In case of a unidirectional ply, there are two principle axes; one parallel and one perpendicular to the fibres. The material has a tensile and compressive strength in each of the two material axes. A fifth strength parameter is the shear strength of the unidirectional lamina.

$\sigma^T_{1,u}$ *ultimate longitudinal tensile strength (1-direction)*

$\sigma^C_{1,u}$ *ultimate longitudinal compressive strength (1-direction)*

$\sigma^T_{2,u}$ *ultimate transverse tensile strength (2-direction)*

$\sigma^C_{2,u}$ *ultimate transverse compressive strength (2-direction)*

$\tau_{12,u}$ *ultimate in-plane shear strength (12-plane)*

Unlike the stiffness parameters, the strength parameters cannot be transformed directly for angled plies. Failure theories have been developed to predict the capacity of the individual plies. Four common theories are discussed.

3.3.3.2 Maximum stress failure theory

The maximum stress theory is similar to those applied to isotropic materials. The stresses acting on a ply are resolved into the local axis. Failure is assumed to occur if any of the normal or shear stresses is equal to or exceeds the corresponding ultimate strength parameters. To avoid failure, the working stresses should fulfil:

$$\begin{aligned} -\sigma_{1,u}^{C} < \sigma_1 < \sigma_{1,u}^{T} \\ -\sigma_{2,u}^{C} < \sigma_2 < \sigma_{2,u}^{T} \\ -\tau_{12,u} < \tau_{12} < \tau_{12,u} \end{aligned} \tag{3.22}$$

3.3.3.3 Maximum strain failure theory

The maximum strain theory is similar to the maximum stress theory, except that strains are used instead of stresses. Failure is assumed to occur if any strain in the principal material axes is equal to or exceeds the corresponding ultimate strain parameters. To avoid failure, the strains should fulfil:

$$\begin{aligned} -\epsilon_{1,u}^{C} < \epsilon_1 < \epsilon_{1,u}^{T} \\ -\epsilon_{2,u}^{C} < \epsilon_2 < \epsilon_{2,u}^{T} \\ -\gamma_{12,u} < \gamma_{12} < \gamma_{12,u} \end{aligned} \tag{3.23}$$

The ultimate strains can be found directly from the ultimate strength parameters and the elastic moduli, assuming linear-elastic until failure.

3.3.3.4 Tsai-Hill failure theory

The Tsai-Hill theory considers the distortion energy in the material. It is assumed that failure takes place if the distortion energy is greater than the failure distortion energy of the material, which relates to the strength parameters. To avoid failure, the following equation should not be violated:

$$\left(\frac{\sigma_1}{\sigma_{1,u}^{T}}\right)^2 - \left(\frac{\sigma_1 \cdot \sigma_2}{{\sigma_{1,u}^{T}}^2}\right) + \left(\frac{\sigma_2}{\sigma_{2,u}^{T}}\right)^2 + \left(\frac{\tau_{12}}{\tau_{12,u}}\right)^2 < 1 \tag{3.24}$$

The Tsai-Hill theory gives a better fit to experimental data, as it accounts for the interaction between strengths and failure modes.

3.3.3.5 Tsai-Wu failure theory

The Tsai-Wu failure theory is more general than the Tsai-Hill theory, as it distinguishes between the compressive and tensile strengths of the plies. To avoid failure, the following equation should not be violated:

$$H_1 \cdot \sigma_1 + H_2 \cdot \sigma_2 + H_6 \cdot \tau_{12} + H_{11} \cdot \sigma_1^2 + H_{22} \cdot \sigma_2^2 + H_{66} \cdot \tau_{12}^2 + 2 \cdot H_{12} \cdot \sigma_1 \cdot \sigma_2 < 1 \tag{3.25}$$

Where the Tsai-Hill theory only requires the five strength parameters from section section 3.3.3.1, the Tsai-Wu criterion requires an additional biaxial tensile test to obtain the H_{12} parameter. The determination of the H-components can be found in literature; for example [Kaw, 2006, section 2.8.6].

3.3.3.6 Comparison

Both the Tsai-Hill and Tsai-Wu failure theories are in good agreement with experimental results. The maximum stress and strain theories are more conservative, especially at the laminate angles around the point where the failure mode changes. This is reflected in the cups that appear in the maximum normal tensile stress plots as in fig. 3.26. The Tsai-Hill and Tsai-Wu theories both result in smooth function, which closer resembles experimental results.

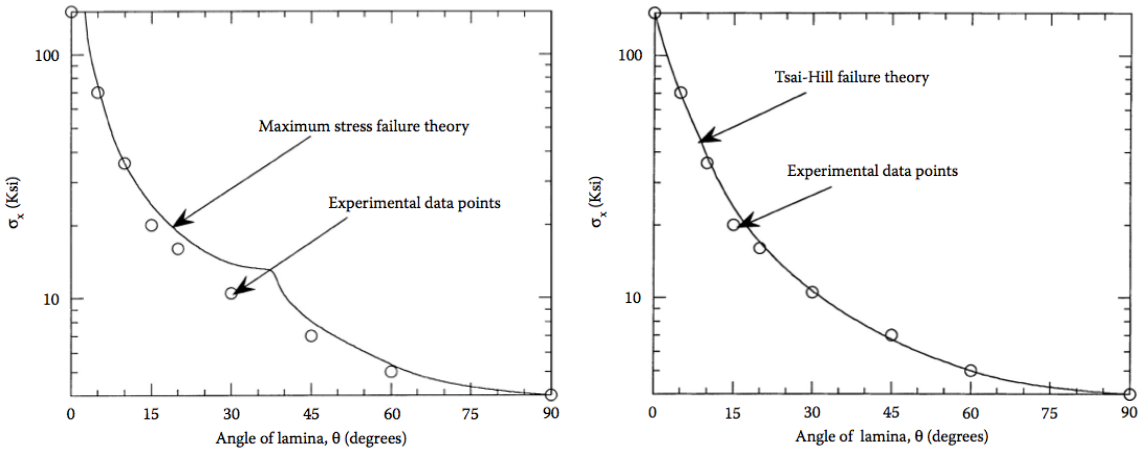

(a) Maximum stress theory

(b) Tsai-Hill theory

Figure 3.26: *Comparison between failure theories and experimental results [Kaw, 2006]*

3.3.3.7 Reserve factor

The failure theories can be used to determine whether a lamina has failed, by checking if any of the inequalities is violated. By comparing the applied loads to the maximum failure load, the reserve factor of each of the plies can be determined:

$$RF = \frac{\text{Failure load}}{\text{Applied load}} \tag{3.26}$$

A reserve factor above unity indicates that the lamina is safe, and the applied stress can be increased by a factor equal to RF. Similarly, a reserve factor below unity indicates that a lamina is unsafe, and the applied stress needs to be reduced by a factor equal to RF.

3.3.4 Laminate analysis procedure

The following steps summarise the procedure to analyse laminated composites, as treated in the previous sections:

1. For each ply, find the values of the reduced stiffness matrix $[Q]$ from the material's four elastic moduli; E_1, E_2, ν_{12} and G_{12}
2. For each ply, find the values of the transformed reduced stiffness matrix $[\overline{Q}]$ by multiplication with the transformation matrix $[T]$ to obtain the stiffness properties in the global axis system of the element
3. For each ply, find the coordinates of the top and bottom surface with respect to the midplane of the laminate
4. Use the reduced stiffness matrices and coordinates from step 2 and 4 to assemble the three stiffness matrices $[A]$ $[B]$ and $[D]$
5. Substitute the stiffness matrices and applied forces and moments in eq. (3.17), and solve the six simultaneous linear equations to find the midplane strains and curvatures
6. For each ply, use the coordinates from step 3 to find the global strains in top and bottom surface
7. For each ply, find the global stresses from the global strains
8. For each ply, find the local stresses and local strains by multiplication with the transformation matrix $[T]$
9. For each ply, use the local stresses and strains to find the reserve factor. Multiplication of the reserve factor with the applied load gives the load level of the first ply failure
10. For each failed ply, fully degrade the stiffness. Assemble a new ABD-matrix for the damaged laminate and find the strength ratio in the undamaged plies
11. Repeat previous step until all plies in the laminate have failed. The load level at catastrophic failure is called the last ply failure

There is a number of software packages available to automate the analysis process, as discussed in section 4.5. Such packages produce the strength and stiffness properties of laminates and individual plies after entering the elastic moduli, thickness and orientation of the individual plies in the composite layup. These properties can subsequently be used as input for finite element analysis of the composite structure.

3.3.5 Sandwich composites

As discussed, laminates are not particularly suitable for out-of-plane loading. As there are no fibres in this direction, these strength and stiffness properties are of the same order as those of the polymer matrix; low. The same holds for the face sheets of composite sandwich panels, which are basically unidirectional laminates. The structure of sandwiches is however such that the dominant loading of the face sheets is in the plane, resulting in membrane forces. The strong face sheets are at the structure's surface, where the flexure stresses are high. The core, which is in the low stress region, carries the transverse shear loads and acts as a spacer for the face sheets. The core also contributes to the energy absorption and impact resistance of the panel.

Structural analysis of sandwich panels is relatively complex, especially when the face sheets are of composite material. The analysis can be simplified by considering only symmetric sandwich panels having identical thin face laminates. Because the faces are thin compared to the core, it is assumed that local flexural rigidity of the faces is negligible. This means that there are no stresses in the out-of-plane direction, and that normal stress is constant throughout the faces. The core is assumed to be considerably less stiff than the faces, and does not contribute significantly to the bending rigidity. The core shear stresses are assumed to be constant throughout the depth of the core. Furthermore, the deflections are assumed to be small. There is no strain in the midplane of the panel from transverse displacements. The effects of shear deflection in the core are considerable, thus the ordinary beam theory must be extended to account for the effects of shear deformation in the core.

3.3.5.1 Flexural stiffness

The flexural stiffness (D) of the sandwich panel is the sum of the flexural rigidities of the different parts, with respect to the centroidal axis of the section. The first term in the equation accounts for the local flexural rigidity of the faces about the own centroidal axis. The second term is the Steiner contribution of the faces. The last term is the flexural rigidity of the core, which centroidal axis coincides with that of the entire section.

$$D_\kappa = E_f \cdot \frac{b \cdot t^3}{6} + E_f \cdot \frac{b \cdot t \cdot d^2}{2} + E_c \cdot \frac{b \cdot c^3}{12} \tag{3.27}$$

In which:

D_κ	*flexural stiffness of the panel*
E_f	*Young's modulus of the face sheets (in loading direction)*
E_c	*Young's modulus of the core*
t	*face thickness*
d	*distance between centroidal axis of face sheets*
c	*core thickness*
b	*element width*

If the considered panel has thin faces ($d/t > 5.77$), the first term can be neglected, as it accounts for less than 1% to the flexural rigidity. Similarly, the third term accounts for less than 1% (and may consequently be ignored) when:

$$\frac{E_f}{E_c} \cdot \frac{t \cdot d^2}{c^3} > 16.7 \tag{3.28}$$

3.3.5.2 Shear stiffness

It is assumed that the face layers do not contribute to the shear stiffness of the section. The shear stiffness D_γ is determined by:

$$D_\gamma = G_c \cdot b \cdot c \tag{3.29}$$

In which:

D_γ *shear stiffness of panel*

G_c *shear modulus of core material*

3.3.5.3 Deflections

The displacement of any symmetrically loaded sandwich beam with a thin faces and a weak core is found by superimposing the bending and shear deflections. Two examples are given below.

The deflection at midspan for a simply supported beam loaded by a point load F:

$$\delta = \frac{1}{48}\frac{F \cdot L^3}{D_\kappa} + \frac{1}{4}\frac{F \cdot L}{D_\gamma} \tag{3.30}$$

The deflection at midspan for a simply supported beam loaded by a uniformly distributed load q:

$$\delta = \frac{5}{384}\frac{q \cdot L^4}{D_\kappa} + \frac{1}{8}\frac{q \cdot L^2}{D_\gamma} \tag{3.31}$$

3.3.5.4 Stresses

It is assumed that sections remain plane and perpendicular to the centroidal axis. The flexural stresses in the faces and cores per unit width are respectively:

$$\sigma_f = \frac{M \cdot z}{D_\kappa} \cdot E_f \tag{3.32a}$$

$$\sigma_c = \frac{M \cdot z}{D_\kappa} \cdot E_c \tag{3.32b}$$

Stresses from normal forces per unit width:

$$\sigma_f = \frac{N}{2 \cdot t} \tag{3.33}$$

The shear stress is assumed to be constant over the thickness of the core, as it is too weak to provide a significant contribution to the flexural rigidity of the sandwich. The constant shear stress in the core for thin faces is given by:

$$\tau = \frac{Q}{b \cdot d} \tag{3.34}$$

3.3.5.5 Failure modes

Sandwich panels can fail in several modes. Next to failure of the face layers in tension or compression, and core failure in shear, sandwich panels may fail locally. In determining the panel's ultimate strength, it may be necessary to check more than one failure mode to determine the governing one.

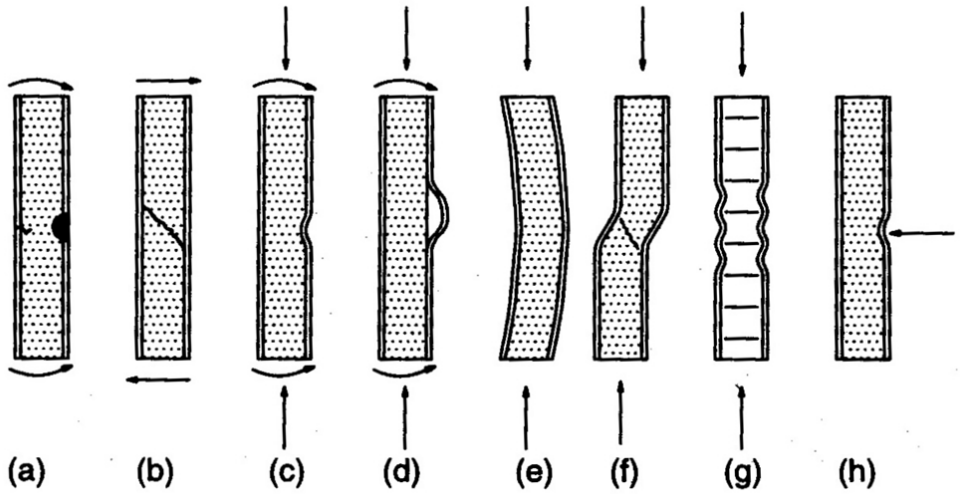

Figure 3.27: *Failure modes in sandwich elements: (a) face fracture, (b) core shear failure, (c-d) face wrinkling, (e) general buckling, (f) core crimpling, (g) face dimpling and (h) local indentation [Carlsson and Kardomateas, 2011]*

Face fracture The failure of the face laminate can be analysed by the failure theories as discussed in section 3.3.3.

Core shear failure The core will fail under shear when the applied shear force exceeds the material's shear strength. Assuming brittle failure, the maximum transverse shear stress in the core is given by:

$$\tau_{c,u} = \left[\left(\frac{\sigma_c}{2} \right) + \tau_c^2 \right]^{\frac{1}{2}} \tag{3.35}$$

Local indentation of the core can occur at concentrated loads. It can be avoided by distributing the load over a sufficiently large area.

Face wrinkling There is a number of models to predict the buckling stress for the face wrinkling failure mode, as discussed in literature, for example [Carlsson and Kardomateas, 2011, section 8.1]. The most elementary model approaches the faces on the core as a plate on an elastic foundation, i.e. supported by an array of continuously distributed linear springs. The critical stress in the face is given by:

$$\sigma_{cr,f} = \frac{1}{2} \cdot \sqrt[3]{E_f \cdot E_c \cdot G_c} \tag{3.36}$$

Core crimping Core crimping is shear deformation of the core at buckling of the face. The critical stress in the face is given by:

$$\sigma_{cr,f} = \frac{G_c \cdot d}{2 \cdot t} \tag{3.37}$$

Face dimpling In cellular core structures, the skins may wrinkle between the cell walls. This failure mode is called dimpling. The critical stress in the face is given by:

$$\sigma_{cr,f} = 2 \cdot \frac{E_f}{1 - \nu_{xy}^2} \cdot \left(\frac{2 \cdot t}{a} \right)^2 \tag{3.38}$$

In which:

a *cell size; diameter of the inscribed circle*

Local identation In the vicinity of a localised lateral load, such as a point load or line load, high local deflections and thus stress concentrations may occur. Next to global bending of the sandwich element, a local bending of the loaded face about its own axis is implied, as displayed in fig. 3.27(h). Just as for face wrinkling, the analysis of this failure mode is based on the elastic foundation model. The distribution of the external load to the core can be determined, and should be lower than the compressive strength of the core material. The procedure to calculate local deflection and stresses can be found in [Zenkert, 1997, chapter 8].

Delamination Although not displayed in the figure, the connection between the face and the core may fail from yielding. This can however easily be avoided by selecting an appropriate adhesive and manufacturing method. The elongation of the connection layer must be lower than the critical elongation of the adhesive.

3.4 Structural design

3.4.1 Fatigue

Fatigue loading results in the initiation and progression of cracks in the fibres, the resin or the interface. As a result of these cracks, the strength and stiffness of the affected element is reduced with progressive fatigue damage. Ultimately, the composite will fail catastrophically as the remaining cross-section is unable to bear the applied load.

For typical applications, the ultimate fatigue life is an order of 10 larger than the service life of the structure. This shows that fatigue effects in composite structures are generally not a governing design criterion, in contrast to steel structures. The underlying reason is not only that crack propagation is slower in composites, but also that the applied cyclic stresses are generally low compared to the ultimate stress. The latter reason results from the fact that deformation is typically the governing design criterion, making the working strain the limiting factor instead of working stress [Vassilopoulos, 2010].

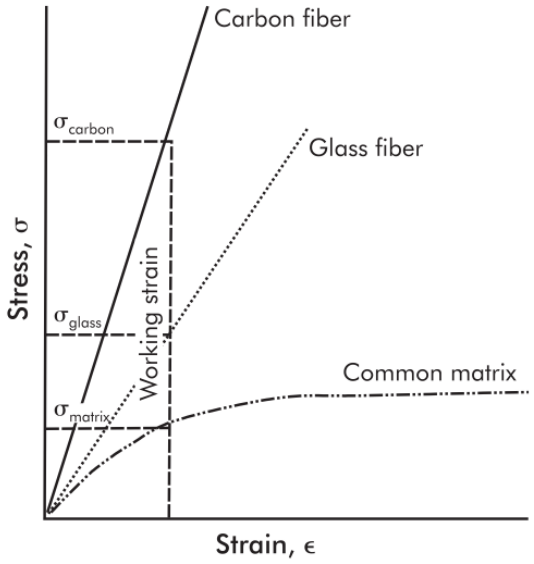

Figure 3.28: *Working strain criterion results in relatively low fatigue stresses [Strong, 2008]*

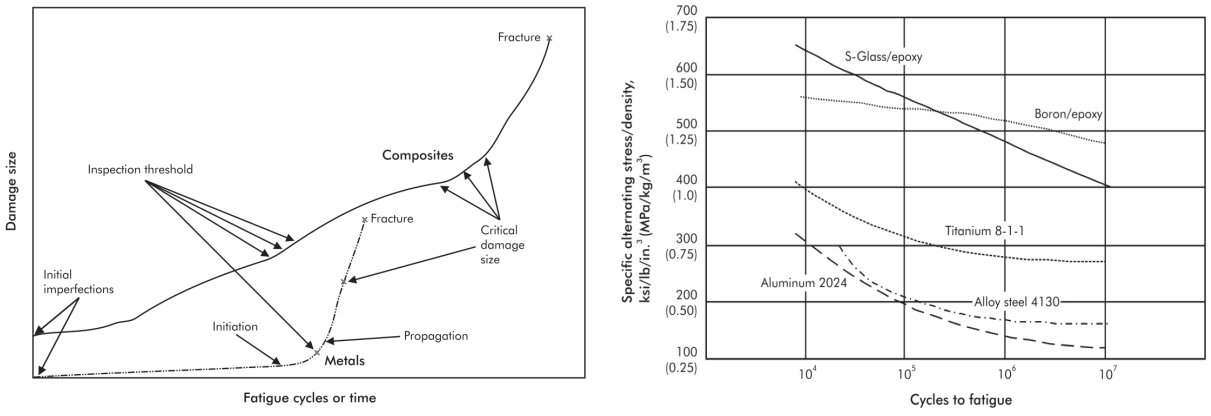

(a) Crack behaviour

(b) S-N curves

Figure 3.29: *Comparison between fatigue behaviour of composite material and metals [Strong, 2008]*

3.4.1.1 Fatigue strength

Like any composite material property, the fatigue strength is influenced by many factors. Therefore it is virtually impossible to develop a fatigue life prediction method to cover all these parameters. However, a growing number of test results is gathered in databases, which enables the estimation of the required fatigue parameters for general applications.

The mean stress level generally does not influence the fatigue life of notched steel section, such as welded structures, as a result of residual stresses and stress concentrations in the welds. The fatigue life of steel structures is determined by the connection details. Composite structures are however notch-insensitive, due to inhomogeneous nature of the material. In contrast to plain metals, the composite material already has micro-cracks prior to loading. The propagation of these micro-cracks is much slower than in metals, and is generally limited within a single ply of the laminate.

Under fatigue loading, composites behave more similar to concrete than to steel. The mean stress effect on the fatigue life of material is very pronounced. This effect can be accurately modelled by means of so-called Constant Life Diagrams (CLD), which can be assembled from a number of S-N curves at different stress ratios (minimum stress over maximum stress) [Nijhof, 2004].

3.4.1.2 Fatigue design

Composite elements that are expected to be subjected to cyclic loading during its service life must be checked for fatigue. The procedure is as follows [CUR-96+, 2012]:

1. Determine the load spectrum of the governing element for its projected service life. For movable bridge design, one should consider both the traffic fatigue load models and the opening/closing cycles. The load spectrum should be displayed in a table in which for every unique combination of mean stress and stress amplitude the expected amount of cycles is given.
2. For each entry in the load spectrum table, the number of allowable cycles should be determined from a supplied CLD. If the CLD for the used composite are not readily available, one can estimate the fatigue properties or perform fatigue tests to establish the CLD.
3. Apply the Miner-rule to determine the accumulated damage. If summation results in a value below 1, the selected material and composition is adequate to withstand the modelled fatigue loads during its design service life. If not, one should adapt the material or composition and start from step 2.

Miner-rule:

$$D = \sum_{i=1}^{k} \frac{n_i}{N_i} \quad \leq \quad 1.0 \tag{3.39}$$

The stiffness reduction as a result of progressing fatigue damage is taken into account by a conversion factor γ_{cf} in the serviceability limit state design section 4.3.2.

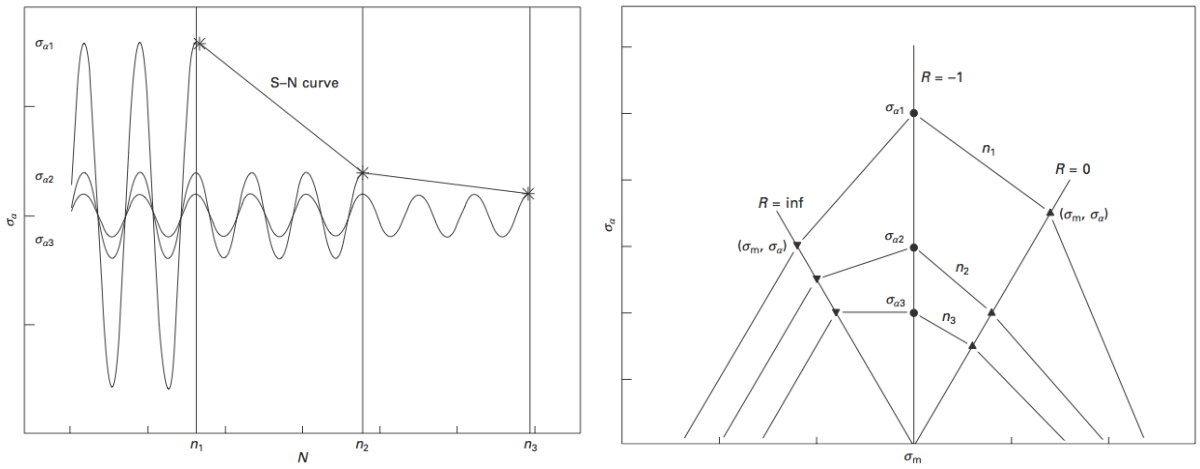

(a) Derivation of S-N curve at certain stress ratio

(b) CLD from several S-N curves

Figure 3.30: *Assembling of CLD from a set of S-N curves at different stress ratios R [Carlsson and Kardomateas, 2011]*

3.4.2 Creep

Creep is the time dependent deformation of a material under a constant load. In composites, creep is primarily a feature of the matrix deformation, as fibres exhibit near-zero creep. It is therefore unlikely that significant creep problems will arise in loading along the fibre direction of the material, while loading in the off-axis direction may result in excessive deformations. The creep process in a material is described by an effective reduction of the stiffness modulus in time; the higher the creep modulus, the smaller the creep. In general terms, the creep modulus of a composite element increases for [Clarke, 1996]:

- a higher degree of cross-linking in the resin
- a higher fibre volume fraction
- a stronger bond between fibre and matrix
- a higher heat distortion temperature of the resin

On the loading side, the following factors enhance the creep:

- a higher stress level
- a higher orthogonality between the fibres and the applied load
- a higher temperature
- a higher moisture content

3.4.2.1 Creep design

Ideally, the creep modulus of the material should be determined from experiments. Experimental data should be checked for conformity in environmental conditions between the test data and the service conditions. Alternatively, the creep behaviour can be taken into account by application of a creep conversion factor γ_{cc} in the serviceability limit state design (see section 4.3.2). In the ultimate limit state design, the effects of creep only have to be considered for stability checks [CUR-96+, 2012].

$$\gamma_{cc} = t^{n} \tag{3.40}$$

In which:

t *load duration in hours*

n *fibre factor, to be found in [CUR-96+, 2012, section 2.5.3.2.3]*

3.4.3 Joints

In principle, there are three established methods of structurally joining composite sections; mechanically, adhesively, and by a combination of both. The following table presents a qualitative comparison between these three joint categories.

Table 3.3: *Qualitative comparison between three joint categories [Clarke, 1996]*

	Joint type		
	Mechanical	Bonded	Combined
Stress concentration at joint			
Strength/weight ratio			
Water tightness			
Thermal insulation			
Electrical insulation			
Smoothness			
Fatigue strength			
Sensitivity to peel loading			
Ease of disassembly			
Ease of inspection			
Tooling costs			
Time to develop full strength			

In the early development of structural composite components, the focus was on material substitution; using elements as a replacement to and in the shape of traditional materials, as described in section 3.2.3.1. Not only were the shapes of steel section was adopted, but also the connection technology was traditional. At the edges of the bolt holes in steel sections, generally yielding and redistribution of stresses occurs during loading. Since composite material does not exhibit the capacity to plastically deform, the area of the joint is always critical. Furthermore, the introduction of stresses transverse to the fibre direction is practically unavoidable.

Bonding elements is a far more material-adapted connection method. Forces are more uniformly introduced into the matrix, before they are transferred to the strong fibres. This results in higher strength-to-weight ratios, and a superior fatigue and impact resistance of the joint. Bonded joints however require more specialist engineering skills and tools, making it more costly. Furthermore, bonded joints fail in a catastrophic way; without any warning prior to failure.

Combined joints can be efficient if a higher degree of end restraint is required. The bond minimised the stress concentration at the bolt/hole zone, while the mechanical connection offers ductility. An additional advantage is that the mechanical system can provide the clamping force, which is necessary during the curing process of the bond. The analysis and design of combined joints is complex due to the difference in stiffness of the alternative load paths. Analysis requires the use of nonlinear techniques, which are available in finite element software packages [Mosallam, 2011].

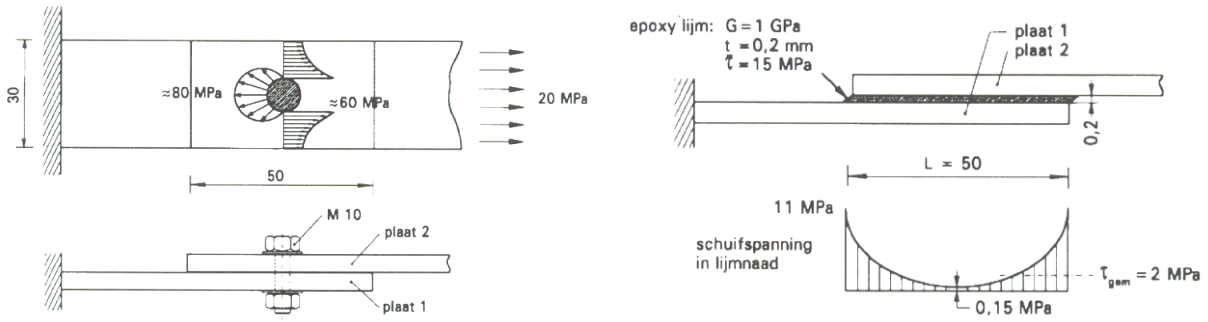

(a) Mechanical bond

(b) Adhesive bond

Figure 3.31: *Stress comparison between equivalent bonded and mechanical joint [de Winter, 1999]*

3.4.3.1 Mechanical joints

Screws, rivets or bolts can be used as fasteners to mechanically join composite sections. It is however unlikely to achieve a connection strength that exceeds 50% of the plain material strength at constant dimensions. For durability reasons, it is advised to always use stainless or galvanized steel as fastener material. Furthermore, threaded bolts or screws are not recommended.

Failure modes In the design of mechanical joints, the following failure modes as illustrated in fig. 3.32 should be considered. Of these failure modes, bearing and tension failure are material-dependent. The other modes can easily be avoided by proper dimensioning and fastener selection. Shearout and cleavage failure can be avoided by retaining an adequate edge distance, pull-through by selection of a sufficiently wide head, and fastener failure by selection of a proper diameter. If an adequate fastener is applied at a proper edge distance, the joint integrity mainly depends on the local laminate bearing strength.

The joint strength is influenced by several factors [Kolstein, 2008]:

- Geometrical factors: width, edge distance, thickness, hole diameter
- Material factors: matrix and fibre type, additives, fibre surface treatment
- Fastener factors: type of fasteners, fastener size, hole size and tolerance, and applied torque
- Design factors: joint type, load directions, loading rate, static versus dynamic loading
- Long-term and environmental exposure factors: creep and creep rupture, humidity, temperature cycling, chemical attacks and stress corrosion

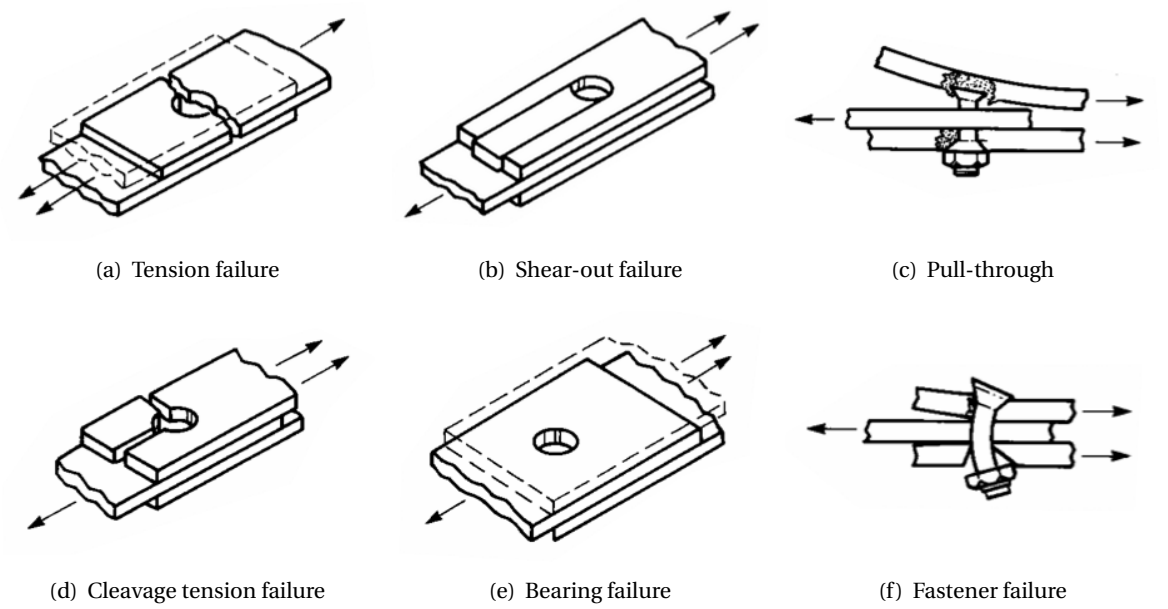

(a) Tension failure (b) Shear-out failure (c) Pull-through

(d) Cleavage tension failure (e) Bearing failure (f) Fastener failure

Figure 3.32: *Failure modes in single bolt tension connections [Strong, 2008]*

Design If the laminate properties are known, joint analysis is quite straightforward and similar to that of traditional materials. The EUROCOMP handbook [Clarke, 1996] is generally considered the most comprehensive design guide for composite connections. The major manufacturers of pultrusion profiles have published their own design manuals, which are mainly based of the EUROCOMP handbook.

3.4.3.2 Bonded joints

In contrast to mechanical joints, bonded joints can be as strong and stiff as the adherent itself. Design, analysis and installation however do require specialist knowledge and skills. Quality control is furthermore difficult and costly.

Failure modes The are four basic stresses associated with bonded joint behaviour; tensile, shear, cleavage and peel. Joints developing direct tension or shear stresses are generally stronger and more reliable than those subjected to cleavage and peel stresses. The latter two stresses can be avoided by designing joint in a symmetrical, non-eccentric way. Alternatively, a sufficient overlapping length and a tapered coupling plate can reduce peel stresses to an acceptable level. The strength of non-symmetrical joints is not proportional to its size, due to stress concentrations at the edges.

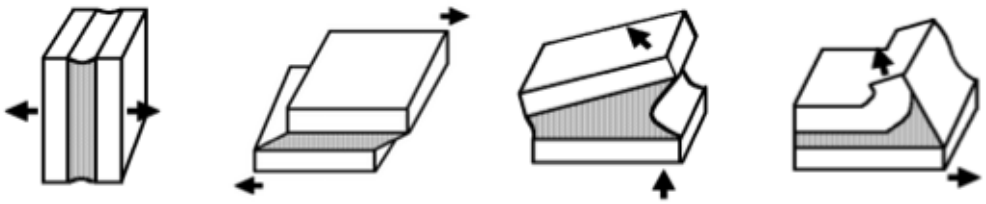

(a) Tensile (b) Shear (c) Cleavage (d) Peel

Figure 3.33: *Deformations from stresses in bonded joints [Creative Pultrusions Inc., 2004]*

The stresses can lead to three primary failure modes; adhesive failure, cohesive failure of adhesive, and cohesive failure of the adherend. Adhesive failure can be avoided by selection of an appropriate adhesive and proper application (surface treatment and curing). If the adhesive is adequate, the integrity of the joint mainly depends on the local interlaminar shear strength of the laminate.

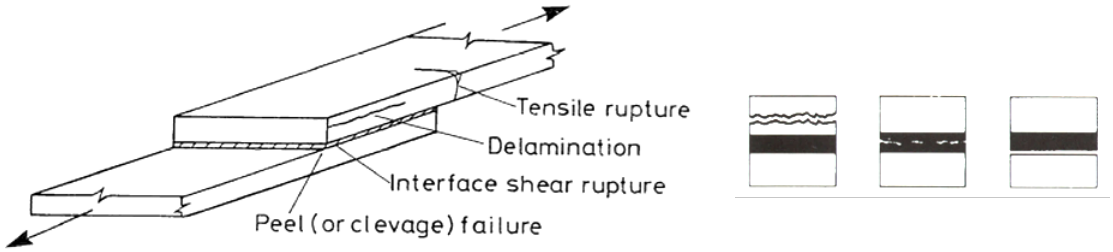

(a) Single-lap bonded joint (b) Adhesive and cohesive failure

Figure 3.34: *Failure modes of bonded joints [de Winter, 1999; Mottram and Turvey, 1998]*

The joint capacity and integrity is influenced by several factors [Mosallam, 2011]:

- Geometrical factors: lap length, eccentricity, thickness of adhesive and adherents
- Material factors: adherent and adhesive capacity and compatibility
- Application factors: surface preparation, curing
- Environmental conditions: moisture, UV-radiation, temperature, load duration

Design The most common bonded joint configurations are [Mosallam, 2011]:

- Single-lap bonded
- Double-lap bonded
- Single-strap bonded
- Double-strap bonded
- Stepped-lap joint
- Scarf joint

The latter two joint types are superior, and can also be used to join laminates to metals. Interlaminar shear stresses due to thermal expansion of the dissimilar materials must be considered. Titanium seems to be the most compatible, steel is acceptable, aluminium is known to be problematic.

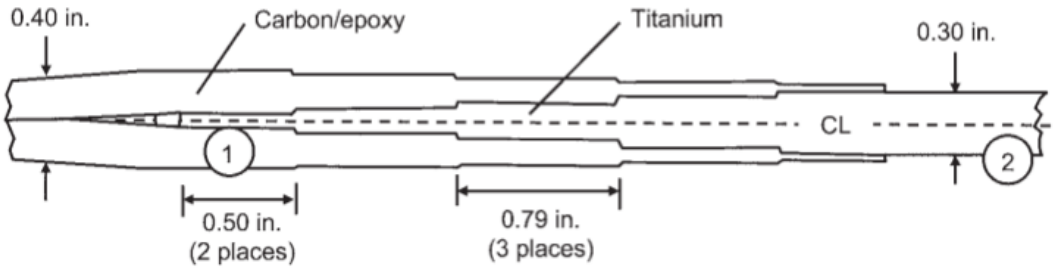

Figure 3.35: *Typical composite-metal stepped-lap joint [Strong, 2008]*

Some design guidelines are available for bonded joint configurations. However, due to the complexity of the problems, EUROCOMP recommends to either analyse each case by means of finite element software, of by physical testing of specimens. Neither option is likely to be straightforward not without additional cost [Mottram and Turvey, 1998].

3.4.3.3 Combined joints

Combined joints, in which both mechanical fasteners and adhesives are used, can provide joints of great capacity and reliability. The combined joint strength is obviously not the algebraic sum of the individual bonded and bolted strengths. Generally, the adhesive provides a much stiffer load path than the fasteners, resulting in a combined joint which is not stronger compared to the bonded joint alone. The application of adhesives with a relatively low stiffness however does allow for load sharing and thus results in a higher overall capacity.

Combined mechanical-adhesive joints exhibit the following advantages over the use of fasteners or adhesives alone [Mosallam, 2011]:

- Higher overall capacity and rigidity
- Greater resistance to environmental and thermal deterioration
- Less subject to peel or cleavage failures
- Improved joint stress distribution
- Improved fatigue and impact characteristics
- Providing clamping force during curing

Design It is common practice to design combined joints, such that the adhesive bond as well as the mechanical fasteners can both transfer the serviceability loads. At the failure of the adhesive, the fasteners secure the structural integrity. This change in load-path is accompanied by significant deformations, warning the users of potential danger. Combined joints can thus help in creating redundant and ductile structures.

If the stiffness of the adhesives is of the same order as the mechanical joint, the structural analysis becomes complex and requires nonlinear techniques [Clarke, 1996].

3.4.4 Impact toughness

Impacts are a notorious weak spot of composite structures. Several bridges have prematurely failed from crack propagation, initiated by the energy of an impact. Runway debris, dropped tools, falling cargo and collisions are examples of low-velocity impacts that can typically occur on road bridges.

In most cases the damage is confined to the matrix, and the fibres remain mostly intact. The in-plane tensile strength of the laminate may therefore not be weakened. The matrix may however be damaged significantly; therefore the ability to stabilise the fibres can be seriously degraded. The laminate can lose up to 60% of its undamaged static compressive strength, and the cyclic load-carrying capacity is compromised [Campbell, 2010].

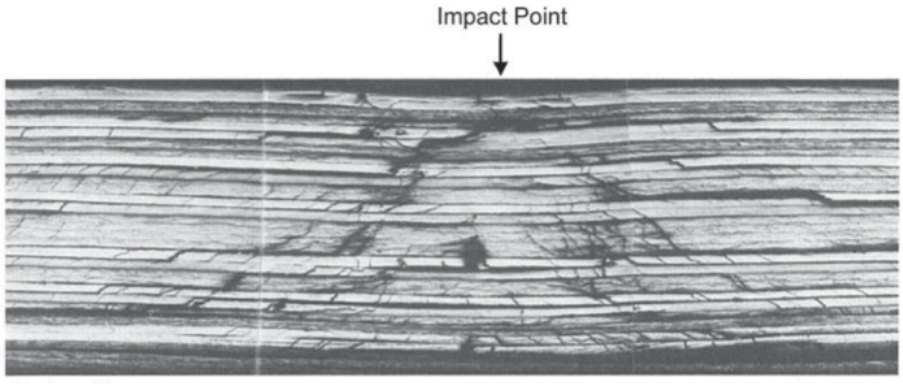

Figure 3.36: *Impact damage in carbon-epoxy laminate [Campbell, 2010]*

Impact damage can be difficult to detect visually. In fig. 3.36 one can see that there is very little evidence of the damaged at the surface of the laminate. Inspection by means of ultrasonic, radiographic or thermographic equipment is still possible, however comes at a cost.

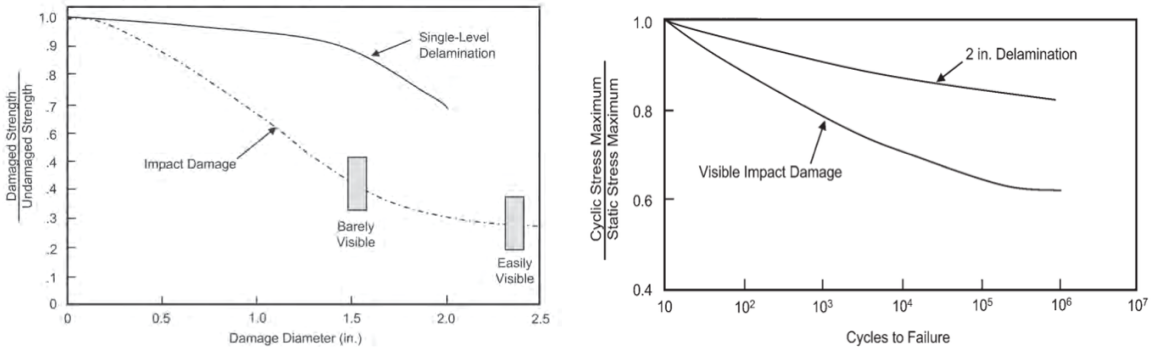

(a) Static strength

(b) Fatigue capacity

Figure 3.37: *Effect of impact damage on material properties [Campbell, 2010]*

Improvements The fibre type, matrix material and shape of the product determine the impact performance of a laminate. As mentioned in section 3.1.1, S-glass and aramid (Kevlar) fibres exhibit superior energy absorption over typical E-glass and carbon fibres. As for the matrix, special toughened epoxies have been developed to obtain greater toughness. A last method of improving the damage tolerance is to use through-the-thickness reinforcement, by applying three-dimensional weaves. However, this generally results in a reduction of the in-plane properties.

3.4.5 Structural safety

Structures should be designed as to give a reasonable and adequate warning of failure prior to reaching an ultimate limit state. This can be achieved by ensuring that a serviceability limit state is reached prior to the ultimate limit state of the considered failure mode. Such serviceability limit states may involve excessive deformations or local buckling or wrinkling [Clarke, 1996].

Composites do not exhibit ductile behaviour beyond a certain point in the linear stress-strain relation of a selected composition. Failure of the material is likely to occur locally, soon after this point has been reached. The inability to redistribute sectional forces makes it more challenging to design structures that warn for failure.

In practice, the warning requirement is not an issue for glass fibre reinforced composites. Since the strength-to-stiffness ratio of this material is much lower than steel, structural design is mainly driven by deflection criterions. As a result, nominal working stresses in the cross-section are well below the ultimate material strength. This may however not be the case in the application of carbon or aramid fibres, which exhibit a higher stiffness.

The following sections present different strategies to obtain safe composite structures.

3.4.5.1 Hybrid fibre arrangements

By applying a certain mixture of carbon and glass fibres (roughly 20 and 80 percent), a pseudo-ductile behaviour can be achieved. Prior to failure, loads are mainly carried by the much stiffer carbon fibres. After their failure the load bearing is transferred to the glass fibres, accompanied by a large increase in deformation. In order to be able to rely on the pseudo-ductility, the production process of hybrid fibre materials should have a high degree of quality assurance. Small changes in fibre volume fractions and cross-sectional placement of different fibres affects the mechanical properties, which may prevent ductile behaviour [Bakis et al., 2001].

3.4.5.2 Combined joints

As mentioned in section 3.4.3.3, the combination of an adhesive bond together with mechanical fasteners can result in a higher safety factor and ductility in a structure. As the bonded load-path is generally stiffer than the mechanical path, the load transfer in the serviceability limit state is mainly provided by the adhesive bond. After failure of the bond, the full load is transferred through the mechanical fasteners. This change of load-path is usually accompanied by an increase in deformation, and emits noises that could function as a warning signal [Mosallam, 2011].

3.4.5.3 Failure sequence

When fibre composites are used in combination with other construction materials, the sections can be designed such that the accompanying material fails prior to the composite. In a steel-FRP construction, the ductility of steel can be exploited. In combination with concrete the development of cracks in the tension zone, or crushing of concrete in the compressive zone, should provide a warning mechanism for imminent failure.

3.4.5.4 Fibre optic sensor monitoring

By embedding fibre optic sensors (FOS) in the composite matrix, actual strains variation can be measured in the structure. The integration of sensors is done in the pultrusion process, allowing for a good mechanical connection and protection. The high sensitivity sensors are able to pick up strains of about 1 mm/m, making it possible to keep track of both short- and long-term deformations. One could set up an automatic system that warns if critical strains are reached.

One step further is the development of so-called 'smart structures', which are equipped with both sensors and actuators. This technology could lead to structures that are able to measure changes in actions and actively control the vibrational damping accordingly [Keller, 2003].

3.4.5.5 Redundancy

If structures are designed with sufficient redundancy, the lack of material ductility can at least partially be compensated for. Redundancy can be achieved on both element and structural level. Element redundancy can be achieved by over-dimensioning; only partially capitalising the material's strength properties. As mentioned before, over-dimensioning is typical to glass fibre composite design as a result of serviceability requirements.

Structural redundancy can be achieved by creating a fail-safe design. This does not mean that failure is impossible or improbable, but rather that the system's design prevents or mitigates unsafe consequences of the system's failure. A typical approach to design fail-safe structures in building engineering is the implementation of an alternative load path, which is activated in the event of failure of certain structural elements.

4 Design input

Movable bridges are generally designed to have a service life of fifty to a hundred years, in which the structure should comply with the functional requirements without requiring excessive maintenance or rehabilitation efforts.

Norms and guidelines have been developed to define standards in safety and reliability of construction works, and help engineers to prove compliance with these requirements. First of all, codes quantify the actions that are exerted on the structure. Secondly, they provide methods to analyse the structural behaviour under the influence of these actions. Lastly, they define the boundaries between which the structure is considered sufficiently safe and reliable. The following sections present the applicable norms for the design of a bascule bridge in the Netherlands according to the Eurocode and, where applicable, the Dutch National Annex.

4.1 Requirements and conditions

According to the Eurocode, a structure shall be designed and executed in such a way that it will remain fit for the use for which it is required during its intended service life, and sustain all actions and influences likely to occur during execution and use. Because no structure can guarantee to fulfil this requirement unconditionally, the codes state that this should be "with appropriate degrees of reliability and in an economical way".

Different levels of reliability may be adopted for structural resistance and serviceability. For instance a bridge should not collapse during a storm, but it may be put out of service at certain wind speeds. The levels of reliability can be achieved by a combination of structural robustness, preventive measures and quality management during execution and use. The performance of the structure may not be impaired during the service life. An adequately durable structure is achieved by assessing the future use and deterioration of the structure under the environmental conditions [NEN-EN 1990, 2002].

The requirements and conditions establish the required service life, together with the foreseeable actions and the permissible reactions of the structure. At least the following items should be defined [CUR-96, 2003]:

- The use of the construction
- The required performance of the structure
- The expected ambient conditions
- The composition, properties and performance of the materials
- The shape and details of structural elements
- The level of craftsmanship and quality control during production and assembly
- The specific protective measures
- The expected maintenance during the projected service life

4.2 Actions

Actions are classified by their variation in time as follows [NEN-EN 1990, 2002]:

- Permanent actions (G): e.g. self-weight, fixed equipment and actions by shrinkage and settlements
- Variable actions (Q): e.g. imposed loads, wind/snow/temperature actions
- Accidental actions (A): e.g. explosions, impact from vehicles

For movable bridges, the actions on both the structural elements as well as the operational systems should be evaluated during the following four situations [NEN 6786, 2001]:

- Closed bridge
- Unclosed bridge
- During opening/closing cycle
- Outside opening/closing cycle

Where quantified, actions are presented as being both secluded and characteristic. For load combinations, the accompanying values of variable actions have to be determined by multiplication with a combination factor (ψ). For typical loads on bridges, these factors can be found in [NEN-EN 1990/A1, 2006, Table A2.1]. Design values of actions are derived by multiplication with partial safety factors (γ_f) accounting for unfavourable deviations of actions, inaccurate modelling of actions and uncertainties in the assessment of the considered limit state [Clarke, 1996].

4.2.1 Self-weight

The self-weight of a bascule bridge is composed of the mass of the permanent structural elements. These include the load bearing components, counterweight, bridge deck, asphalt layer and non-structural components such as hand rails, kerbs and other bridge furniture [NEN-EN 1991-1-1, 2011].

The nominal densities of traditional construction materials are enumerated in the Eurocode. Fibre reinforced composites are however not included in these tables, as the material is not (yet) standardised. The weight of composite elements depends on the types and proportions of fibres and matrix. For commercially available products, the weight is usually specified by the manufacturers. Otherwise, the density of laminates can be estimated by applying the rule of mixtures:

$$\rho = V_f \cdot \rho_f + V_m \cdot \rho_m \tag{4.1}$$

In which:

ρ	*total density*
ρ_f	*desity of fibres*
V_m	*matrix volume ratio*
ρ_m	*density of matrix*

Most common composites have a density ranging from 1300 to 1800 kg/m^3 [Strong, 2008, p. 318].

4.2.2 Traffic

The Eurocode defines imposed loads associated with road and rail traffic, and actions from pedestrians and bikes. For carriageways up to 200 meters in length, the characteristic loads are represented by four different load models. The first two models describe the most general load cases, whereas the third and fourth models describe occasional loads from exceptional traffic and crowds. In the scope of this thesis, rail traffic is not considered.

The characteristic loads are multiplied with adjustment factors, specified in the national annex, to calibrate the models for projections of actual traffic loads in a reference period of 100 years.

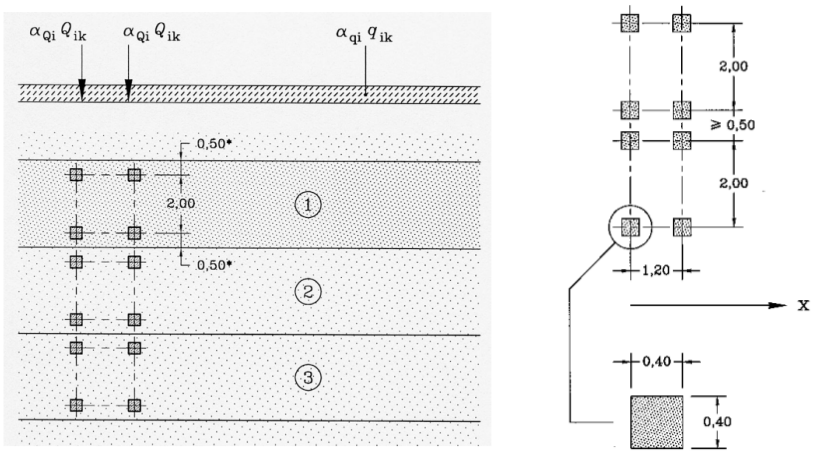

(a) Application on lanes (b) Local verification

Figure 4.1: *Application of LM1 [NEN-EN 1991-2, 2003]*

4.2.2.1 Load Model 1

This load model covers flowing, congested or traffic jam situations with a high percentage of heavy trucks, including special vehicles up to 600 kN. The effects of traffic actions are modelled by both uniformly distributed and concentrated loads (tandem system). The model should be used for general and local verifications.

Tandem system The concentrated load of this model is composed of a double-axle tandem system, with each axle imposing the following specified load (in which α_Q represents the adjustment factor):

$$\alpha_Q \cdot Q_k$$

No more than one, and only complete tandem system should be taken into account per notional lane. The load of each tandem is equally distributed over two square surface contact areas of 0.40 meter, positioned at each side of the axle. Four of these contact areas have to be applied in a 1.2 by 2 meter grid at each notional lane. The minimum distance between the grids of two adjacent vehicles should not be below 0.50 m.

Characteristic load values The characteristic load values are displayed in table 4.1

Table 4.1: *Characteristic load values LM1 [NEN-EN 1991-2, 2003]*

Location	Tandem system Q_{ik} [kN]	Uniformly distributed load q_{ik} [kN/m^2]
Lane number 1	**300**	**9**
Lane number 2	**200**	**2.5**
Lane number 3	**100**	**2.5**
Other lanes	**0**	**2.5**
Remaining area	**0**	**2.5**

Adjustment factor For bridges being built in the Netherlands, one should account for more than 2.500.000 trucks per traffic lane per year [Rijkswaterstaat, 2013b, p. 53]. The carriageway is divided in a number of notional lanes. The traffic loads on these notional lanes is subsequently adjusted by the following factors from the Dutch national annex:

$\alpha_{qi} = 1.15$ *for bridges with one or two traffic lanes*

$\alpha_{q1} = 1.15$ and $\alpha_{qi} = 1.40$ for $i > 1$ *for three or more lanes*

4.2.2.2 Load Model 2

To check local effects, LM2 consists of the following single axle load:

$$\beta_Q \cdot Q_{ak}$$

In which Q_{ak} is equal to 400 kN. This characteristic value includes a dynamic amplification factor, however tan additional factor should be applied in the vicinity of expansion joints. The contact area of this load is should be taken as a rectangle of 0.35 and 0.60 m, corresponding to twin-tires. The centre-to-centre distance of these contact areas is set at 2 meters. The adjustment factor β_Q should be equal to α_{Q1}, according to the Dutch National Annex.

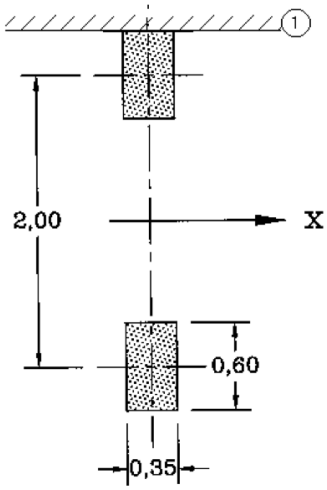

Figure 4.2: *Application of LM2 [NEN-EN 1991-2, 2003]*

4.2.2.3 Load Model 3

LM3 describes special vehicles. This model is only applied if this is specified in the requirements of a specific project. The number of vehicles, maximum axle loads and distances between axes must be given and analysed. These requirements can be imposed by for example the military or local industries making use of the bridge.

4.2.2.4 Load Model 4

LM4 accounts for crowd loading during special occasions, and is modelled by a uniformly distributed load equal to 5 kN/m^2. This load includes a dynamic amplification. It should be placed on all relevant parts of the bridge, including central reservations.

4.2.2.5 Horizontal forces

Breaking and acceleration of vehicles introduces horizontal forces along the longitudinal axis at the surfacing level of the bridge. The corresponding load model is defined as a fraction of the Load Model 1 at the first notional lane as follows:

$$Q_{1k} = 0.6 \cdot \alpha_{Q1} \cdot (2 \cdot Q_{1k}) + 0.1 \cdot \alpha_{q1} \cdot q_{1k} \cdot w_1 \cdot L \quad \leq \quad 800\ [kN] \tag{4.2}$$

The Dutch National Annex specifies a maximum horizontal acceleration load of 800 kN over the total width of the bridge. Horizontal forces are also induced by centrifugal forces in case of a curved carriageway, which is not considered in the scope of this thesis. Furthermore, models of transverse loading from wind effects and collision on kerbs are assumed to provide sufficient capacity for skew braking and skidding.

4.2.2.6 Footways and cycle tracks

The imposed loads by pedestrians, cyclists and occasional service vehicles are accounted for by separate load models for these areas of the bridge. First model is a uniformly distributed load:

$$q_{fk} = 2.0 + \frac{120}{L+30} \qquad 2.5 < q_{fk} < 5.0\ [kN/m^2] \tag{4.3}$$

The second model is a concentrated load acting on a square surface of sides 0.1 meter.

$$Q_{fwk} = 7\ [kN]$$

A last model account for a service vehicle. Four wheels in a 3 by 1.75 meter grid, having a square contact surface of sides 0.25 meter are applied with the following axle load:

$$Q_{serv} = 25\ [kN]$$

Horizontal actions from pedestrians and cyclists do not have to be taken into account for traffic bridges.

4.2.2.7 Multi-component action

The simultaneous action of vertical- and horizontal loads of traffic and loads on footways and cycle tracks needs to be checked. For this purpose, the Eurocode specifies groups of traffic loads in [NEN-EN 1991-2, 2003, table 4.4a]. This table specifies the combinations of action that have to be taken into account. The Dutch National Annex redefines these load combinations by making use of adjustment factors.

4.2.3 Fatigue

Fatigue actions are often a governing criterion in the design of heavy traffic bridges. The Eurocode specifies a number of fatigue load models, taking into account different vehicle geometries, axle loads, vehicle spacing, composition of traffic and its dynamic effects.

The first two load models are used to determine whether a structure may be considered to have an unlimited fatigue life or not, under the influence of a constant stress amplitude. The other three models are intended for fatigue life assessment by reference to fatigue strength curves.

4.2.3.1 Traffic categories

A traffic category has to be determined for the selected bridge structure, which corresponds to a modelled number of heavy vehicles per year per lane as indicated in the table below. The Dutch National Annex specifies that each notional lane has to be considered as heavy-traffic lane.

Table 4.2: *Indicative number of heavy vehicles expected per year and per slow lane [NEN-EN 1991-2, 2003]*

Traffic category	Heavy vehicles 10^6 N_{obs} [1/year/lane]
1: Highway (A-roads)	**2.0**
2: Motorways (N-roads)	**0.5**
3: Main roads	**0.125**
4: Local roads	**0.05**

4.2.3.2 Fatigue Load Model 1

The FLM1 is configured in accordance to LM1, applying a partial factor over the applied distributed and concentrated loads:

$$\begin{aligned} Q_{ik,FLM1} &= 0.7 \cdot Q_{ik,LM1} \\ q_{ik,FLM1} &= 0.3 \cdot q_{ik,LM1} \end{aligned} \tag{4.4}$$

The maximum and minimum stresses following from this model should be determined from the possible load arrangements on the bridge.

4.2.3.3 Fatigue Load Model 2

FLM2 is more accurate than the conservative FLM1, consisting of a set of frequent trucks. The maximum and minimum stresses should be determined for the governing truck travelling along the carriageway. The frequent trucks are defined in [NEN-EN 1991-2, 2003, table 4.6]

4.2.3.4 Fatigue Load Model 3

This load model considers a single vehicle consisting of four axles, each carrying a load of 120 kN. The configuration and dimensions of the contact surfaces is indicated in the figure below. The maximum and minimum stresses result from the transit of the model along the bridge.

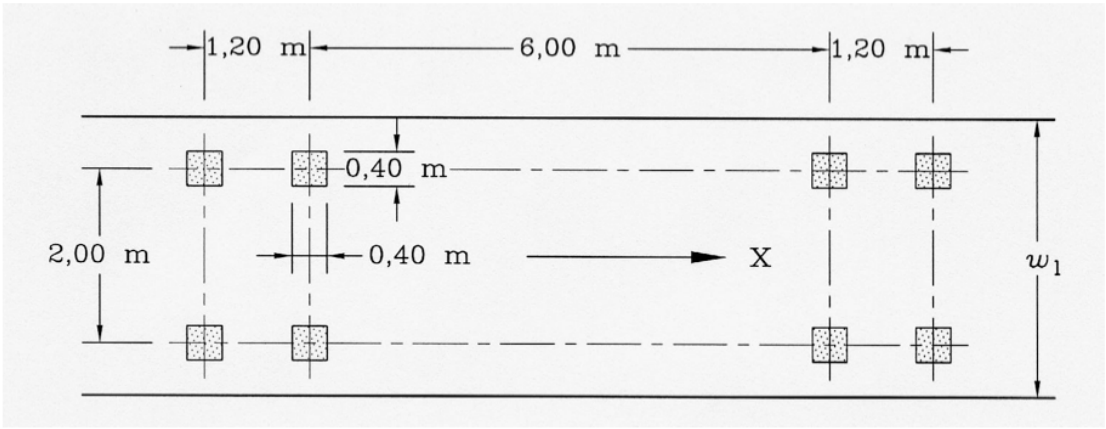

Figure 4.3: *Application of FLM3 [NEN-EN 1991-2, 2003]*

4.2.3.5 Fatigue Load Model 4

FLM4 models typical traffic as found on the European roads, consisting of sets of standard trucks. Five different standards trucks have been specified to simulate the equivalent fatigue damage due to actual traffic of the corresponding traffic categories. These sets of equivalent trucks can be found in [NEN-EN 1991-2/NB, 2011, table NB.6 and NB.8]

This model is suitable for application on construction materials which fatigue strength depends on both the stress range as well as the average stress. Fibre-reinforced polymers exhibit this fatigue behaviour, as discussed in section 3.4.1. The stress range spectrum and corresponding number of cycles from each passage of individual trucks on the bridge should be determined using the 'rainflow' or the 'reservoir' counting method.

4.2.3.6 Fatigue Load Model 5

This last load model is based on recorded road traffic data, supplemented with appropriate statistical and projected extrapolations for future actions. Complete specification and application of this model is given in [NEN-EN 1991-2, 2003, annex B].

4.2.4 Wind

Wind loading can be a governing action on a movable bridge, not only for the superstructure but also for the substructure and the operating machinery. High stresses and stress fluctuations can occur in structural members under the influence of wind. Especially long span single leaf bascules are susceptible to wind loading, as the spans extend high above the water level in the opened position.

Wind can blow from any direction, and in all states of the bridge. However, in order to limit the amount of calculations, the Eurocode [NEN 6786, 2001] allows to consider only the longitudinal actions working on the fully opened wind profile of the bridge as it is in operation. In the closed position, the uplifting effect of the wind and the load in transverse direction are considered.

4.2.4.1 Transverse direction

The models for wind actions on the bridge in closed state are defined in [NEN-EN 1991-1-4, 2005]. The calculation procedure is relatively elaborate, depending on a range of parameters related to the wind action and structural properties. A simplified method is however presented, which may be applied if is assessed that a dynamic response procedure is not necessary. As the dynamic properties of the structure are separately considered, this simplified method is assumed to be sufficient in preliminary design stages. The wind force in the transverse direction of the bridge should be modelled by:

$$F_{w,x} = \frac{1}{2} \cdot \rho \cdot v_b^2 \cdot C_x \cdot A_{ref,x} \tag{4.5}$$

In which:

v_b	*basic wind speed*
C_x	*wind load factor*
$A_{ref,x}$	*reference area*
ρ	*density of air*

Basic wind speed The basis wind speed, defined as a function of wind direction and time of year at 10 meter above ground of terrain category II is modelled by:

$$v_b = c_{dir} \cdot c_{season} \cdot v_{b,0}$$

In which:

c_{dir}	*directional factor, set equal to unity*
c_{season}	*season factor, set equal to unity*
$v_{b,0}$	*fundamental value of basic wind velocity in respective wind areas in the Netherlands*

Table 4.3: *Basic wind speeds in the Netherlands [NEN-EN 1991-1-4/NB, 2011]*

Wind area	I	II	III
Wind speed *[m/s]*	**29.5**	**27.0**	**24.5**

Wind load factor The wind load factor is an aerodynamic coefficient, determined by:

$$C_x = c_e \cdot c_{f,x} \tag{4.6}$$

In which:

c_e	*exposure factor for flat terrain in the different wind areas, as a function of the construction height; to be found in [NEN-EN 1991-1-4/NB, 2011, table NB.5]*
$c_{f,x}$	*force coefficient without free-end flow, depending on the shape of the structure and the face normal to the wind direction (including traffic); to be found in [NEN-EN 1991-1-4, 2005, figure 8.3]*

Alternatively, one could use [NEN-EN 1991-1-4/NB, 2011, table NB.18] to determine the wind load factor for bridges.

Reference area The reference area is the face surface of the considered structure normal to the wind direction. Next to the construction itself, road furniture and traffic are considered for the wind profile in the transverse direction of the bridge. For traffic, an additional height of 2 meters from the level of the carriageway should be added at the most unfavourable length.

Density of air The density of air is set at ρ=1.25 kg/m^3

4.2.4.2 Vertical direction

The lifting force may have a significant effect on lightweight bascule bridges. In case no live load is present on the bridge, the magnitude of the uplifting force could approach the same order as the dead load working on the rest pier. This may cause the leaf to flutter, causing impact stresses and most probably noise hindrance. The imbalance of the bridge, causing the dead load to partially be supported on the live load shoes, must be adjusted to compensate for uplifting effects of both traffic and wind.

The determination of the wind force in vertical direction is analogous to the transverse direction:

$$F_{w,z} = \frac{1}{2} \cdot \rho \cdot v_b^2 \cdot C_z \cdot A_{ref,z} \tag{4.7}$$

Wind load factor The wind load factor in vertical direction is again the product of the exposure factor and a force coefficient factor.

$$C_z = c_e \cdot c_{f,z} \tag{4.8}$$

The force coefficient factor $c_{f,z}$ depends on the angle of the wind with respect to the plane of the bridge deck. For horizontal terrain, the angle of the wind direction relative to the horizontal plane may be taken as $\alpha = 5°$. Adding up the superelevation of the bridge itself leads to a wind impact angle θ. Together with the deck's width-to-height ratio, the force coefficient factor can be determined from the relation plotted in [NEN-EN 1991-1-4, 2005, figure 8.6]

4.2.4.3 Longitudinal direction

In the closed position of the bridge, and outside of operational cycle, the Dutch National Annex prescribes the wind force in longitudinal direction of the bridge as a percentage of the wind force in transverse direction:

$$F_{w,y} = 0.4 \cdot F_{w,x} \tag{4.9}$$

During an operational cycle, wind load has to be taken into account according to the 'rules for the design of movable bridges'. These norms take a semi-probibalistic approach to determine the maximum design wind pressure, in order to achieve a certain reliability of operation. The number of days per year that the bridge is permitted to be out of service due to wind effects depends on the relative importance of the waterway it spans. These reliability requirements are within a range of 0.25 to 3 days per year, as defined in [NEN 6786, 2001, section 8.2.1.2, table 1]

Table 4.4: *Serviceability requirement movable bridges [NEN 6786, 2001]*

Type of waterway	Clearance *[m]*	Maximum days out of service *[day/year]*
Sea route		**0.5**
Main transport axis	**> 9.1 m**	**1**
	< 9.1 m	**0.25**
Main waterway	**> 6.0 m**	**2**
	< 6.0 m	**0.5**
Other		**3**

Based on these reliability requirements and the classification of the wind area at the location of the bridge, the design mean hourly wind speeds U_R are determined in [NEN 6786, 2001, section 8.2.1.2]. The pressure on the opened structure can subsequently be determined using the following relation:

$$p_w = \frac{1}{2} \cdot \rho \cdot \left\{ U_R \cdot \frac{\ln\left(\frac{h}{z_0}\right)}{\ln\left(\frac{z_{ur}}{z_0}\right)} \right\}^2 \cdot \left\{ 1 + \frac{7}{\ln\left(\frac{h}{z_0}\right)} \right\} \tag{4.10}$$

In which:

p_w	*wind pressure at the tip of the leaf*
U_R	*mean hourly windspeed at height z_{ur}; from [NEN 6786, 2001, section 8.2.1.2, table 3]*
h	*distance between mean waterlevel and the tip of the leaf*
z_0	*roughness length; from [NEN 6786, 2001, section 8.2.1.2, table 3]*
z_{ur}	*height above surface level at which U_R is determined; $z_{ur} = 10m$*

The characteristic pressure, which should be taken constant over the height of the opened leaf, is derived by multiplication with shape and dynamic factors:

$$P_{w,rep} = C_{dim} \cdot C_t \cdot \phi_w \cdot p_w \tag{4.11}$$

In which:

C_{dim}	*dimensional factor; $C_{dim} = 0.95$*
C_t	*wind shape factor of bascule; from [NEN 6786, 2001, section 8.2.1.2, Figure 5]*
ϕ_w	*dynamic amplification factor; $\phi_w = 1.15$*

4.2.5 Snow

The characteristic values for snow load on movable bridges are small compared to those on for example roof structures, as the removal of snow is accounted for. The following value for electromechanical and hydraulic bridges should be used [NEN 6786, 2001, section 8.2.2]:

$$p_{sn} = 0.1 \ [kN/m^2]$$

4.2.6 Thermal

Working thermal actions strongly depend on the shape of the structure and its material properties, such as density, specific heat capacity and thermal conductivity. The Eurocode prescribes different thermal actions for steel and concrete bridges, in several different configurations. Fibre composite bridges are not included, so these actions should be estimated.

These thermal actions impose strains in the structural elements, which relate through material specific thermal expansion coefficients. For composites, this coefficient again depends on chosen material properties such as fibre percentage and direction.

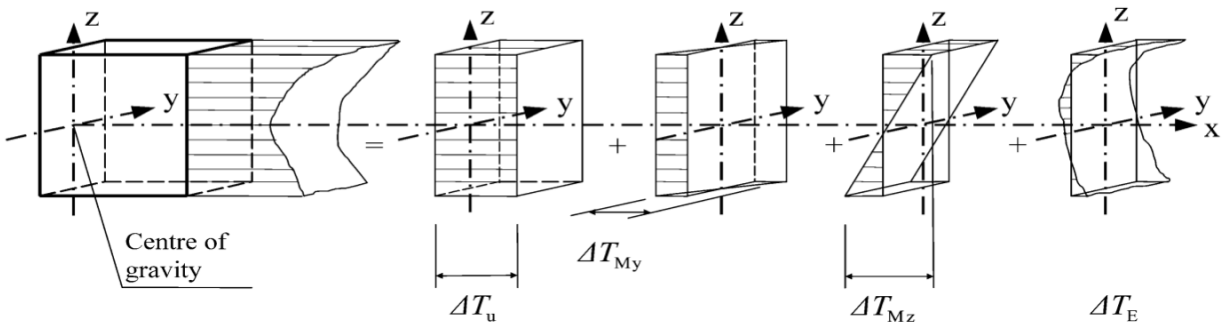

Figure 4.4: *Representation of temperature profile components [NEN-EN 1991-1-5, 2011]*

4.2.6.1 Uniform temperature component

A change in uniform temperature of an unrestrained structure results in a change of element length. Therefore, this uniform thermal action is mainly important for the design of bearings and expansion joints. If the elongation of the structure exceeds the dilatation between span and abutment, the leaf is trapped between the abutments. In this stage, the bridge can not be operated and introduced forces could lead to buckling of elements.

The minimum and maximum temperature component of the bridge is correlated to the minimum and maximum air temperature in the shade, as defined in [NEN-EN 1991-1-5/NB, 2011, section 5.3]

$$T_{max} = 30\ [^{\circ}C]$$
$$T_{min} = -25\ [^{\circ}C]$$

Subsequently, the uniform temperature components can be determined from [NEN-EN 1991-1-5/NB, 2011, figure NB.1]. The different lines in this graph correspond to different three distinguished bridge deck types; steel, steel-concrete and concrete. Depending on the structural layout, one of these relations should be chosen.

Occurring stresses at restrained deformation of elements are calculated using the temperature range from initial restriction to maximum temperature:

$$\begin{aligned} \Delta_{N,con} &= T_0 - T_{e,min} \\ \Delta_{N,exp} &= T_{e,max} - T_0 \end{aligned} \tag{4.12}$$

4.2.6.2 Vertical temperature component

A vertical temperature component in the cross-section of the bridge is the result of heating and cooling of the bridge deck's upper surface, caused by sunlight and radiation. If the curvatures caused by this temperate difference are restrained, additional stresses are introduced in the structure.

The Eurocode [NEN-EN 1991-1-5, 2011, section 6.1.4] specifies both a linear- and a non-linear vertical temperature model. Both methods make a distinction between different types of bridge deck; in material as well as in shape.

Linear temperature difference The design temperature range between the upper- and lower fibre in the cross-section of the bridge are specified in [NEN-EN 1991-1-5/NB, 2011, table 6.1]. The values given in this table are based on a depth of a surface finishing layer of 50 mm. For other depths, the values should be multiplied by a surface depth factor k_{sur} which can be found in [NEN-EN 1991-1-5/NB, 2011, table 6.2].

Non-linear temperature difference The non-linear temperature models take more account of thermal properties of different structural layouts. Thermal inertia, the degree of slowness with which the temperature of a body approaches that of its surroundings, is an important parameter for the non-linear models. A more uneven distribution of thermal inertia over the cross-section results in a higher non-linearity of the vertical temperature component. The model values can be found in [NEN-EN 1991-1-5, 2011, table 6.2a-6.2c].

4.2.6.3 Temperature difference between elements

As a result of orientation with respect to the sun, a temperature difference can occur between elements. To account for this effect, a uniform temperature difference of 15 °C between the main structural elements has to be considered.

4.2.7 Operation

During an operational cycle, stresses in the structure radically change along with the opening angle of the leaf. Furthermore, acceleration and deceleration impose dynamic effects. This load case should be taken into consideration for both strength and fatigue calculations.

The degree of severity of this load case for the fatigue life of the structure depends mainly on the number of operational cycles. The Eurocode prescribes to account for 100.000 opening/closing cycles per year [NEN 6786, 2001].

4.2.8 Accidental actions

The likelihood of occurrence and associated consequences of accidental actions should be considered by assessing risk levels of such events. The potential failure of the structure arising from an unspecified cause can be mitigated to acceptable levels by the one or more of the following measures:

- Preventing the action from occurring
- Protecting the structure against the effects of the action
- Ensuring sufficient robustness of structure

For example; the event of a vehicle collision against the bridge structure can be prevented by providing adequate clearance. Protecting the structure at occurrence of this event can be achieved by a physical separation between the roadway and the structural elements. Ensuring sufficient robustness of the structure can be achieved by taking the load case into account in the structural design. The selection of materials that are capable of absorbing significant strain energy without rupture or providing an alternative load path are ways of improving a structure's robustness.

4.2.8.1 Emergency stop

The Eurocode specifies a time interval in which the nominal movement of the bridge leaf should be able to be brought to a halt, in case of emergencies. The sharp deceleration imposes a dynamic load on the structure which is much larger than regular decelerations during an operational cycle.

The time intervals depend on the surface size of the bascule leaf; a maximum of 3 seconds is prescribed for leafs up to 125 m^2, and a maximum of 6 seconds for larger ones. [NEN 6786, 2001, section 8.2.11.1]

Next to the prescribed time interval, the severity of this load case depends on the nominal speed of operation and the structure's mass moment of inertia relative to the rotation axis.

4.2.8.2 Impact by ship

A bridge span crossing a waterway must be designed to withstand the impact of a ship in a transverse direction to the longitudinal axis. This accidental action can occur in the event of a premature closure of the bridge. The impact of a vessel against the bridge deck may be modelled as a hard impact, where the energy is mainly dissipated by the impacting body. It is assuming that the structure is rigid and immovable and that the colliding object deforms linearly during the impact phase. The most significant parameters determining the impact forces are the vessel speed, impact angle and the hydrodynamic mass [Parke and Hewson, 2008].

The Eurocode prescribes an equivalent static force due to the impact of a ship of 1 MN, acting over a surface of 0.25 m height and 3.0 m width [NEN-EN 1991-1-7, 2006, section 4.6.2]. This force is relatively small compared to frontal collision forces against vertical structures, such as bridge piers. This is due to the fact that only a part of the vessel interacts with the bridge deck.

4.2.8.3 Vehicle on footway or cycle tracks

The footway and cycle tracks on bridge decks should be designed to withstand the load of accidental events in which a vehicle leaves the roadway. If safety barriers of an appropriate containment level are provided, wheel or vehicle loading beyond this protection need not to be taken into account. Where this protection is provided, one accidental axle load corresponding to $\alpha_{Q2} \cdot Q_{2k}$ (see section 4.2.2.1) should be placed at the most unfavourable position on the bridge. In the absence of safety barriers, the accidental axle load is applicable up to the edge of the deck.

4.3 Design values of material- and product properties

Material properties of materials and products are presented by nominal- and/or characteristic values with corresponding fractiles, statistical distribution and testing conditions. In the limit state verification, upper and lower characteristic values of the respective material properties shall be taken into account as the following fractiles:

5%	*in case a low property value is unfavourable*
95%	*in case a high property value is unfavourable*

Subsequently, the design value is determined by:

$$X_d = \frac{X_k}{\gamma_m \cdot \gamma_c} \tag{4.13}$$

In which:

X_k	*Characteristic or nominal value of material- or product property*
γ_m	*Material factor; to account for uncertainties in material properties*
γ_c	*Conversion factor; to account for degradation under influence of time, temperature, load characteristics and environmental factors (moisture, UV)*

The safety factors are somewhat arbitrary, as no established design codes exist. In absence thereof, the recommendations of [CUR-96+, 2012] are maintained.

4.3.1 Material factor

The material factor for composites has two components:

$$\gamma_m = \gamma_{m,1} \cdot \gamma_{m,2} \tag{4.14}$$

In which:

$\gamma_{m,1}$ *Partial safety factor related to the level of uncertainty in deriving the section characteristics:*

- *1.35 if determined from tables or empirical methods*
- *1.15 if determined by physical tests on specimens*

$\gamma_{m,2}$ *Partial safety factor related to the production process and curing conditions*

Table 4.5: *Partial material factors $\gamma_{m,2}$ for different production methods [CUR-96+, 2012]*

Production method	Partial material factor	
	Fully postcured	Not fully postcured
Spray application	**1.6**	**1.9**
Hand lay-up	**1.4**	**1.7**
Resin transfer moulding	**1.2**	**1.4**
Filamentwinding	**1.1**	**1.3**
Pre-preg lay-up	**1.1**	**1.3**
Pultrusion	**1.1**	**1.3**

4.3.2 Conversion factor

The conversion factor has four components, related to the influences of temperature, moisture, creep and cyclic loading:

$$\gamma_c = \gamma_{ct} \cdot \gamma_{cv} \cdot \gamma_{ck} \cdot \gamma_{cf} \tag{4.15}$$

In which:

γ_{ct} *Partial conversion related to temperature effects*

γ_{cm} *Partial conversion related to moisture effects*

γ_{cc} *Partial conversion related to creep effects*

γ_{cf} *Partial conversion related to fatigue effects*

The applicability of the partial conversion factors depends on the limit state that is considered, as indicated in the following table [1]:

[1] Creep-related factor only has to be applied for long-term actions. Vibration limit state has to be considered both with and without conversion factors

Table 4.6: *Applicability of partial conversion factors [CUR-96+, 2012]*

Conversion	Ultimate Limit State			Serviceability Limit State		
	Strength	Stability	Fatigue	Deflection	Vibration	Cracking
Temperature	X	X	X	X	X	X
Moisture	X	X	X	X	X	X
Creep		X		X		X
Cyclic loading		X		X	X	X

The quantifications of these partial conversion factors depend on the conditions which the material is exposed to during its service life, and can be found in [CUR-96+, 2012, section 2.5.3.2].

4.4 Limit states

In the Eurocode, a distinction is made between the ultimate limit state (ULS) and the serviceability limit state (SLS). The ULS concerns the safety of people and the structure, whereas the SLS concerns the functionality of the structure. Different levels of reliability may be adopted for both limit states, which is reflected in partial load factors as prescribed in [NEN-EN 1990, 2002].

4.4.1 Ultimate limit state

The ultimate state is a physical situation of a structure that involves excessive deformations leading to collapse of a component or the structure as a whole. In order to avoid this, the ULS should be respected considering the loss of equilibrium (stability), failure by excessive deformations (strength) and failure caused by fatigue.

4.4.1.1 Stability

This limit state considers the loss of static equilibrium of the structure or any part of it as a rigid body. Minor variations in the value or the spatial distribution of actions from a single source are significant. The strength of construction materials is generally not governing.

When considering a limit state of static equilibrium of the structure, it shall be verified that:

$$E_{d,dst} \leq E_{d,stb} \tag{4.16}$$

In which:

$E_{d,dst}$ *design value of destabilising actions*

$E_{d,stb}$ *design value of stabilising actions*

The design values of actions are derived by multiplication of permanent and variable actions with partial safety factors for favourable and unfavourable effects, according to [NEN-EN 1990, 2002, table A1.2(A)].

All elements of the structure have to be checked for the following failure modes:

- Rigid body movement
- Buckling
- Flexural-torsional buckling
- Lateral-torsional buckling
- Local instability

4.4.1.2 Strength

The strength limit state considers internal failure (rupture) or excessive deformations of the structure or structural members, in which the strength of construction materials is governing.

When considering the strength limit state, it shall be verified that:

$$E_d \leq R_d \tag{4.17}$$

In which:

E_d *design value of internal forces or moments*
R_d *design value of corresponding resistance*

The design values of actions are derived by multiplication of permanent and variable actions with partial safety factors, according to [NEN-EN 1990, 2002, table A1.2(B-C)]

All cross-sections of the structure have to be checked for the effects of:

- Axial tension
- Axial compression
- Bending moment
- Shear
- Torsion
- Any unfavourable combination of above mentioned

4.4.1.3 Fatigue

Repeated cyclic loading may lead to progressive and localised structural damage in the construction material. The formation of micro-cracks in the matrix or resin-fibre interface leads to the degradation of strength and stiffness properties of composites.

When considering the fatigue limit state, it shall be verified that the accumulated damage of the expected load spectrum does not exceed unity:

$$D = \sum_{i=1}^{k} \frac{n_i}{N_i} \quad \leq \quad 1.0 \tag{4.18}$$

In which:

n_i *number of contributing cycles at a constant stress reversal* S_i

N_i *number of cycles to failure of a constant stress reversal* S_i

Only cyclic loads with either of the following specifications have to be considered in the load spectrum [CUR-96+, 2012, section 6.4.1]:

$n_i > 1000$ *repeated over 1000 times during service life*

$\sigma_{max} > 0.4 \cdot f_y$ *absolute maximum stress over 40% of ultimate load*

4.4.2 Serviceability limit state

The serviceability limit defines the performance criteria beyond which the structure cannot fulfil its service requirements with respect to functionality, comfort and aesthetics. These requirements are generally expressed in limit states for deflections, vibrations and local defects (not jeopardising global structure).

4.4.2.1 Deflection

There is an ongoing debate on deflection criterions to be maintained in the design of composite structures. These serviceability criterions are usually governing in the design, due to the relatively low stiffness of glass fibre composites. In case of stringent deflection requirements, the strength potential of the material is not fully utilised. This results in a less economical structure, having an excessively high safety factor for ultimate limit states.

No norms exist that quantify the deflection limits for composite structures. Most research papers however obey the AASHTO[1] design guides for aluminium and concrete structures, which prescribe the following deflection limits:

Table 4.7: *AASHTO deflection limits for alumunium and concrete stuctures [AASHTO, 2013]*

Type of action	Support system	Deflection
Traffic	Simply supported	**L/800**
Traffic + pedestrian	Simply supported	**L/1000**
Traffic	Cantilever	**L/300**
Traffic + pedestrian	Cantilever	**L/375**

[1]American Association of State Highway and Transportation Officials

Other reports have suggested a less conservative deflection limit of L/400, as long as strains are limited to 20% of the composite's minimum guaranteed ultimate strength, in order to avoid long-term creep [O'Connor, 2013].

Another reference could be design codes for timber structures, which material properties are more in line with composites. The Dutch National Annex for the design of timber bridges prescribes the deflection limits as presented in table 4.8. Please note that these limits represent a deflection range due to variable traffic load only.

Table 4.8: *NEN deflection limits for timber bridges [NEN-EN 1995-2/NB, 2011, section 7.2]*

Type of action	Support system	Deflection
Traffic	Simply supported	**L/400**
Traffic + pedestrian	Simply supported	**L/200**

Transverse stiffness In addition to global deflection limits, requirements to the gap between bridge and abutment are prescribed in [NEN-EN 1993-2/NB, 2011, table NB.4]. The vertical clearance, which is largely determined by the transverse stiffness of the bridge, should be limited to 5 millimetres to ensure a smooth transition for traffic.

4.4.2.2 Vibration

Understanding and controlling the dynamic performance is gaining importance as ever more innovations are implemented in bridge engineering. New structural shapes and construction materials are employed to comply with increased demands to design bridges with high aesthetic appeal and economic performance. These innovations call for a more rigorous dynamic assessment, as codified pseudo-static load factors and empirical rules may not be sufficient to ensure stability [Parke and Hewson, 2008].

Dynamic analysis of bridge structures basically comes down to establishing the characteristics of cyclic actions, induced by either human or natural forces. A frequency domain analysis of the structure can be performed by finite element software. Subsequently, it has to be assured that the natural frequencies of the structure's modal shapes do not coincide with those of the actions in order to comply with serviceability and ultimate limit states.

Dynamics of composites The dynamic response of bridges depends on the structure's mass, stiffness and damping properties. For composites, the characteristics of these parameters are significantly different from conventional construction materials. In a comparative study by [Zhang et al., 2006] between the dynamic performance of composite and concrete bridge decks, it was concluded that the dynamic impact factors as specified by AASHTO are safe to be applied to composite bridges. The accelerations of the composite bridge are however significantly higher compared to an equivalent concrete variant, which may affect long-term durability and comfort of users. Due to the lower mass of the composite structure, the natural frequencies of the modal shapes are higher.

As with all material properties, the damping of fibre composites is largely influenced by the fibre fraction and orientation. Generally, the dissipation of energy is higher the direction perpendicular to the fibre orientation, in which case the damping is dominated by the polymeric matrix. It was found that the damping properties of composites can be readily predicted by application of the the laminate theory [Adams and Maheri, 2003].

Dynamic behaviour is also influenced by the applied joint type. As mechanical joints exhibit friction during movement, higher damping ratios can be achieved when using bolted instead of bonded joints. On the other hand, the lowest natural frequency also becomes smaller, which may have a detrimental or favourable effect depending on the nature of the actions [Bai and Keller, 2008].

Wind induced vibration Slender structures are generally more susceptible to lower frequency actions, in which case the aerodynamic response of the structure can be significant. Wind actions induce deflections, which alter the flow pattern around the structure. The coupling of motion and aerodynamic forces causes dynamic instability. A limited amplitude response may cause people to feel unsafe, and can also result in overstress or fatigue damage to the structure. However if the response causes a divergent amplitude, a catastrophic collapse will be the result. A famous example is the Tacoma Narrows Bridge, which collapsed in 1940 due to classical flutter.

The susceptibility of structures to aerodynamic forces depends on many factors and is difficult to predict in the design phase. The Eurocode indicates that a dynamic response procedure for wind loads is generally not needed for 'normal bridges' with a span of less than 40 meters. A bridge is categorised as normal if its shape of cross-sections and construction material are conventional. Hence, a fibre composite bridge will always require verification of dynamic stability.

The Eurocode presents criteria to assess the susceptibility of a structure to different types of instability caused by wind actions [NEN-EN 1991-1-4, 2005, Annex E] . If these criteria are met, it is recommended to acquire a specialist's advice. A specialist will then assess the aerodynamic properties of the structure by wind tunnel testing or computer modelling.

Traffic and pedestrian induced vibration Due to the configuration and mass of typical highway bridges, the traffic induced vibrations are generally not detrimental to these structures. This may however be different for lightweight composite bridges. Therefore it should be assessed how the structure will respond to frequencies of a typical traffic spectrum of cars and trucks. The imposed vibrations are generally within a frequency range of 5 to 25 Hz. Furthermore, it has been found that the smoothness and state of the running surface of the bridge has a major influence on the dynamic effects of traffic.

Pedestrian traffic can pose a considerable dynamic loading on slender or lightweight bridges, having a lateral or torsional natural frequency below 1.5 Hz. Groups of people, for example during a sports event or parade, tend to synchronise and adjust their pace to the initial lateral vibration of the structure to maintain balance. This 'synchronous lateral excitation' excites the structure in its natural frequency, providing a positive feedback to the initial sway. This type of dynamic loading caused the Millennium Bridge in London to heavily excite right after opening. Tuned mass dampers had to be installed in order to reduce the effects of synchronous excitation, which cost an additional 5 million pounds. These design flaws should be avoided by checking the dynamic response of the bridge in the design phase [Parke and Hewson, 2008, p 138].

The Eurocode prescribes serviceability limits for the deformations and vibrations road- and footbridges [NEN-EN 1990/A1, 2006, section A2.4.2]. The dynamic response of the bridge to traffic should be verified with respect to the uplift of the bridge deck at the supports, as well as damage to the structural bearings. Limits to ensure the comfort of pedestrians is more stringent; the following maximum accelerations should be enforced:

0.7 $[m/s^2]$	*vertical vibrations*
0.2 $[m/s^2]$	*horizontal vibrations*
0.4 $[m/s^2]$	*exceptional crowd loading*

These comfort criteria only have to be verified if the fundamental frequencies of the deck are less than:

5 $[Hz]$	*vertical frequency*
2.5 $[Hz]$	*lateral and torsional frequencies*

4.5 Computer-aided design tools

The structural design of composites is an interactive process in which the material design, the structural design and the manufacturing process must be considered simultaneously. For practical reason, the design process generally starts at a high level and iterates towards a low-level detailed design. Different commercial software packages are available to support the engineer in each of the four design stages that can be identified [Meunier and Knibbs, 2007]:

- Conceptual design
- Detailed structural design
- Design for manufacture
- Design for production

Different design tools should be used in different stages of the design process. Some of the industry leading tools are compared in appendix A.

4.5.1 Laminate design tools

Laminate design tools enable engineers to carry out ply calculations and subsequently design and evaluate laminates.

4.5.1.1 Ply calculation

One of the first key steps in composite design is establishing the engineering constants and the thermal and hygrothermal expansion coefficients of each of the plies. Preferably, this data is determined by coupon tests. If test data is not readily available, one can call on data that is gathered in databases. As a last resort, the engineering constants can be derived from the micromechanic theories, as discussed in section 3.3.1. The ply calculation modules of the laminate design tools allow the engineer to easily apply the theories on different ply configurations.

4.5.1.2 Laminate design

Optimisation of the laminated composite can be a time consuming procedure. Laminate design tools aim at simplifying this optimisation process. The engineer can specify design constraints in terms of weight, cost, geometry, strength and deformation. Based on these constraints, the software identifies complying laminates that are constructed from the selected ply material.

4.5.1.3 Laminate evaluation

The behaviour of the selected laminate can evaluated for in- and out-of-plane loads. The analysis is based on the classical laminate theory, as discussed in section 3.3.2. The software can present the result layer-by-layer, which enables the engineer to tailor the stacking sequence. The failure theories, as discussed in section 3.3.3, are used to verify at which load the first ply fails. Most software packages can furthermore compute the additional load carrying capacity up to last-ply-failure.

Some packages have additional modules to carry out hygrothermal stress analysis, moisture diffusion prediction, heat conductivity analysis, fatigue analysis and progressive crack prediction [Meunier and Knibbs, 2007].

4.5.2 Analytical design tools

Some laminate design tools are equipped with code to provide solutions to problems where an exact elastic analytical solution exists. These tools can assist in the conceptual design by providing insight in the deformation, buckling and dynamic behaviour of composite elements, such as plates, beams, tubes, shells and sandwich panels. Some packages are furthermore able to analytically determine the strength of bonded and bolted joints.

The combination of an analytical and laminate tool can help the engineer establish a conceptual design. The loads from the analytical tool are used as input for the laminate tool, which determines the strains and stresses in the plies. Based on the results of the failure theories, the laminate can be optimised [Meunier and Knibbs, 2007].

4.5.3 Finite element software

It is common practice to verify and optimise the conceptual design using finite element software. Also for composites, most traditional FEA code can be used as long as it is able to handle orthotropic plates. The laminate will have to be simplified into a homogeneous orthotropic plate by assuming a perfect bond. As only special symmetric laminates can be analysed this way (in which extorsional and flexural behaviour is uncoupled), the design may not be fully optimised. Furthermore, the first-ply-failure will have to be evaluated by hand or by feedback to a laminate design tool.

For more accurate and convenient designing, most of the major FEA packages nowadays offer modules to handle composite material. Special meshing elements are developed to consider the plies individually and in their interaction with the load conditions. Furthermore the composite material failure criteria are included, and specific failure modes such as delamination and impact damage can be evaluated. Many programs have support for pre- and post-processors for more laminate input or interpretation of results [Meunier and Knibbs, 2007].

4.5.4 Production design tools

In the design of complex shapes, the manufacturability plays a major design role. Production design tools allows to drape a laminate over a CAD shape to simulate the manufacturing lay-up. The software indicates impossible curvatures and generates folds and darts to allow for a better fit of the fabric around the model.

Once the design is completed and verified the software exports the model as ply books and template drawings, which are used during the manufacturing process [Meunier and Knibbs, 2007].

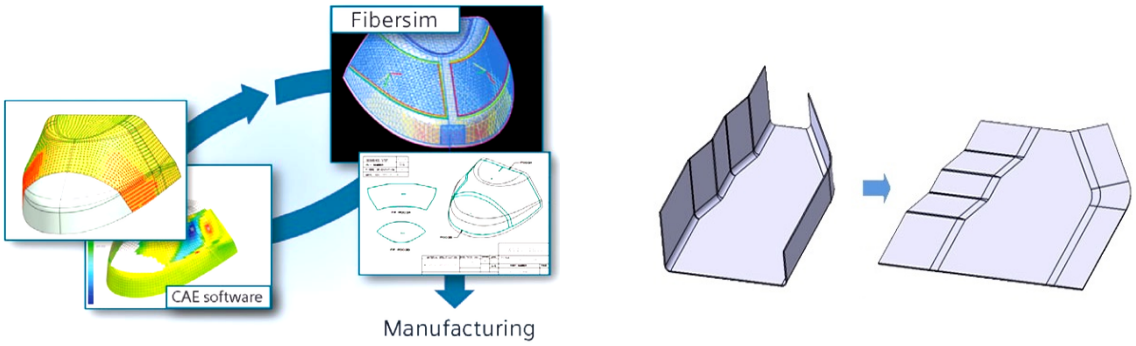

(a) Fibersim workflow

(b) Part flattening in CATIA

Figure 4.5: *Production design tools for composite structures [Meunier and Knibbs, 2007]*

Part II

Design study

5 Quantification of design input

5.1 Rehabilitation philosophy

As discussed in section 3.2, fibre reinforced composites can be utilised to strengthen, rehabilitate or replace structurally deficient bridges. Strengthening and rehabilitation are proven concepts in the field of movable bridges, potentially extending the service life of a structure by some decades. Many reference projects are available, and the design is relatively straightforward. The solutions are generally easy to implement, and require relatively minor investments. The most common rehabilitation technique is the application of a new composite deck panels on top of the existing steel superstructure, as discussed in section 3.2.2.2.

In the scope of this thesis however, it is decided to focus on the complete replacement of the superstructure and operation system. This is a major operation, but might prove to be cost effective as the service life can be extended by many decades. In order to control the initial investment, the aim is to retain the substructures at the abutments of the bridge. Components such as the bascule chamber and the live load pier are composed of concrete, and are generally in much better condition than the steel components.

Retaining the substructure does however impose strict boundary conditions to the rehabilitation project. First of all, the global geometry of the bridge is retained; the span- and tail length of the bridge are more or less fixed. Secondly, it should be ensured that the forces introduced in the substructure are not increased with respect to the current situation. Special attention should be given to the shear capacity of the concrete structures, as this aspect was often overestimated in structures originating from before the 70's [Rijkswaterstaat, 2007]. Some minor modifications may prove to be necessary, but total reconstruction of the concrete parts should be avoided. Lastly, it should be considered to what extend the operational- and safety systems can be reused. Retaining these restricts the design freedom even further.

5.2 Boundary conditions

The focus in this thesis is on bascule bridge structures within the main road network of the Netherlands, originating from the 60's and 70's of the last century, as many of these structures are subject to imminent rehabilitation.

In order to be able to quantify some basic boundary conditions, the 'Koningin Julianabrug' in Alpen aan den Rijn is used as a reference bridge. Some design parameters have been (conservatively) truncated for simplicity.

5.2.1 Geometrical

As indicated, only minor modifications to the substructure are allowed. Next to that, the connection from the abutments to the bridge should be smooth with respect to both height and width. Lastly, the clearance for vessels (in closed position) may not be reduced with respect to the current situation. These requirements impose the following geometrical boundary conditions to the new superstructure. A graphical representation of the geometrical boundary conditions is included in appendix B.1.

- Width $W = 15.0\ [m]$
- Approximated distance between pivot axis and support $L = 16.0\ [m]$
- Span between both abutments $L_1 = 14.3\ [m]$
- Bascule chamber internal length $L_{int} = 7.5\ [m]$
- Bascule chamber internal height $H_{int} = 6.5\ [m]$
- Structural height between supports $H = 1.1\ [m]$

5.2.2 Weight

To avoid strengthening of the substructure, it is determined that the weight of the superstructure may be increased by a maximum of 5%. The total weight of the current structure, including both the span, tail and counterweight, is estimated to be 156 metric tons. The weight of the steel span, including the pivot axis, is estimated at 61 tons.

5.2.3 Reliability

The economic and social consequences of the failure of malfunction of the structure are considerable. Therefore, the reliability of the structure must be in accordance with the CC2 consequence class, as determined by [NEN-EN 1990/NB, 2011, table NB.20].

5.2.4 Operational- and stability systems

The operational- and stability systems are considered not to be in good enough condition to be retained, and shall thus be taken into account in the design.

5.3 Functional requirements

The functional requirements define the required behaviour of the structure. Together with the boundary conditions, the functional requirements define the design space for the new bridge.

5.3.1 Spatial demands

5.3.1.1 Traffic

The bridge should be able to accommodate vehicular-, cycle- and pedestrian traffic. Each of these traffic flows should have a single lane in both directions. In the current situation, there is a pedestrian lane at either side of the bridge. The design speed of the vehicular traffic is set at 50 km/h.

The following minimum widths are prescribed in the Dutch recommendations for road geometry [Stichting CROW, 2012]:

- Double-lane vehicular traffic 6.0 $[m]$
- Safety barrier at either side of double-lane 0.5 $[m]$
- Double-lane cycle path 3.0 $[m]$
- Pedestrian lane 1.5 $[m]$

The summation of these widths reveals that the transverse profile easily fits within the geometrical boundary conditions. The residual width can be used for physical barriers to separate vehicular traffic from cyclists and pedestrians, windshields and other road furniture.

5.3.1.2 Vessels

The horizontal and vertical clearance for vessels in both closed- and opened position of the bridge must (at least) be retained with respect to the current situation.

In closed position, this is achieved by maintaining the current level of the supports and geometries of the superstructure. In the opened position, the horizontal clearance is unrestricted. The vertical clearance is determined by the length between both abutment piers, and the angle of rotation of the opened span. In the current situation, this angle has a maximum of $\theta = 85°$.

5.3.2 Balance

The distance between the pivot axis and the gravitational axis determines the magnitude of the intentional imbalance of the structure, and should follow from the stability requirements. If the intentional imbalance provides insufficient resistance to counteract the uplifting effects, an additional 'setting force' can be applied at the tail-side of the bascule. The Dutch regulations for the design of movable bridges (VOBB) requires a minimum total pre-pressure at the supports of 20 kN for movable traffic bridges [NEN 6786, 2001, section 9.9].

In order to allow for recalibration of the balance during the service life of the bridge, the counterweight must be adjustable by at least 5% with respect to the initial weight.

5.3.3 Deflections

Based on considerations as discussed in section 4.4.2.1, both a global and a local criterion is drafted for the maximum deflection in the serviceability limit state.

5.3.3.1 Global deflection

For the maximum global deflection a value of L/400 is maintained, in accordance with the deflection limit for timber bridges as prescribed by the Eurocode. Considering the geometry of the structure, this comes down to a total deflection of 40 millimetres in closed position.

As no people are present on the deck during opening/closing cycle of the bridge, the deflection requirement can be less strict. It is chosen to limit the global deflection of the cantilever construction to L/250, which comes down to 64 millimetres.

5.3.3.2 Transverse deflection

The vertical clearance between the bridge span and the abutment should be limited in order to assure a smooth transition for vehicular traffic. The deflection of the bridge at the line joints at either abutment side of the bridge should be limited to a maximum of 5 millimetres.

5.3.4 Vibrations

Based on the dynamic behaviour of composite material, as discussed in section 4.4.2.2, it is chosen to follow the Eurocode requirements for steel traffic/pedestrian bridges. The fundamental frequencies of the structure should be smaller than:

- Vertical frequency 5 $[Hz]$
- Lateral and torsional frequencies 2.5 $[Hz]$

Modal shapes may only exceed these limit frequencies if the response of the structure is limited to the following accelerations:

- Vertical vibrations 0.7 $[m/s^2]$
- Horizontal vibrations 0.2 $[m/s^2]$
- Exceptional crowd loading 0.4 $[m/s^2]$

5.3.5 Durability

5.3.5.1 Design service life

According to the Eurocode, the design service life of common civil engineering structures should be within 50 to 100 years [NEN-EN 1990, 2002, Table 2.1]. Under normal conditions, only minor repair and maintenance shall be required within this period.

In order to achieve this durability requirement, partial safety factors are introduced in the structural design. On the resistance side, a material factor is introduced to account for uncertainties in the derivation of section characteristics, as discussed in section 4.3.1. In addition, conversion factors are introduced to account for the degradation of material properties over time, resulting from influences of temperature, moisture, creep and fatigue, as discussed in section 4.3.2. On the action side, load factors are introduced to account for uncertainties in representative loads.

5.3.5.2 Damage tolerance

Structural damages due to the effects of environmental conditions and accidental actions can be acceptable up to a certain level, depending on the probability and consequences of occurrence.

Major damage in rare cases can be accepted, provided that there is a fail-safe mechanism. As mentioned in section 4.2.8, the risks associated with accidents can be mitigated to acceptable levels by preventing actions from happening, and by protecting the structure against its effects.

No damage tolerated Actions that may not result in structural damage include:

- Sunlight; UV-radiation and high temperatures
- Rainwater; hydrolysis and osmosis
- Chemicals; de-icing salts and small amount of aggressive chemicals
- Temperature fluctuations
- Frost
- Impact; runway debris, dropped tools, falling cargo
- Vehicle on cycle/pedestrian track

Minor damage tolerated Actions that may result in damage that can easily be repaired include:

- Fire; small vehicle
- Impact; traffic accident
- Vandalism

Major damage tolerated Actions that may result in damage that requires major restoration include:

- Impact by ship
- Fire; fuel-tank, ship
- Other catastrophes

5.3.5.3 Maintenance

To make up for the (potentially) higher initial cost of a composite structure, the required maintenance during the service life should be small compared to traditional materials.

Inspection On completion of the structure, and at predetermined intervals, all structural composite components should be given a full visual inspection. This inspection should be easy to execute, which can be achieved by ensuring accessibility of these parts.

Surface treatment By application of a proper surface finish, composite elements will not require any paint or preserving measures. If a colour is however desired for aesthetic reasons, pigments can be added to the resin material at the surface laminate.

If considered necessary, composite surfaces can be cleaned with detergent and water. Wire wool and coarse abrasives shall not be used, and the cleaning agents shall be approved by the resin manufacturer. Corrosion of mechanical joints should be avoided by making use of stainless steel fasteners [Clarke, 1996].

5.3.6 Operational

5.3.6.1 Movement

The duration of the opening/closing cycle, as prescribed by [NEN 6786, 2001], depends on the surface of the leaf. The reference bridge has a total surface of 240 m^2, resulting in the specifications listed below. Furthermore, in case of emergency, the nominal movement of the bridge should be brought to arrest within a specified time interval.

- Total time for single rotation movement $t_{tot} = 60\ [s]$
- Acceleration time $t_{acc} = 12\ [s]$
- Deceleration time $t_{dec} = 12\ [s]$
- Emergency stop time $t_{stop} = 6\ [s]$

5.3.6.2 Reliability

As discussed in section 4.2.4.3, the serviceability requirements of movable bridges depend on both the importance of the waterway and the vertical clearance in closed position of the bridge. The reference bridge spans a main waterway, and has a clearance of approximately 5 meters in closed position. According to table 4.4, the bridge is allowed to be out of service for only 0.5 days per year.

This requirement partly determines the design mean hourly wind speed, which the opened structure should be able to withstand. Next to that, the reliability of the mechanical systems must be in accordance with this requirement.

5.4 Actions

The relevant permanent, variable and accidental actions have been identified in section 4.2. In this section, the actions will be quantified with respect to the reference bridge. The presented values are characteristic, and should be multiplied by load factors for limit state validation (see section 5.4.6.1).

5.4.1 Traffic

The different traffic load models have been discussed in section 4.2.2. The considered load models are projected on the reference bridge, and are depicted in appendix B.2.

5.4.1.1 Load Model 1

LM1 consists of a concentrated double-axle load system and a simultaneously acting uniformly distributed load. The driving lane is divided in two 3-meter wide notional lanes on which the following loads have to be applied. The most conservative value for α_Q is chosen, as prescribed by [Rijkswaterstaat, 2013b]. The application of LM1 is depicted in fig. 4.1.

$$\begin{aligned} Q_{LM1,1} &= \alpha_Q \cdot Q_{1k} = 1.0 \cdot 300 = \quad 300\ [kN] \\ Q_{LM1,2} &= \alpha_Q \cdot Q_{2k} = 1.0 \cdot 200 = \quad 200\ [kN] \\ q_{LM1,1} &= \alpha_q \cdot q_{1k} = 1.15 \cdot 9.0 = \quad 10.35\ [kN/m^2] \\ q_{LM1,2} &= \alpha_q \cdot q_{2k} = 1.15 \cdot 2.5 = \quad 2.88\ [kN/m^2] \end{aligned} \tag{5.1}$$

5.4.1.2 Load Model 2

LM2 consists of a concentrated single-axle load system, which includes a dynamic amplification factor. The load system should be applied at any location on the carriageway, in order to check for local effects. Where relevant, only a single wheel of half the axle load should be used if this is unfavourable. The adjustment factor β_Q is taken equal to α_{Q1}, as prescribed in [NEN-EN 1991-2/NB, 2011]. The application of LM2 is depicted in fig. 4.2.

$$Q_{LM2} = \beta_Q \cdot Q_{a,k} = 1.0 \cdot 400 = 400\ [kN] \tag{5.2}$$

5.4.1.3 Load Model 4

LM4 consists of a uniformly distributed load, applied at all relevant parts of the bridge; including carriageway, cycle- and pedestrian paths and central reservations. The load system accounts for crowd loading during special occasions, and includes a dynamic amplification factor.

$$q_{LM4} = 5.0\ [kN/m^2] \tag{5.3}$$

5.4.1.4 Horizontal loads

The horizontal loads from braking and acceleration of vehicular traffic is accounted for by a load model consisting of a distributed force acting in the longitudinal direction of the bridge.

$$\begin{aligned} F_{hor} &= 0.6 \cdot \alpha_{Q1} \cdot (2 \cdot Q_{1k}) + 0.1 \cdot \alpha_{q1} \cdot q_{1k} \cdot w_1 \cdot L \\ &= 0.6 \cdot (2 \cdot 300) + 0.1 \cdot 1.15 \cdot 9.0 \cdot 3.0 \cdot 16.0 = 410\ [kN] \end{aligned} \tag{5.4}$$

5.4.1.5 Footways and cycle tracks

The loads on footways and cycle tracks are accounted for by three mutually exclusive load models, consisting of a uniformly distributed load q_{fk}, a concentrated load Q_{fwk} and a double-axle load representing a service vehicle Q_{serv}. The uniformly distributed load is quantified by using the influence length of the reference bridge; $L = 16.0$ m. The application of the loads is prescribed in section 4.2.2.6.

$$\begin{aligned} q_{fk} &= 2.0 + \frac{120}{L+30} = && 4.6\ [kN/m^2] \\ Q_{fwk} &= && 7.0\ [kN] \\ Q_{serv} &= && 25\ [kN] \end{aligned} \tag{5.5}$$

5.4.1.6 Multi-component action

The simultaneous occurrence of traffic loads is taken into account by multi-component models, which are defined in [NEN-EN 1991-2/NB, 2011, Table NB.3]. The components of the traffic load combinations are summarised in the following table. The occurrence of the traffic load combinations is mutually exclusive, but should be considered in combination with non-traffic loads as defined in section 5.4.6

Table 5.1: *Multi-component actions for traffic loads [NEN-EN 1991-2/NB, 2011, Table NB.3]*

	Load combinations				
	gr1a	gr1b	gr2	gr3	gr4
LM1	**1**		**0.8**		
LM2		**1**			
LM4					**1**
Horizontal	**0.8**		**1**		
Foot & cycle	**0.4**		**0.4**	**1**	**1**

Multi-component model 'gr5' will not be used in the design, as the special vehicles for LM3 are not defined in the functional requirements.

5.4.2 Wind

This section quantifies the wind load models, as discussed in section 4.2.4.

5.4.2.1 Transverse direction

The wind load in transverse direction on the reference bridge is modelled by:

$$\begin{aligned} F_{w,x} &= \frac{1}{2} \cdot \rho \cdot v_b^2 \cdot C_x \cdot A_{ref,x} \\ &= \frac{1}{2} \cdot 1.25 \cdot 29.5^2 \cdot 1.577 \cdot 49.6 = 42.5\ [kN] \end{aligned} \tag{5.6}$$

Basic wind speed The basic wind speed depends mainly on wind area classification at the location of the bridge. As the design should be applicable throughout the whole country, the most conservative wind area is chosen as design input; level I. In reality, the location of the reference bridge (Alphen aan den Rijn) is classified as a level II wind area. The directional- and season factor are prescribed to be equal to unity by the [NEN-EN 1991-1-4/NB, 2011].

$$v_b = c_{dir} \cdot c_{season} \cdot v_{b,0} = 29.5\ [m/s] \tag{5.7}$$

Wind load factor The reference bridge is positioned at a height of approximately 5 meters above the water level. The peak velocity pressure q_p at this height in wind area I is determined from [NEN-EN 1991-1-4/NB, 2011, table NB.5]:

$$q_p = 0.78\ [kN/m^2] \tag{5.8}$$

The exposure factor is given by:

$$c_e = \frac{q_p}{\frac{1}{2} \cdot \rho \cdot v_b^2} = \frac{780}{\frac{1}{2} \cdot 1.25 \cdot 29.5^2} = 1.434\ [-] \tag{5.9}$$

The force coefficient factor depends on the shape of the bridge, and is determined from [NEN-EN 1991-1-4, 2005, figure 8.3]. The height of the bridge is the summation of the structural height of 1.1 meter and a traffic band of 2 meter height:

$$c_{f,x} = 1.1\ [-] \tag{5.10}$$

The wind load factor in the transverse direction of the bridge is the product of the exposure factor c_e and a force coefficient factor $c_{f,x}$:

$$C_x = c_e \cdot c_{f,x} = 1.577\ [-] \tag{5.11}$$

Reference area The reference area of the bridge is the surface on which the wind pressure acts. This surface is equal to the product of the bridge length and structural height, plus an additional traffic band of 2 meters high.

$$A_{ref,x} = L \cdot (H + 2.0) = 49.6\ [m^2] \tag{5.12}$$

5.4.2.2 Vertical direction

The wind load in vertical direction, causing an uplifting force on the closed bridge structure, is modelled by:

$$\begin{aligned} F_{w,z} &= \frac{1}{2} \cdot \rho \cdot v_b^2 \cdot C_z \cdot A_{ref,z} \\ &= \frac{1}{2} \cdot 1.25 \cdot 29.5^2 \cdot 1.291 \cdot 240 = 168.5\ [kN] \end{aligned} \tag{5.13}$$

Wind load factor The wind load factor in the vertical direction of the bridge is the product of an exposure factor c_e and a force coefficient factor $c_{f,z}$. The exposure factor remains equal to that calculated in eq. (5.9). The force coefficient factor is taken equal to a conservative value of 0.9, so that the wind load factor is:

$$C_z = c_e \cdot c_{f,z} = 1.291\ [-] \tag{5.14}$$

Reference area The reference area of the bridge is the surface on which the uplifting wind pressure acts, which is equal to the footprint of the bridge:

$$A_{ref,z} = L \cdot W = 240\ [m^2] \tag{5.15}$$

5.4.2.3 Longitudinal direction

Closed state In the closed state of the bridge, the wind force in the longitudinal direction of the bridge is modelled as a percentage of the wind force in transverse direction:

$$F_{w,y,closed} = 0.4 \cdot F_{w,x} = 17\ [kN] \tag{5.16}$$

Opened state During the operational cycle, the bascule bridge structure has to be designed in accordance with [NEN 6786, 2001]. As determined in the functional requirements, the bridge is allowed to be out of service for only 0.5 days per year (see section 5.3.6.2). Based on this reliability requirement and the classification of the wind area, the design mean hourly wind speed at 10 meter above surface level U_R can be determined from [NEN 6786, 2001, table 3].

$$U_R = 18.1\ [m/s] \tag{5.17}$$

Using this value, the wind pressure at the tip of the leaf is calculated by eq. (4.10):

$$p_w = \frac{1}{2} \cdot 1.25 \cdot \left\{ 18.1 \cdot \frac{\ln\left(\frac{5+16}{0.1}\right)}{\ln\left(\frac{10}{0.1}\right)} \right\}^2 \cdot \left\{ 1 + \frac{7}{\ln\left(\frac{5+16}{0.1}\right)} \right\} = 637.4\ [N/m^2] \tag{5.18}$$

This pressure has to be taken constant over the total height of the leaf, which gives the following resultant force acting at the centre of the reference area:

$$F_{w,y,opened} = 153.0\ [kN] \tag{5.19}$$

5.4.3 Snow

The snow load models has already been quantified in section 4.2.5:

$$P_{sn} = 0.1\ [kN/m^2] \tag{5.20}$$

5.4.4 Thermal

This section quantifies the thermal load models, as discussed in section 4.2.6. Only the uniform temperature component and the linear vertical temperature component will be considered.

5.4.4.1 Uniform temperature component

As composites are not considered in the Eurocode, the thermal models for steel bridges (type 1) are used. The minimum and maximum uniform temperature components of the bridge are correlated to the minimum and maximum air temperatures in the shade by [NEN-EN 1991-1-5/NB, 2011, figure NB.1]:

$$\begin{aligned} T_{e,max} &= T_{max} + 16 = \quad 46\ [^\circ C] \\ T_{e,min} &= T_{min} - 3 = \quad -28\ [^\circ C] \end{aligned} \tag{5.21}$$

The characteristic value of the range of uniform bridge temperature component is thus:

$$\Delta T_N = T_{e,max} - T_{e,min} = 74\ [^\circ C] \tag{5.22}$$

5.4.4.2 Linear vertical temperature component

The characteristic temperature range between the upper- and lower fibre in the cross-section of a bridge structure, having a surface layer of 50 mm, is determined by [NEN-EN 1991-1-5/NB, 2011, table NB.1]:

$$\begin{aligned} \Delta T_{M,heat} &= \quad 18\ [^\circ C] \quad && \textit{Top surface warmer than bottom} \\ \Delta T_{M,cool} &= \quad 13\ [^\circ C] \quad && \textit{Bottom surface warmer than top} \end{aligned} \tag{5.23}$$

5.4.5 Accidental

This section quantifies the three accidental actions that have been identified in section 4.2.8. Note that these actions are mutually exclusive.

5.4.5.1 Emergency stop

As specified in section 5.3.6.1, the nominal movement of the bridge should be decelerated to zero within a time span of 6 seconds. The mechanical breaks impose a torque to the structure, dependent of the nominal angular speed and mass moment of inertia of the structure. The nominal angular speed of the bridge, given that the opening angle is $\theta = 85°$:

$$\omega_{nom} = \frac{\theta}{t_{tot} - \frac{1}{2} \cdot t_{acc} - \frac{1}{2} \cdot t_{dec}} = 3.1 \cdot 10^{-2}\ [rad/s] \tag{5.24}$$

The constant deceleration to arrest this movement within the specified time span is:

$$\alpha_{stop} = \frac{\omega_{nom}}{t_{stop}} = 5.2 \cdot 10^{-3} \; [rad/s^2] \tag{5.25}$$

The mass moment of inertia of the bascule structure, with respect to the pivot axis, can be calculated when the total mass of the structure and counterweight (m) and the distance from pivot axis to the gravitational centre (r) are known:

$$I_m = m \cdot r^2 \tag{5.26}$$

The imposed bending moment by the emergency stop is given by:

$$M_{stop} = I_m \cdot \alpha_{stop} \tag{5.27}$$

5.4.5.2 Impact by ship

The Eurocode prescribes an equivalent static force from the impact of a ship. This force is uniformly distributed over a rectangular surface of 0.25 m height and 3.0 m width [NEN-EN 1991-1-7, 2006, section 4.6.2]:

$$F_{ship} = 1000 \; [kN] \tag{5.28}$$

Note that the functional requirements (section 5.3.5.2) prescribe that major damage to the structure is tolerated after the impact of a ship.

5.4.5.3 Vehicle on footway or cycle tracks

Apart from an occasional service vehicle, the structure must be able to withstand the load of a vehicle that accidentally left the roadway. The axle load corresponds to a tandem system at lane number 2 of LM1 (see section 4.2.2.1):

$$\begin{aligned} Q_{accident} &= Q_{LM1,2} = \alpha_{Q2} \cdot Q_{2k} \\ &= 1.0 \cdot 200 = 200 \; [kN] \end{aligned} \tag{5.29}$$

The accidental load has been included in the projection of load models on the reference bridge, as depicted in appendix B.2. Note that the position of the load system becomes less extreme if physical barriers are applied.

5.4.6 Load combinations

The multi-component actions for traffic, as given in table 5.1, can be extended to account for the simultaneous occurrence of traffic and non-traffic actions.

Table 5.2: *Load combinations for traffic bridges [NEN-EN 1990/NB, 2011, table NB.16]*

	Load combinations								
	gr1a	gr1b	gr2	gr3	gr4	W	T	S	A
Self-weight	**1**	**1**	**1**	**1**	**1**	**1**	**1**	**1**	**1**
LM1	**1**		**0.8**			**0.8**	**0.8**		**0.8**
LM2		**1**							
LM4					**1**				
Horizontal	**0.8**		**1**			**0.64**	**0.64**		**0.64**
Foot & cycle	**0.4**		**0.4**	**1**	**1**	**0.32**	**0.32**		**0.32**
Wind	**0.3**		**0.3**			**1**	**0.3**		
Temperature	**0.3**		**0.3**		**0.3**	**0.3**	**1**		
Snow								**1**	
Accidental									**1**

5.4.6.1 Design load combinations

All actions and load combinations have been defined by using characteristic values. In order to obtain a sufficient degree of reliability to comply with the specified consequence class of the structure, these characteristic values have to be multiplied by load factors. As discussed in section 5.2.3, the consequence class of the reference bridge is set at CC2, resulting in the following load factors for the verification of the ultimate limit states [NEN-EN 1990/NB, 2011, table NB.13]:

$$\begin{aligned}
&\gamma_{G,sup} = 1.30 && \textit{for unfavourable permanent actions}\\
&\gamma_{G,inf} = 0.90 && \textit{for favourable permanent actions}\\
&\gamma_{Q} = 1.35 && \textit{for unfavourable variable actions}\\
&\gamma_{Q} = 0 && \textit{for favourable variable actions}\\
&\gamma_{A} = 1.50 && \textit{for accidental actions}
\end{aligned} \tag{5.30}$$

For serviceability limit state verifications, the load factors should be taken equal to unity.

5.5 Material

In order to make the composite design a viable alternative to a traditional design, the main challenge lies in optimising the structure with respect to cost, while being in compliance with the functional requirements and boundary conditions. The selection of production technique and the composition of the fibre reinforced polymer material are the most essential parameters that determine the efficiency of the structure.

It should be noted that the term 'cost' refers not only to the initial investment, but rather the total cost of ownership over the service life of the structure. Optimising with respect to cost thus means finding the optimum in material- and manufacturing cost, assembly, service life, maintenance- and repair requirements and energy consumption.

5.5.1 Structural shape

Driven by both structural and non-structural considerations, there is a tendency in the composite industry to move away from linear construction elements, and to adapt surface shaped elements (see section 3.2.3). As the material cost generally dominate the initial investment, material-adapted concepts aim at reducing the structure's complexity and minimising the use of high grade (expensive) material in sections where it is not strictly required.

The bridge structure, which is mainly loaded by out-of-plane actions, has to cope with high flexural- and shear stresses. Sandwich elements have proven to be very efficient under flexural loading, utilising the full potential of the composite material (see fig. 3.15). High-grade material (composite laminate) is positioned in the high flexural stress region, while low-grade core material acts as a spacer for the face sheets. The shear loads are either transferred by composite webs, or by the core material. In the first case, the core material provides stability agains buckling of the webs. In the second case, higher-grade material must be applied for the core to allow for the transfer of shear stresses.

The most efficient cross-sectional shape and associated materials should be evaluated in the design stage.

5.5.2 Production techniques

The choice to use sandwich elements reduces the number of suitable production methods. The available techniques have to be compared by their limitations with respect to geometrical flexibility, finishing requirements, quality assurance, fibre volume fraction, tolerances and equipment- and production cost.

The most suitable techniques to produce large hollow or core-filled plate-shaped elements are hand lamination, pultrusion and closed-mould resin transfer processes (such as VARTM, vacuum- or pressure bag).

5.5.2.1 Comparison

As can be seen from table 5.3, the properties of hand lamination and pultrusion techniques are opposite poles. It is clear that hand lamination is very suitable for a wide range of single-unit products, whereas pultrusion is suitable for high volumes of specific products. Closed-mould techniques offer properties that are somewhat in between these two extremes.

Table 5.3: *Qualitative comparison between relevant production techniques [CUR-96, 2003; Kolstein, 2008]*

	Production technique		
	Hand lamination	Pultrusion	Closed mould
Fibre fraction			
Size limitation			
Geometrical flexibility			
Detail tolerance			
Quality assurance			
Equipment cost			
Production cost			

The main problem with hand lamination is the relatively low achievable fibre fraction (40 to 50%), and lack of quality assurance. These two reasons make that the technique is not very suitable for a high-performance bridge.

Pultrusion on the other hand can offer high-quality products, with fibre fractions ranging from 60 to 70%. The main issue is the size limitation of the panels, which ranges up to 1 meter in width. The implies that many joints will be required to assemble the structure, which drives the installation and maintenance cost and offers a lower durability. Next to that, the joints will inevitably result in a less efficient structure.

Closed-mould techniques can be used to process unitised full-size bridges, which do not exhibit any joints (see section 3.2.3.2). The fibre volume fractions range between 50 and 60%. There is a high degree of geometrical flexibility, high quality consistency and a reasonable price tag for single-unit projects. Furthermore, the lack of resin-dominated joints increases the impact resistance and overall efficiency of the structure.

5.5.2.2 Choice of production technique

An important consideration is that the production should be scaleable; the concept should be applicable to a range of bascule bridges that require rehabilitation. If the concept proves to be successful, a handful of these bridges could be produced per year. The structures will have to meet high quality standards at a reasonable prise.

To fulfil this requirement, a production technique should be selected that is both capable of adapting to changing boundary conditions and functional requirements, while at the same time offering a certain degree of automatisation.

Considering the above, it is clear that closed-mould resin transfer techniques are the most promising for the production of the superstructure.

5.5.3 Fibres

As discussed in section 3.1.1, the most common fibre materials for structural applications are glass, carbon and aramid. An indicative comparison of bare fibre properties was given in table 3.1. It must be noted that there is a big differentiation in properties for each fibre material, making the material applicable for a range of product classes. It is clear that the acceptable price per unit material is very different when considering, for example, a space shuttle and a bridge. In order to keep the design realistic, the composite material should be selected accordingly.

5.5.3.1 Glass

Of all the fibres available for structural applications, E-glass is by far the most used and least expensive. It can be applied where the higher stiffness of carbon fibres is not required, thereby reducing the material cost. Higher grade glass-fibre types (such as S-glass) may have increased strength properties, but the stiffness increases less significant. Next to that, the increase in price is disproportional. It thus makes sense to use E-glass where possible. Where higher strength or stiffness is required, one can better switch to carbon fibres then applying higher glass-fibre grades.

Considering the above, it is chosen to use a typical E-glass fibre; Gevetex 21xK43.

5.5.3.2 Carbon

Carbon fibres are classified into low (40-200 GPa), standard (200-275 GPa), intermediate (275-345 GPa), high (345-600 GPa) and ultra-high (600-965) modulus classes. The difficulty of the production process, and thus the price of the fibres, increases with higher stiffness classes. Standard- and intermediate modulus fibre classes are generally recognised as most suitable for commercial and industrial applications. These fibres provide the highest value in terms of cost/performance ratio. The use of higher performance carbon fibres can only be justified on rare occasions. At present, the most universally used carbon fibres for structural applications have a tensile modulus of about 230 GPa, tensile strength of 3200-3500 MPa and a strain to failure of 1.5% [Clarke, 1996].

Considering the above, it is chosen to use a widely available and well-documented carbon fibre; Toray T300.

5.5.3.3 Aramid

In contrast with glass- and carbon fibres, only few types of aramid fibres are available. There are basically two distinct types of aramid fibres; those having an elastic modulus comparable to glass fibre, and those with a modulus of twice that level. As discussed in section 3.1.1.3, aramid fibres are relatively prone to fatigue and creep. In additions, they exhibit low compressive strengths; at about one-quarter of the tensile strength. This makes their application in either compressive or flexural situations problematic. Aramids do however provide high energy absorption and impact resistance, which makes the material very suitable for application in the sacrificial layer.

The most common aramid fibre in the higher-strength category is chosen; Kevlar 49.

5.5.3.4 Properties

For design purposes, more detailed properties of the selected fibre types are presented in the tables below. Note that the glass and carbon fibre types were tested under equal circumstances, as they were part of an exercise to compare composite laminates, as described in [Soden et al., 1998].

Table 5.4: *Characteristic bare-fibre properties [Componeering Inc., 2013; Soden et al., 1998]*

	Direction	Symbol	Unit	E-glass (Gevetex)	Carbon (T300)	Aramid (Kevlar 49)
Density	-	ρ_f	kg/m^3	**2560**	**1760**	**1440**
Young's modulus	longitudinal	E_{f1}	GPa	**80**	**230**	**124**
	transverse	E_{f2}	GPa	**80**	**15**	**6.9**
Shear modulus	12-plane	G_{f12}	GPa	**33.3**	**15**	**2.8**
	23-plane	G_{f23}	GPa	**33.3**	**7**	**2.8**
Poisson ratio	12-plane	ν_{f12}	-	**0.2**	**0.2**	**0.36**
	23-plane	ν_{f23}	-	**0.2**	**0.07**	**0.23**
Tensile strength	longitudinal	X_{ft}	MPa	**2150**	**2500**	**3620**
Compressive strength	longitudinal	X_{fc}	MPa	**1450**	**2000**	**868**
Tensile failure strain	longitudinal	ε_{ft}	%	**2.687**	**1.086**	**2.9**
Compressive failure strain	longitudinal	ε_{fc}	%	**1.813**	**0.869**	**0.7**
Thermal expansion coefficient	longitudinal	α_{f1}	$°C^{-1}$	$\mathbf{4.9 \cdot 10^{-6}}$	$\mathbf{-0.7 \cdot 10^{-6}}$	$\mathbf{-5.2 \cdot 10^{-6}}$
	transverse	α_{f2}	$°C^{-1}$	$\mathbf{4.9 \cdot 10^{-6}}$	$\mathbf{12 \cdot 10^{-6}}$	$\mathbf{41.4 \cdot 10^{-6}}$

5.5.4 Matrix

The choice for resin material mainly depends on the selected fibre and production process. The reinforcement fibres are surface coated by the manufacturer (a process called sizing), which makes it specifically compatible with a type of resin. For the production process, the viscosity and curing conditions of the resin are important.

The compatibility of the resin with the fibre mostly depends on the adhesion between both. Adequate adhesion is necessary to ensure that stresses are transferred to, and thus carried by, the fibres. Too high adhesion however, can make the composite brittle as the resin does not allow the growth of cracks along the fibre in an impact situation.

Five types of resins were discussed in section 3.1.3, of which epoxy is most common for structural applications. It offers high resistance to environmental conditions, and behaves less brittle than higher strength resins. The high viscosity of the resin makes it applicable for closed-mould processing, and the shrinkage during curing is very low.

Considering the above, an commercial epoxy resin (3501-6, manufactured by Hercules) is chosen as matrix constituent for the fibre composite material. The data of the resin material comes from the same source at the fibre properties.

Table 5.5: *Characteristic resin properties [Soden et al., 1998]*

	Symbol	Unit	Epoxy (Hercules)
Density	ρ_m	kg/m^3	**1260**
Young's modulus	E_m	GPa	**4.2**
Shear modulus	G_m	GPa	**1.57**
Poisson's ratio	ν_m	-	**0.34**
Tensile strength	Y_{mt}	MPa	**69**
Compressive strength	Y_{mc}	MPa	**250**
Shear strength	S_m	MPa	**50**
Tensile failure strain	ε_{mt}	%	**1.7**
Thermal expansion coefficient	α_m	$°C^{-1}$	**$45 \cdot 10^{-6}$**

5.5.5 Plies

The structural laminate is composed of a number of stacked lamina. Each lamina has a single layer of reinforcement material. As discussed in section 3.1.2.1, the reinforcement of each lamina can be applied as simply unidirectional, a woven fabric, or even more complex rovings.

For the laminate in the superstructure of the bridge, a certain degree of orthogonality is required to be able to transfer the applied forces efficiently to the supports. This can be achieved by either applying orthogonal fabrics, or by stacking unidirectional lamina while changing the orientation of the layers. The advantage of the unidirectional stacking approach is that it allows to fully customise the material properties in either direction. Next to that, unidirectional material is cheaper than woven fabrics, as it does not undergo a weaving process.

As discussed in section 3.3.2.2, certain special mechanical behaviour can be obtained by using a particular sequence and orientation of unidirectional lamina. The symmetry or antisymmetry of the constructed laminate has a large influence on the coupling between in-plane and out-of-plane behaviour of the laminate.

Considering the above, only unidirectional lamina will be used to compose the laminate.

5.5.5.1 Nominal engineering constants

The nominal material properties of the individual lamina can be determined from the properties of its constituents, as discussed in section 3.3.1. For fibre fractions above 15%, the lamina properties can accurately be determined by the semi-empirical Halpin-Tsai material model [CUR-96+, 2012].

The fibre percentage of the lamina is chosen such, that it is compatible with the selected production process of resin transfer moulding; a fibre volume fraction of 60%.

The following table presents the characteristic values of unidirectional lamina, composed of the selected fibre and matrix types. The values have been calculated by making use of the equations from section 3.3.1.4, while applying the factors as prescribed by [CUR-96+, 2012]; $\xi = 2$ and $\phi_{UD} = 0.97$. Subsequently, the values have been checked by the ESAComp ply calculation module.

Table 5.6: *Nominal engineering constants of UD-lamina*

	Direction	Symbol	Unit	E-glass (Gevetex)	Carbon (T300)	Aramid (Kevlar 49)
Density	-	ρ	kg/m^3	**2040**	**1560**	**1368**
Young's modulus	longitudinal	E_1	GPa	**48.2**	**135.5**	**73.8**
	transverse	E_2	GPa	**17.0**	**8.8**	**5.5**
Shear modulus	12-plane	G_{12}	GPa	**5.2**	**4.4**	**2.1**
Poisson ratio	12-plane	v_{12}	-	**0.256**	**0.256**	**0.352**

5.5.5.2 Nominal strength properties

To calculate the laminate strength properties, the CUR96+ prescribes to use a linear failure strain of 1.2% for tension and compression in both longitudinal and transverse direction of the ply. This is however only applicable for glass-fibre reinforcement, and would lead to non-conservative values for carbon and aramid fibres. The reason for this is obvious when comparing the moduli of the different fibre types from table 5.6; carbon and aramid plies are relatively weak in the off-axis direction compared to glass fibres.

The failure strain properties are therefore derived from actual test results of the considered material, and taken from the ESAComp material database [Componeering Inc., 2013][1].

Table 5.7: *Characteristic failure strains of UD-lamina [Componeering Inc., 2013]*

	Direction	Symbol	Unit	E-glass (Gevetex)	Carbon (T300)	Aramid (Kevlar 49)
First tensile failure strains	longitudinal	$\varepsilon_{X,t}$	%	**2.13**	**1.28**	**1.87**
	transverse	$\varepsilon_{Y,t}$	%	**0.20**	**0.50**	**0.45**
	normal	$\varepsilon_{Z,t}$	%	**0.20**	**0.50**	**0.45**
First compressive failure strains	longitudinal	$\varepsilon_{X,c}$	%	**1.07**	**0.80**	**0.33**
	transverse	$\varepsilon_{Y,c}$	%	**0.65**	**2.75**	**1.82**
	normal	$\varepsilon_{Z,c}$	%	**0.65**	**2.75**	**1.82**
First shear failure strains	longitudinal	ε_S	%	**1.23**	**1.60**	**1.14**
	transverse	ε_R	%	**1.23**	**1.60**	**1.14**
	normal	ε_Q	%	**1.00**	**1.20**	**1.00**

Multiplication of these failure strains with the given lamina moduli gives the first failure stresses, as displayed in the table below.

[1] Typical data at room temperature (25 °C), with moisture weight content of 0.5% and void volume content of less than 3.0%

Table 5.8: *Nominal failure stresses of UD-lamina*

	Direction	Symbol	Unit	E-glass (Gevetex)	Carbon (T300)	Aramid (Kevlar 49)
First tensile failure stress	longitudinal	X_t	MPa	**1027**	**1734**	**1380**
	transverse	Y_t	MPa	**34**	**44**	**25**
	normal	Z_t	MPa	**35**	**44**	**25**
First compressive failure stress	longitudinal	X_c	MPa	**516**	**1084**	**244**
	transverse	Y_c	MPa	**111**	**242**	**100**
	normal	Z_c	MPa	**111**	**242**	**100**
First shear failure stress	longitudinal	S	MPa	**64**	**70**	**24**
	transverse	R	MPa	**64**	**70**	**24**
	normal	Q	MPa	**52**	**53**	**21**

5.5.6 Core

Selecting the core material requires a comparison between the three most common types; balsawood, expanded polymer foam and honeycomb. The material-adapted design philosophy should again be embraced; minimise the use of high grade (expensive) material in sections where it is not strictly required. Several types of core can be applied in those areas in which they are best utilised.

5.5.6.1 Balsa

It is clear that balsa offers the best strength-to-density ratio. The problem is however that balsa is not available in big chunks, as the dimensions are limited by the size of the tree. The interfaces between the blocks will have to be bonded in order to achieve these high strength properties, which will significantly increase the cost, and reduces the quality consistency. Next to that, the material deteriorates under the influence of moisture, and combusts when catching fire. A service life of 100 years can probably not be guaranteed. It is therefore considered not to be suitable for the superstructure of the bridge.

Table 5.9: *Qualitative comparison of different core types [Kindinger, 2001]*

	Core type			
	Balsa	Foam High density	Foam Low density	Honeycomb
Density				
Cost				
Strength and stiffness				
Moisture resistance				
Chemical resistance				
Flammability resistance				
Impact resistance				
Fatigue strength				
Abrasion resistance				
Formability				

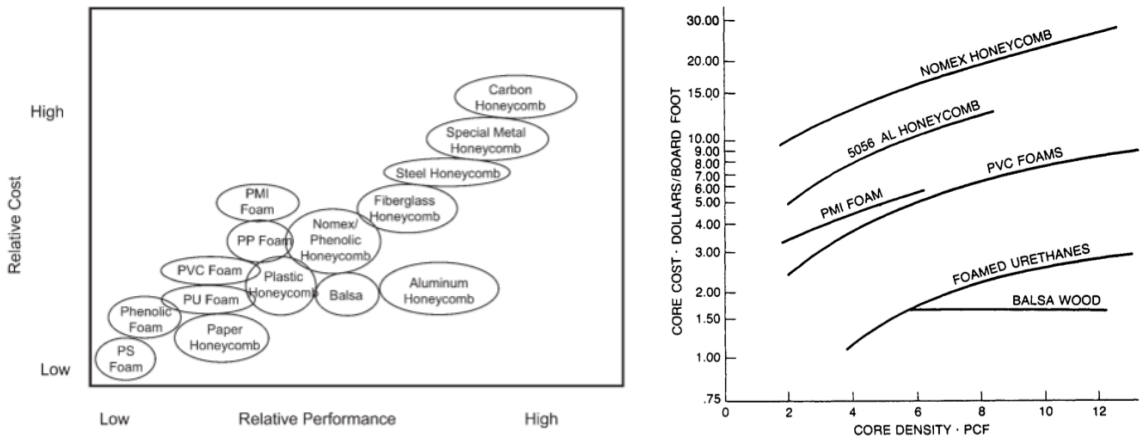

(a) Cost-performance (b) Cost-density

Figure 5.1: *Relative comparison of different core types [Campbell, 2010]*

5.5.6.2 Foam

Foamed polymers are relatively cheap and easy to process in large volumes and shapes. It is very stable under different environmental conditions. The mechanical properties are generally proportional to the density of the material. Three types are chosen for the comparison below; a low-, medium- and high-density foamed PVC core.

5.5.6.3 Honeycomb

Aluminium corrugated plates seem to be the honeycomb core with the highest cost-performance ratio. Apart from their price, they outperform the other core types in all properties. Honeycomb cores are however not easy to use in the selected closed-mould production technique, as the ingression of resin in the hollow core should be prevented.

Table 5.10: *Quantitative comparison of different core types [Componeering Inc., 2013]*

	Symbol	Unit	Basla	LD Foam	MD Foam	HD Foam	Honeycomb
Density	ρ_c	kg/m^3	**110**	**40**	**100**	**250**	**77**
Young's modulus	E_c	GPa	**3.23**	**0.037**	**0.115**	**0.282**	**1.02**
Shear modulus	G_c	GPa	**0.15**	**0.013**	**0.04**	**0.095**	**0.26**
Poisson's ratio	ν_c	-	**0.23**	**0.42**	**0.44**	**0.48**	**0.5**
Tensile strength	Z_t	MPa	**9.4**	**0.7**	**2.7**	**7.5**	**4.55**
Compressive strength	Z_c	MPa	**10.0**	**0.45**	**2.0**	**6.6**	**4.55**
Shear strength	S	MPa	**10.0**	**0.45**	**1.7**	**4.7**	**4.55**

5.5.7 Design properties

As discussed in section 4.3, partial material and conversion factors must be used to derive more conservative design properties for the lamina and core materials. The applicability of the partial conversion factors depends on the considered limit state. The following table presents partial factors, which are the result of multiplication of the factors as quantified in the following sections[2].

Table 5.11: *Material- and conversion factors for different limit states [CUR-96+, 2012]*

Conversion	Ultimate Limit State			Serviceability Limit State		
	Strength	Stability	Fatigue	Deflection	Vibration	Cracking
Temperature	X	X	X	X	X	X
Moisture	X	X	X	X	X	X
Creep		X		X		X
Cyclic loading		X		X	X	X
Conversion factor	1.21	1.53	1.21	1.53	1.33	1.53
Material factor	1.50	1.50	1.50	1.38	1.38	1.38
Total factor	1.82	2.30	1.82	2.11	1.84	2.11

5.5.7.1 Lamina

Material factor The material factor accounts for the uncertainty in deriving the material properties, and the level of quality consistency of the production process.

Post-curing the composite after the moulding process gives a better bond between matrix and fibres, and thus provides a much better assurance of quality. Next to that, it is assumed that coupons of the composite material will be tested to verify the strength properties that have been assigned to it. These two measures, post-curing and coupon testing, have a drastic impact on the material factor that has to be retained in the structural design. Using the information from section 4.3.1, the material factor for a fully cured resin transfer moulded composite, which material properties were verified by coupon testing, is:

$$\gamma_m = \gamma_{m,1} \cdot \gamma_{m,2} = 1.15 \cdot 1.2 = 1.38\ [-] \tag{5.31}$$

For ultimate limit state verification, the CUR96 requires $\gamma_m \geq 1.50$.

Temperature factor The conversion factor for temperature effects is:

$$\gamma_{ct} = 1.1\ [-] \tag{5.32}$$

[2]Creep-related factor only has to be taken into account for long-term actions. Vibration limit state has to be considered both with and without conversion factors

Moisture The conversion factor for moisture effects, when exposed to changing humidity conditions, is:

$$\gamma_{cv} = 1.1 \tag{5.33}$$

Creep The conversion factor accounting for creep has to be applied for prolonged load conditions, such as self-weight. For unidirectional plies, the creep factor over a 100-year service life is:

$$\gamma_{ck} = t^n = (100 \cdot 365 \cdot 24)^{0.01} = 1.15 \tag{5.34}$$

Fatigue The conversion factor for the effects of fatigue is:

$$\gamma_{cf} = 1.1 \tag{5.35}$$

5.5.7.2 Core

The CUR96+ does not prescribe a safety factor for core material, but indicates that there will be one when the guideline is finalised. Therefore, the following partial material factor is assumed:

$$\gamma_{m,c} = 1.3 \tag{5.36}$$

6 Parametric analysis of sandwich plate

6.1 Basic sandwich plate

As a first step the problem is heavily simplified in terms of loading- and boundary conditions, such that simple hand calculations can be used to investigate the effects of certain design parameters on the behaviour and price of the structure. The aim is to determine the technical and economical feasibility of the selected materials, and get a feeling for the dimensioning of the structure.

As a result of the high strength to stiffness ratio, the structural design of fibreglass composites is generally predominated by the deflection criteria. Hence, the SLS criteria are used as the driving design parameter, and the effective stresses are verified afterwards. Note that the stress criterion will be of higher importance as the percentage of carbon fibres increases, since the higher structural stiffness results in higher stresses.

6.1.1 Model parameters

The most elementary composite leaf design would be a plain sandwich panel, consisting of two identical face sheets which are separated by a foamed core layer. The influence of the following design parameters for the basic sandwich panel is investigated:

- Structural height
- Skin thickness
- Core thickness
- Skin material
- Core material

Depending on the results of the model, the sandwich panel can be further optimised in subsequent design steps. One could think of adding shear stiffeners, honeycomb core material, varying the thickness of the construction, etcetera.

By applying symmetric sandwich skins, the sandwich panel behaves as a orthotropic plate; supported at the abutment sides, unsupported at the longitudinal sides. Due to these free edges, the leaf can also simply be modelled as a wide beam. Hence, its behaviour can be studied by application of the Timoshenko beam theory.

The hand calculations of this model have been included in appendix C.

6.1.1.1 Plate to beam

In order to be able to model the 2-dimensional plate as a 1-dimensional beam, the following has to be considered.

Stiffness modulus A sandwich beam is generally considered to be wide if the width is greater than the core depth (b>c). For simply supported plates, it is reasonable to assume that the strains in the lateral direction are zero, as the lateral deformation is restricted by adjacent material. Therefore, the stiffness modulus in the longitudinal direction of the beam has to be adjusted by [Timoshenko, 1959]:

$$E' = \frac{E}{1-\nu^2} \tag{6.1}$$

In this case however, the plate is only simply supported at two sides, whereas the other two are unsupported. The plate is thus free to curve in the yz-plane. Therefore, the stiffness modulus does not need to be adapted [DIAB Group, 1999].

Effective width The plate is loaded by LM1, which consists of a uniformly distributed load (UDL) and a set of concentrated loads (TS). As the plate has a width of 15 meters, and the concentrated load is acting in the middle, it is clear that the plate will not be activated uniformly. The area surrounding the concentrated load will be subjected to higher stresses and deflection than the edge of the plate.

This problem can be approached by assuming an effective width. The complex non-uniform stress distribution is translated into an equivalent uniform stress distribution over a portion of the plate's width. This effective width concept is the basis of design codes for plates of traditional materials. For any other material, including orthotropic sandwich panels, no approximations are readily available. The effective width for specific panels will have to be determined from finite element modelling.

The approach in this hand-calculation is to set the effective width equal to the total width of the beam. The results are subsequently compared with two FEM results, in which the concentrated loads are either introduced as a line-load or as prescribed by the Eurocode (as depicted in fig. 4.1)

6.1.1.2 Support system

As discussed in section 2.1, the self-weight of the leaf is balanced by the self-weight and counterweight at the tail of the structure. When considering the case of zero imbalance, there is no vertical reaction force on the support at the liveload pier. The deflection line of the balanced structure, as sketched in fig. 6.1(a), gives a good insight on the behaviour of the structure under the combination of self- and counterweight; there is a positive influence on the deflection at midspan. Obviously, this is not a stable equilibrium, which is why in practice a span-heavy imbalance is created. The positive effect of the dead load is thereby nullified. It is however clear that, due to the balance, the effect of self-weight on the deformation of the structure is small compared to the live loads.

When live loads are applied on the leaf, the construction will deform as if it were simply supported at both abutments. The tail-end of the structure will not restrain the deformation of live loads, and thus remains straight. The partial deflection for (uniformly distributed) live loads is sketched in fig. 6.1(b).

The resulting deflection of the structure is obtained by superimposing dead- and live load deflections. The contribution in the deflection from the dead load balance is however small compared to the contribution from live loads.

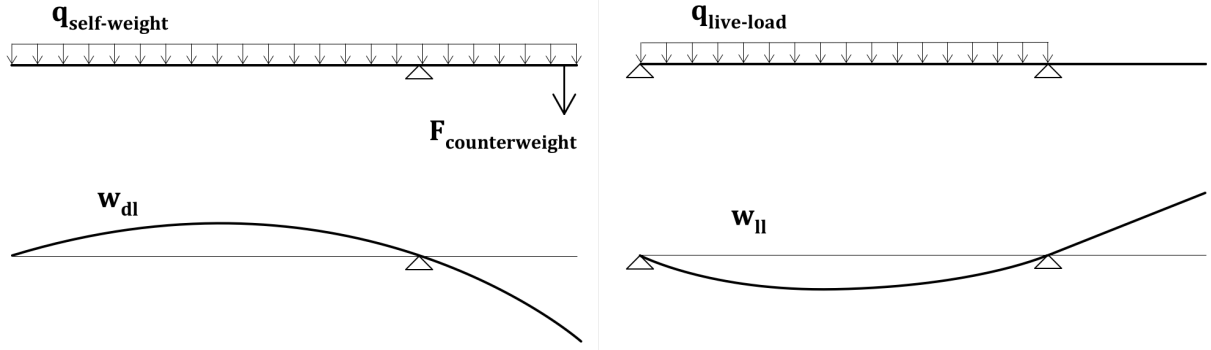

(a) Partial deflection from dead load

(b) Partial deflection from live load

Figure 6.1: *Sketch of partial deflection lines for dead- and live load*

6.1.1.3 Loads

Considering the small contribution in deflections from self-weight, only the effects of live loads are considered in this hand calculation. From the load combinations, as presented in table 5.2, the 'gr1a' combination is considered to be most detrimental for the global deflections. The effects from horizontal-, wind- and temperature loads are not considered.

The uniformly distributed load for the beam model is composed by averaging the distributed load over the different sections of the bridge; traffic lanes, footways and cycletracks, and remaining area. Both traffic lanes of the bridge, covering a total width of 6.1 meters, should be considered heavy-traffic lanes. The footways and cycle tracks cover a width of 4.5 meters, leaving a remaining width of 4.4 meters. Using the distributed loads, as quantified in section 5.4.1, the following resultant distributed load is composed:

$$q_d = \gamma_Q \cdot \left(6.1 \cdot q_{LM1,1} + 4.5 \cdot q_{fk} + 4.4 \cdot q_{LM1,r}\right) = 130.3\ [kN/m] \tag{6.2}$$

For simplicity, the double-axle tandem system of is considered to act as one pointload at midspan of the beam:

$$Q_d = \gamma_Q \cdot 2 \cdot Q_{LM1} = 810\ [kN] \tag{6.3}$$

6.1.1.4 Material

The influence of the face- and core material on the structural behaviour is point of investigation. In this first estimation, optional carbon layers are only applied in the longitudinal direction of the span.

Face laminates The resultant stiffness of the face material is derived from the proportion between E-glass and carbon layers in the laminate. The CUR96 recommendations for the composition of laminates are respected. The face laminates are constructed of unidirectional plies, which are oriented in four principle directions with respect to the longitudinal axis of the structure; 0°, +45°, -45° and 90°. Each of these principle directions must contain at least 15% of the total available fibre volume, in order to account for unpredicted loads in these directions. As the applied loads will have to be transferred to the abutments , the amount of fibres in the longitudinal direction is maximised (55% of total fibre volume). The averaged stiffness modulus of the face sheets can subsequently be estimated by:

$$E_{f,k} \approx 0.55 \cdot (p_{gls} \cdot E_{gls,1} + p_{crb} \cdot E_{crb,1}) + 0.3 \cdot \frac{1}{2} \cdot (E_{gls,1} + E_{gls,2}) + 0.15 \cdot E_{gls,2} \tag{6.4}$$

In which:

p_{gls}	*percentage of glass-fibres in face laminates*
p_{crb}	*percentage of carbon-fibres in face laminates*
$E_{gls,1}$	*stiffness of glass reinforced UD-lamina in longitudinal direction (see table 5.6)*
$E_{gls,2}$	*stiffness of glass reinforced UD-lamina in transverse direction*
$E_{crb,1}$	*stiffness of carbon reinforced UD-lamina in longitudinal direction*

The characteristic values of the material properties are converted to design values by division with the material and conversion factors, as discussed in section 5.5.7:

$$E_{f,d} = \frac{1}{\gamma_m \cdot \gamma_c} \cdot E_{f,k} \tag{6.5}$$

Core No shear stiffeners are used in the initial model. Instead, the core is composed of a uniform layer of medium- or high-density foam. Low-density foam is not applied, as it was obvious that this material would not be feasible without the use of shear stiffeners. The characteristic material properties can be found in table 5.10.

The design properties are derived by application of the material factor for the core:

$$E_{c,d} = \frac{1}{\gamma_{m,c}} \cdot E_{c,k} \tag{6.6}$$

Sandwich panels Four basic sandwich panels are composed from the selected material set, each consisting of either a medium- or high density core, and either $p_{gls} = 1$ or $p_{crb} = 1$. The panel configurations are displayed in table 6.1

Table 6.1: *Four sandwich panel configurations*

		Core	
		Medium-density PVC	High-Density PVC
Face laminate	55% glass 15% glass 15% glass 15% glass	**Panel A**	**Panel B**
	55% carbon 15% glass 15% glass 15% glass	**Panel C**	**Panel D**

6.1.1.5 Material cost

After proving the technical feasibility of the materials, the structure will be optimised with respect to material cost. In order to do so, unit prices for the materials have been assumed. It should be noted that the information, coming from multiple sources, may not be very accurate or up-to-date. It is however the ratio between these unit prices that gives insight in the economical feasibility of the different materials. The following unit prices were used:

Table 6.2: *Unit prices for selected sandwich materials [NauticExpo, 2014]*

	Unit	Medium-dens Foamed PVC	High-dens Foamed PVC	Glass/Epoxy 60% UD	Carbon/Epoxy 60% UD
Mass price	[EUR/kg]	**1.0**	**1.0**	**4.0**	**20.0**
Density	[kg/m^3]	**100**	**250**	**2040**	**1560**
Volume price	[EUR/m^3]	**100**	**250**	**8.160**	**31.200**

6.1.1.6 Assumptions

As discussed in section 3.3.5, the structural analysis of fibre reinforced sandwich panels is relatively complex. The problem can however be simplified to allow for hand calculations, by making the following set of assumptions:

- Both the face sheets and the panel itself are symmetric with respect to the structural midplane → no coupling between in-plane extrosional and flexural behaviour ($[B] = 0$)
- The face sheets are thin compared to the core → the faces do not contribute to the shear rigidity of the section; normal stress is constant throughout the depth of the face
- The core is considerably less stiff than the face sheets → the shear stresses are constant throughout the depth of the core
- Deflections are small with respect to the structural height → no strains in the midplane of the panel from transverse displacement

The maximum deflections are determined by applying the elementary beam equations, accounting for both bending- and shear deformation.

6.1.2 Result

This section presents the results from the hand calculation model, as can be found in appendix C. The aim is to investigate the influence of the design parameters, as listed in section 6.1.1.

6.1.2.1 Contribution from bending and shear

The deformation of the sandwich structure can be decomposed in two parts; deformations due to bending moments (w_b), and deformations due to transverse forces (w_s). The following graphs show the partial deflections for the four panel types, having a fixed skin thickness of 60 mm. Notice that the shear contribution is considerable, especially for the panels composed of a medium-density foam core (A and C). Furthermore, the bending contribution is clearly higher for glass-fibre reinforced face laminates (A and B).

Table 6.3: *Bending- and shear contribution to the midspan deflection*

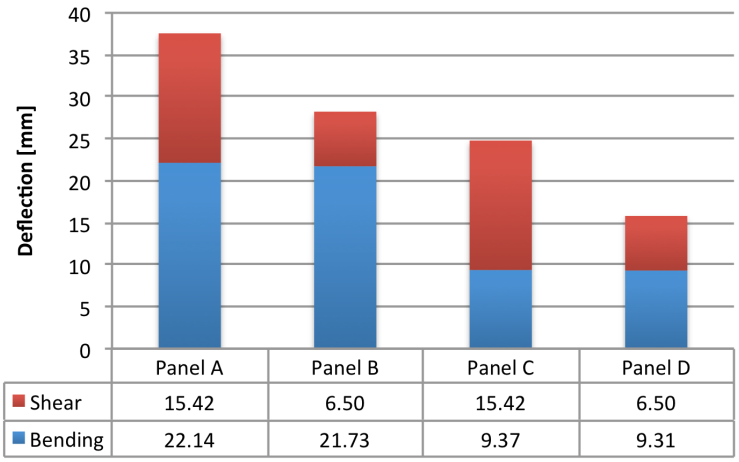

The bending deformation is determined by the bending stiffness of the sandwich face sheets, whereas the shear deformation is determined by the shear stiffness of the core. The influence of the skin thickness becomes apparent in the following figure, in which the skin thickness is varied for a fixed structural height of 1100 mm.

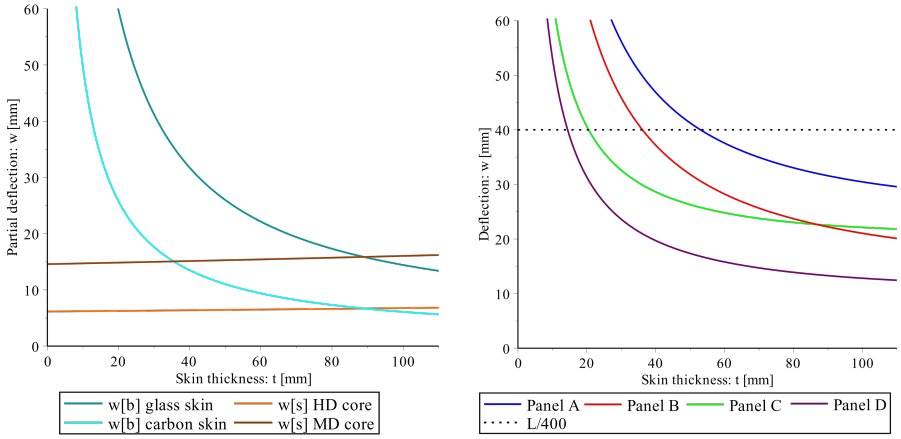

(a) Shear- and bending contribution

(b) Total deflection and limit state

Figure 6.2: *Partial- and total deflections for fixed structural height of H=1100 mm*

6.1.2.2 Panel configurations for fixed deflection

By expressing the deformation in terms of structural height (H) and skin thickness (t), the panel configurations for which the maximum deflection is constant can be plotted. The plots in fig. 6.3 show all combinations of H and t for which the maximum midspan deflection of the structure under the given load case is L/400=40 mm.

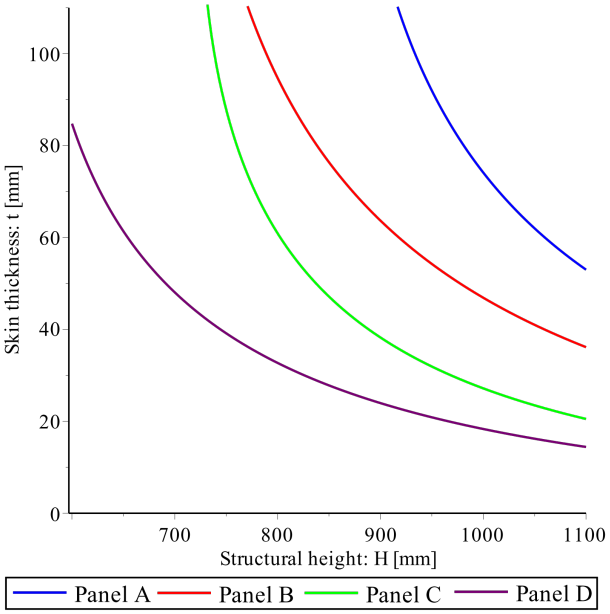

Figure 6.3: *Panel configurations that comply with L/400 limit state*

6.1.2.3 Self-weight

For all combinations of structural height and skin thickness that comply with the L/400 limit state (i.e. the plotted functions in fig. 6.3), the self-weight of the structure is determined by multiplication with the material densities. The result is displayed in fig. 6.4.

As the structural height increases, the relatively dense face laminate can be thinner. For panel D, apparently the weight reduction from slimming down the skin thickness does not weigh up to the increase of weight from the thicker (high-density) core. The other three panels all become lighter with increasing structural height (within the geometrical boundary of 1100 mm).

For comparison, the average weight per square meter of the steel orthotropic leaf of the Julianabridge (55 ton) is added to the figure. It can be concluded that, without any structural refinements, only panel C is able to outperform the old structure with respect to weight.

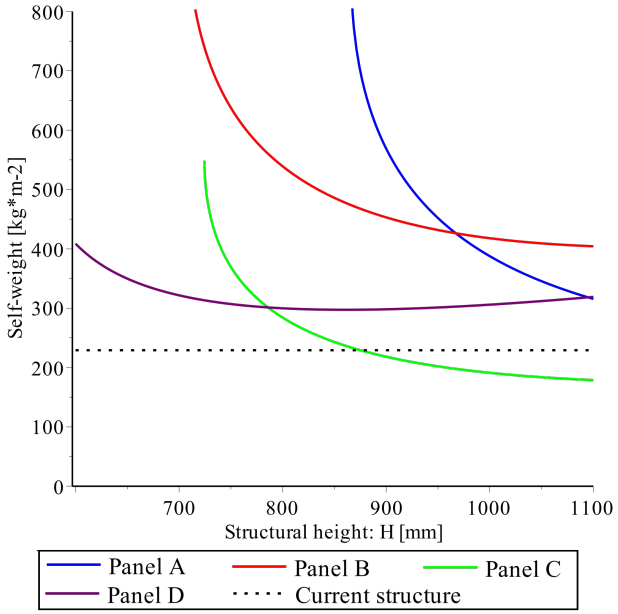

Figure 6.4: *Self-weight for all panel configurations that comply with L/400 limit state*

6.1.2.4 Material cost

Similar to the determination of the weight for all combinations of sandwich configurations, the material cost can be calculated by multiplication with the unit prices from table 6.2.

As the structural height increases, the relatively expensive face laminate can be thinner. As a result, the total material cost decreases for an increasing structural height. It is clear that the panels with a high-density core (B and D) are more cost-effective than the ones having a lower-density core. The higher price of the core is outweighed by the reduction of the skin thickness. In general, it can be concluded that an increased structural height will result in a more cost-effective solution.

For comparison, the estimated price for an equivalent steel leaf is added to the figure. This price is based on a material unit price of 5 euro per kilogram, multiplied by a total weight of 55 metric tons. It must however be noted that, next to material cost, this steel unit price also includes assembly, transport and conservation. All of these additional costs have not been considered for the composite unit prices.

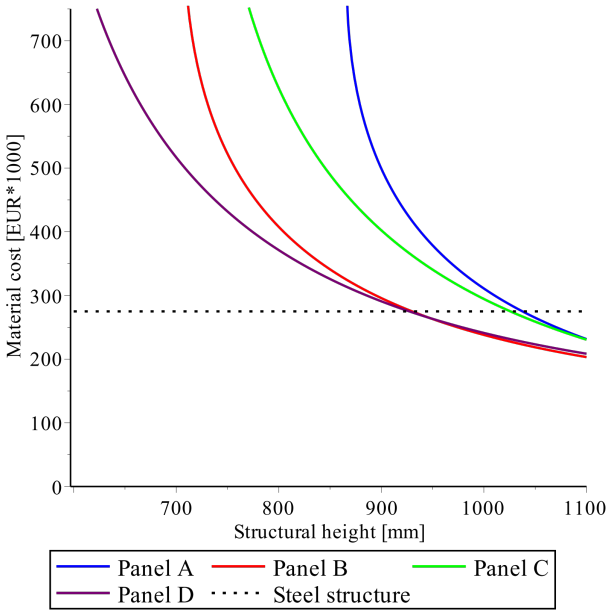

Figure 6.5: *Estimated material cost for all panel configurations that comply with L/400 limit state*

6.1.2.5 Stresses

It is assumed that the deformations would be governing. To verify this assumption, the effective stresses in the face sheets and core will be checked.

Face laminates The average flexural stresses in longitudinal direction, which are solely transferred through the face sheets, can be determined from eq. (3.32). For the panel configurations as given in fig. 6.3, the resulting average flexural stresses in the face laminates are plotted in fig. 6.6(a). The maximum bending moment occurs when the concentrated load is positioned at midspan of the beam:

$$M_{max} = \frac{1}{8} \cdot q_d \cdot L^2 + \frac{1}{4} \cdot Q_d \cdot L = 7409\ [kNm] \tag{6.7}$$

It should be noted that, in this hand calculation, the stresses are assumed to be uniform over the height of the face sheet. In reality, the stresses in the laminate vary from layer to layer, dependent of the layer's stiffness in the direction of the stresses. The highest stresses thus occur in those layers that are reinforced by high-modulus (carbon) fibres, and in which the fibres are aligned with the stress direction.

Core The shear stresses in the core can be determined from eq. (3.34). The maximum shear stresses occur in the cross-section when the concentrated load is positioned right next to one of the supports:

$$V_{max} = \frac{1}{2} \cdot q_d \cdot L + Q_d = 1852\ [kN] \tag{6.8}$$

The resulting core shear stress for the considered panel configurations are displayed in fig. 6.6(b).

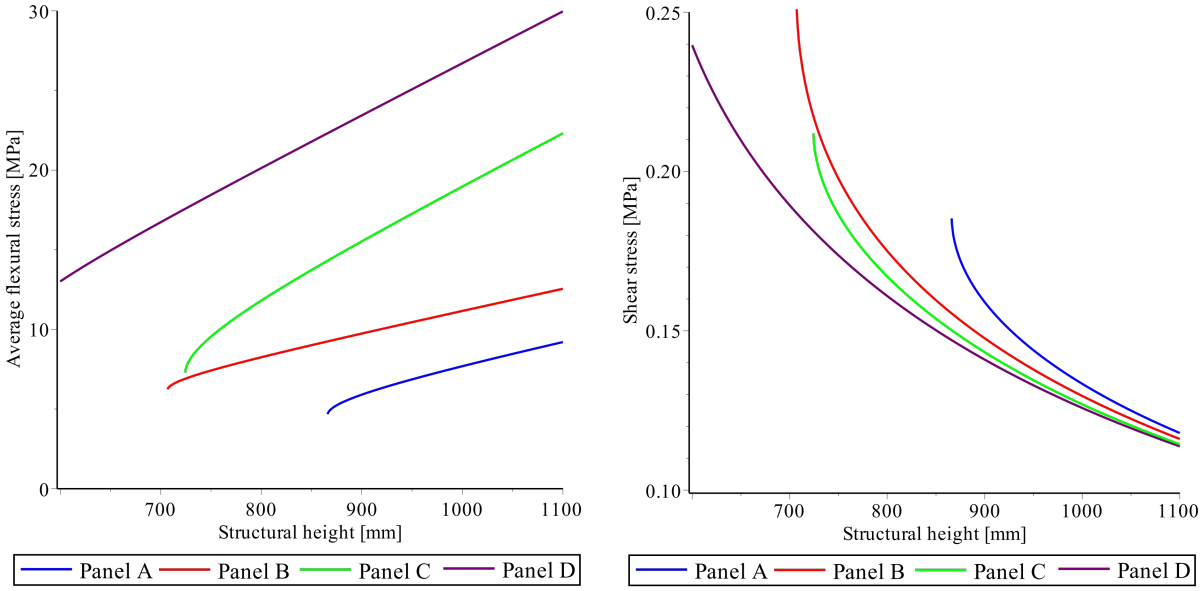

(a) Average longitudinal stress in face laminates $\sigma_{f,1}$

(b) Shear stress in core τ_c

Figure 6.6: *Average face- and core stresses for all panel configurations that comply with L/400 limit state*

6.1.2.6 Reserve factor

Calculating the reserve factor is a way of quantifying the safety with respect to failure of a structure. The factor is defined as the ratio of the failure stresses to the effective stresses, as discussed in section 3.3.3.7. A reserve factor smaller than unity ($0 \leq RF \leq 1$) indicates that the sandwich exceeds the critical stress for the corresponding failure mode, and is thus unsafe.

In order to determine the reserve factor of a structure under a defined load, all applicable failure modes (as displayed in fig. 3.27) will have to be considered in each section of the structure. The reserve factor, which varies along the length of the beam, is determined by the governing failure mode for each section.

Note that for these ultimate limit states, a smaller conversion factor can be applied than for the serviceability limit states (see table 5.11).

Face fracture As discussed, the hand calculation only results in averaged stresses for the face laminates. These average stresses are well below the ultimate failure stresses of the face laminates. This does however not guarantee that none of the individual plies has fractured. To check if the first-ply-failure criterion is violated, the local ply stresses in the laminate will have to be derived by making use of the Classical Laminate Theory (see section 3.3.2.1). This will not be done in the hand calculation, but the local stress-state of the individual plies will be checked by a CLT-based design tool in section 6.1.3.3.

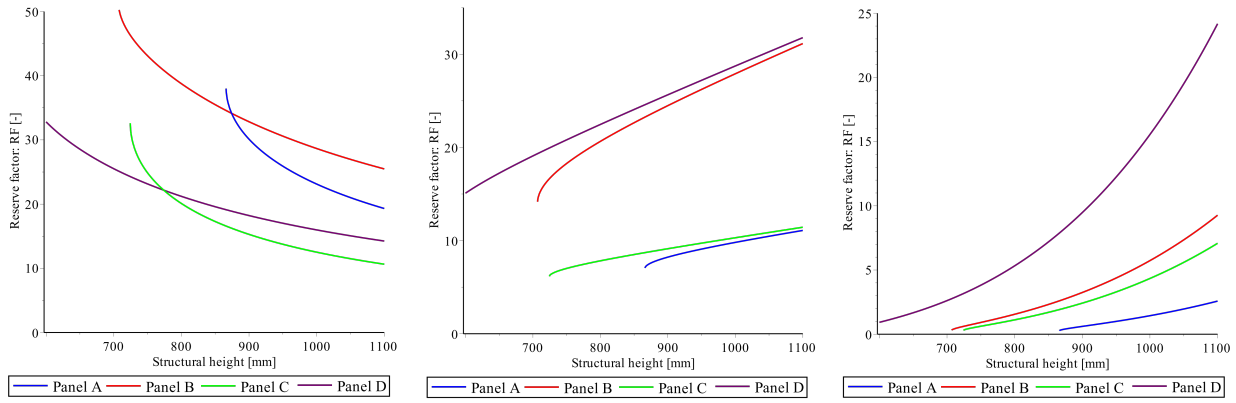

(a) Face wrinkling (b) Core shear (c) Core crimping

Figure 6.7: *Reserve factors for maximum stresses in panel configurations that comply with L/400 limit state*

Face wrinkling Unlike for the face fracture failure mode, the check for face wrinkling uses the average stress in the laminate. The critical average face stress is given by eq. (3.36). The reserve factor for this failure mode, at the average flexural stresses from fig. 6.6(a), is plotted in fig. 6.7(a).

Core shear failure The critical core shear stress is given by eq. (3.36). The reserve factor for this failure mode, at the shear stresses from fig. 6.6(b), is plotted in fig. 6.7(b).

Core crimping The critical core shear stress is given by eq. (3.37). The reserve factor for this failure mode, at the shear stresses from fig. 6.6(b), is plotted in fig. 6.7(c). This failure mode proves to be governing for most of the considered panel configurations, and is actually critical for some configurations.

6.1.3 Comparison with analytical design tool

The hand calculations are compared with results achieved from the computer-aided design tool 'ESAComp'. For this comparison, both the analytical beam design tool and the FEM-based plate design tool was used. Both tools rely on CLT to derive their results.

6.1.3.1 Laminate properties

An estimation of the averaged stiffness properties of the face laminates was made by eq. (6.4). It should be verified how the estimation holds up against the laminate design tool, which is based on CLT. The comparison in fig. 6.8 shows that laminate properties are slightly overestimated using the simple equation.

It should be noted that all hand calculations of the above-discussed results were based on the laminate properties as derived by the laminate tool.

Table 6.4: *Comparison between estimated and CLT-derived laminate stiffness in main principle direction*

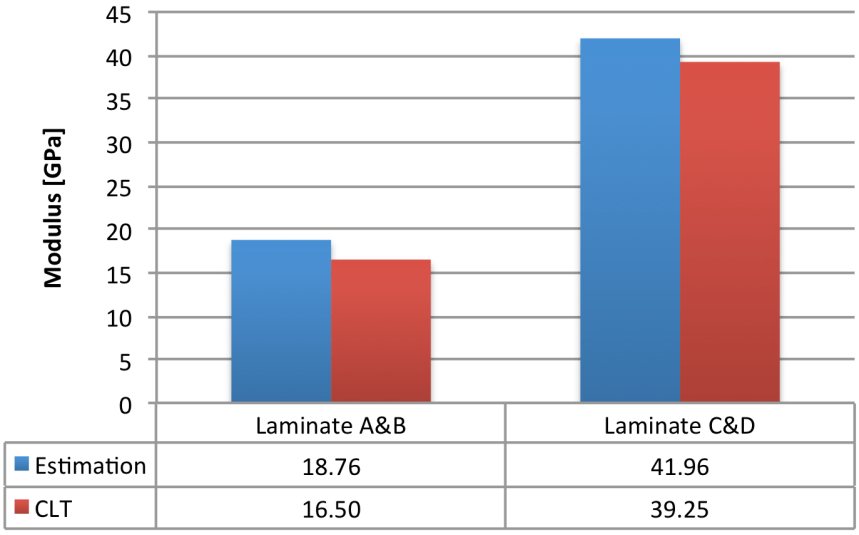

6.1.3.2 Deflection

In order to verify the results from the hand-calculation, the following four panel configurations have been tested in the analytical and numerical tools of ESAComp. All plies have a thickness of 1 millimetre. Both the face laminates, as well as the sandwich panel itself, are symmetric and balanced. Note that the number of angled plies approximately corresponds to a 55%-15%-15%-15% fibre distribution.

Table 6.5: *Sandwich configurations modelled in ESAComp*

Material	Angle *[deg]*	Panel A *[mm]*	Panel B *[mm]*	Panel C *[mm]*	Panel D *[mm]*
Glass UD	0	**29**	**21**	**0**	**0**
	45	**8**	**5**	**3**	**2**
	-45	**8**	**5**	**3**	**2**
	90	**8**	**5**	**3**	**2**
Carbon UD	0	**0**	**0**	**12**	**9**
MD Foam	-	**994**	**0**	**1058**	**0**
HD Foam	-	**0**	**1028**	**0**	**1070**
Total	-	**1100**	**1100**	**1100**	**1100**

Note that the combination of structural height and skin thickness of the four panels are close to the solutions plotted in fig. 6.3. Hence, the results should indicate a maximum midspan deflection of 40 mm.

In ESAComp's beam tool, the introduced loads are equal to the ones used in the hand-calculation. For the panel tool however, the applied concentrated load had to be transformed into an equivalent load on the surface of the 2D panel. This was done in two different ways:

- as a 54 kN/m uniformly distributed line-load over the width of the plate
- as a double-axle tandem system, consisting of four concentrated loads of 202.5 kN with a 2.0x1.2 meter spacing

The results of the analytical beam tool and the numerical panel tool are displayed in fig. 6.10, along with the results from the hand-calculation. The results seem to correspond quite well.

Table 6.6: *Comparison between maximum panel deflection from hand-calculation and ESAComp*

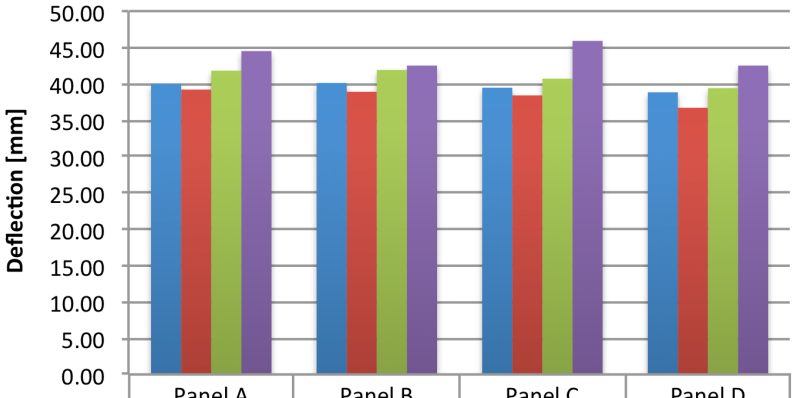

	Panel A	Panel B	Panel C	Panel D
Beam [Hand-calculation]	40.00	40.11	39.46	38.83
Beam [ESAComp]	39.2	38.9	38.4	36.7
Plate: Line-load [ESAComp]	41.8	41.9	40.7	39.4
Plate: TS [ESAComp]	44.5	42.5	45.9	42.5

The tandem system load case clearly results in higher maximum deflections compared to the three others. This is due to the fact that this load is not spread over the full width of the plate, so that the plate suffers from a higher local deformation in the vicinity of the concentrated loads. Note that this effect is more pronounced for panels A and C, which contain a lower-density core.

6.1.3.3 Stresses

The hand-calculated average face stresses and the core shear stresses can be compared to the ESAComp results as well. The comparison for the face stresses of the selected panel configurations is given in table 6.7. As discussed, the flexural stresses are however not uniform over the height of the face laminates, as a result of stiffness differences between the lamina. This effect is clearly shown in the face stress distribution plots, which are included in fig. D.1. The maximum effective ply stresses can be a factor 1.5 to 2.0 higher than the average laminate stress.

Both the flexural- as well as the shear stresses are slightly overestimated by the hand calculation. This is a result of the assumptions, as stated in section 6.1.1.6. In the ESAComp results, which are based on the CLT, the faces and core respectively do contribute to the shear- and flexural rigidity of the section.

Table 6.7: *Comparison between average face stress from hand-calculation and ESAComp*

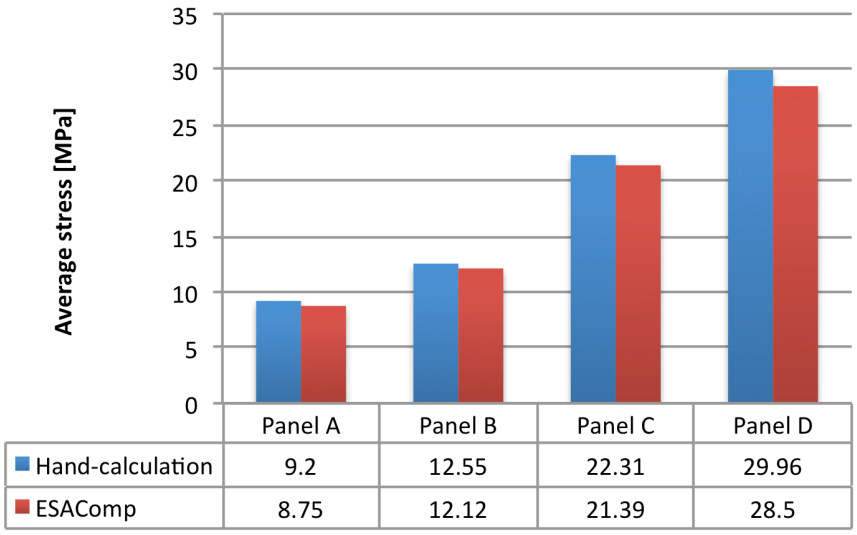

	Panel A	Panel B	Panel C	Panel D
Hand-calculation	9.2	12.55	22.31	29.96
ESAComp	8.75	12.12	21.39	28.5

6.1.3.4 Reserve factor

Unfortunately, the software does not allow to plot the reserve factor for the individual failure modes. Instead, only the RF of the governing failure mode is displayed. The face fracture criterion can however be checked by analysing the laminate section under the effect of the maximum effective bending moment in the plate.

Note that the inverted reserve factor (RF^{-1}) is used in the different plots, as this gives much clearer visual results.

Face fracture The reserve factor of the face laminates is determined by the weakest layer in the given stress direction. For all four sandwich panels, this weakest layer is the one furthest away from the neutral axis, having a fibre direction perpendicular to the stresses. The results are included in fig. D.3.

Note that failure of these layers would not lead to a catastrophic failure of the section, as the layers in the stress direction (transferring most of the load) have much higher RF-factors.

Governing RF loaded panel The reserve factor of the panel, under the influence of the uniformly distributed load (q_d) and the double-axle tandem system (Q_d), can be found in fig. D.4 and fig. D.5 respectively. The combined governing reserve factor is derived by superimposing the two, as displayed in fig. D.6.

All of the governing inverted reserve factors prove to be well below unity, which means that the panels are all over-dimensioned with respect to strength. It is clear that the serviceability limit state is indeed governing over the ultimate limit state, even when only considering the first-ply-failure. Another conclusion from comparing the reserve factors of the panels, is that the sandwiches composed of higher-modulus materials better utilise the strength potential of the face laminates. In other words, these panels are less over-dimensioned with respect to strength.

6.1.4 Conclusion

This parametric study has shown that sandwich panels have the potential to comply with the functional requirements and boundary conditions of the considered bascule bridge, both in serviceability- and ultimate limit state. The following conclusions can be drawn:

- The shear contribution in the deflection is significant (see table 6.3)
- In the basic sandwich shape, the required panel configuration is generally more heavy than a orthotropic steel bridge leaf (see fig. 6.4)
- Using more lightweight materials does not automatically lead to a more weight-efficient structure (see fig. 6.4)
- Using cheaper materials does not automatically lead to a more cost-efficient structure (see fig. 6.5)
- Increasing the structural height of the sandwich (thus minimising the skin thickness) results in lower total material cost (see fig. 6.5)
- Face-related failure modes are governing in high flexural stress areas (at midspan), whereas core-related failure modes are governing in high shear stress areas (at supports)
- The serviceability limit state is governing over the ultimate limit state (see fig. D.6)
- Using higher-modulus materials results in a lower governing reserve factor

In the next phase, the structural design will have to be refined in order to optimise with respect to cost and weight. Stiffening the panel, and tapering the plate edges are two examples to accomplish this. Next to refining the structure, the model will have to be extended to better reflect the actual loads and conditions.

6.2 Stiffened plate

The analysis of the basic sandwich plate indicates that the concept is technically feasible, but optimisation with respect to cost and weight is required to be competitive to conventional building materials. This section shows that significant efficiency improvements can be achieved by the addition of longitudinal stiffeners to the sandwich, connecting the face sheets.

6.2.1 Shear rigidity improvements

From fig. 6.2(a), it is clear that shear deformation accounts for a significant contribution to the deflection of the structure. This shear deformation is concentrated in the relatively weak core material between the stiff face sheets. Hence, to tackle the shear deformation, this low-grade material has to be substituted by higher-grade material.

6.2.1.1 Core shear modulus

A higher sectional shear rigidity can naturally be obtained by selecting a core material that offers better shear stiffness properties. Better properties however go hand-in-hand with a higher density and price of the material. For this comparison, it is assumed that the density and price of the core material are linearly proportional to the shear modulus. Other types of cores, such as balsa or honeycombs, are not considered for reasons mentioned under section 5.5.6.

6.2.1.2 Stiffeners

A second way of increasing the sectional rigidity is the addition of composite shear stiffeners (see section 3.2.3.2). Similar to I-beams, the bending stresses of such panels will be transferred through the flanges (face sheets), while the shear stresses are transferred through the web (stiffeners). Due to the high stiffness of the webs, the foam core between the laminates is spared from high stresses and thus deformation.

Two laminate compositions are considered; glass- and carbon reinforced lamella consisting of 60% fibres, and impregnated by epoxy resin. The stacking sequence complies with the recommendations of the CUR96, while being optimised for transferring shear forces. Of the total amount of fibres, 30% is divided over the in the 0° and 90° angle with respect to the longitudinal direction of the bridge. The remaining 70% is oriented at an angle of 45° and -45° with respect to the longitudinal axis.

6.2.1.3 Effectiveness of improvement methods

In order to evaluate which method is most effective, the performance with respect to structural weight and material cost is determined. By parameterisation of the core shear modulus (G_c) and the total stiffener percentage over width of the bridge (t_s), the relative performance of the methods could be plotted. fig. 6.8 shows the result for a core stiffness range of $0 < G_c < 130$ MPa, and a total stiffener percentage range of $0 < t_s < 15\%$ of the structure's width.

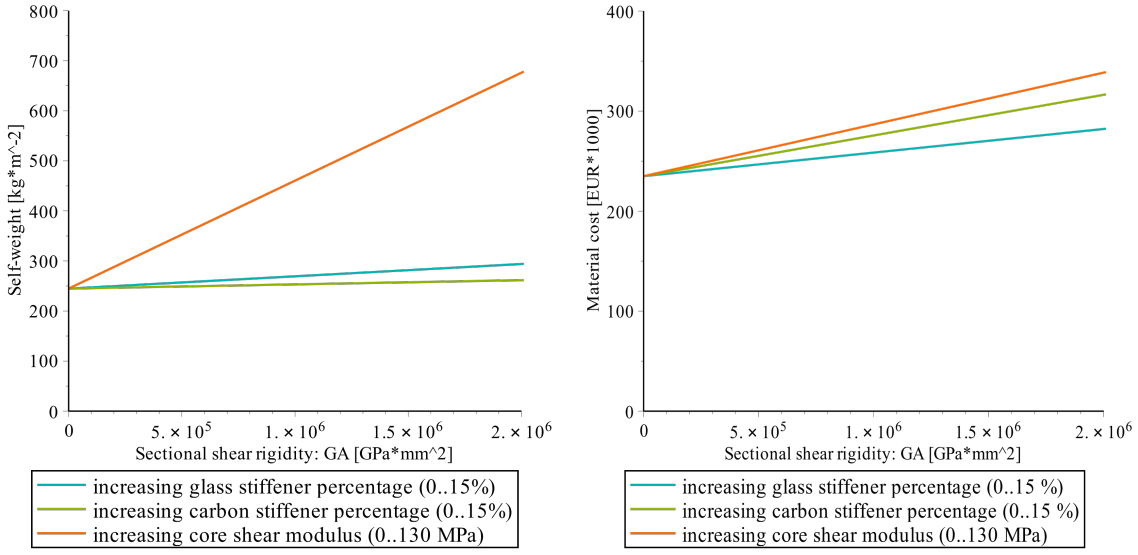

(a) Self-weight (kg/m^2)

(b) Material cost (Euro $\cdot 10^3$)

Figure 6.8: *Relative performance of stiffeners and core shear modulus*

The figures clearly show that the addition of shear stiffeners is a more efficient way to increase the shear rigidity of the panel compared to the use of higher-density foam. Furthermore, it seems that glass-reinforced stiffeners offer a higher value-for-money than carbon-reinforced stiffeners do. Hence, in the following model, only glass-reinforced stiffeners are considered.

6.2.2 Model parameters

The changes in the hand-calculation model, with respect to the input and assumptions of section 6.1, are given in this section.

6.2.2.1 Stiffeners

The configuration of the stiffeners is discussed under section 6.2.1.2. Only glass-reinforced stiffener laminates are considered, since these offer the highest value-for-money.

6.2.2.2 Panel configurations

As the shear force is mainly transferred through the stiffeners, it is possible to completely omit the foam core. Hence, two new panel types (E and F) are introduced for comparison. Note that these hollow panel types are fictitious, as the selected production method requires some sort core to act as a mould for the laminating process.

Table 6.8: *Six sandwich panel configurations*

		Core		
		Medium-density PVC	High-Density PVC	Hollow
Face laminate	55% glass 15% glass 15% glass 15% glass	**Panel A**	**Panel B**	**Panel E**
	55% carbon 15% glass 15% glass 15% glass	**Panel C**	**Panel D**	**Panel F**

6.2.2.3 Loads

For simplicity, the load model is limited to the uniformly distributed load (q_d) only. Omitting the concentrated load (Q_d) avoids having to deal with effective widths, allowing the stiffener thickness to be expressed per unit width of the bridge. Subsequent analysis should be performed in order to investigate the behaviour of the stiffeners under the influence of concentrated loads.

6.2.2.4 Deflection limit

As the uniformly distributed load is considered as load model, the deflection limit for of the structure has to be changed accordingly. Previous analysis has shown that this load model roughly accounts for 50% of the total deflection of the structure. Hence, a limit state of $L/800 = 20$ mm is maintained.

6.2.3 Contribution from bending and shear

Analogous to the approach in section 6.1.2.1, the bending- and shear contribution to the deformation is investigated for a range of design parameters. Figure 6.9(a) shows that the shear contribution rapidly decreases for an increasing stiffener thickness per unit width of the bridge. Figure 6.9(b) shows the total deflection of the different panel configurations.

It can be concluded that the shear modulus of the core is of minor importance if the thickness of the stiffeners account for more than 2% of the structure's width. For increasing stiffener width, the total deflections of the panels converge to the partial deflection from bending deformation only.

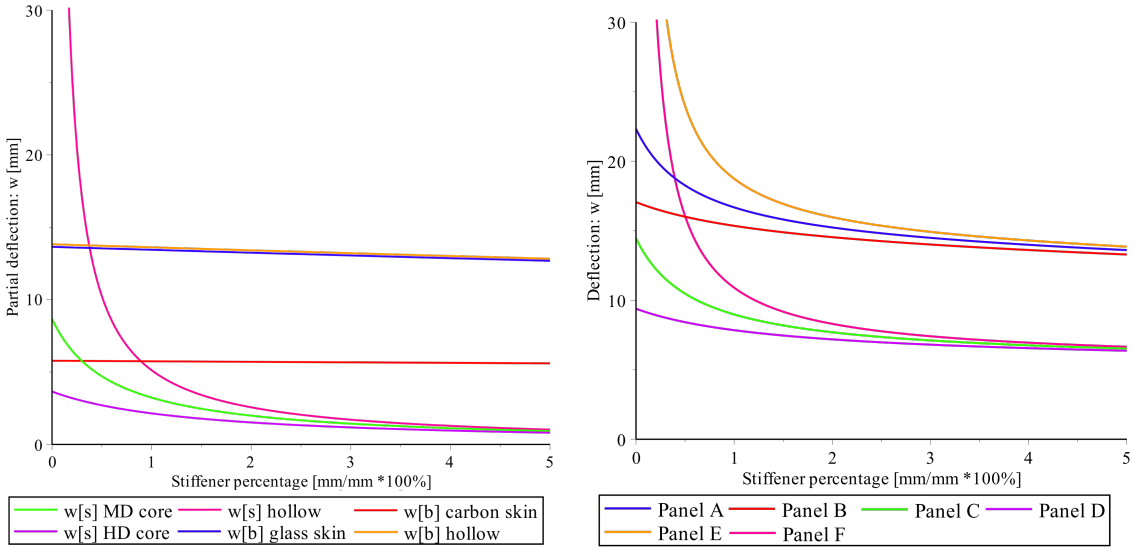

(a) Shear- and bending contribution

(b) Total deflection of panel configurations

Figure 6.9: *Partial- and total deflections for fixed structural height of H=1100 mm*

6.2.4 Performance of panel configurations

Figure 6.9 shows that the addition of stiffeners is effective in the reduction of the deflections. However, as fig. 6.8 shows, the stiffeners also contribute to a higher self-weight and material price at a constant panel configuration. The addition of stiffeners only helps optimising the efficiency of the panel if the beneficial effects outweigh the detrimental effects.

To investigate for which set of parameters the stiffeners are of added value to the structure, a similar analysis as for the basic sandwich panel is conducted. The following parameters are investigated:

- Skin thickness
- Skin material
- Core material
- Stiffener percentage

Note that construction height is no longer considered as a parameter, since it is established that maximising this height is most efficient. Hence, the construction height is maximised within the boundary conditions; $H = 1100$ mm.

For the six different material sets (A to F), and a range of stiffener percentages, a panel configuration is determined that complies with the deflection limit state of L/800. Subsequently, the self-weight and material cost for these configurations are determined by using the input from table 6.2. Figure 6.10 summarizes the result of this analysis.

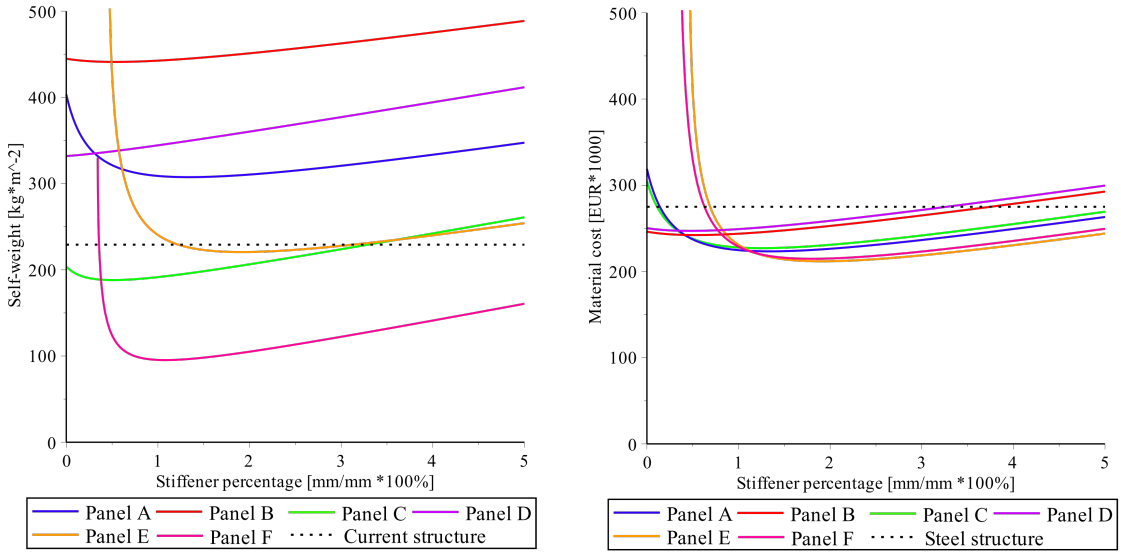

(a) Self-weight (kg/m^2)

(b) Material cost (Euro $\cdot 10^3$)

Figure 6.10: *Optimisation of stiffener percentage for all panel configurations that comply with L/800 limit state, having a fixed structural height of H=1100 mm*

There seems to be a different optimum in the stiffener percentage for each defined material set, lying somewhere between 0.5 and 1.5% per unit width. A clear optimum can be identified for all hollow- and low-density core panels, whereas an optimum is less pronounced for the high-density core panels (B and D). Obviously, the hollow panels are unable to transfer any type of loading without the use of stiffeners, hence the solution goes to infinity at $t_s = 0\%$. The carbon-reinforced panels on the other hand, already comply with the limit state without any stiffener. Hence, the efficiency decreases for an increasing stiffener percentage.

Considering both weight and price, it is clear that a the use of stiffeners allows for a more efficient design. This optimum percentage may slightly change as concentrated load models are considered as well, which will be done in a next phase.

6.2.5 Conclusions

From fig. 6.10(a) and fig. 6.10(b) it can be concluded that, by decreasing the density of the core, the panels become more efficient with respect to weight and price. Furthermore, carbon-reinforced panels are not necessarily more expensive, whereas they offer a much higher efficiency with respect to weight. Lastly, when the right material set is chosen, the stiffened sandwich panel is competitive with an equivalent steel structure in terms of weight and price.

It must be noted that only global deformation has been considered in this analysis. Local buckling of the stiffeners may however prevail over global deformation, especially in the case of hollow panels. Non-linear finite element models can be used to analyse the local stability of the stiffeners under the influence of distributed and concentrated loads.

7 Bascule design

7.1 Tail design

The previous chapter has shown that fibre-reinforced composites can be a viable alternative to steel as construction material for the leaf of a bascule bridge. One end of the leaf rests on the supports of the abutment, whereas the other end is connected to the tail of the bridge. In orthotropic steel structures, the tail usually consists of an extension of the main girders. These girders make a kink to fit underneath the roof of the bascule chamber, and are subsequently attached to the counterweights. The trunnions are usually connected at the position of the kink, where the construction height of the girder is maximised. The required stabilising- and operating mechanisms are generally attached between the kink and the counterweights.

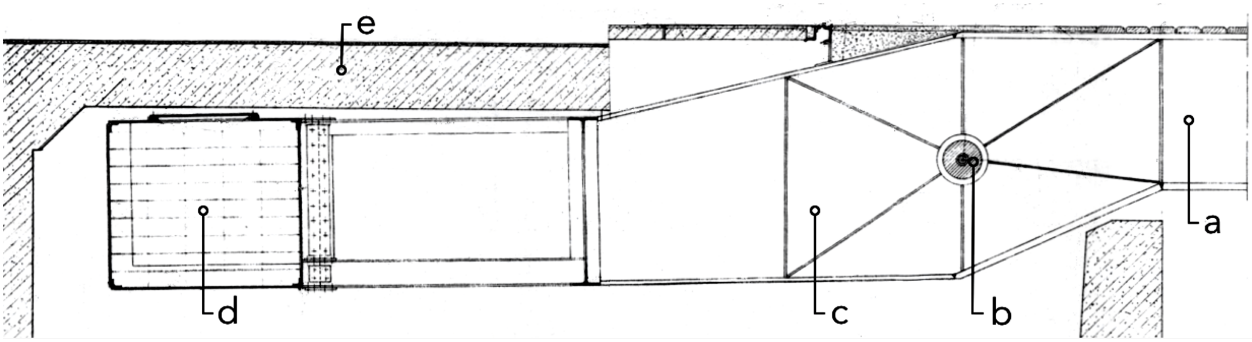

Figure 7.1: *Detailed drawing of trunnion bascule bridge tail-section: (a) bridge leaf, (b) trunnion, (c) stiffened kink in main girders, (d) counterweight and (e) bascule chamber roof - courtesy of Witteveen+Bos [edited]*

Most modern bascule bridges in the Netherlands have a tail configuration similar to what is displayed in fig. 7.1, as apparently it is an effective solution. In this thesis however, the used construction material is very different from these traditional steel bridges. Therefore, for an integrated design, the tail must be reconsidered in the process.

7.1.1 Construction material

All structural mass that is located at the tail-side of the the pivot axis is beneficial to the balance of the structure. Therefore, it is basically counterproductive to execute the bascule tail in lightweight (and expensive) composite material. The obvious solution for the tail design would thus be connecting the composite leaf to a steel tail structure. Doing so would be beneficial for the balance, but more importantly, the challenges with respect to local stress concentrations around the pivot axis would be simplified.

The same conclusion was drawn in the feasibility study for the Andel bascule bridge, as discussed in section 2.5.3. A connection between the composite leaf and the steel tail structure was developed and tested. A double-strap combined joint (both fastened and bonded) was used to transfer the cross-sectional forces from leaf to tail. The details of this connection are discussed in the section underneath fig. 2.16.

7.1.1.1 Steel

When connecting the composite leaf to a steel tail structure, a conventional steel trunnion pivot system can be used. This trunnion design has proven to be effective and quite durable, in contrast to any new solutions that can be thought of. On the other hand, other complications are introduced. First of all, the steel part of the structure would require more frequent maintenance than the composite part, thereby abolishing one of the biggest advantages of the composite structure. Furthermore, the suggested connection for the Andel bridge is rather complex and thus expensive. Load transfer primarily depends on adhesive bonds, which long-term performance under the influence of environmental- and cyclic loading cannot be guaranteed. Lastly, mechanical fasteners are applied as a secondary load-path in case of adhesive bond failure. This however implies that that the composite material must be designed to withstand the localised peak stresses in the vicinity of the fasteners. Hence, the localised stress problem has not been solved, but is rather relocated to a somewhat more convenient location.

7.1.1.2 Composite

As discussed in chapter 3, fibre-reinforced composite material is in some ways very different from construction steel. As opposed to metals, composites are both inhomogeneous and anisotropic; the properties dependent of location and orientation within the material. Furthermore, the material does not have the ability to plastically deform and redistribute stresses to adjacent material. These differences in material characteristics impose a big challenge in the tail- and pivot design, in which one has to deal with high localised loads in different directions.

The conclusion of the Andel bridge feasibility study was that a fully composite structure was too complicated and expensive to produce. It must however be noted that the production techniques have considerably advanced in the past two decades since this study was performed. The design team of the Andel bridge only had access to hand lay-up production, offering a maximum fibre fraction of 35%. The modern resin transfer moulding technique allows for more complex shapes and much higher fibre fractions. The entire structure could be moulded and impregnated in a single production, thereby creating a unitised structure without abrupt cross-sectional discontinuities. Furthermore, the whole structure will require the same low maintenance frequency. The stress concentration problem is however not yet solved, as peak stresses in the composite material will now occur in the vicinity of the pivot axis.

7.1.2 Position of deck joint

Another important decision is the location of the joint between the bridge deck of the fixed and the movable part of the bridge. Basically, three different configurations are possible, as schematised in fig. 7.3.

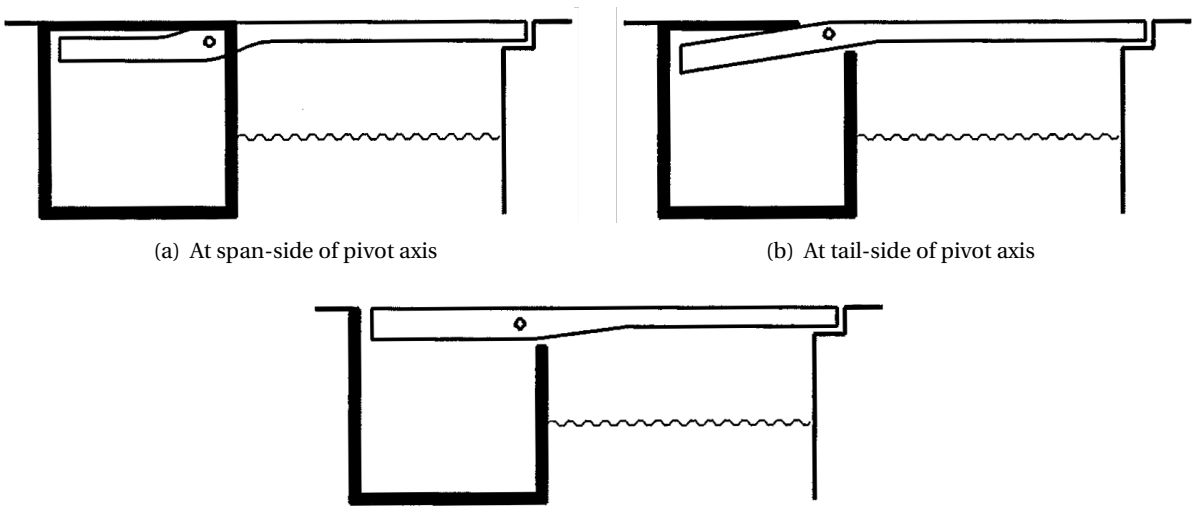

(a) At span-side of pivot axis

(b) At tail-side of pivot axis

(c) At counterweight

Figure 7.2: *Three possible deck joint locations [Oosterhoff and Coelman, 1999]*

7.1.2.1 Joint at span-side of pivot axis

Figure 7.3(a) shows the most common deck joint location for modern bascule bridges; at the span-side of the pivot axis.

Advantages This configuration is often preferred, as it allows for a somewhat protected environment inside the bascule chamber. Apart from some cutouts for the continuous main girders, the chamber is closed off from water and dirt. Furthermore, in this configuration the tail is never subjected to traffic loads.

(a) View from across waterway

(b) View from pivot-side

Figure 7.3: *The Julianabridge in Alphen aan den Rijn features a deck joint at the span-side of the pivot axis*

Disadvantages The closed character of the chamber complicates the assembly of the bridge. The roof of the chamber can only be installed after the completing the assembly of the bridge, and must furthermore be removable for renovation works. The tail structure is required to have a kink, so that there is sufficient space for the chamber roof.

7.1.2.2 Joint at tail-side of pivot axis

Figure 7.3(b) shows a configuration in which the deck joint is located at the tail-side of the pivot axis. The bascule chamber is only partly closed. A closed look a the differences between this joint location and the one discussed above is given by fig. 7.4.

Advantages This configuration was preferred before the 1940's, as it is much easier to execute. During the construction, the fully assembled bridge structure can be lifted into the bascule chamber, through the hole in the chamber roof. Furthermore, just a single bend in the tail section will suffice to allow space for the chamber roof.

Disadvantages In the opened position of the bridge, one could see straight down into the bascule chamber. This also implies that all dirt on top of the movable bridge deck can fall through this gap. In order not to affect the operating machinery, the dirt must be intercepted or the machinery must be protected. Figure 7.4(b) shows a simple solution for this problem; a valve above the deck joint that should prevent dirt from falling into the chamber. Another disadvantage is that a small part of the tail is subjected to traffic loads, which must be counterbalanced to avoid unintentional opening of the leaf.

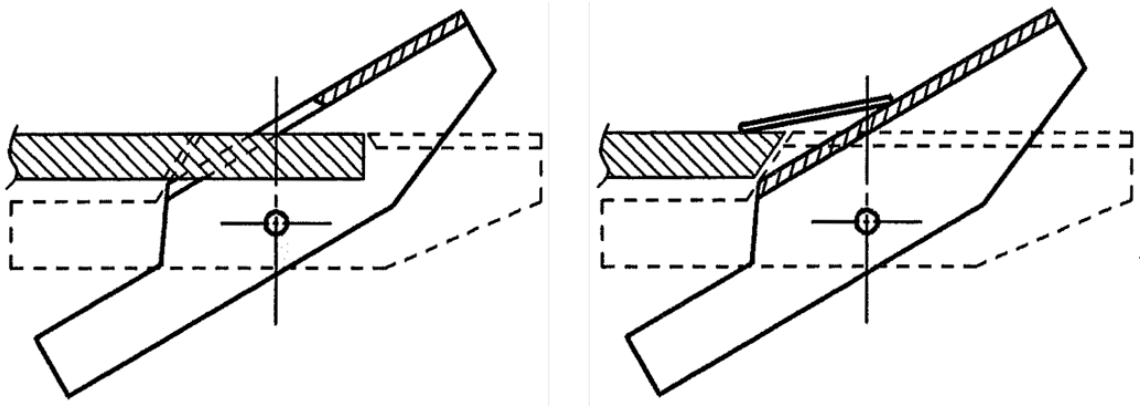

(a) Span-sided deck joint (b) Tail-sided deck joint

Figure 7.4: *Detail at pivot axis for different joint locations [Oosterhoff and Coelman, 1999]*

7.1.2.3 Joint at counterweight

Figure 7.2(c) shows a configuration in which the joint between the fixed and movable part of the bridge is positioned at the abutment side of the bascule chamber, right at the counterweight. This implies that traffic loads are not just exerted on the span, but on the full length of the structure.

Advantages The main advantage of this configuration is that no kink in the main girders is required. The continuous cross-sectional profile along the length of the structure results in a more uniform distribution of stresses. Next to that, the weight of the road deck and furniture at the tail-side positively contributes to the balance of the structure. Furthermore, the assembly of the bridge is much easier, due to the absence of a bascule chamber roof. Also the joint itself is the more simplistic than for the alternatives.

Disadvantages The main disadvantage of this joint position is the relatively complex stabilising system that is required. One can imagine the effect on the balance of the bridge as a heavy truck drives onto the tail-side of the bridge. To assure stability under this load, the bridge basically requires to be fixed in the closed position. This can be achieved by installing an additional set of live load supports near the counterweight. The bridge is lifted on top op these supports at the end of the closing cycle, disconnecting the pivot system. Such a system is both expensive and would require frequent maintenance. A second disadvantage is the fact that dirt on top of the bridge deck will end up in the bascule chamber during an opening cycle.

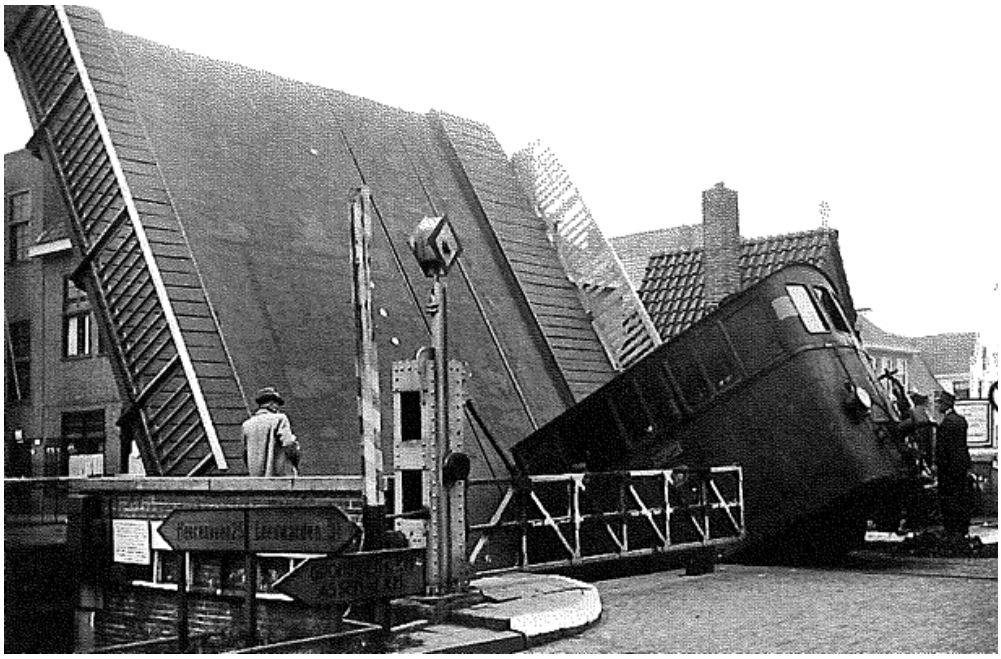

Figure 7.5: *Safety is one of the disadvantages of a traffic-subjected tail [Oosterhoff and Coelman, 1999]*

7.1.2.4 Comparison

The considered pros and cons with respect to the location of the deck joint are translated into the following table for a qualitative comparison.

Table 7.1: *Qualitative comparison of deck joint location*

	Position of deck joint		
	Span-side of pivot	Tail-side of pivot	Counterweight-side
Composite compatibility			
Environment bascule chamber			
Tail subjected to traffic loads			
Complexity girder shape			
Complexity installations			
Ease of assembly			
Maintenance requirement			

7.1.3 Design approach

Based on the considerations from section 7.1.1, it would be desirable to use composite material for the tail of the bascule construction. This option will therefore first be considered in the design process. As demonstrated in chapter 6, the main challenge in the span design is the stiffness of the structure. When looking at the pivot design, it becomes apparent that not stiffness but strength will be critical. The focus in the design should therefore be at reducing the effective stresses on one hand, and increasing the structural resistance on the other. The following design principles can contribute to a technically feasible solution:

- reducing the overall weight of the structure
- increasing the contact areas that transfer the reaction forces
- avoiding cross-sectional discontinuities
- avoiding complex and tension-loaded joints
- tailoring the fibre-reinforced composite to the expected stresses
- substituting composite material by more suitable material (primarily steel) where necessary

The third item, avoiding cross-sectional discontinuities, suggests that the cross-sectional configuration of the tail should be similar to the leaf of the bridge. This would rule out the possibility of having the deck joint at the span-side of the pivot axis, as this requires the continuation of only the main girders (as can be seen in fig. 7.3(b)). Considering the remaining two options, the qualitative comparison from table 7.1 shows that a tail-sided deck joint is more favourable. Hence, in the further course of this chapter, the focus will be on designing a composite tail with a deck joint at the tail-side of the pivot axis.

7.2 Pivot sytem

In this section, the possibilities for a pivot system of the composite bascule structure are investigated. As mentioned before, local peak stresses will pose the biggest challenge in a composite tail design. In order to find a suitable solution, the design principles as listed under section 7.1.3 should be respected.

As discussed in chapter 2, a bascule bridge consists of a single moving element, which pivots about a horizontal line near its centre of gravity so that the weight on either side of the pivot axis is balanced. During the evolution of the bascule bridge, several variations of pivot systems have been developed. These different types can roughly be classified in two categories; trunnion-bascule and rolling-bascule bridges (see section 2.1).

The trunnion pivot system is nowadays the standard choice; the latest rolling bascule in the Netherlands dates back to 1939 [Oosterhoff and Coelman, 1999]. Apparently, the trunnion pivot system is favourable for modern steel bascules. This is however not necessarily the case for other structural types and materials. Therefore, both options will be kept open, and a comparative analysis should lead to the most suitable pivot system for the composite structure.

7.2.1 Trunnion bascule system

A trunnion pivot system relies on metal shafts (trunnions) that connect the main girders to the bearings, which allow the structure to pivot around a static axis. The trunnion is normally rigidly connected to the web of the girder by means of a hub. At the location of the hubs, the webs of the main girders are strengthened in order to bear the stresses at every opening angle of the bridge, as can be seen from fig. 7.6. The assembly of the trunnion pivot system is shown in fig. 2.3.

(a) View from inside bascule chamber

(b) Deteriorated part of Julianabridge

Figure 7.6: *Web stiffening at the location of trunnions*

7.2.1.1 Composite implementation

Steel bascule structures generally have two main girders that are extended into the tail. Two separate small trunnions connect the girders to the bearings at either side of the structure. To provide force equilibrium, a compressive strut is installed at the inboard side of the main girders (see fig. 2.4). The sandwich composite structure, in which the cross-section of the tail is similar to the span, does not have two distinct main girders. Instead, the sandwich panel has a number of vertical stiffeners, which are confined by structural foam. The trunnion bearing can therefore not be positioned right next to the stiffeners, but must be positioned at either side of the structure.

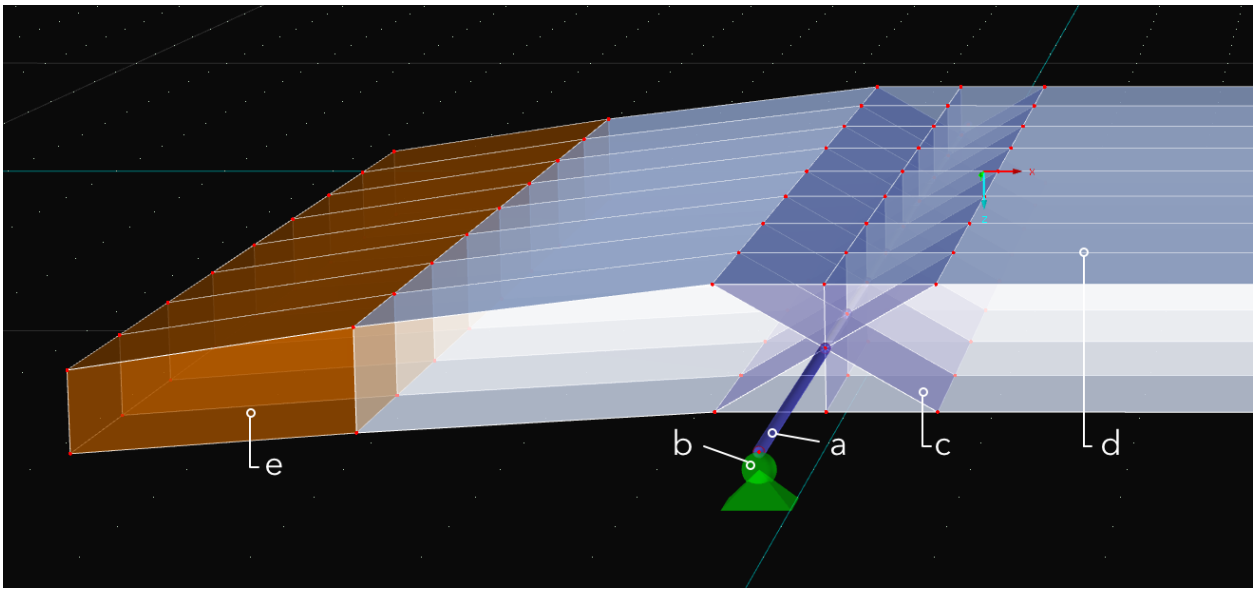

Figure 7.7: *Impression of trunnion implementation in composite structure: (a) steel trunnion, (b) trunnion bearing, (c) transverse stiffeners, (d) longitudinal stiffeners and (e) counterweight*

7.2.1.2 Structural details

Transverse stiffeners In order to avoid localised loads from the trunnion on the longitudinal stiffeners, a transverse composite stiffener will be required at the position of the trunnion. This transverse stiffener will also act as the compressive strut between the trunnion bearings. Additionally, two stiffeners in a 60° and 120° angle with respect to the face sheets are provided, in order to have sufficient strength and stiffness during the opening cycle.

Joints between laminates The transverse stiffeners intersect with the longitudinal stiffeners, while both are also connected to the face sheets. These intersections result in relatively complex joints. The resin transfer moulding technique however enables to create such joints, in which the fibres are continuous between the laminates of the face sheets and the stiffeners. As discussed in section 3.2.3.2, the structure is created by wrapping the core foam blocks with continuous unidirectional fibre mats, which are subsequently impregnated. The course of the continuous fibres must be carefully considered, such that kinks in the fibre direction are minimised. Furthermore, laminate connections that are subjected to tension should not purely transfer stresses through an adhesive bond. This can be achieved by providing additional mid-laminate plies. Figure 7.8 shows a possible fibre configuration in the longitudinal cross-section, in which the tension joints are reinforced with mid-laminate plies. Please note that the laminates are not drawn to scale.

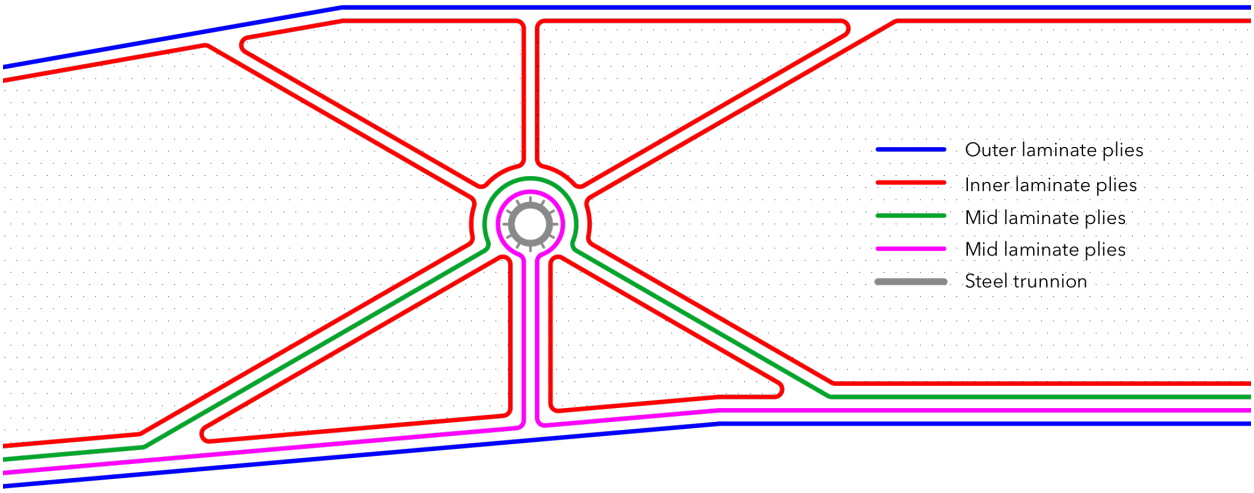

Figure 7.8: *Configuration of continuous fibres, creating a unitised structure with embedded trunnion*

Joints between stiffeners and trunnions Trunnions are normally composed of steel, which offers a high resistance to wear and tear from friction during the rotation. A rigid connection between the cylindrical steel trunnion and the transverse stiffeners can be provided by an embedded steel hub. This connection technique, developed in the automotive industry, relies on the transfer of stresses by steel pins on the exterior of a cylindrical mandrel. These pins are subsequently embedded in the woven laminates of the transverse stiffeners. A uniform transfer of stresses is achieved by tapering the edge of the mandrel. The joint concept is shown in fig. 7.9.

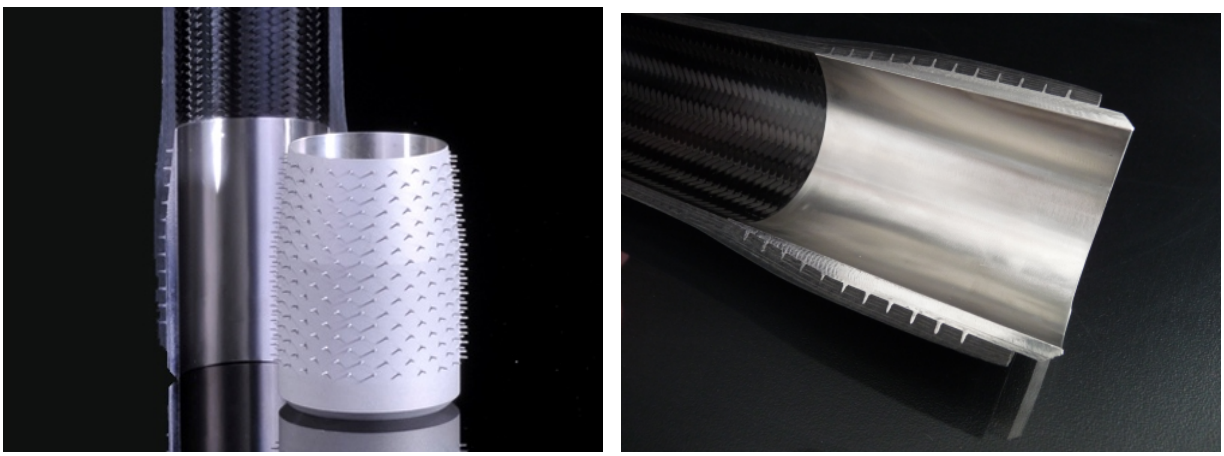

(a) Pinned steel mandrel

(b) Mandrel integration in composite

Figure 7.9: *Composite-metal shaft connection [Teufelberger Composite, 2014]*

7.2.2 Rolling bascule system

Rolling bascule bridges translate backwards during the opening rotation, resembling the motion of a rocking chair. The structure is suspended near the gravitational axis on a cylindrical shaped bulge, known as the quadrant. Slipping of the quadrant on the tracks is avoided by threaded plates, or by pegs and sockets (see fig. 7.12(b)).

There are two basic types of rolling bascule bridges; one having the rolling quadrants located below the driving deck, and the other having them above the deck. The latter type was seldomly applied in the Netherlands, and it does not require a bascule chamber. Allowing this in this study would open the way for many other types of movable bridges. Hence, this type is not further considered.

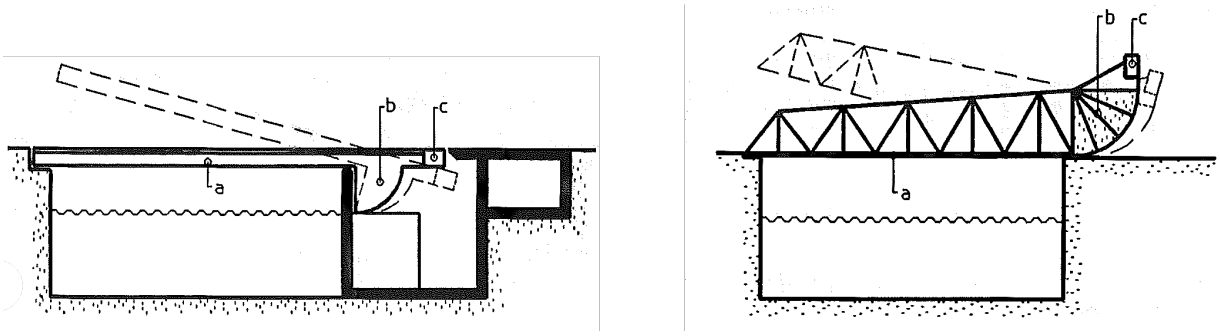

(a) Quadrants below deck

(b) Quadrants above deck

Figure 7.10: *Two basic types of rolling bascule bridges [Oosterhoff and Coelman, 1999]*

7.2.2.1 Composite implementation

Steel rolling bascule bridges are normally suspended on a number of individual rolling quadrants, attached under the main girders of the structure. The foreseen composite structure does not have main girders, but is based on a number of longitudinal stiffeners distributed over the cross-section. The rolling quadrant should subsequently also stretch over the full width of the structure, creating a line support at the pivot-side of the span.

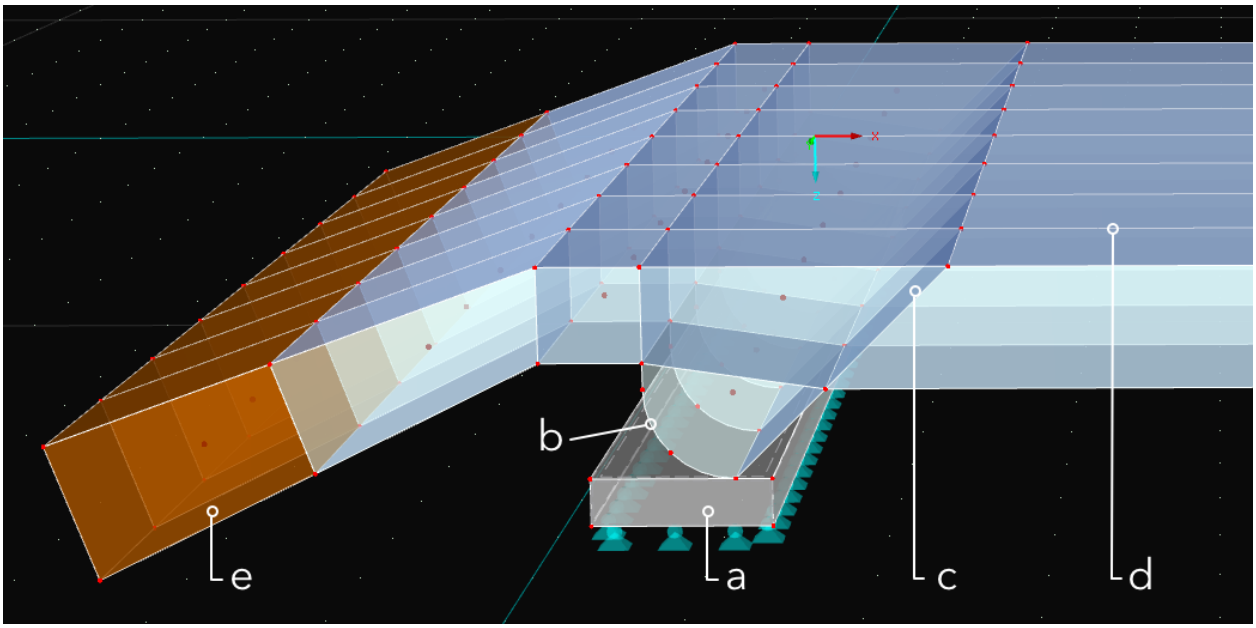

Figure 7.11: *Impression of rolling system implementation in composite structure: (a) front wall bascule chamber, (b) rolling segment, (c) transverse stiffeners, (d) longitudinal stiffeners and (e) counterweight*

7.2.2.2 Structural details

Rolling quadrant The quadrant is subjected to both dead- and live loads in the closed state of the bridge. In the opened state, the full weight of the structure is transferred through the quadrant. In every position of the bridge, the reaction forces must be transferred to the longitudinal stiffeners and subsequently the face laminates of the panel. The core of the rolling quadrant will be made of high density foam. The improved strength and stiffness properties of this core will support the face laminates and slightly release the stresses in the stiffeners.

During the opening movement, the contact surface between the structure and the substructure travels along the perimeter of the quadrant. The associated localised stresses will be dealt with by a steel skin, which will be attached to the perimeter of the quadrant. The steel skin will furthermore offer resistance to wear and tear as a result of friction. Furthermore, the steel can accommodate the sockets that align with pegs on the substructure. To be able to fulfil all these functions, the steel layer must be several centimetres thick.

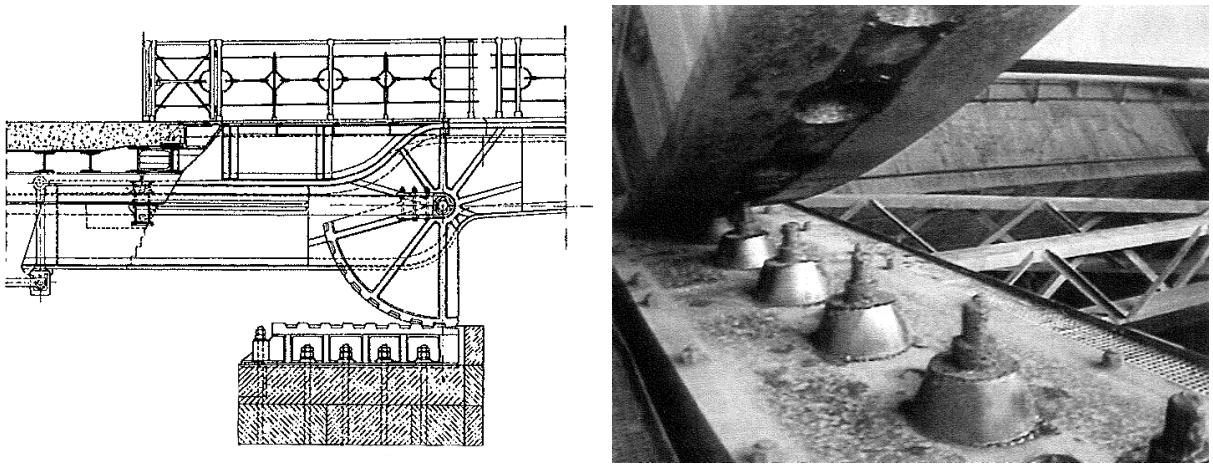

(a) Rolling quadrant and track

(b) Pegs and sockets

Figure 7.12: *Traditional cast steel design of rolling quadrants and tracks [Oosterhoff and Coelman, 1999]*

Joint between quadrant and superstructure The resin transfer moulding production technique provides the freedom to create complex structural shapes. It allows to create a fully unitised composite bridge structure, in which the rolling quadrant is incorporated. Again, kinks in the laminate direction should be minimised and resin-dominated joints under tension stresses must be avoided. Figure 7.13 gives an example of a proper laminate configurations in the longitudinal cross-section at the quadrant.

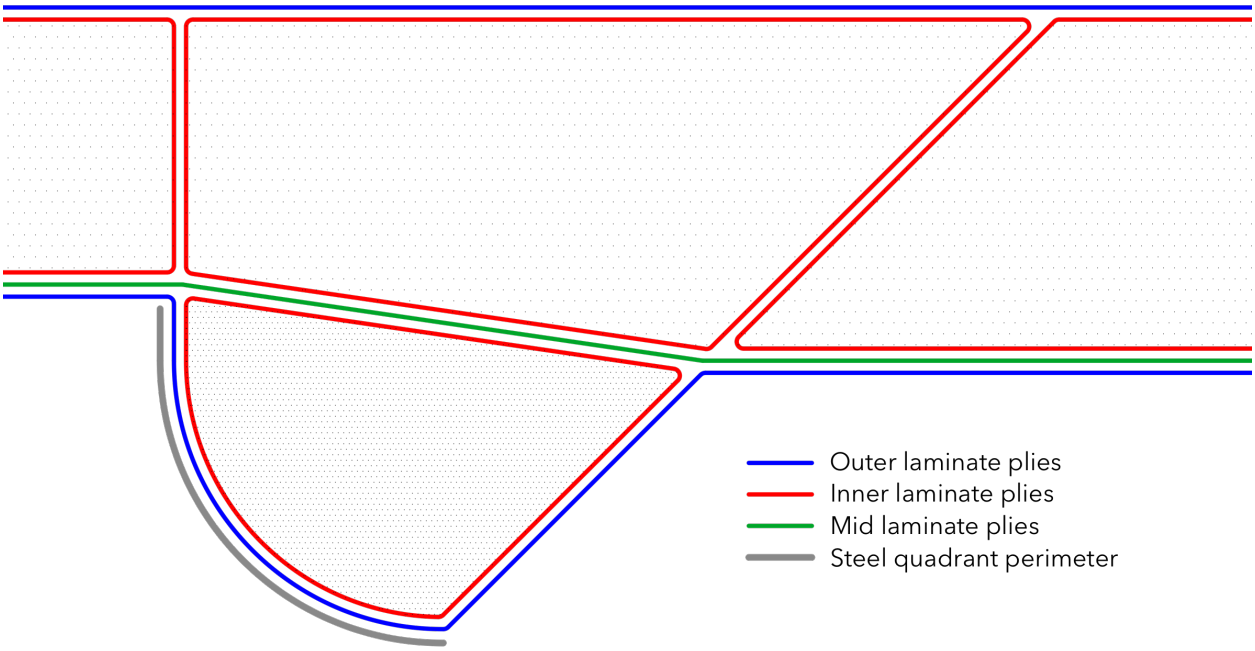

Figure 7.13: *Configuration of continuous fibres, creating a unitised structure with quadrant*

7.2.3 Comparison

The previous sections have shown how both the trunnion- and the rolling pivot system can be implemented in the composite structure. The characteristics of both pivot systems will be compared in this section.

7.2.3.1 Composite compatibility

The compatibility of the pivot systems with the composite structure is evaluated on the basis of the design principles as discussed in section 7.1.3.

Load distribution As discussed, localised stresses are a decisive factor in the vicinity of the pivot axis. Therefore, the aim is to maximise the area over which the support loads are distributed.

The trunnion bascule is suspended by two trunnion bearings at either side of the structure. The rolling bascule structure, on the other hand, is supported over the full width of the bridge. Hence, it is clear that the trunnion pivot system results in higher localised stresses than the rolling pivot system.

Material use and complexity When comparing the longitudinal cross-section of both structures, it is clear that creating the rolling pivot system requires more material than creating the trunnion pivot. The trunnion structure however requires more complex joints, both between the composite parts and between the composite and steel trunnion.

Complexity of laminate joints is mainly determined by the number of laminates that come together at one point. In the rolling bascule structure, the maximum number of meeting laminates is four. These joints are merely subjected to compressive stresses. In the trunnion structure, the number of laminates meeting at the pivot axis is six. Furthermore, this joint is partly loaded in tension. Hence, the composite joints of the trunnion structure are much more complex (see fig. 7.8 and fig. 7.13)

Also the joint between the composite material and the steel part is more complex for the trunnion pivot system. The steel plate at the perimeter of the rolling quadrant is merely subjected to compression, and can therefore simply be adhesively joined to the laminate. The trunnion-composite connection, on the other hand, relies on the joint as displayed in fig. 7.9.

7.2.3.2 Global structure

Both pivot systems can comply with the specified geometrical boundary conditions of the reference bridge. A graphical representation of the implementations of the two alternatives is included in appendix E.

Opening angle and span The functional requirements state that the horizontal and vertical clearance must be retained with respect to the current situation. In the opened state, the full width of the channel must be available for vessels. The vertical clearance within this width must be unlimited. These requirements are met by a combination of the opening angle, and the location of the pivot axis.

For the trunnion bascule, the maximum required opening angle of 85° is maintained. The location of the pivot axis, for which the vertical clearance is unlimited, results in a span length of 16.35 meter. The rolling bascule translates backwards during the opening rotation. Therefore, an opening angle of 83° is already sufficient to comply with the vertical clearance requirement. The resulting span length is 15.25 meter.

A smaller span length directly translates into a more efficient structure. Since the spanning length is taken to the fourth power in the deflection, the following rule-of-thumb shows that the 7% decrease in span length roughly results in a 24% increase in efficiency:

$$\frac{16.35^4 - 15.25^4}{16.35^4} * 100\% = 24\% \tag{7.1}$$

Tail length The tail should be designed such that the structure fits within the boundaries of the bascule chamber, while maximising the lever arm of the counterweight.

For the trunnion bascule, the tail can extend all the way to the back of the bascule chamber, resulting in a tail length of 5.83 meter. The length of the tail for the rolling bascule is restricted by the height of the bascule chamber, which is limiting in the opened position. The maximum tail length is 5.67 meter.

A larger lever arm directly translates into a smaller required counterweight. As this effect is linear, the longer lever arm of trunnion structure results in roughly a 3% smaller counterweight.

7.2.3.3 Other considerations

Bascule chamber renovation When comparing the concrete cross-section of the bascule chamber from appendix E, it becomes apparent that the rolling bascule alternative requires a more drastic renovation to the bascule chamber than the trunnion bridge. In both alternatives, the chamber's roof will have to be replaced by one that spans over the full width of the structure. For the rolling bascule chamber, also the wall at the waterway-side requires much work.

Durability One of the concerns with rolling bascule bridges, is that the have found to be prone to wear and tear. This is one of the reasons why this type of pivot system is rarely used in the past decades. As a result, the advancement of the technique have stalled. Trunnion pivot systems, on the other hand, are widely applied and have become a speciality for some companies.

The risk of rapid deterioration of the rolling quadrant is reduced by the thick steel layer that is attached at the perimeter of the composite quadrant. Next to that, the contact area for traditional steel rolling bascules is much smaller, as the bridge was generally suspended on a small number of individual quadrants. The composite quadrant, on the other hand, extends over the full width of the structure.

7.2.3.4 Conclusion

The considered pros and cons of both pivot systems are translated into the following table. The trunnion system is favourable in more aspects than the rolling bascule. However, those aspects in which the rolling bascule is favourable are considered more important. Especially the lower localised stresses and reduced structural complexity can make the difference in weather the composite bascule structure is feasible of not. Hence, it is chosen to continue with the rolling pivot system.

Table 7.2: *Qualitative comparison of pivot system*

	Type of pivot system	
	Trunnion bascule	Rolling bascule
Localised stresses		
Material use		
Structural complexity		
Span length		
Lever arm counterweight		
Construction works chamber		
Durability		

7.3 Operating system

As discussed in section 2.2.4, the term 'operating system' refers to the collection of mechanical and/or hydraulic components that drive the bridge during the opening/closing cycle. The purpose of these components is to convert the low-torque high-speed output for the prime mover to a high-torque low-speed rotation that is required to move the span.

In traditional bascule structures, the tail of the structure consists of the extension of two or more main girders. The components of the operating system are generally positioned between these main girders, such that the structure does not interfere with the operating system during its movement. Since the proposed composite tail structure has a continuous surface over the width and length of the tail, the interference space is much bigger. Therefore, the positioning of the operating system within the bascule chamber is more challenging for the composite tail.

In this section, a number of possible operating system configurations for the composite rolling bascule bridge will be introduced and evaluated.

7.3.1 Rack-pinion systems

Rack and pinion systems comprise a pair of gears, which convert a rotational motion (from the generator) into a linear motion. The circular gear, called the pinion, translates over the linear gear, called the rack. Two common rack-pinion combinations as the driving mechanism of bascule bridges are discussed.

7.3.1.1 Horizontal rack

The combination of a driven pinion and a horizontal rack is among the most common driving mechanisms for rolling bascule bridges. The driven pinions are rigidly connected to the main girders of the structure, at the position of the rolling axis. This axis remains at the same horizontal level during the combined rotation/translation of the structure. The rotation of the pinions on the racks introduces a horizontal pulling or pushing force at the rolling axis, driving the motion of the span.

As discussed, the composite tail design is not based on main girders. Therefore, the pinions can only be fixed to the two external webs at either side of the structure. As a consequence, the full operational force is divided over just two locations, resulting in high localised stresses during operation.

7.3.1.2 Segmental rack

Segmental rack-pinion systems were commonly applied in trunnion bascule bridges, before more advanced systems (such as the panama-wheel) were invented. The installation is comparable to the horizontal rack-pinion, however the pinion is now located at the counterweight-end of the tail. The pinion moves along a circular rack segment during its rotation, which introduces an opening/closing force at the end of the tail. The implementation in a rolling bascule bridge would require an elliptical rack segment instead of a circular one, since the structure translates backwards during the cycle.

The main advantage of the segmental rack-pinion installation with respect to the horizontal alternative, is the greatly improved lever arm. Due to this larger lever arm, a smaller force is required during the opening cycle. This is beneficial for the magnitude of the localised stresses in the composite, in the vicinity of the connected pinion. Next to that, less torque is required during the operation.

A second advantage is that the rack segments are positioned outside the interference space of the moving structure. Therefore, one can apply as many pinions over the width of the bridge as necessary, thereby spreading the opening/closing loads. This in contrast to the horizontal alternative, where only one driving pinion can be positioned at either side of the structure.

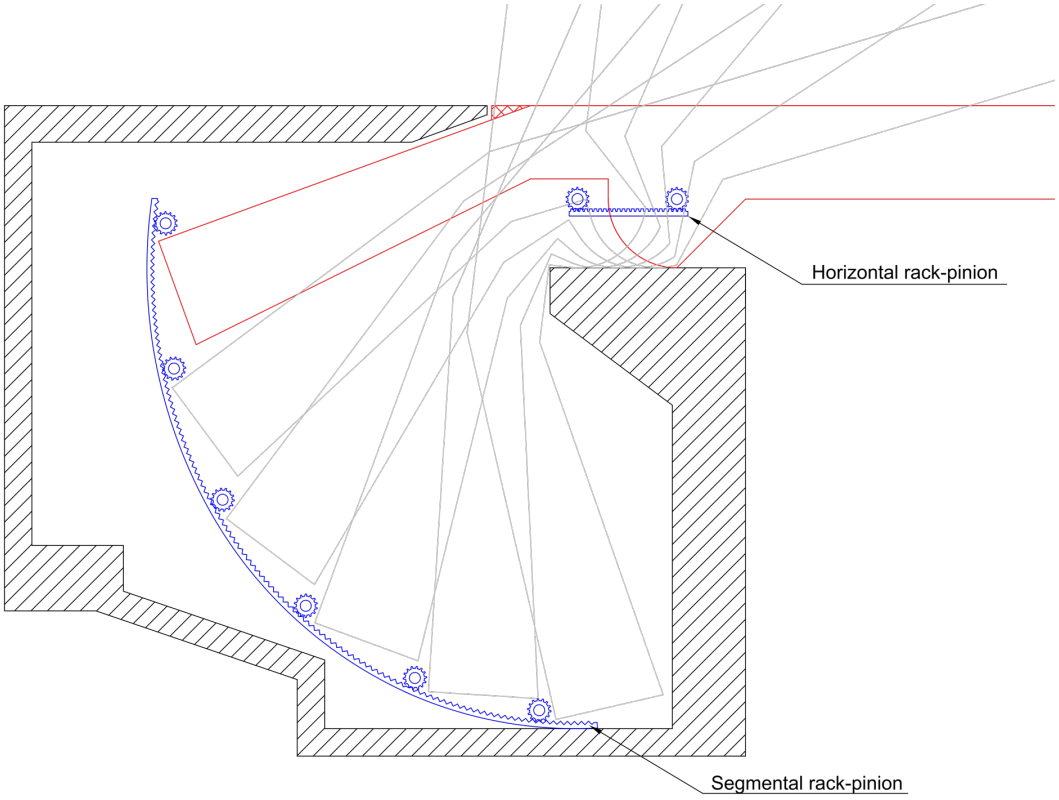

Figure 7.14: *Implementation of horizontal- and segmental rack-pinion driving mechanism*

7.3.2 Hydraulic systems

Hydraulic cylinders are linear actuators; the motion produced is along a straight line with respect to the longitudinal axis of the cylinder. The forces during operation are produced by pressurising fluids in the cylinder, which subsequently act on the pistons. The pressure in the cylinders is generated by an electrically driven pump. Hydraulic systems allow for a powerful installation in a very small space.

Hydraulic systems are well suited for the operation of large mechanisms, and are increasingly being used for movable bridges. This is especially true for bridge renovations, in which hydraulic cylinders can be installed to substitute deteriorated mechanical systems. The obsolete systems have to be disconnected, but do not necessarily have to be removed from the chamber.

The hydraulic systems can be designed with 'off the shelf' components. Hence, the systems are known for their low initial cost and fast installation. Reliability and durability, on the other hand, are the weak points of hydraulics. Fluid levels should be checked regularly and replaced after certain intervals.

Telescopic cylinders, which extend and retract in multiple stages, are much more expensive and require more maintenance. Therefore, the aim is to stick to conventional non-telescopic cylinders. This does however limit the implementation possibilities within the bascule chamber.

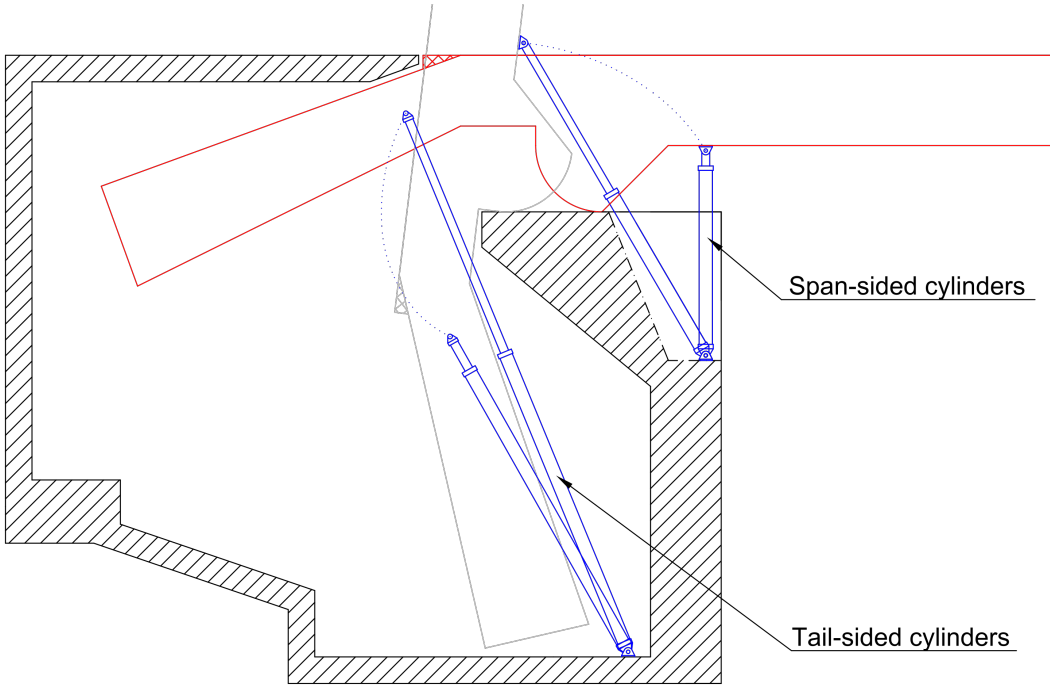

Figure 7.15: *Implementation of span- and tail-sided hydraulic driving mechanism*

7.3.2.1 Span-sided cylinders

The most common position is to install driving cylinders is at the front wall of the bascule chamber. The tops of the cylinders are attached to the bottom face of the sandwich, so that the span-side is pushed upwards during the opening cycle.

The advantage of the positioning at span-side, is that the cylinders are outside the interference space of the moving structure. Hence, one can apply as many cylinders over the width of the bridge as necessary. The cylinders are relatively small in size, while the lever arm is reasonable.

The major disadvantage of the span-sided location, is that the total bridge will have to be shifted backwards in order to accommodate the cylinders. This effectively means that the spanning length of the bridge is increased, and the lever arm of the counterweight decreased. This has a big influence on the need for strength and stiffness of the structure. In the implementation as displayed in fig. 7.15, the bridge has been shifted backwards by as much as 600 millimetres with respect to the rack-pinion alternative from fig. 7.14. Analogous to eq. (7.1), one can calculate that this shift results in an efficiency decrease of roughly 15%. Next to that, the positioning at the span-side requires additional works to the concrete front wall of the chamber, as cutouts are required to accommodate the cylinders.

7.3.2.2 Tail-sided cylinders

Since only the use of non-telescopic cylinders is considered, the configuration options within the chamber are very limited. The most promising option would be fixing the cylinders in the bottom-right corner of the chamber.

Although not showing from fig. 7.15 (in which both types have been combined for simplicity), the advantage of positioning the cylinders at the tail-side is that the bridge does not have to be shifted backwards. Also, no additional works to the concrete chamber are required.

On the other hand, all options within the bascule chamber do interfere with the moving structure and must therefore be positioned at the sides of the tail. This implies that the opening/closing loads are concentrated at the sides of the structure, instead of being distributed over the full width. The required cylinders are longer, whereas the lever arm is not improved with respect to the span-sided configuration.

7.3.3 Comparison

As discussed, localised stresses in the laminates of the sandwich panel are expected to be decisive in the tail-design. Hence, the focus in the selection of a operating system is on minimising the stresses associated to the opening/closing cycle. The stresses can be reduced in two ways; increasing the number of driving points over the width of the structure, and otherwise by increasing the lever arm from the driving point to the rolling axis.

The segmental rack-pinion system turns out to be the most favourable operating system as is comes to localised stresses. The second most interesting alternative would be a span-sided hydraulic system. Both alternatives are rather complex to produce and install, which drives the initial cost. The maintenance requirements and reliability of the mechanical rack-pinion system are however expected to be much better than for the hydraulic system.

Based on the qualitative comparison between the considered operating systems, it is decided to use a segmental rack-pinion mechanism for this case study.

Table 7.3: *Qualitative comparison of operating systems*

	Type of operating system			
	Rack-pinion		Hydraulic	
	Horizontal	Segmental	Span-sided	Tail-sided
Force distribution over width				
Lever arm to rolling axis				
Complexity / initial cost				
Durability / reliability				

7.4 Balance

As discussed in section 2.3, the location of the gravitational centre with respect to the rolling axis has a major effect on the energy efficiency, safety and complexity of the bridge. The four principle locations, as displayed in fig. 2.7, all have their pros and cons.

The common practice in the Netherlands is to position the gravitational centre at the span-side of the pivot axis, as displayed in fig. 2.7(b). This is not the most energy efficient solution, however it does provide the highest safety and reliability for traffic. The stability of the bridge in the closed position does not depend on a locking system, which rules out risks associated with a failure of such systems. Due to bridge's tendency to close from the opened position, the bridge can manually be closed in the event of a failure of the operating mechanism. Furthermore, the balance is less sensitive to small changes in the location of the gravitational centre. As the self-weight of the composite bridge is relatively low, this issue becomes more important.

In line with the Dutch common practice, the gravitational axis in this case study will be positioned at the span-side of the rolling axis. The required magnitude of the imbalance and setting force to ensure rotational stability outside the opening/closing cycle will be calculated. The size, shape, location and density of the counterweight will subsequently be defined.

7.4.1 Uplifting effect

The main uplifting effect in the closed position of the bridge derives from wind loads, creating pressure at the bottom and suction at the top of the bridge deck. Uplifting effects introduced by traffic loads are not considered, as these have been accounted for in the minimum pre-pressure requirement.

The uplifting effect from wind must be addressed by a point-load acting at the centre of the span, according to [NEN-EN 1991-1-4, 2005]. The load has been quantified for the case study bridge in section 5.4.2.2. The reference area of the span has however slightly changed with respect to the initial assumptions. The updated vertical uplifting wind load is slightly smaller, as the result of a decreased span length:

$$\begin{aligned} F_{w,z,rep} &= \frac{1}{2} \cdot \rho \cdot v_b^2 \cdot C_z \cdot A_{ref,z} \\ &= \frac{1}{2} \cdot 1.25 \cdot 29.5^2 \cdot 1.291 \cdot 15.25 \cdot 15.0 = 161 \; [kN] \end{aligned} \tag{7.2}$$

In accordance with [NEN 6786, 2001, section 8.4.2.5.2], the design value for the uplifting load is:

$$\begin{aligned} F_{w,z,d} &= \gamma_w \cdot F_{w,z,rep} \\ &= 1.1 \cdot 161 = 177 \; [kN] \end{aligned} \tag{7.3}$$

7.4.2 Rotational stability

The rotational stability of the bridge has to be ensured by (a combination of) an intentional imbalance, a setting force from the operating system or a locking system.

7.4.2.1 Intentional imbalance

An intentional imbalance is achieved by not fully counterbalancing the weight of the span, resulting in a positive support force at the resting pier. Obviously, the larger the intentional imbalance, the less energy efficient the bridge during the operational cycle. It is therefore desirable to minimise the magnitude of the imbalance, by combining the imbalance with a setting force or a locking system.

7.4.2.2 Setting force

A setting force can be introduced by slightly overstressing the operating system after the completion of the closing cycle. The maximum magnitude of the setting force is determined by the type and size of the driving mechanism. Overstressing the operating mechanism can result is an accelerated deterioration, as live loads will introduce cyclic stresses in the driving mechanisms.

7.4.2.3 Locking system

Locking systems do not cause a positive support load at the rest pier, but rather stop the opening movement itself. Locks can be installed at either the tip of the leaf (locking upward motion) or at the tail (locking downward motion). The main disadvantage of a locking system, is that they require regular maintenance and pose a risk in the event of failure. Hence, if not strictly required, the use of such a system should be omitted.

7.4.3 Counterweight

The supporting load at the rest pier is positive, as long as the closing momentum (from imbalance and setting) is greater or equal than the opening momentum:

$$F_{set} \cdot d_{set} + G \cdot d_G \geq F_{w,z,d} \cdot d_w \tag{7.4}$$

In which:

F_{set}	*setting force from operating system*
d_{set}	*distance between rolling axis and point of application of driving mechanism*
G	*total weight of the superstructure, including the counterweight*
d_G	*distance between rolling axis and gravitational axis of the superstructure*
$F_{w,z,d}$	*design resultant uplifting wind load on span*
d_w	*distance between rolling axis point of application of wind load*

7.4.3.1 Setting force

It is difficult to assess how much setting force the chosen segmental rack-pinion driving mechanism can provide. Therefore, it is simply assumed that the setting force accounts for 50% of the stabilising momentum, where the intentional imbalance accounts for the remaining half. Since $d_{set} = L_{tail} = 5666$ mm and $d_w = \frac{1}{2} \cdot L_{span} = 7625$ mm, the setting force can be determined:

$$F_{set} = 50\% \cdot \frac{177 \cdot 7625}{5666} = 120\ [kN] \tag{7.5}$$

7.4.3.2 Dimensions of counterweight

In order to roughly estimate the required dimensions of the counterweight, the following set of assumptions is made:

$q_{span} = 1.2\ [kN/m^2]$	*distributed weight of the composite panel*
$H_{cw} = 1.0\ [m]$	*height of the counterweight*
$B_{cw} = 15.0\ [m]$	*width of the counterweight*

The material that constitutes the counterweight will be integrated inside the composite sandwich, acting as the core material of the panel. The height and width of the counterweight are therefore fixed to the established inner dimensions of the panel. The total mass of the counterweight is further determined by the following two parameters:

ρ_{cw}	*density of counterweight*
a_{cw}	*length of the counterweight, in the longitudinal direction of the bridge*

The distance between the rolling axis and the gravitational axis of the superstructure (d_G) can now be expressed in terms of the above parameters:

$$d_G = \left(\frac{L_{span} + L_{tail}}{2} - L_{tail} \right) \cdot q_{span} - \left(L_{tail} - \frac{1}{2} \cdot a_{cw} \right) \cdot H_{cw} \cdot B_{cw} \cdot a_{cw} \cdot \rho_{cw} \tag{7.6}$$

After substitution of eq. (7.6) into eq. (7.4), the set of satisfying combinations of counterweight length and density can be plotted. The result is displayed in the figure below.

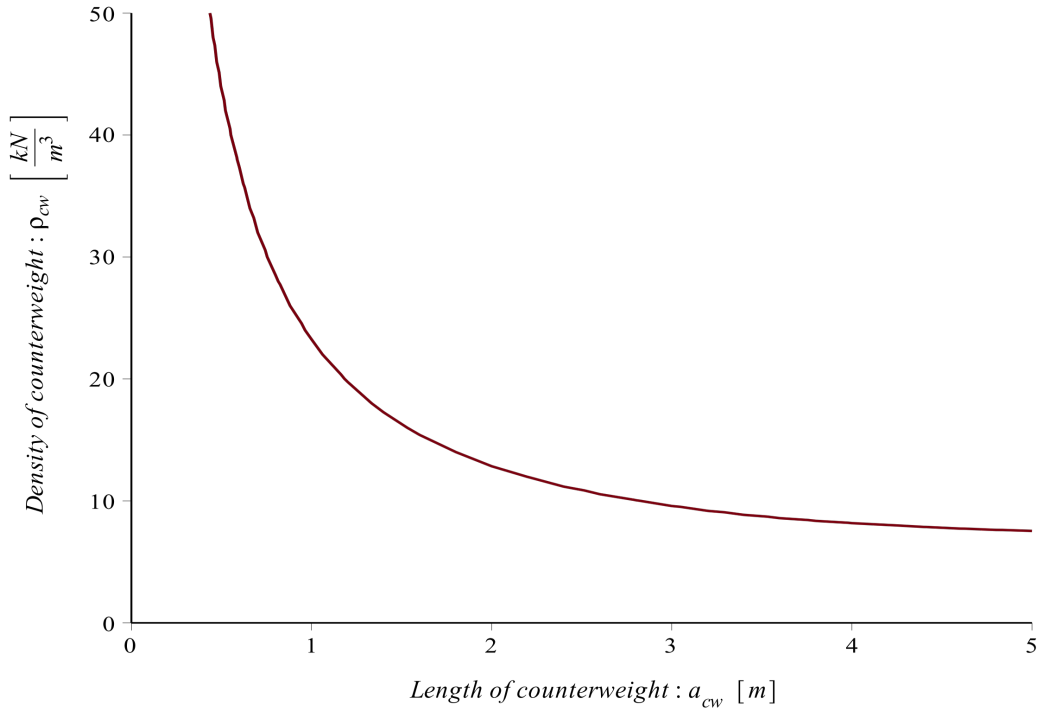

Figure 7.16: *Set of counterweight parameters which satisfy the rotational stability requirement*

From the plot, it can be concluded that the required counterweight easily fits within the maximum length of 5.66 meter (total length of tail). In fact, even relatively low-density materials such as sand and concrete can be used as counterweight. This will drastically reduce the material cost of the structure.

Please note that this section presents a rough estimation of a the counterweight design. A more detailed calculation can be made in the process of the FEM-analysis, as will be presented in the following chapter.

7.5 Stabilising system

As discussed in section 2.2.5, the stabilising system is a collective term for elements that assure the rotational stability of the bridge in the desired position. The required provisions are discussed in the following sections.

7.5.1 Bearing at rest-pier

Live loads on the bridge are transferred through the rolling segment at the pivot-side, and through the bearings at the rest-pier. The bearings must provide sufficient shear stiffness to transfer horizontal forces, while at the same time having adequate flexibility to accommodate translational- and rotational movement arising from temperature changes and traffic loading.

7.5.1.1 Bearing type

One of the design principles from section 7.1.3 states that the transferring contact areas should be maximised, in order to reduce localised peak stresses. One way to achieve a large contact area is providing a continuous bearing over the full width of the structure.

An important consideration when using line bearings is flapping of the leaf on the support. When high traffic loads are exerted at one side of the bridge, this causes an uplifting effect at the opposite side of the line support. On removal of the load, the uplifted deck impacts on the bearing. Repetitive flapping can result in nuisance and eventually damage to the structure.

This behaviour can be avoided by providing a bearing with a relatively low shear stiffness. Due to the reduced stiffness the asymmetric loads are distributed over a larger area, which reduces the uplifting effects. Next to that, eventual impacts are mitigated by the elasticity of the material. Elastometric material, composed of vulcanised rubber or neoprene, can provide the right properties. These elastomeric bearings also come in strips, which can be assembled into a continuous line bearing.

(a) Bearing strip (b) Translational flexibility

Figure 7.17: *Elastomeric bearings [Granor Rubber & Engineering, 2014]*

7.5.1.2 Bearing properties

The mechanical properties of a standard elastomeric bearing strip are taken from the product catalog of a producer [Granor Rubber & Engineering, 2014]:

$l = 1850$	$[mm]$	*length*	
$w = 200$	$[mm]$	*width*	
$h = 20$	$[mm]$	*height*	
$u_{max} = 10$	$[mm]$	*maximum shear deformation*	(7.7)
$\phi_{max} = 0.01$	$[rad]$	*maximum rotation*	
$E_c = 333$	$[kN/mm/m]$	*compressive stiffness*	
$E_s = 9.0$	$[kN/mm/m]$	*shear stiffness*	

7.5.2 Centring device

A movable bridge may slightly displace after each opening/closing cycle, both in transverse direction and by rotation about the z-axis. This displacement can become a problem after many cycles. A centring device can prevent this displacement, by correcting the final movement of the bridge.

The centring of the bridge will be controlled by the pegs and sockets on the perimeter of the rolling quadrant, as shown in fig. 7.12(b). Therefore, no additional centring device is required.

7.5.3 Machinery breaks

In the opened position, the bridge has the tendency to close as a result of the intentional imbalance and wind loads. This movement has to be prevented by a machinery break on the operating system. Secondly, the breaks must be able to arrest the movement of the span within the specified time interval of 6 seconds (see section 5.3.6.1).

7.5.4 Buffer cylinders

The closing movement of the bridge has to be controlled, since the gravitational centre of the superstructure is at the span-side of the rolling axis. In order to dissipate the kinematic energy at the end of the closing cycle, buffer cylinders should be installed. The most convenient location would be at the counterweight-side of the tail.

7.5.5 Bumper blocks

Bumper blocks are provided at the front wall of the bascule chamber, to prevent over-travelling of the structure during the opening cycle. The tail of the structure rests at the blocks in the opened state, so that opening wind-loads can be transferred to the substructure.

8 Finite element analysis

A global shape of the span and tail of the bridge has been proposed in the previous two chapters. This chapter should be seen as a 'proof-of-concept', in which the behaviour of the proposed design is analysed and verified with respect to the drawn functional requirements and boundary conditions (see chapter 5).

The analysis is done by means of computational models, with use of the finite element software package 'Dlubal RFEM 5'. This package provides a set of tools that enable to model and analyse composite sandwich structures.

8.1 Global model

8.1.1 Initial shape

The shape of the structure is more or less defined in the previous chapters. The resulting profile, which fits the geometrical boundary conditions of the case study bridge, is displayed in appendix E.2. The configuration of the transverse stiffeners around the integrated rolling segment is displayed in fig. 7.13. Both drawings form the basis for the three-dimensional structural shape, which will be further optimised in the modelling process. The first raw shape of the is displayed in fig. 8.1. Note that longitudinal axis of the bridge is in the x-direction, the transverse axis is in the y-direction and the thickness is in the z-direction.

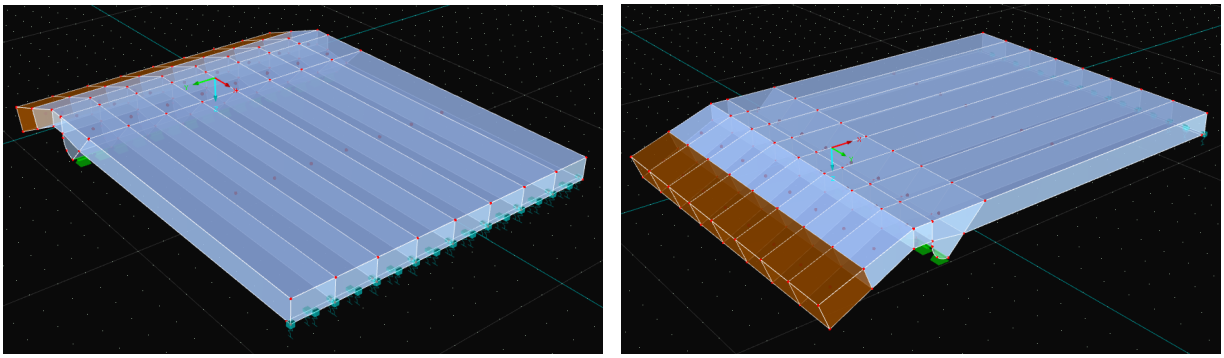

(a) Front view (b) Rear view

Figure 8.1: *Inital structural shape based on geometrical boundary conditions*

8.1.2 FEM elements

The core of the panel is composed of lightweight foamed PVC, while the faces and stiffeners are composed of fibre reinforced composite laminates. The materials behave very differently on loading, and should be modelled accordingly to achieve realistic results.

8.1.2.1 Laminates

Previously, the structure was assumed to be loaded by pure normal- and bending stresses, and all laminates were considered to be thin and symmetrical. This would allow the use of typical plate elements with only in-plane degrees of freedom, resulting in a computationally inexpensive analysis.

In the global model, the definition of the laminates and loads is more realistic and complex. For optimisation purposes, most cross-sections are not always symmetrical, so that coupling between in-plane extensional and out-of-plane flexural deformation occurs. Furthermore, shear stresses cannot be neglected in the vicinity of patch-loads and supports. More complex elements are thus required to achieve realistic results.

In theory it would be possible to stack three-dimensional brick elements, in which each layer of bricks represents a single ply of the composite laminate. This would however lead to a very expensive analysis. It is much more practical to define rotations and translations in the mid-thickness plane of the laminate, thereby limiting the number of degrees of freedom. By application of the Mindlin theory, the shell elements can account for transverse shear strains [Matthews et al., 2000].

This approach does require an extra pre-processing step, in which the properties of the stacked plies are translated into mid-plane properties. This is done by means of the classical laminate theory, as described in section 3.3.2.1. The Dlubal software package offers a module, called RF-Laminate, which handles this link between ply and laminate properties. During pre-processing, one can simply input and edit laminate configurations, after which the module computes the stiffness matrices of the shell elements in accordance with CLT. During post-processing, the module translates the stress results from the integration points of the shell elements into the stresses over the thickness of the laminate. The stress states of the individual plies can therefore be analyzed, so that the first-ply failure criterion can easily be verified.

8.1.2.2 Cores

As discussed, the core material is composed of lightweight foamed PVC. The main purpose in the finalized structure is providing buckling stability for the slender laminates that are under compression. Under these load conditions, the core elements are subjected to a three-dimensional stress state. Hence, three-dimensional solid brick elements were used to model the core material, as displayed in fig. 8.2(b).

At the interface between laminate and core material, the nodes of the Mindlin shell-elements and the linear brick elements are aligned and coupled.

8.1.2.3 Connections

The full structure is basically a single monolithic sandwich panel, which has been impregnated in a continuous process. Furthermore the plies inside the connections between composite laminates are positioned in such a way, that continuous fibres are assured in direction of possible tensile stresses. Since both the fibres and the resin are continuous, the laminate connections can be assumed rigid.

The connection between the face sheets and the core are provided by resin, which partly permeates the foamed core material. By assuring proper surface treatment and curing, it can be assumed that the sections are not are not dominated by adhesive failure within the laminate-core connection. Hence, a perfectly bond between the face sheets and the core is used in the model.

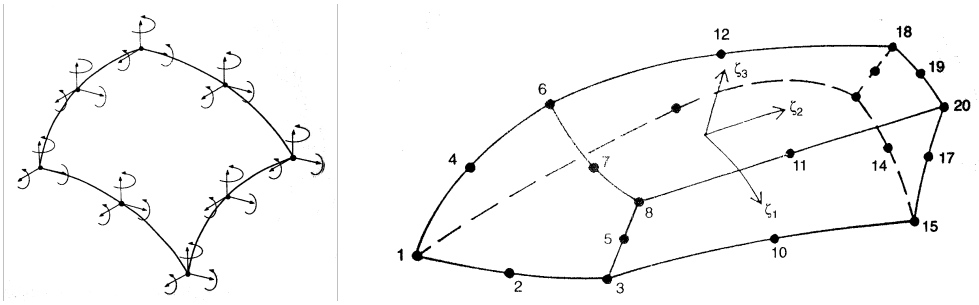

(a) 8-noded Mindlin shell element (b) 20-noded curvilinear brick element

Figure 8.2: *Degrees of freedom of applied finite elements [Matthews et al., 2000]*

8.1.3 Material properties

Based on the conclusions from chapter 6, a total of four materials are used in the model; two core materials and two unidirectional plies for the laminates.

8.1.3.1 Laminates

Two types of unidirectional plies are used in the configurations of the laminates; glass-fibre and carbon-fibre epoxies with a fibre volume fraction of 60%. The engineering constants of both ply materials can be found in table 5.6. The nominal strength properties can be found in table 5.8.

The material properties of the laminates (stacked plies) are computed by the software. The recommendations of the CUR-96 with regard to the stacking sequence are respected; each of the four principle directions should at least contain 15% of the available fibre material.

Based on the considered limit states, the material properties are divided by certain material- and conversion factors. These factors can be found in table 5.11.

8.1.3.2 Cores

Two types of core materials are used in the global model; low-density (40 kg/m^3) and high-density (250 kg/m^3) foamed PVC. The material properties of both materials can be found in table 5.10. The properties are divided by a material factor of $\gamma_{m,c} = 1.3$ (see section 5.5.7.2).

8.1.4 Supports

The structure is supported over the full width at both abutments. The properties of the bearings are discussed below.

8.1.4.1 Tail-sided support

Translation is restricted in all directions at the tail-sided support, as movement is prevented by the aligned pegs and sockets on the perimeter of the rolling segment. No spring constant is applied in the model, as the concrete support surface reacts relatively stiff compared to the composite structure. Rotation is only unrestricted about the y-axis, which is enabled by the round shape at the support line. The other two rotational degrees of freedom are restricted.

In practice, the rolling segment causes a coupling between translation in the x-direction and a rotation about the y-axis of the bridge; the rocking motion during the opening/closing cycle. Rotation at the supports from live loads will therefore also introduce a slight translation of the bridge, causing the line of contact to shift along the perimeter of the rolling segment. In the global model, this coupling of rotation and translation is however neglected in the closed state of the bridge. The location of the line support thus remains unchanged under small rotations at the support.

8.1.4.2 Span-sided support

The span-sided support is equipped with a 200 mm wide elastomeric bearing strip, provided over the full width of the structure. The degrees of freedom are supported by the spring constants of the elastomeric support, as given under section 7.5.1.2. The support in the z-direction is non-linear; the contact fails if negative contact stresses occur. This allows the structure to open under the uplifting effects of wind- and non-symmetric traffic loads. The stability limit state of the structure can thus be verified by means of a non-linear analysis.

8.1.5 Loads

The considered live loads on the bridge have been introduced in chapter 4 and quantified in chapter 5. A projection of the traffic loads on the reference bridge is given in appendix B.2. Those loads that contribute to the considered limit states are used in the modelling process.

8.2 Model verification

Any type of modelling should start by verification and calibration of the model. For a simple problem, the results from the Dlubal package will be compared to those from the ESAComp package, and subsequently to an analytical solution.

8.2.1 Sandwich configuration

The considered sandwich panel is composed of a 300 mm thick low-density foam core, and an 8 mm thick face sheet on either side. Both face laminates are identical and the composition is symmetric:

Table 8.1: *Face sheet laminates of sandwich verification model*

Ply material	Thickness [mm]	Angle [°]	E_x [GPa]	E_y [GPa]	G_{xy} [GPa]
Carbon (T300)	**1.0**	**0**	**135.5**	**8.8**	**4.4**
Glass (Gevetex)	**1.0**	**-45**	**48.2**	**17.0**	**5.2**
Glass (Gevetex)	**1.0**	**45**	**48.2**	**17.0**	**5.2**
Glass (Gevetex)	**1.0**	**90**	**48.2**	**17.0**	**5.2**
Glass (Gevetex)	**1.0**	**90**	**48.2**	**17.0**	**5.2**
Glass (Gevetex)	**1.0**	**45**	**48.2**	**17.0**	**5.2**
Glass (Gevetex)	**1.0**	**-45**	**48.2**	**17.0**	**5.2**
Carbon (T300)	**1.0**	**0**	**135.5**	**8.8**	**4.4**

8.2.2 Laminate stiffness matrices

The first verification concerns Dlubal's laminate module RF-Laminate. As fig. 8.3 shows, the generated laminate stiffness matrices from Dlubal are consistent with those from ESAComp. This suggests that the implementation of the classical laminate theory in both packages is similar.

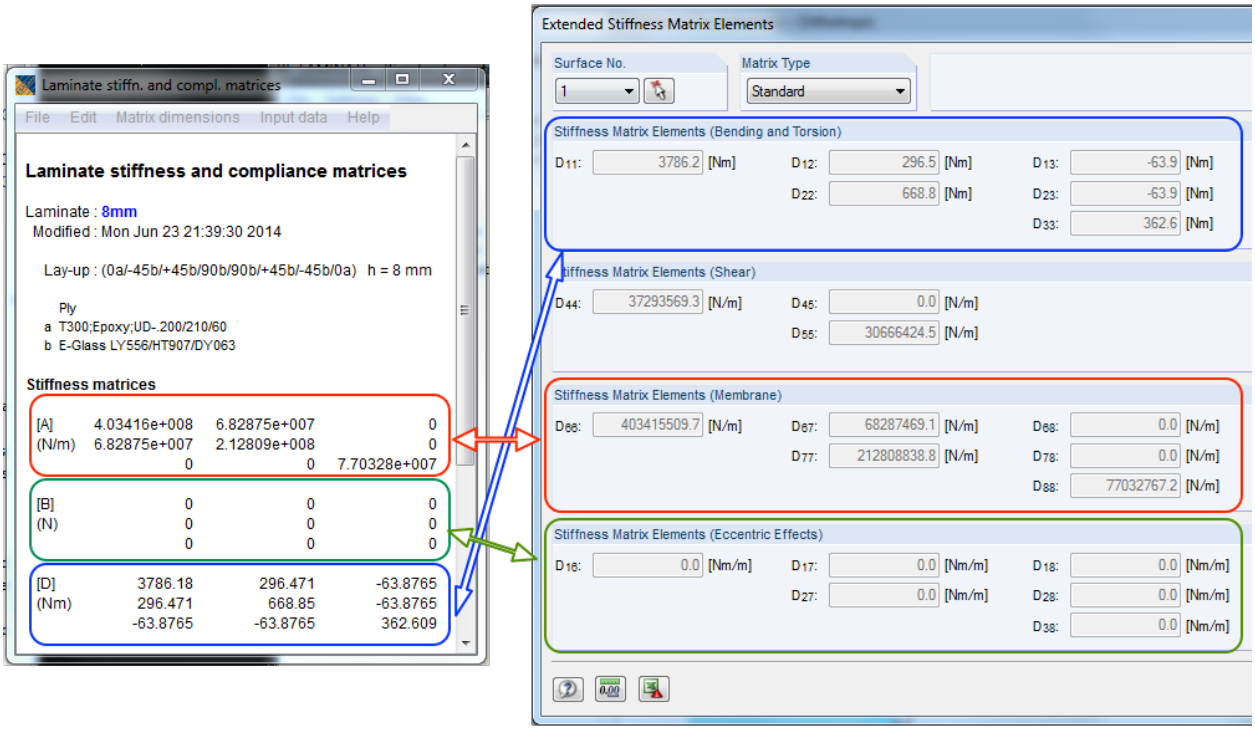

Figure 8.3: *Laminate stiffness comparison between ESAComp (left) and Dlubal (right)*

8.2.3 Panel deflection

The verification model concerns a rectangular sandwich panel with sides L x W, which is subjected to an uniformly distributed load of 100 kN/m^2. Two opposite sides are simply supported, while the other two are clamped.

8.2.3.1 Analytical approximation

Approximate solutions for the deformation of rectangular sandwich panels exist for a number of boundary conditions, as can be found in [Zenkert, 1997]. The three-dimensional deformed shape of the panel can be plotted by means of these analytical solutions. The engineering constants of the laminates are required as input, and are taken from ESAComp. The core properties can be found in table 5.10.

$$\begin{aligned} E_x &= 47.69\ [GPa] \\ E_y &= 25.16\ [GPa] \\ G_{xy} &= 9.63\ [GPa] \\ \nu_{xy} &= 0.324\ [-] \end{aligned} \tag{8.1}$$

The flexural, shear and torsional stiffness of the panel can be determined by the equations from section 3.3.5:

$$\begin{aligned} D_x &= E_x \cdot \left(\frac{t^3}{6} + \cdot \frac{t \cdot d^2}{2} \right) + E_c \cdot \frac{c^3}{12} && [kN \cdot mm] \\ D_y &= E_y \cdot \left(\frac{t^3}{6} + \cdot \frac{t \cdot d^2}{2} \right) + E_c \cdot \frac{c^3}{12} && [kN \cdot mm] \\ D_{xy} &= 2 \cdot G_{xy} \cdot \left(\frac{t^3}{6} + \cdot \frac{t \cdot d^2}{2} \right) + G_c \cdot \frac{c^3}{12} && [kN \cdot mm] \\ S_x &= G_c \cdot c && [kN/mm] \\ S_y &= S_x && [kN/mm] \end{aligned} \tag{8.2}$$

The analytical solution for the deformation of the panel is given by:

$$w(x,y) = w_{max} \cdot \sin\left(\frac{\pi \cdot x}{L} \right)^2 \cdot \sin\left(\frac{\pi \cdot y}{W} \right) \tag{8.3}$$

In which maximum deformation can be expressed in a contribution from shear and bending. The total maximum deformation is the sum of both contributions:

$$\begin{aligned} w_{s,max} &= \frac{16 \cdot q \cdot W^2}{\pi^3 \cdot \left(4 \cdot S_x \cdot \left(\frac{W}{L} \right)^2 + 3 \cdot S_y \right)} && [mm] \\ w_{b,max} &= \frac{16 \cdot q \cdot W^4 \cdot \left(1 - \nu_{xy}^2 \right)}{\pi^5 \cdot \left(16 \cdot D_x \cdot \left(\frac{W}{L} \right)^4 + 8 \cdot \left(1 - \nu_{xy}^2 \right) \cdot D_{xy} \cdot \left(\frac{W}{L} \right)^2 + 3 \cdot D_y \right)} && [mm] \\ w_{max} &= w_{s,max} + w_{b,max} && [mm] \end{aligned} \tag{8.4}$$

8.2.3.2 Comparison

In Dlubal, the rectangular sandwich panels are modelled by a combination of solid elements for the core and shell elements for the face laminates, as discussed in section 8.1.2. An additional comparison was made with the finite element solver of ESAComp. This solver uses another approach, in which the full sandwich is modelled with shell element instead of using solid elements for the core. The solutions of the three methods are compared for the following configurations:

Table 8.2: *Comparison of results for different sandwich panel configurations*

Sandwich configuration					Calculated maximum deflection		
W [mm]	L [mm]	t [mm]	c [mm]	Core type	Dlubal	Analytical	ESAComp
5000	5000	8	300	LD	**54.54**	**53.79 (1.39%)**	**57.53 (5.57%)**
5000	5000	16	300	LD	**50.22**	**49.52 (1.41%)**	**47.58 (5.33%)**
5000	5000	8	600	LD	**27.03**	**25.28 (6.95%)**	**27.95 (3.63%)**
5000	5000	8	300	HD	**14.19**	**15.05 (5.77%)**	**13.36 (5.51%)**
10000	5000	8	300	LD	**87.46**	**78.17 (11.88%)**	**86.76 (0.89%)**

For square panels, the computed maximum deflection of the three methods are within a reasonable range to each other; up to 7% for the analysed configurations. For other aspect ratios, the analytical approximation seems to give less accurate results. The Dlubal result is in this case however still close to the ESAComp result.

The shape of the deformation can also be compared, by means of contour plots. It is clear that the finite element approaches result in a more symmetric deflection than the analytical result. The influence of the clamped boundaries seems to be overestimated by the analytical approximation.

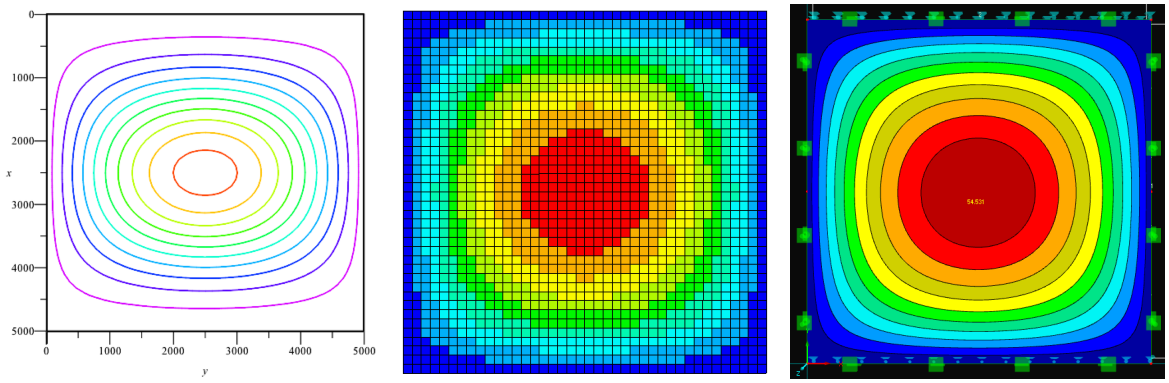

(a) Analytical (b) ESAComp (c) Dlubal

Figure 8.4: *Contourplot of deformation of rectangular sandwich panel*

Based on the comparison between the methods, it can be concluded that the accuracy of the Dlubal package is sufficient for the global evaluation of composite sandwich elements.

8.3 Limit states

Based on the considered load combinations and opening angles of the bridge, a number of serviceability- and ultimate limit states needs to be verified.

8.3.1 Serviceability limit states

Both in the opened and closed state, the allowed maximum deformation of the bridge under the influence of live loads is limited in order to ensure the wellbeing of its users. Characteristic loads should be used for serviceability limit state verifications; the applied load factors are equal to unity.

8.3.1.1 Deformation in closed position

In the functional requirements, the maximum deformation at midspan was set at L/400. Considering the length of the span, this comes down to a deflection of:

$$w_{mid} \leq L/400 = 38.1\ [mm] \tag{8.5}$$

The maximum deflection occurs under the influence of load combination 'gr1a' (see table 5.2). The contribution from self-weight is not considered, as only the additional deflection from live load is regarded.

8.3.1.2 Deformation in opened position

The maximum deformation in the opened position was set at L/250, which comes down to the following deflection at the tip of the leaf:

$$w_{tip} \leq L/250 = 61.0\ [mm] \tag{8.6}$$

The deflection is caused by the horizontal wind load, acting on the opened bridge span. Again, the contribution from self-weight is not considered.

8.3.1.3 Vibration in closed position

To ensure the comfort of pedestrians, the accelerations of the deck should be smaller than:

$0.7\ m/s^2$	*vertical vibrations*
$0.2\ m/s^2$	*horizontal vibrations*
$0.4\ m/s^2$	*exceptional crowd loading*

These comfort criteria have to be verified if the fundamental frequencies of the deck are less than:

5 Hz	*vertical frequency*
2.5 Hz	*lateral and torsional frequencies*

8.3.2 Ultimate limit states

Both the stability and strength of the structure for the different loads combinations and opening angles are verified by means of ultimate limit states. For the strength verifications of the laminates, the stress state of the individual plies must be evaluated as prescribed by the CUR-96. The conservative first-ply-failure criterion is applied, which implies that the whole laminate is considered to fail upon failure of one of the constituent plies.

Design loads are to be used for ultimate limit state verifications, which is done by introducing the load factors as prescribed in section 5.4.6.1.

8.3.2.1 Stability closed position

The stability of the closed bridge under the influence of uplifting wind loads is verified by this limit state. As discussed in section 7.4.3, the stability is determined by the following loads:

- Self-weight (including counterweight)
- Setting force (see section 7.4.3.1)
- Vertical wind load at span-side (see section 5.4.2.2)

This limit state is used to calibrate the balance of the structure, and to precisely determine the required size of the counterweight. The combination of loads must be such, that the support force at the tip of the leaf approaches zero. In that case the rotational stability is assured, while the imbalance (and thus the energy consumption during an opening cycle) is minimised.

8.3.2.2 First-ply-failure in closed position

The strength of the core and laminates under the influence of different load combinations is verified. The following load combinations are considered (see table 5.2):

- Load combination ‘gr1a-1’: self-weight + LM1 (TS at midspan) + foot & cycle
- Load combination ‘gr1a-2’: self-weight + LM1 (TS at abutment) + foot & cycle
- Load combination ‘gr1b’: self-weight + LM2
- Load combination ‘gr3’: self-weight + foot & cycle (service vehicle)
- Load combination ‘A’: self-weight + LM1 + foot & cycle + accidental (vehicle on footway)

Note that only the most important load combinations have been considered. Furthermore, breaking-, wind-, snow- and temperature loading have not been taken into account in the ultimate limit states.

8.3.2.3 First-ply-failure in (half-)opened position

The strength of the core and laminates in the (half)-opened position is verified under the influence of self-weight and horizontal wind loads. At the moment of opening, the full span acts as a cantilever. Hence, the influence of self-weight on the stress state in the laminates is relatively high. When the opening angle increases, the importance of the horizontal wind load increases, while the influence of self-weight decreases. Three different opening angles are therefore considered and verified; just opening (0°), halfway opened (41.5°) and fully opened (83°). The following load combinations are considered:

- Self-weight + opening wind load (see section 5.4.2.3)
- Self-weight + closing wind load
- Self-weight + opening emergency stop (see section 5.4.5.1)
- Self-weight + closing emergency stop

As a result of the imbalance, the structure is not stable in the opened position. In practice, the balance is maintained by a breaking load from the operating mechanism. This is simulated by simply supporting the tail end of the structure, restricting the bridge to rotate about the rolling axis.

8.4 Optimisation

The goal of the modelling process is to find the most efficient structural shape that complies with the established functional requirements and boundary conditions. This chapter describes a process to derive the optimal shape for sandwich structures.

8.4.1 Efficiency

The degree of efficiency of the structure can be expressed in terms of money. Therefore, certain structural properties must be translated into investment cost. The following aspects are considered to have most impact on the price of the structure:

- Volume of applied materials
- Price of applied material
- Complexity of structural shape (manufacturing cost)
- Total weight of structure (operating mechanism cost)

The material volumes and the total weight follow from the output of the software. For the determination of the total material cost, the unit prices from table 6.2 are used. The complexity will be judged qualitatively.

8.4.2 Optimisation parameters

The most efficient structural shape can be found by means of an optimisation process, in which the following parameters are considered:

- Cross-sectional shape
- Number of longitudinal stiffeners
- Laminate and core material properties
- Laminate layup and thickness
- Support system properties
- Counterweight properties

Changing any of these parameters has its effects on the balance, strength and stiffness on one hand, and on the price of the structure on the other. The effects of these parameters should be investigated by means of a sensitivity analysis, in which each of the parameters is changed and evaluated individually. In each optimisation step, only that combination of parameters should be changed that offer the highest increase in structural efficiency. An optimum is found after a sufficient number of iterations.

One must be aware that the derived optimum may not be equal to the global optimum. The iteration process should therefore be performed from multiple starting points, so that the discovered local optima can be compared to find the global optimum.

8.4.3 Sensitivity analysis

The focus of this chapter is on the methodology behind optimisation of composite structures, rather than the actual result of the optimisation process in this specific case study. Therefore, just a single example of a sensitivity analysis will be discussed in detail before presenting the final design concept.

8.4.3.1 Considered parameters

This sensitivity analysis example helps to identify which of the following actions has the highest beneficial effect on the structure's deflection at midspan:

- Increasing thickness of top laminate
- Increasing thickness of bottom laminate
- Increasing thickness of longitudinal stiffener laminate
- Increasing number of longitudinal stiffeners
- Replacing glass- by carbon fibre in top laminate
- Replacing glass- by carbon fibre in bottom laminate
- Replacing glass- by carbon fibre in longitudinal stiffener laminate

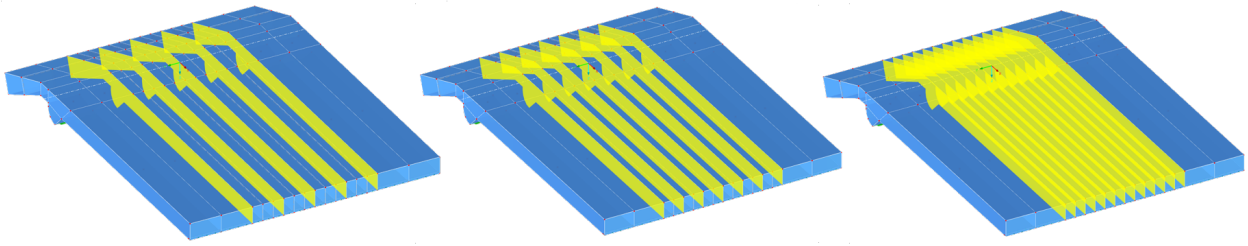

Figure 8.5: *Models to investigate effect of increasing number of longitudinal stiffeners*

8.4.3.2 Result

These seven different parameters are all investigated individually, by creating separate models. The decrease of the midspan deflections are subsequently plotted against the increase in material cost, which are based on the information from table 6.2.

Figure 8.6 shows the resulting sensitivity of the considered parameters. The slopes of the diagrams show the effectiveness of the actions; how much can the midspan deflection be reduced per unit extra material cost? In this example, increasing the thickness of the top laminate appears to be the most effective action to reduce the midspan deflection. Note that this may change if another reference situation is used.

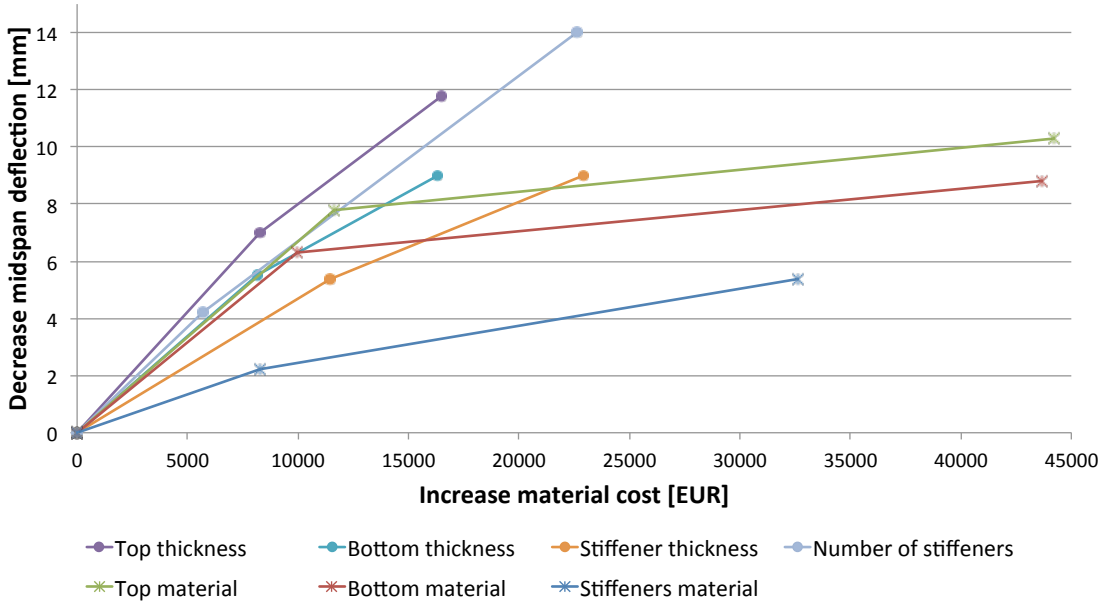

Figure 8.6: *Results of optimisation example*

Notice that the diagrams corresponding to the replacement of glass- by carbon fibres are bi-linear. This results from the order in which the fibres are replaced. In this example, the first branch of the diagram represents the replacement of the fibres in the 0° direction. The second branch of the diagram represents the replacement of the fibres in the 45°, -45° and 90° angle. It is clearly much more effective to only upgrade the longitudinal plies with carbon fibres, instead of upgrading the full laminate.

8.4.4 Process

The optimisation process starts with the raw structural shape, as displayed in fig. 8.1. By means of the iterative steps, the structure is first adapted to satisfy the midspan deflections of the serviceability limit state. Subsequently, the structure is further optimised to satisfy the ultimate limit states. Lastly, these same steps are performed in the half-opened and fully opened state of the bridge. After each major change in the structure, the balance of the bridge must be recalibrated by adapting the counterweight accordingly. This process is very laborious when done by hand, due to its unpredictable and iterative character. Special pre- and post-processors for finite element solvers exist, that automate the optimisation process. The final solutions in this theses, as presented in the following sections, were derived by hand and leave room for further optimisation (see section 8.7.2).

8.5 Final design

The final design is the result of several dozen iteration steps, which will not be discussed in detail. This chapter merely presents the characteristics of the final design. Subsequently, the response to a number of load combinations will be verified on basis of the limit states.

8.5.1 Shape

One of the conclusions from chapter 7 was that the construction should be continuous between span- and tail-side. The global shape of the bridge is derived by simply extruding the two-dimensional design, as displayed in appendix E.2. However, during the optimisation process it became clear that a lot of material could be saved by reducing the width of the tail section. The removal of these tail sections did however introduce local peak stresses at the 'armpit' ; the location of the discontinuity. This challenge was overcome by introducing a transition between span and tail, in which a triangular-shaped section restores the continuity between the laminates. The laminates in this 'armpit' (displayed in yellow in fig. 8.7) are around twice as thick as the surrounding laminates, and are fully composed of carbon reinforced plies. This extra material is however easily compensated by the material that is saved by narrowing the tail section.

8.5.2 Laminates

Based on the output of the stress analysis, the laminate thickness and configuration of the failing panels are adapted after each iteration. After a number of iterations, one ends up with a set of laminate groups. The more iterations are completed, the more of these groups will be created. During the iterations to derive the final design, a number of 12 laminate groups have been created. The detailed configurations and locations of these laminate groups can be found in appendix F.

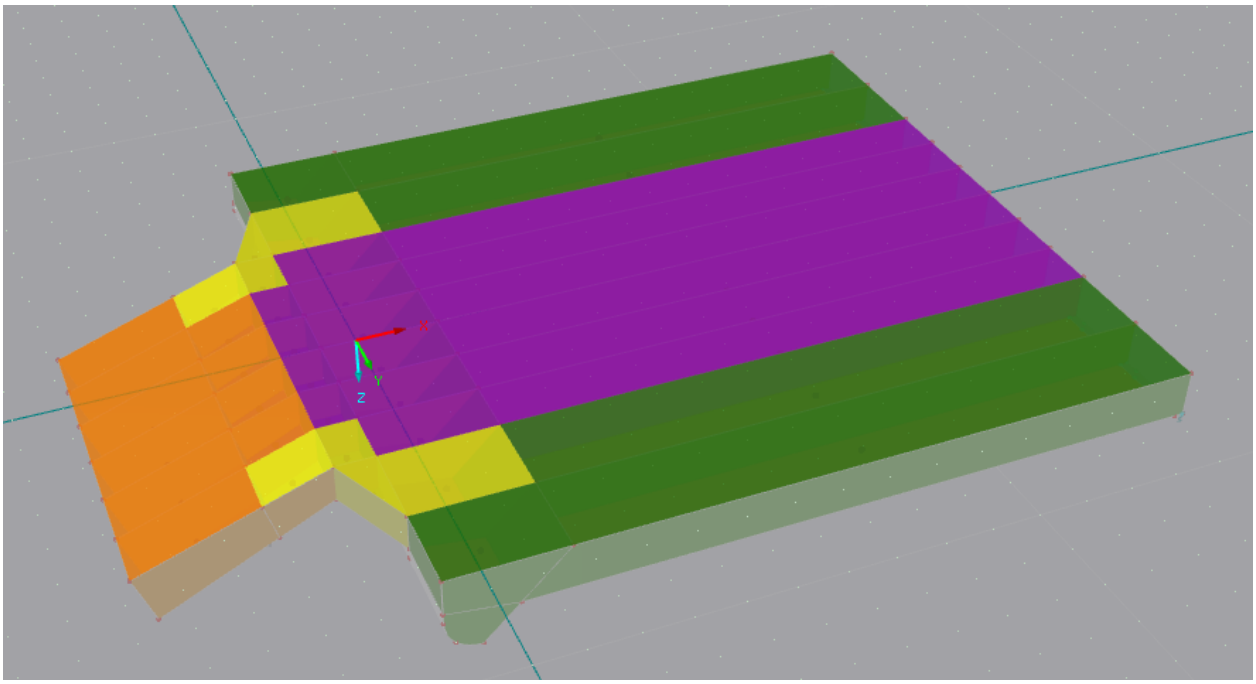

Figure 8.7: *Four different laminate groups at the topside of the structure*

8.5.2.1 Face laminates

The configurations of the face laminates at the span of the structure were mostly determined by the serviceability limit states. In order to meet the deflection requirement, most of the fibres in the laminates are pointing in the longitudinal direction. In the middle section, these longitudinal plies are composed or carbon fibres.

For the tail-sided laminates, the ultimate limit states in the opened state of the bridge proved to be decisive. In order to cope with the combination of self-weight and a closing horizontal wind load, these laminates had to be drastically strengthened. At the connections of the longitudinal stiffeners with the face laminates, high strength is also required in the 90° direction. The face laminates therefore have a more isotropic ply configuration than at the span side.

8.5.2.2 Stiffeners

From fig. 8.6 it can be seen that increasing the thickness and number of stiffeners is much more effective than upgrading the material as it comes to increasing the structural stiffness. Therefore, the span-sided stiffeners are all reinforced by glass fibres. The middle part of the structure, which accommodates the traffic lanes, is provided with twice as many stiffeners as the sides. Next to that, the these stiffeners are 66% thicker than those at the location of the footway and cycle lanes.

The tail part of the stiffeners are severely loaded during the opening cycle, under the influence of self-weight and horizontal wind loads. It is therefore necessary to increase their thickness and to upgrade to carbon fibres.

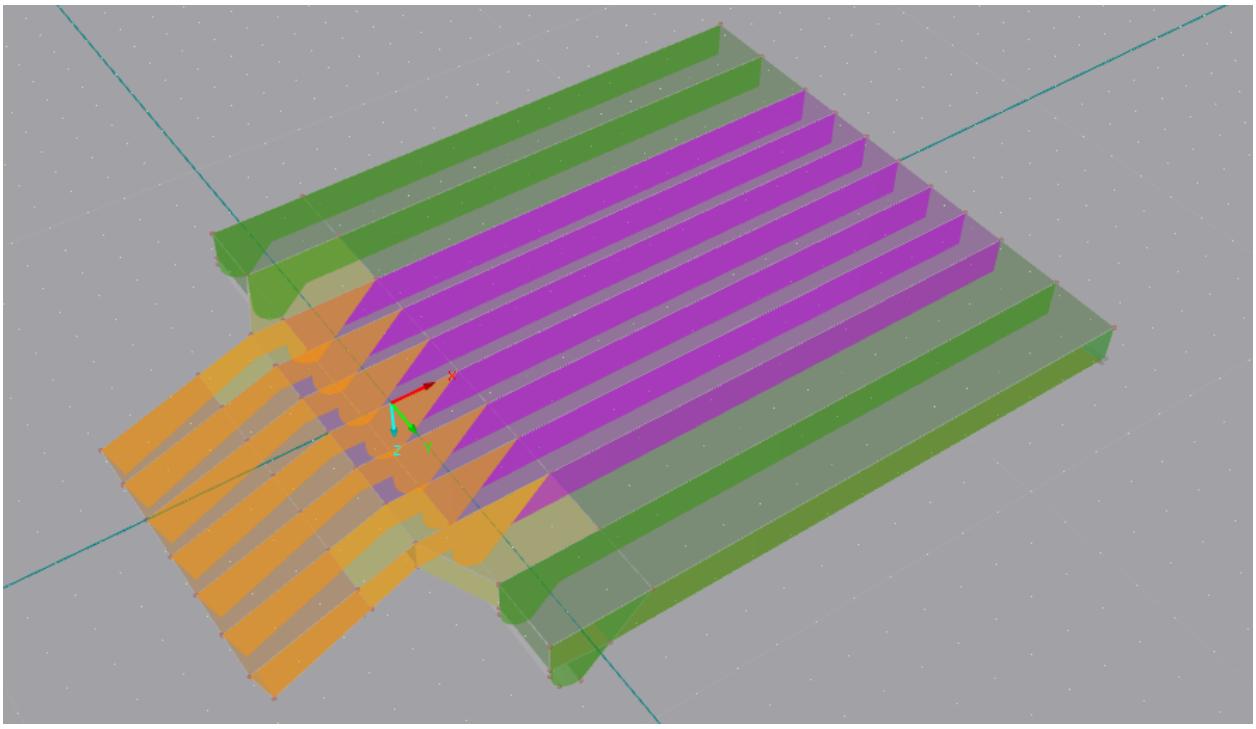

Figure 8.8: *Three different laminate groups for the longitudinal stiffeners*

8.5.2.3 Traffic lane laminate

The face laminate at the middle part of the span, indicated with purple in fig. 8.7, is subjected by heavy traffic loads. The local deflection of the laminate in the vicinity of the tires should be limited, as high curvatures could introduce cracks in the laminate. The bending stiffness of the top face must thus be high enough to avoid excessive local deformation around the tires.

As discussed, the best way to increase the bending stiffness of a laminate is by introducing a core. The laminate's properties can drastically be increased by adding a relatively thin layer of (high density) foam. This basically means that the top face of the structural sandwich is a sandwich by itself. The configuration of the traffic lane laminate is shown in fig. 8.9(a).

While the main goal of this face sandwich is to decrease the local deformations, it has an additional advantage; it protects the surface from severe impact damage. The impact energy, for example from falling cargo, can be absorbed by the additional core layer such that the underlaying laminates are protected. Only the top layers are still vulnerable, but this does not jeopardise the safety of the structure and can easily be repaired.

8.5.2.4 Quadrant

As discussed in section 7.2.2.2 the rolling quadrant is subjected high localised stresses, which travel along the perimeter of the quadrant during the opening cycle. A steel layer of 20 millimetre thickness is therefore attached to the laminate at this position. This layer will reduce the local deformations, protect the laminate from wear and tear, and accommodates the sockets that align with the pegs on the superstructure. The rolling quadrant laminate is displayed in fig. 8.9(b).

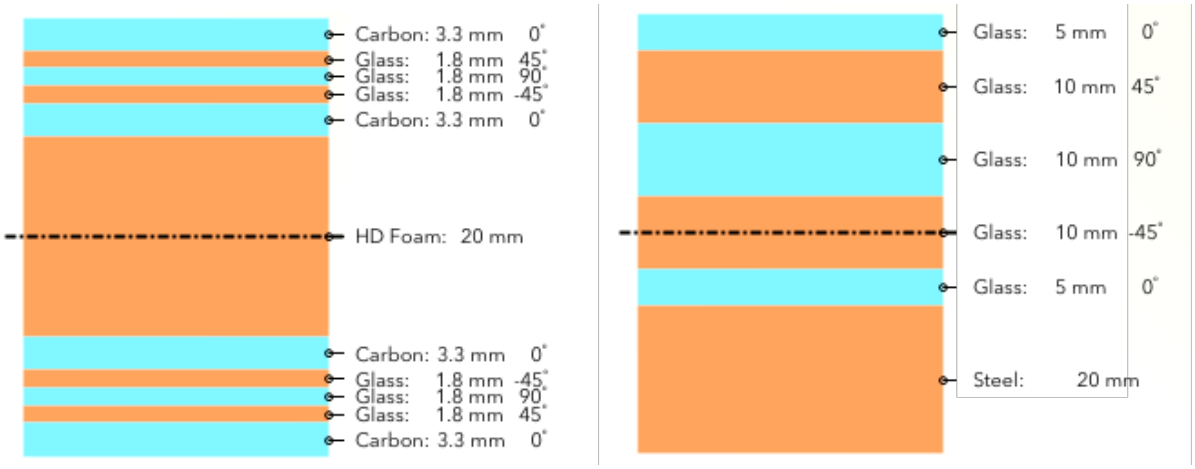

(a) Traffic lane face laminate

(b) Rolling quadrant laminate

Figure 8.9: *Special laminate configurations*

8.5.3 Cores

From chapter 6, it was concluded that a low-density core material contributes most to the efficiency of a sandwich panel. Therefore, low-density foam was applied where possible, and high-density foam where necessary. Two parts of the structure are provided with high-density foam; the traffic lane laminate, and the cores of the quadrants. All other volumes between the laminates are filled with low-density foam.

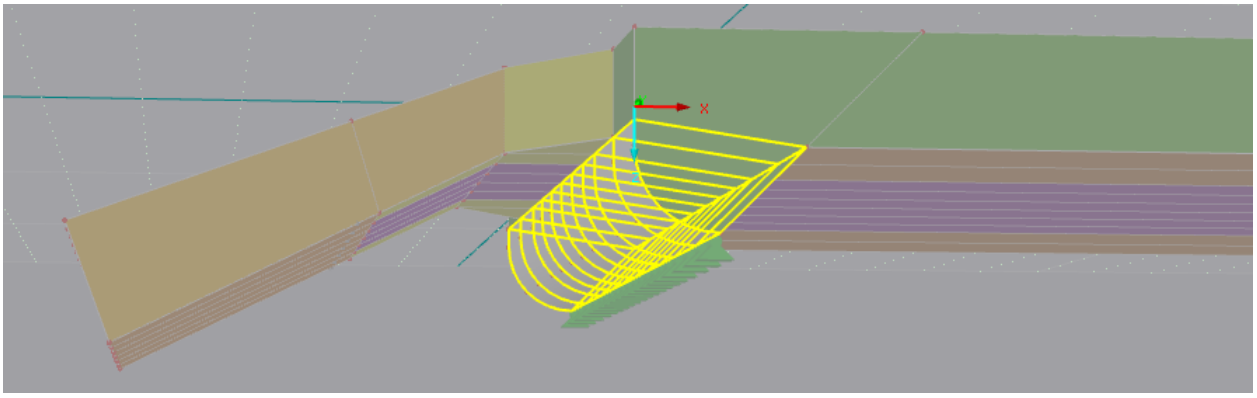

Figure 8.10: *High-density foam is applied in the core of the rolling quadrant*

8.5.4 Counterweight

The required dimensions and density of the counterweight were estimated in section 7.4.3.2. The results showed that, for the assumed densities and dimensions, even sand could be used as counterweight material. In the final design, the counterweight has half the width of that assumed in the estimation. The density is sand of is however still sufficient to balance the structure.

8.5.4.1 Material

Choosing steel as balancing material would make the required length of the counterweight smaller, and therefore the lever arm with respect to the rolling axis bigger. The result is a lower total weight, and consequently smaller loads on the laminates of the tail section. Sand is on the other hand a much cheaper ballast material than steel. It is assumed that this effect outweighs the savings on the laminates. Sand is therefore chosen as ballast material.

In order to avoid shifting of sand during the operation cycle, the sand will be mixed with some cement while it is injected in the sandwich panel. The balance material is therefore basically a low-grade concrete, which is able to retain its shape.

8.5.4.2 Dimensions

The dimensions of the counterweight are roughly 1.2 x 2.8 x 7.5 meter, as indicated in fig. 8.11. With a density of 1600 kg/m^3, the total weight comes in at:

$$G_{cw} = 33.2\ [ton] \tag{8.7}$$

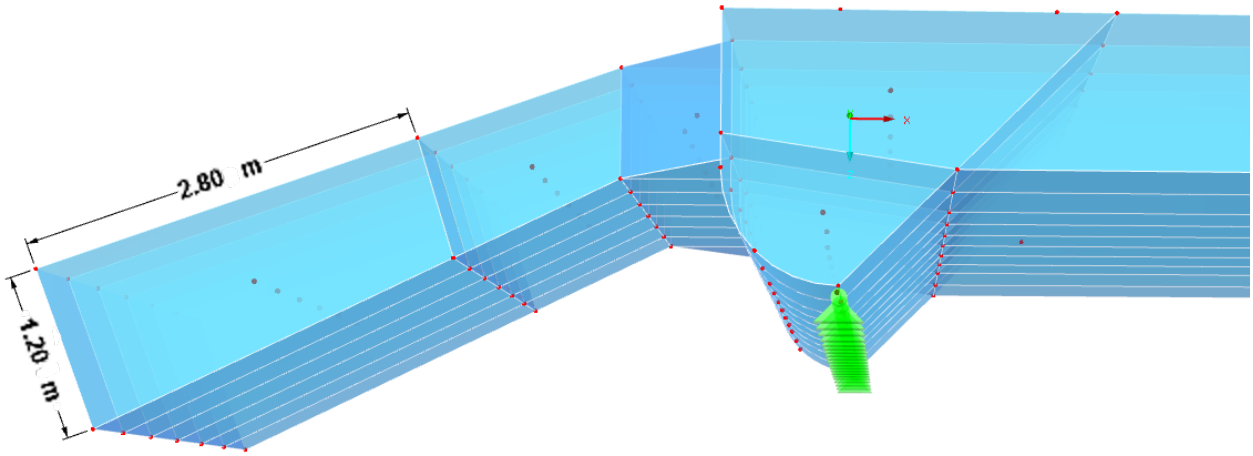

Figure 8.11: *Dimensions of the counterweight*

8.5.5 Gravitational centre

The total weight of the structure in the final configuration, including the counterweight, is:

$$G = 94.0\ [ton] \tag{8.8}$$

In the closed position, the gravitational axis is located at a horizontal distance of about 1.4 meters from the rolling axis. The resulting imbalance is such that it can resist half of the maximum opening momentum that is generated by uplifting wind loads. The other half of the momentum is countered by a setting force from the operating mechanism (see section 7.4.3.2).

As stated in the functional requirements, the gravitational centre in the opened position is also located at the span-side of the rolling axis. The distance between rolling axis and gravitational axis is just 0.13 meter. This distance is chosen small in order to maximise the energy efficiency of an opening/closing cycle. It is however still at the span-side of the rolling axis so that the bridge can manually be closed in the event of a power outage, as prescribed in the functional requirements.

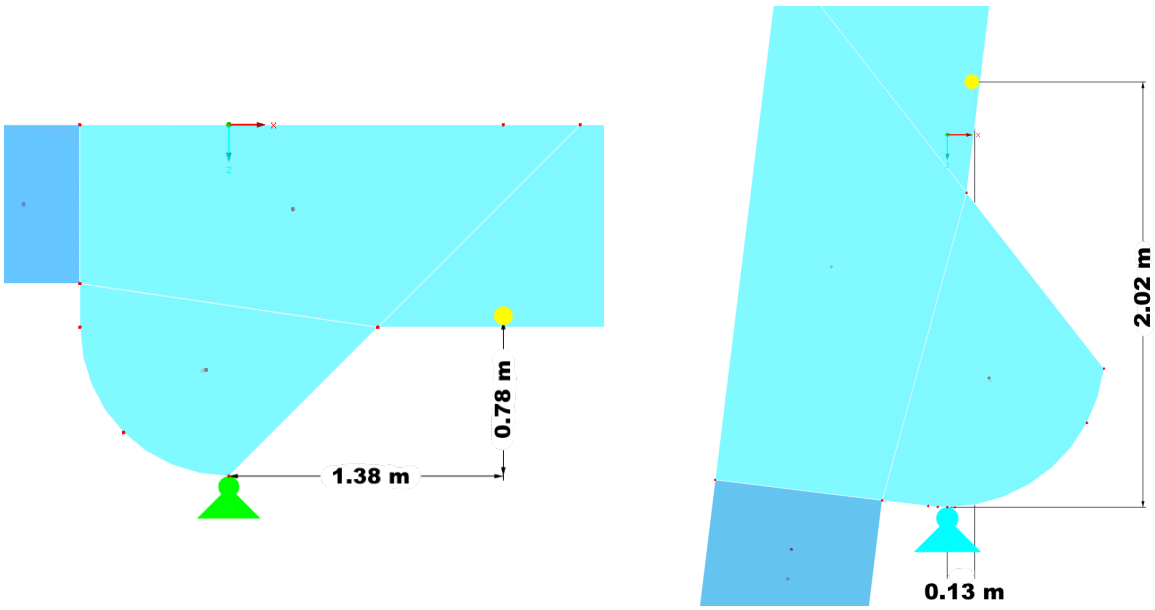

(a) Closed position: 0°

(b) Opened position: 83°

Figure 8.12: *Position of gravitational axis*

8.5.6 Material usage

The structure is composed of six different constituents, of which the volumes are extracted from the model data. From these volumes, one can calculate the the corresponding weights and material-cost by using the information from table 6.2:

Table 8.3: *Distribution of material volume, weight and cost in final design of structure*

Material	Volume [m^3]	Weight [ton]	Unit price [EUR/kg]	Material cost [€*1000]
Glass plies	**15.3**	**31.2**	**4**	**124.9**
Carbon plies	**7.9**	**12.4**	**20**	**247.2**
LD Foam	**257.3**	**10.3**	**1**	**10.3**
HD Foam	**15.6**	**3.3**	**1**	**3.3**
Steel	**0.5**	**3.7**	**1.5**	**5.6**
Sand	**21.8**	**33.2**	**0.1**	**3.3**
Total	**318.5**	**94.0**	**-**	**394.6**

Some interesting conclusions can be drawn from the constituent's contributions to the structure's weight and material-cost. Carbon material, for example, covers only 13% of the structure's weight, it accounts for no less than 63% of the total material cost. The opposite holds for the ballast material, which contributes for 35% in structural weight, while its share in material-cost is under 1%. Another notable conclusion is that 95% of the total material-cost come at the expense of the laminates. These conclusions underline the importance of laminate optimisation.

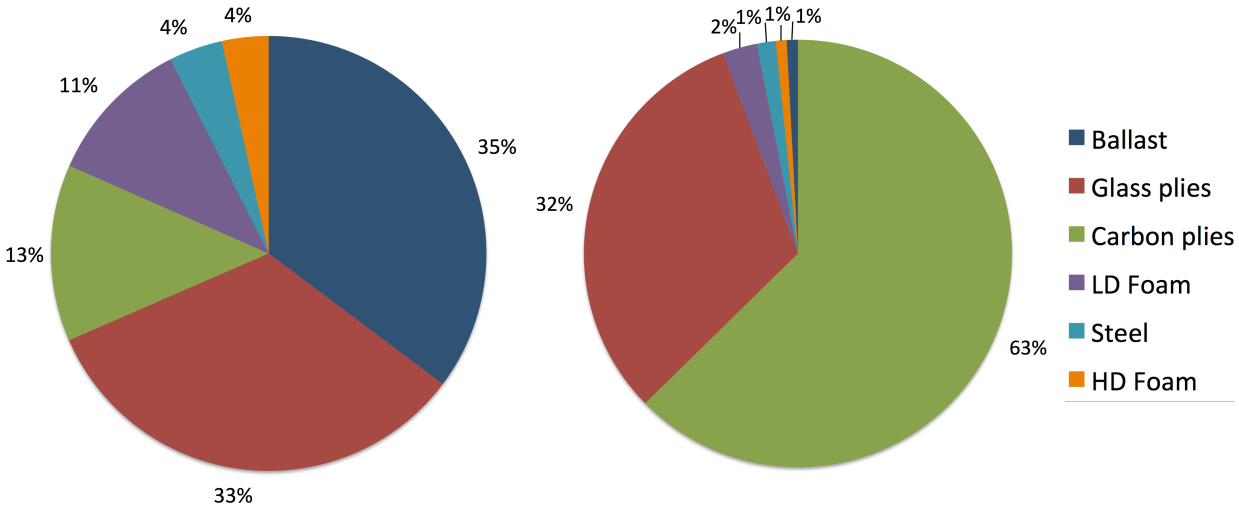

(a) Weight (b) Material-cost (c) Legend

Figure 8.13: *Breakdown of contribution to weight and material-cost from constituents*

8.6 Structural response

The response of the structure to the considered load combinations is evaluated with respect to the limit states. A few relevant and interesting results are discussed in this chapter.

8.6.1 Deflections in closed state

The first step in the optimisation process is to adjust the structure to comply with the serviceability limit state in the closed position. By means of sensitivity analysis and common sense, an optimised shape was derived that complies with the maximum midspan deflection under the influence of load combination 'gr1a'.

Self-weight is not considered in this load combination, as is has a beneficial effect on the midspan deflection (see fig. 6.1). The maximum deflection at midspan under the any load or load case is below the serviceability limit of 38.1 mm, as defined in eq. (8.5).

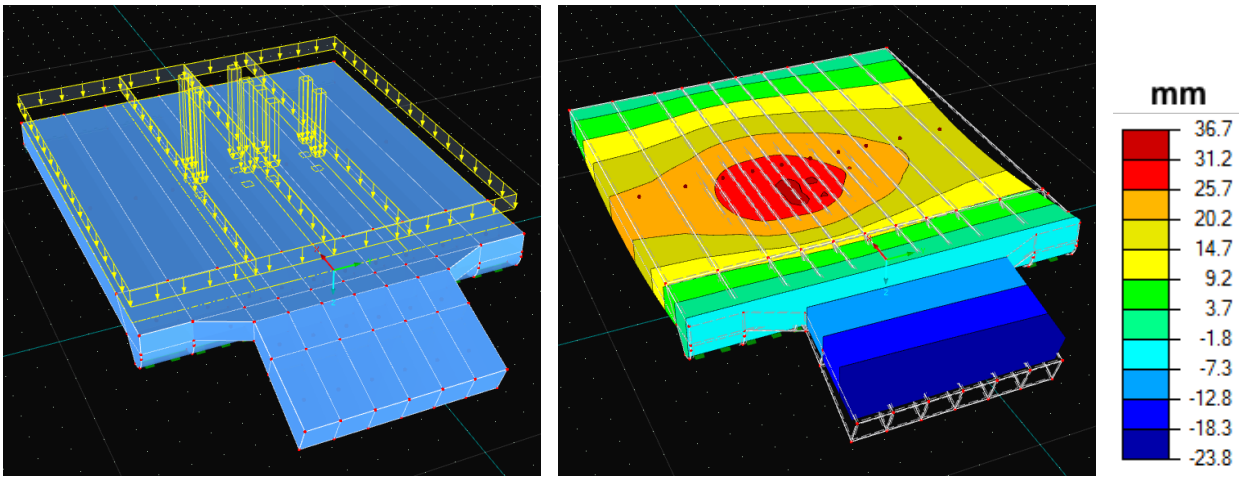

(a) Load combination 'gr1a' (b) Deformation in z-direction (c) Scale

Figure 8.14: *Evaluation of serviceability under load combination 'gr1a'*

8.6.2 Strength in closed state

8.6.2.1 Top laminate at traffic lane

The strength of the top laminate has to be checked at the high stress locations in the vicinity of the patch-loads from the tires. For this purpose, both the load combinations 'gr1a' and 'gr1b' have been applied at different positions on the bridge deck.

The laminate module in the finite element software translates the stress state of the shell element to the stress state in the individual plies. Subsequently, each ply can be verified with respect to the ultimate strength in the principle directions. Figure 8.15(c) displays the stresses in different directions over the thickness of the traffic lane top laminate, clearly showing that the sandwich laminate functions as expected.

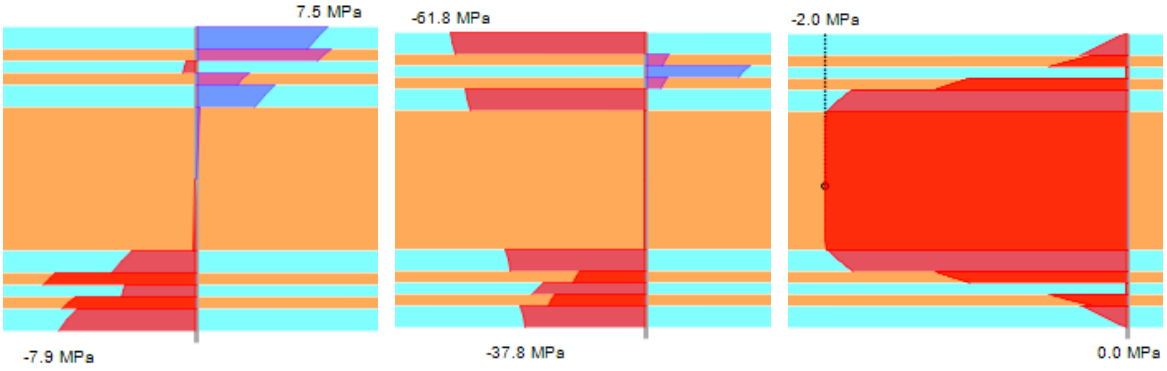

(a) Tension/compression in 0° (b) Tension/compression in 90° (c) Shear

Figure 8.15: *Stresses over the thickness of the top laminate*

Plotting the stress state of an individual ply over the surface of the structure gives a good idea of the force trajectories inside the plies, as can be seen in fig. 8.16. It is clear that the highest stresses occur in the direction of the fibres, in which the stiffness of the ply is highest. It was found that the stresses in the 90° direction were often governing the ultimate limit state, as peak stresses appear at the connection between the face sheets and the longitudinal stiffeners (see fig. 8.18(d)). The laminates therefore had to be strengthened in the transverse direction.

Note that the stress scale of each picture is different, and therefore not given. The figure should just give an impression of the stress trajectories inside the individual plies.

8.6.2.2 Top laminate at pedestrian/cycle lane

Two load combinations are used to evaluate the strength of the laminates at the pedestrian and cycle lanes, shown in fig. 8.17. During the design process, it became clear that complying with the accidental load combination 'A' would require a much stronger top laminate than the other two combinations. Since this would drastically increase the material cost, it was chosen to apply a physical barrier between the traffic lanes and the pedestrian/cycle lanes. The accidental load combination is thereby eliminated from evaluation, as vehicles are unable to end up at this part of the structure as a result of an accident. Much lighter service vehicles are however still allowed on the side parts of the bridge.

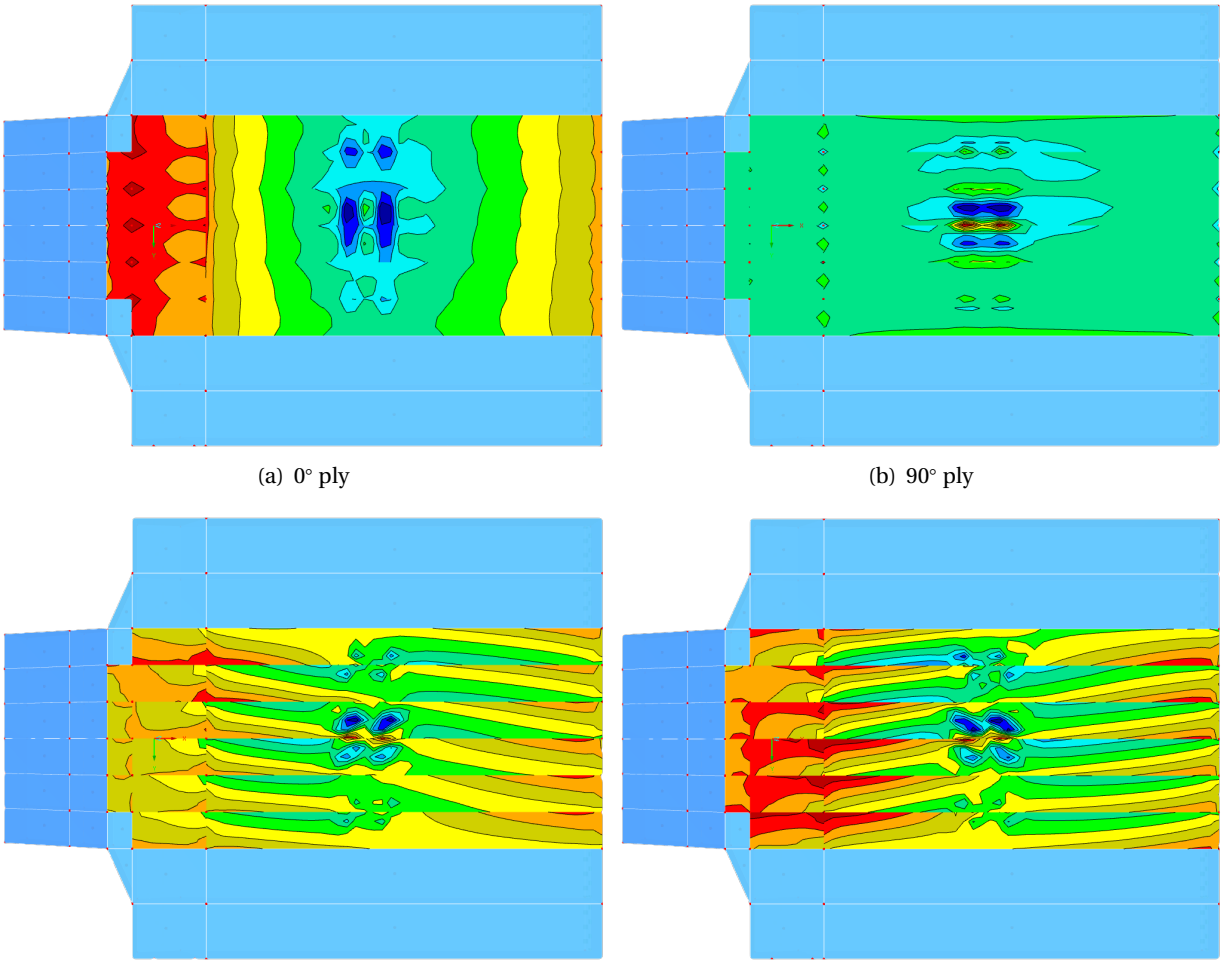

(a) 0° ply (b) 90° ply

(c) 45° ply (d) -45° ply

Figure 8.16: *Stress distribution in individual plies of top laminate under load combination'gr1a'*

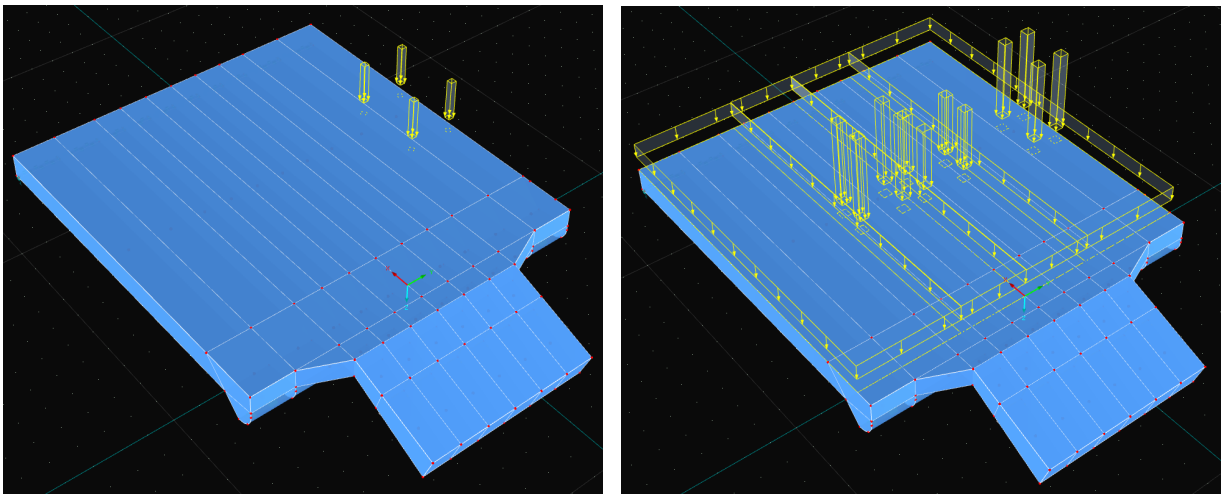

(a) Service vehicle: load combination 'gr3' (b) Vehicle on footway: load combination 'A'

Figure 8.17: *Load combinations for verification of pedestrian/cycle lanes*

8.6.2.3 Stiffeners at traffic lane

The significant deflections in the vicinity of patch loads resulted in peak stresses in the connection between the longitudinal stiffeners and the top laminate. This effect is drastically reduced by the addition of a high-density core layer in the top laminate.

Figure 8.18 shows the stress trajectories in the individual plies of a longitudinal stiffener. The main purpose of the stiffeners is transferring shear stresses, which is most effectively done by the 45° and -45° plies. The 0° plies contribute to the bending stiffness, resulting in a clear tension/compression stress diagram over the height of the stiffener. The 90° plies form the main connection between the top- and bottom face of the laminate, and are relatively uniformly loaded.

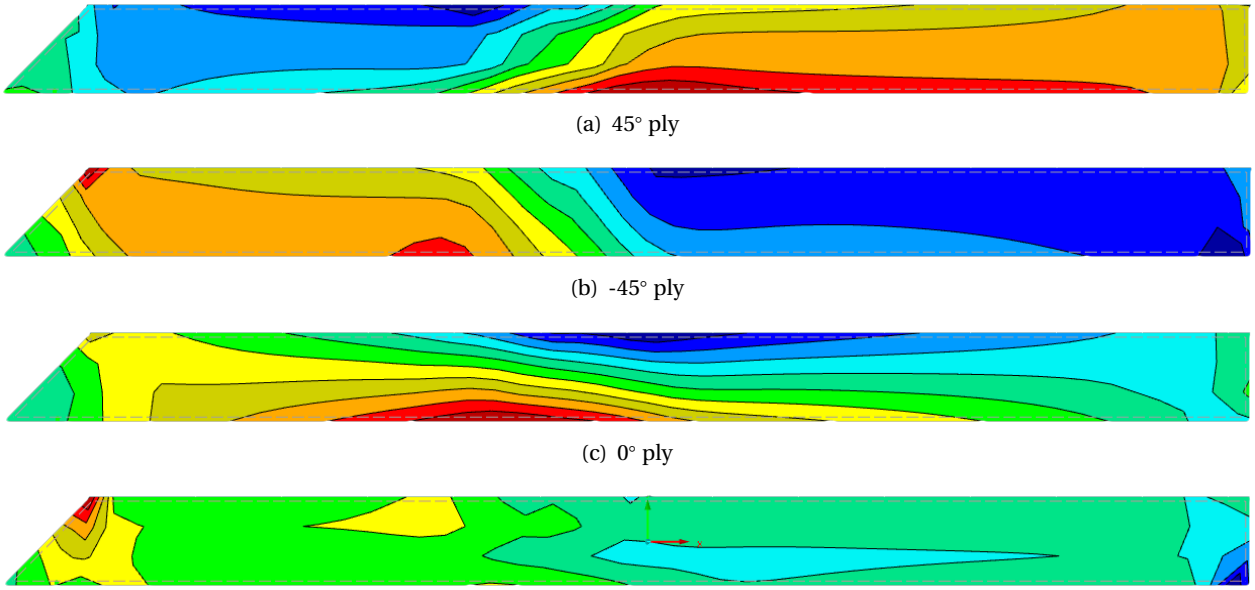

(a) 45° ply

(b) -45° ply

(c) 0° ply

(d) 90° ply

Figure 8.18: *Stress distribution in individual plies of longitudinal stiffener under load combination'gr1a'*

8.6.2.4 Core

The core mainly provides stability to the laminates, and the working stresses are generally low with respect to the ultimate strength. Only at the location right underneath the patch loads from tires, the compressive stresses can approach the strength limits of the low-density foam core. Figure 8.19 shows the solid stresses under the patch load of the 'gr1b' load combination. The maximum occurring stresses remain just under the design ultimate strength of the foam material. Notice that the left patch load is applied directly on top of the longitudinal stiffener, where the right patch load is positioned just next to the stiffener.

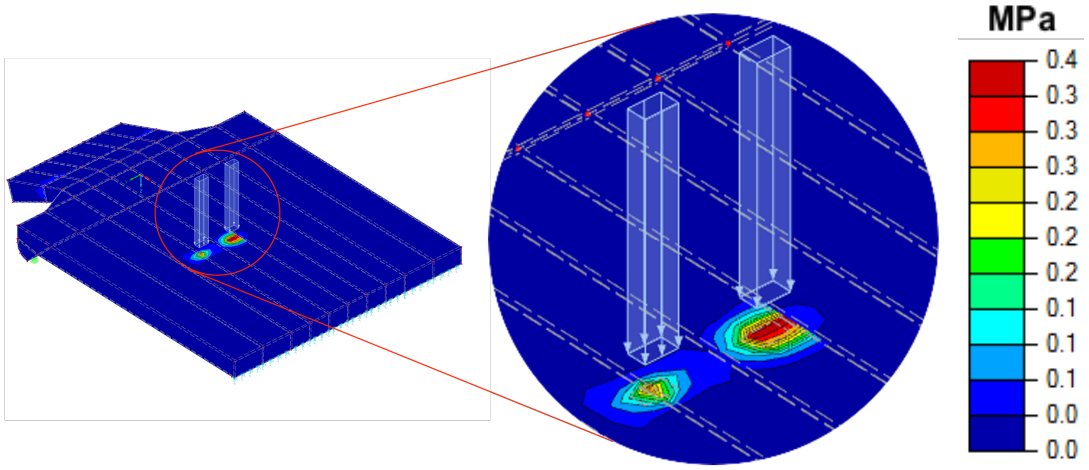

(a) Von-Mises solid stresses in core material (b) Scale

Figure 8.19: *Three-dimensional stress state in core material under load combination 'gr1b'*

8.6.3 Stability in closed position

The rotational stability in the closed position of the bridge is ensured by a combination of intentional imbalance and a setting force, applied at the end of the tail (see section 7.4). The balance of the structure must be calibrated such that the intentional imbalance is minimised, while assuring the rotational stability under the influence of uplifting wind loads. The structure is ideally calibrated if the support reaction at tip of the structure approaches zero. This is however hard to achieve in the software package, as the iterative solving algorithm does not handle this unstable situation well. The solution can however be closely approached. The resulting support reaction at the tip is calculated from the vertical equilibrium:

$$\sum F_z = 0 = G - \left(F_{w,z,d} + F_{set} + F_{sup,1} + F_{sup,2}\right) \tag{8.9}$$

In which:

$$\begin{aligned} G &= 917\ [kN] \\ F_{w,z,d} &= 165\ [kN] \\ F_{set} &= 60\ [kN] \end{aligned} \tag{8.10}$$

The total support reaction at the rolling axis ($F_{sup,1}$) is derived by integrating the distributed support reaction over the width of the structure, as displayed in fig. 8.20:

$$F_{sup,1} = 44.8 \cdot 15.0 = 672\ [kN] \tag{8.11}$$

The support reaction at the rest pier now follows from eq. (8.9):

$$F_{sup,2} = 20\ [kN] \tag{8.12}$$

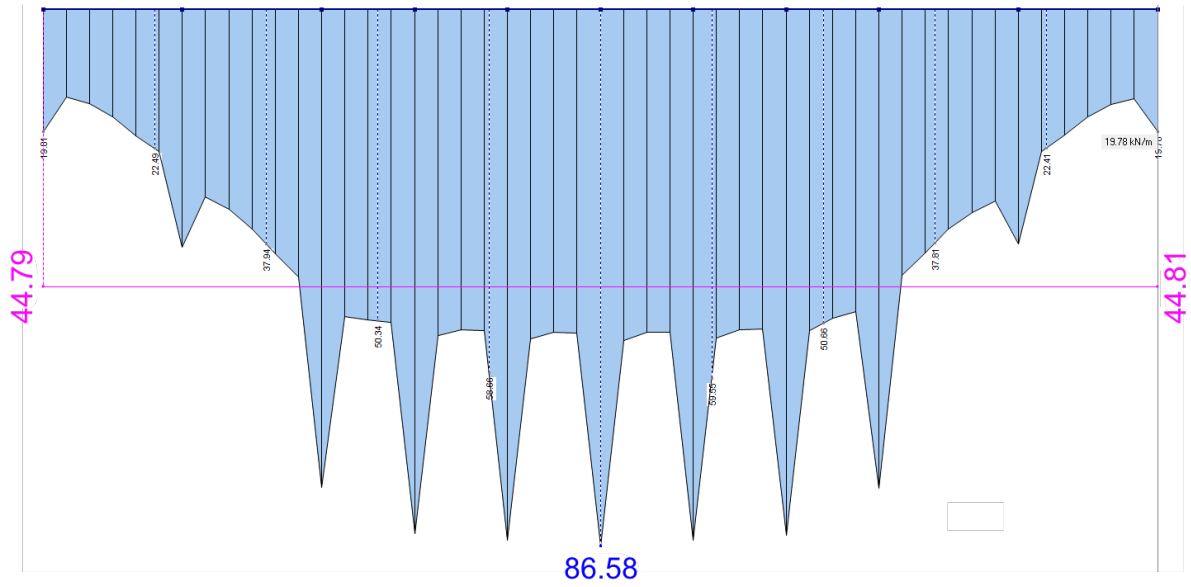

Figure 8.20: *Support reaction at rolling axis under load combination 'uplift' [kN/m]*

Figure 8.21 shows the deformation of the structure when it is about to be lifted up by the wind load. The maximum upward deflection of the span is 1.6 millimetres.

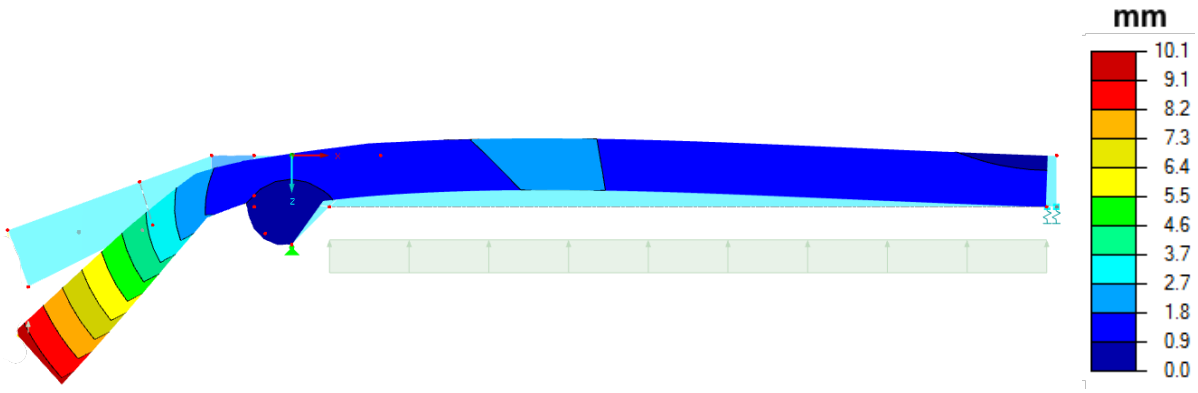

(a) Deformation under load combination 'uplift' (b) Scale

Figure 8.21: *Evaluation of stability under load combination 'uplift'*

8.6.4 Vibration in closed state

While the bending stiffness of the composite bridge is comparable to an equivalent steel structure, its mass and damping characteristics are very different. These differences are beneficial in the case of bridge structures; the material dissipates more energy, and the lower mass of the span results in higher natural frequencies of the modal shapes.

An initial evaluation of the dynamic behaviour can be done by assessing the fundamental frequencies of the structure. If these frequencies are higher than the values as indicated in section 8.3.1.3, it is likely that the accelerations of the deck under the influence of traffic loads will stay below the serviceability limit state (see section 4.4.2.2). The fundamental frequencies of the final model can be calculated by the software. The lowest frequencies of the principle modes are:

$$\begin{aligned} f_1 &= 6.07\ [Hz] \quad && \textit{vertical vibration} \\ f_2 &= 12.61\ [Hz] \quad && \textit{torsional vibration} \\ f_3 &= 19.09\ [Hz] \quad && \textit{lateral vibration} \end{aligned} \tag{8.13}$$

These frequencies are all higher than the boundaries, which is an indication that the traffic-induced vibrations are within the serviceability limit state.

8.6.5 Deflections in (half-)opened state

Under the influence of horizontal wind loads, the maximum sway of the span's tip must be limited. Figure 8.22 shows that the deformations with respect to the static state (under self-weight only) comply with the limit state of eq. (8.6).

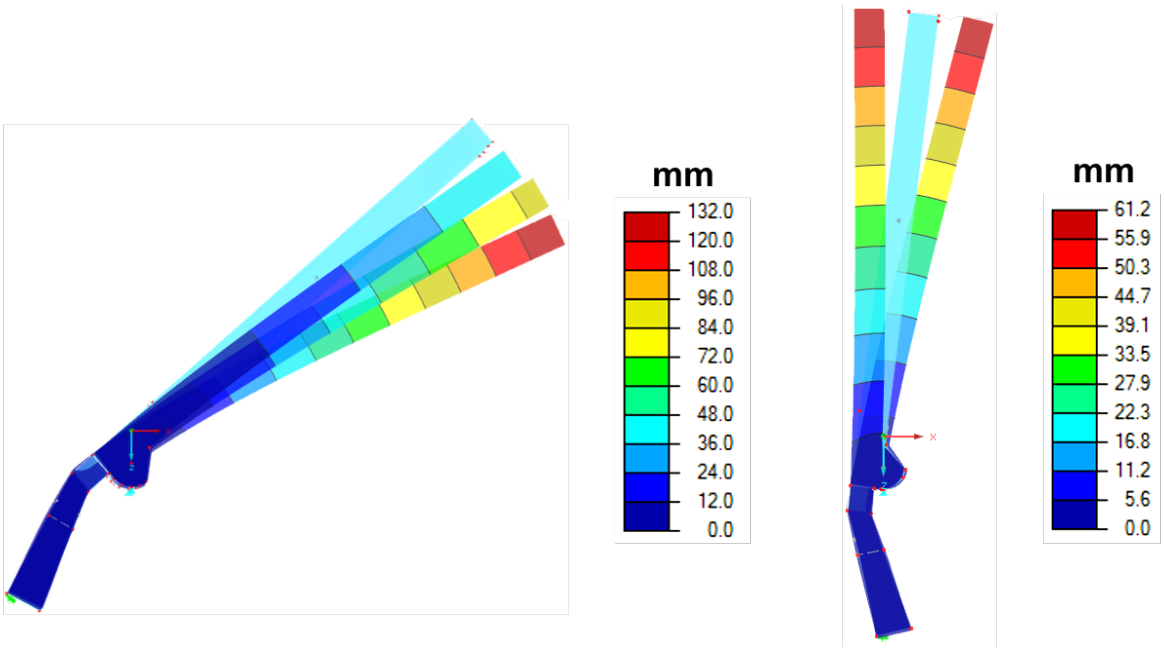

(a) Half-opened state: 41.5°

(b) Fully opened state: 83°

Figure 8.22: *Deflections of cantilever under influence of opening/closing horizontal wind load*

8.6.6 Strength in opened position

The strength of the structure was evaluated in multiple opening angles. It was found that the half-opened position was decisive in the design of the tail section of the structure. In this position, the combination of stresses due to self-weight and horizontal wind loads is maximised. In an iterative process, the failing laminates were thickened and strengthened until all laminates passed the unity checks of the first-ply-failure criterium. The resulting laminate configurations can be found in appendix F.

As expected, the highest peak stresses occur in the 'armpit'; at the transition between the tail and the span. The laminate in this section is very thick compared to the rest of the structure, and fully reinforced by carbon plies.

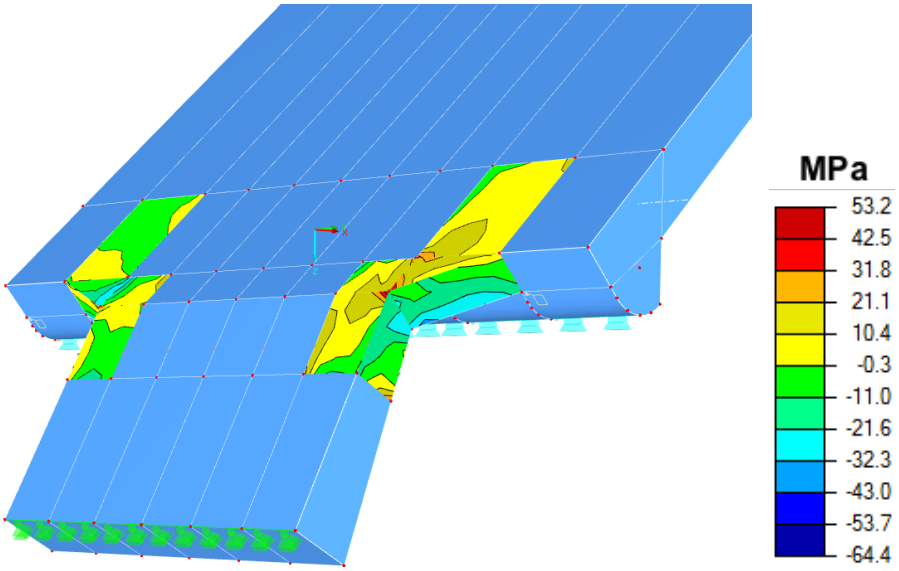

(a) Stresses in 0° plies of 'armpit' (b) Scale

Figure 8.23: *Laminate stresses in half-opened position under closing windload*

8.6.7 Stability in opened position

The stability of the bridge in the fully opened position is guaranteed by the mechanical breaks and the bumper blocks, both positioned at the end of the tail. The support is modelled by restricting the translation in the local z-direction of the line elements at the tail's end, as can be seen in fig. 8.23(a). The support reaction is significant under the influence of horizontal wind loads.

The rolling quadrant is the only vertical support in the opened position. The vertical support reaction should thus add up to the structural weight of 94 ton. Figure 8.24(b) shows the distribution of this support reaction over the width of the structure. Notice that the peaks in the distribution coincide with the position of the longitudinal stiffeners, where the stiffness of the structure is highest.

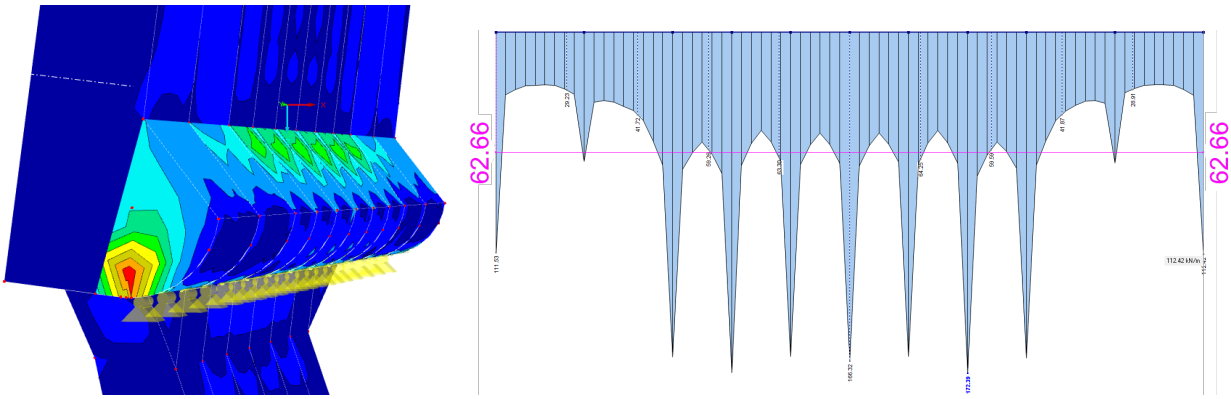

(a) Solid stresses at rolling quadrant

(b) Distribution of support reaction

Figure 8.24: *Support reaction at rolling axis under self-weight [kN/m]*

8.7 Analysis and optimisation recommendations

8.7.1 Further analysis

The conducted structural analysis as presented in this chapter should be seen as a 'proof of concept'; an initial evaluation of the technical feasibility of the proposed bridge design. Although the results do suggest that the design complies with the requirements, more detailed analysis must be conducted to evaluate the functionality and safety under all conditions. Suggested subjects for further analysis are discussed in the following sections.

8.7.1.1 Vibrations

Only an initial check of the dynamic behaviour of the bridge was performed, based on a frequency domain analysis. The Eurocode however states that this check is subject to high uncertainties, and that more detailed analysis is necessary if the criteria are not satisfied with a significant margin [NEN-EN 1990/A1, 2006, section A.2.4.3.2].

A common method to evaluate the dynamic behaviour in higher detail, is by doing an analysis in the time-domain. This entails recording the displacements of the deck in time, while the bridge is subjected to moving axle loads or crowd loads.

If the dynamic behaviour structure proves to be inadequate in further analysis, this should be addressed by adding dampers or by changing the stiffness of the structure. The latter solution can easily be achieved by replacing the used fibre reinforcement by one with other stiffness properties. This can be done in specific locations and directions, which allows to fine-tune the dynamic behaviour.

8.7.1.2 Fatigue

The fatigue limit state is mostly the decisive limit state for traditional steel bridges, resulting from a combination of high peak stresses from traffic loads and a low fatigue resistance of welds. Composite structures, on the other hand, typically have a fatigue life that is a order of magnitude larger than the required service life. As explained in section 3.4.1, this is mostly because the composite structure is overdimensioned with respect to strength, as the serviceability limit state is governing. The cyclic stresses are therefore small compared to the ultimate strength of the material, which is beneficial for the fatigue life. The sheer fatigue strength of composites is also high compared to metals, as indicated in fig. 3.29(b).

Although fatigue is not expected to be a limiting factor, the limit state should still be checked in further analysis.

8.7.1.3 Impact

As discussed in section 3.4.4, impact damage from runway debris or falling cargo is a notorious weak spot of composite bridges. It is tried to improve the impact toughness of the top laminate at the location of the traffic lane, by adding a high-density core layer to the laminate. This additional layer can absorb the impact energy, and thereby protect vital parts of the structure. The top layer of the laminate is still vulnerable, but can more easily be replaced.

In a subsequent design stage, the effectiveness of the proposed solution should be evaluated by computational and/or physical models. Also, a more extensive identification of possible impact loads is necessary. For example, the hooves of horses are known to be able to cause damage to composite surfaces.

8.7.1.4 Material-specific failure modes

In the global analysis, only three failure modes have been considered; face fracture, core shear failure and general buckling. Sandwich elements can however also fail locally, as shown in fig. 3.27. The analysis of such failure modes requires more specific software, in which for example the bond between face laminate and core can be modelled with interface elements.

Next to the considered failure modes, also the selected failure theory should be reviewed. The ‘maximum stress failure theory’ was used in the analysis, which simply assumes that failure occurs if any of the stresses exceeds the corresponding ultimate strength parameter. It is however generally recognised that the multi-directional stress state should be considered, by the application of a more material-specific failure theory such as the ‘Tsai-Hill failure theory’ (see section 3.3.3).

As advised by the CUR-96, the first-ply-failure criterion has been used in the analysis. This is a conservative approach, in which the full laminate is considered to fail upon the failure of one of the constituent plies. In reality, the laminate has residual strength after first-ply-failure, provided that the laminate is composed of multiple layer orientations. Allowing to exploit this residual strength would enable to design more efficiently.

8.7.2 Further optimisation

The structure must also be further optimised in order to make the alternative more economically competitive. Since the price of the composite material is high compared to traditional materials, the level of optimisation of composite structures must be relatively high in order to remain competitive. The automotive-, aerospace and wind-energy industries have made much progression in optimisation techniques for composites. The techniques that have been developed for these high-tech products can be used to design even more lightweight and cost-effective structures.

8.7.2.1 Geometry

Although a lot of effort was put in designing the geometry of the final structure, there is still much to improve. For example, the cross-section of the structure is constant over the full span of the bridge, while the stress distributions of the different load models are not. This suggests that some material can be saved by adapting the structure to the expected loads at that location.

In the width of the structure, the bridge is composed of two different sections; one for vehicular traffic and one for cyclists and pedestrians at either side. There is an abrupt transition between the different sections, which does not coincide with the expected stress distribution over the width. Again, material can be saved by adapting the structure to the expected loads at that location; in this case by creating a more continuous transition in cross-sectional changes.

The final design contains sharp corners in some of the laminates, which is undesirable. A favourable radius for every corner should be derived to further improve the structural efficiency.

8.7.2.2 Laminate clusters

Instead of using just a single laminate composition for the total structure, the final design is composed of a number of different laminates. Adjoined laminates of the same compositions form clusters, which have been indicated with colours in the figures of appendix F. Creating laminate groups allows to tailor the laminates for location-specific needs, and thereby increasing the material efficiency.

The size of the clusters have a big impact on the efficiency of the final structure. In theory, the smaller cluster size, the more material-efficient the design. Very small clusters are however not practical from an design and manufacturing point of view. It is however obvious that the clusters that of the proposed design are too course, and should be refined in order to reduce the material cost.

8.7.2.3 Stacking sequence

The order in which plies are stacked has a big impact on the behaviour of the laminate, as discussed in section 3.3.2.2. Even if one sticks to symmetric laminates, the order of the plies is of importance. The stacking sequence must be optimised with respect to the expected loading conditions, in order to increase the efficiency of the laminates.

8.7.2.4 Fibre reinforcement

The most important way of tailoring laminates to the requirements is by selecting the right reinforcement material. In the proposed design, only two types of fibre material were considered. By diversifying the range of available fibres, it is possible to make better use of the material.

Next to the type of fibre material, also the nature of the reinforcement form is of importance. Based on the recommendation from the CUR-96, only unidirectional plies were applied in the design exercise. The use of two- or three-dimensional woven reinforcement at certain locations can further improve the material efficiency.

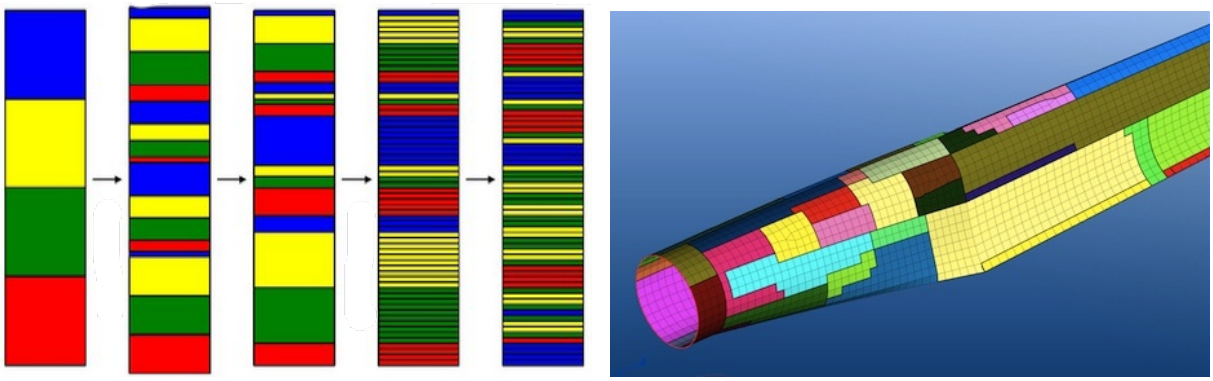

(a) Ply stacking sequence optimisation

(b) Laminate cluster optimisation

Figure 8.25: *Material-specific software 'Hypersizer' can be used to further optimise the structure*

Part III

Concluding summary

9 Conclusions

The objective of this thesis was to find the material-specific potential and challenges of composite material, and to apply the knowledge to design a new superstructure for an existing heavy-traffic bascule bridge. This chapter presents the conclusions that can be drawn for this exercise.

9.1 Literature study

Compared to construction steel, fibre reinforced polymer material is mainly lighter, stronger and more durable. On the downside however, the material is less stiff, brittle, anisotropic and more expensive. As composite material is fundamentally different from conventional materials, it requires a different design approach in order to capitalise the full potential of the material. The following sections describe a good design practice to overcome the challenges of constructing with composite material.

9.1.1 Stiffness

For high fibre percentages, the first-ply-failure strength of laminates is higher than the yielding strength of steel, while the stiffness is much lower. Simply substituting steel elements by equivalently strong composite elements will therefore result in stiffness issues; the limit state regarding maximum deflection becomes governing over the ultimate limit state. A higher bending stiffness should be obtained, which can be achieved by increasing the area moment of inertia of the section. This can be done without adding extra material by moving the load-carrying sections away from the gravitational centre of the cross-section, thereby increasing the 'Steiner' part of the equation. The associated cost with this adaption should be kept as to a minimum. The two most common approaches are creating a framework of linear elements, or otherwise by making a sandwich element by adding a low-grade material between two load-carrying face sheets. The first method allows to make use of the elements produced by the pultrusion process; a highly automated manufacturing technique that offers consistent quality at a relatively low price. On the other hand, joints are introduced in the design, which reduce the structural efficiency and complicate the design and assembly. Therefore, there is a tendency to move away from linear elements and to adopt surface elements for composite structures. Hence, the sandwich configuration was chosen as a starting point for the design of the bascule bridge.

9.1.2 Ductility

Unidirectional composite material does not exhibit much ductility, and will fail in a brittle way without large plastic deformations. Other tricks will have to be applied to ensure that the structure gives an adequate warning prior to failure, such as creating hybrid fibre arrangements, second load-paths or fibre optic sensor monitoring. Alternatively, one can opt for providing redundancy by over-dimensioning the structural elements.

The ductility problem is more severe if fibres with a relatively high stiffness are applied, such as carbon fibres. Compared to glass-fibres, these high-stiffness fibres have a strength-to-stiffness ratio that is much closer to unity. Stiffness is therefore less of an issue in the design. As a result however, carbon composite structures are more likely to be governed by strength rather than stiffness. Since the material will not adequately warn prior to failure, due to the lack of ductility, this can lead to potentially dangerous structures.

Design codes and recommendations for composites acknowledge this potential danger, and prescribe regulations to avoid such situations. The Dutch CUR96 recommendations for composite materials prescribes that each of the principle directions (0°, +45°, -45° and 90°) must contain at least 15% of the available fibre volume. Doing so will introduce some extra ductility; the strongest plies (parallel to load direction) are still intact after the failure of the weakest plies (perpendicular to load direction). Although the additional deformation may not be very noticeable, the progressive failure does manifest itself by showing crack and delamination patterns on the surface. This allows to check the condition of the structure by visual inspection.

9.1.3 Anisotropy

The anisotropic nature of the laminates complicates the design of the composite structures. On the other hand it allows to tailor the material to meet the specific requirements, thereby increasing the material efficiency of the structure.

The anisotropic behaviour of the laminates mainly depends on the stacking sequence of the constituent plies, and can be determined by the classical laminate theory. By stacking the plies in a particular manner, one can create laminates with special properties such as having zero coefficient of expansion or being quasi-isotropic.

9.1.4 Cost

Per unit of volume, composite material is up to four times as expensive as construction steel. Also, the production methods mostly require more manual labor than conventional materials, further driving the cost. The initial investment for a composite structure is therefore often significantly higher than for an equivalent steel structure.

There is however a trend in the construction industry to consider the cost of a structure over the full service life of a structure; from design to demolition. Although such a life-cycle approach is always an estimation, it is not unlikely that a composite bridge structure would outperform a conventional structure in the long run. Especially when considering movable bridges, the corrosion-free and lightweight character of the material is beneficial. The structure is easier to transport and assemble, the operational system can be simpler, the opening/closing cycle requires less energy, and the structure is has a longer service-life while being practically maintenance-free. For rehabilitation projects, there is the additional benefit of being able to reuse the substructure without further strengthening.

Nevertheless, the initial investment is an important consideration for a client. And since the material offers endless laminate combinations and geometrical freedom, it is essential to explore these options to further improve the material efficiency.

9.2 Design study

In the first part (Ch. 6) of the design study, only the span of the bascule bridge is considered. By strongly simplifying the problem, the structure could be analysed by simple equations. A subsequent parametric analysis gave a good impression of the influence of several design parameters on the efficiency of the structure, followed by optimisation with respect to self-weight and cost. The second part (Ch. 7) of the design study focussed on tackling some of the challenges regarding the composite design of a bascule bridge, with a strong emphasis on the tail-part of the structure. Several solutions for these challenges were presented and evaluated based on their compatibility with the composite material. Lastly, in the third part (Ch. 8), the obtained knowledge was used to create a first design for a replacement composite superstructure for the case study bascule bridge. This design was subjected to a number of governing load combinations, and optimised while respecting the functional requirements.

9.2.1 Span design (Ch. 6)

The basic sandwich composition was chosen as starting point for the design process, for the reasons mentioned under section 9.1.1. Hand-calculations show that the serviceability limit state (midspan deflection) is indeed governing over the ultimate limit state (strength), and that the shear contribution to the deformation is significant. A parametric study proves that the most effective way of reducing the midspan deflections is adding longitudinal stiffeners to the sandwich panel, which marginalise the shear deformation with relatively little material.

The parametric study revealed that the structural height of the panel should be maximised within the geometrical boundary conditions, in order to optimise the panel with respect to self-weight and cost. Furthermore, replacing glass-fibre material by more expensive carbon-fibre material can, in some cases, result in a cheaper structure. For example, placing high-stiffness carbon fibres in the spanning direction of the bridge is a very effective way of increasing the bending stiffness of the structure in this direction.

The parametric study, in which different material sets and panel configurations were considered, gave a good insight in the influence of the different design parameters. These are the most important conclusions that were drawn:

- The structural height of the panel should be maximised within the geometrical boundaries
- Using more lightweight material does not always lead to a more weight-efficient structure
- Using cheaper material does not always lead to a more cost-efficient structure
- A composite sandwich panel can comply with the functional requirement and boundary conditions of the span of the case study's bascule bridge
- A spanning composite sandwich panel can be competitive to an equivalent steel structure in terms of weight and material-cost

9.2.2 Tail design (Ch. 7)

While the span of the structure is governed by deformation, the design of the tail is mainly determined by strength criteria. In order to obtain a technically feasible design, the following design principles proved to be most important:

- Minimise the complexity of the structure
- Avoid discontinuities of the laminates
- Minimise localised stresses by increasing contact areas

With these design principles in mind, the geometry and the pivot-, operating- and stabilising systems should be designed. The result is a bascule bridge superstructure that is compatible with the composite material.

9.2.2.1 Geometry

Although it seems counterintuitive to use lightweight material at the counterweight-side of the pivot axis, this proved to be necessary to create a feasible solution. By integrating the tail- and span-sections into a single monolithic composite superstructure, the design can be greatly simplified while ensuring the continuity of the laminates. The full structure can be impregnated in a single production step by using the resin transfer moulding technique.

An important condition for a replacement project, such as the case study, is that the new structure should fit within the confines of the existing bascule chamber. In order to accommodate the roof of the chamber, the tail cannot be straight. Steel structures mostly have a double kink at the position of the rotation shaft. In the composite sandwich structure, local instability of the face laminates in the vicinity of the kink should be considered. The geometry of the kink should be such that the peeling stresses between the plies of the laminate are minimised, in order to avoid delamination. Therefore, a single (concave) kink was used in the conceptual composite design.

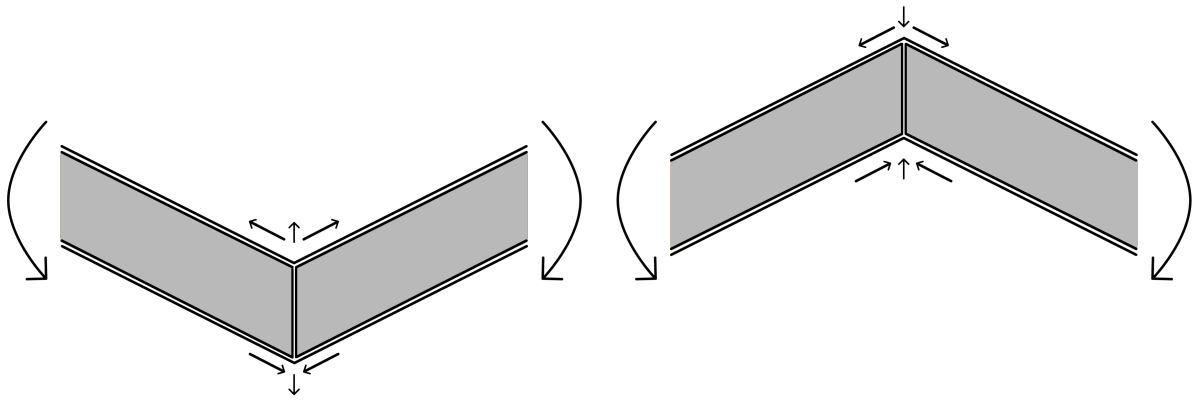

(a) Locally unstable (b) Stable

Figure 9.1: *Force equilibrium in kinked sandwich panel configurations*

9.2.2.2 Pivot system

Conventional steel bascule bridge superstructures are mostly equipped with a trunnion pivot system, in which the main girders are connected to the rotational bearings by a metal shaft. Another pivot system, which has not been applied in the Netherlands for over 60 years, relies on a rolling quadrant on which the bridge is suspended. During the opening cycle, the structure rocks backwards, resembling the motion of a rocking chair.

The evaluation of these two alternatives shows that the rolling pivot system offers better load distribution, a less complex laminate structure and a smaller span length. The rolling quadrant can be integrated into the monolithic structure, while ensuring the continuity of the laminates.

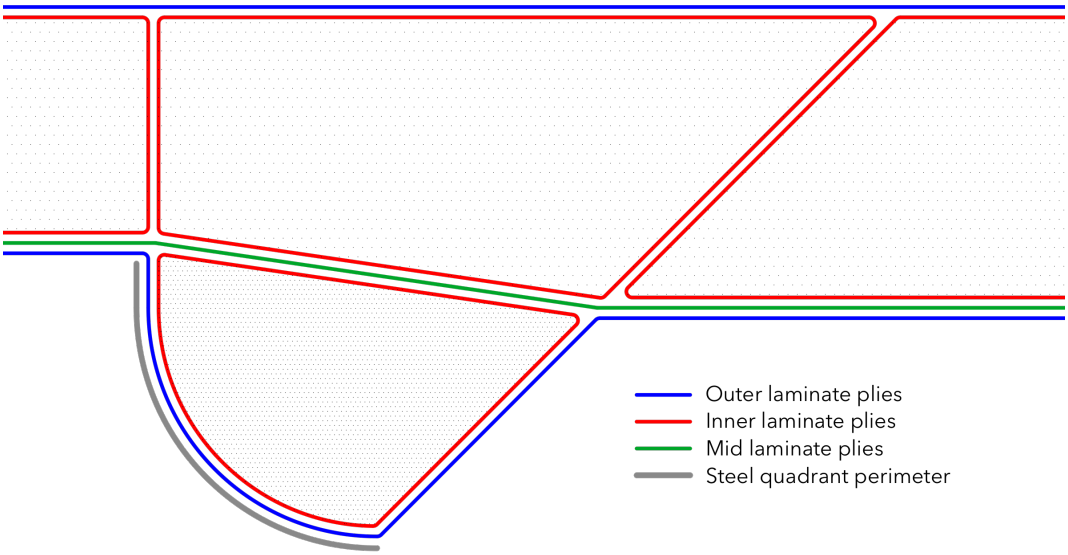

Figure 9.2: *Integration of rolling quadrant in monolithic composite structure*

9.2.2.3 Operating system

The main challenge with the operating system in combination with the composite tail structure is force distribution; localised pulling/pushing on the laminates must be avoided, especially perpendicular to the surface. Secondly, since the tail section is a solid sandwich structure, avoiding physical interference of the mechanical systems with the opening structure is challenging.

Both hydraulic- and mechanical operating mechanisms have been evaluated based on their compatibility with the composite tail structure. A segmental rack-pinion mechanism at the very end of the tail-section maximised the lever arm of the opening force, while allowing to distribute the load over the full width of the structure. Although the system is relatively complex, mechanical systems do offer a higher durability and reliability than hydraulic systems.

9.2.2.4 Stabilising system

The stabilising system, which comprises all elements that ensure the rotational stability of the structure, must also be designed with the composite material in mind. By suspending the superstructure on a line support, the contact area for transferring loads is maximised. An elastomeric bearing strip can offer sufficient flexibility for live load deformations, while avoiding unintentional uplifting from the support.

Since the self-weight of the a composite bridge is low compared to an equivalent steel structure, the counterweight can be much smaller as well. Alternatively, one can use ballast material with a lower density such as sand or concrete. The latter approach was chosen in the design study, as it was estimated that this would be a cheaper solution.

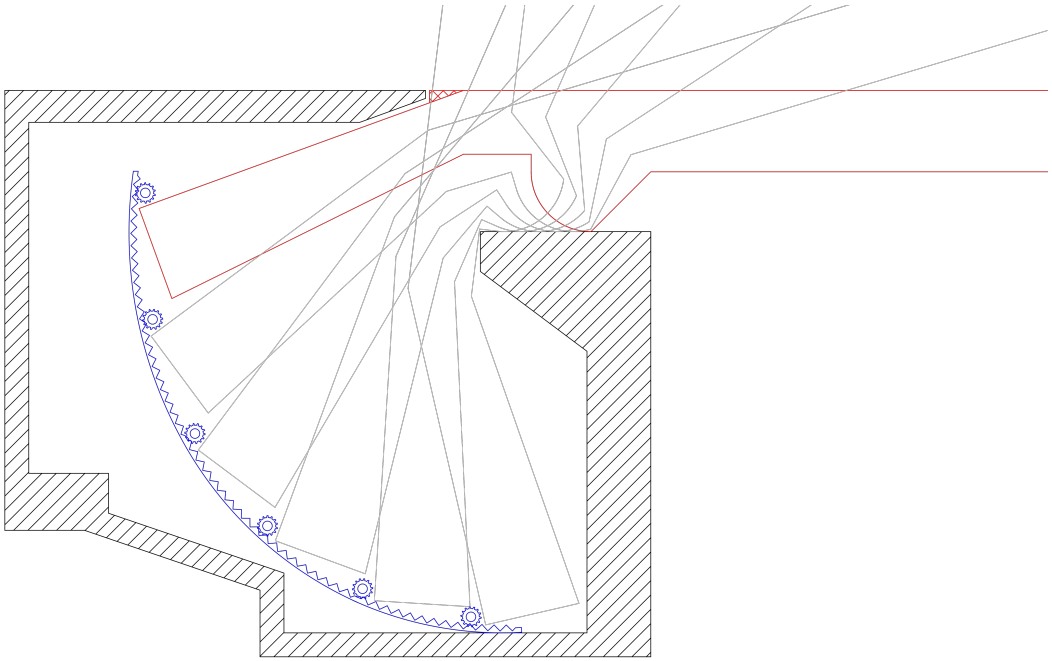

Figure 9.3: *Implementation of mechanical rack-pinion operating system*

9.2.3 Computational modelling (Ch. 8)

On a global level, sandwich composite structures can be modelled and analysed by conventional finite element software that offers both shell and solid elements. The anisotropic properties of the face laminates however need to be pre-processed through the classical laminate theory. During post-processing, the results from the integration points of the shell elements will, again via CLT, have to be translated into the stress states of the individual plies.

The proposed structural geometry was modelled and analysed using the 'Dlubal RFEM' finite element software. The shape and materials were subsequently optimised in an iterative process, until the structure complied with the serviceability- and ultimate limit states under the different load combinations. The conclusions that were drawn from this exercise are now discussed.

9.2.3.1 Stiffness

As a result of the relatively low stiffness of composite material, the serviceability limit state proved to be governing for the span of the structure. In the closed state, the global deformation in combination with local deformation in the vicinity of patch loads quickly exceeds the maximum deformation limits. In the fully-opened state, the horizontal wind loads cause large deformations at the tip of the cantilevered span.

Sensitivity analysis shows that the midspan deflections in the closed state can most effectively be reduced by increasing the stiffness of the face laminate at the location of the traffic lanes, which affects both the global- and the local deformations. The following two methods are most effective to achieve this increased stiffness:

- Use high-modulus (carbon) fibres in the spanning direction of the structure
- Add a high-grade core layer to the face laminate

Note that upgrading the full laminate with high-modulus (and more expensive) fibres is less cost-effective than only upgrading the plies in the spanning direction. The additional core in the face laminate should have a high shear modulus to decrease the local deformation in the vicinity of the patch load.

9.2.3.2 Strength

The combination of self-weight and horizontal wind loads in the half-opened state proves to be decisive for the laminates around the pivot axis of the structure. Especially at the intersections of the face laminates with the longitudinal stiffener panels, the peak-stresses in the 90° angled plies govern the first-ply-failure criterion. Therefore, the face laminates at the tail-section should have a more balanced ply configuration compared to the span-section. This means that the available fibre volume should be more equally distributed over the principle directions, and that also the 90° angled plies should be upgraded to high-strength (carbon) fibres.

9.2.3.3 Self-weight and cost

After a number of optimisation iterations, a configuration was found that complies with the limit states under all considered load combinations. Although the structure leaves a lot of space for further optimisation, the self-weight (94 tons) and estimated material-cost (0.4 million euro) of the final design suggest that the composite alternative can be feasible. An equivalent steel superstructure is estimated to weight around 150 tons, and requires 0.3 million euros of material. Note that only the expenses for the materials are considered; production, transport, assembly, maintenance and operation are not considered in this thesis. Although the initial investment is considerably higher, the composite alternative could outperform the conventional steel structure when considering the cost over the full service life of the structure (see section 9.1.4).

From the breakdown of the expenses, it is found that 95% of the material-cost arise from the composite laminates. This indicates that the material-cost can quickly decrease by further optimisation.

9.2.3.4 Optimisation

As the global structure can be analysed by conventional software packages, the geometry can also be optimised. Composite material can easily be moulded in any shape, and it is recommendable to usefully employ this feature. Since the material-cost are relatively high compared to steel, the extra engineering cost are quickly recouped by the material that can be saved. Geometric optimisation can be partially automated by using scripts, in which a form-finding algorithm uses output from the structural analysis as input for the next step. A well-known plugin for algorithmic modelling is ‘Grasshopper’.

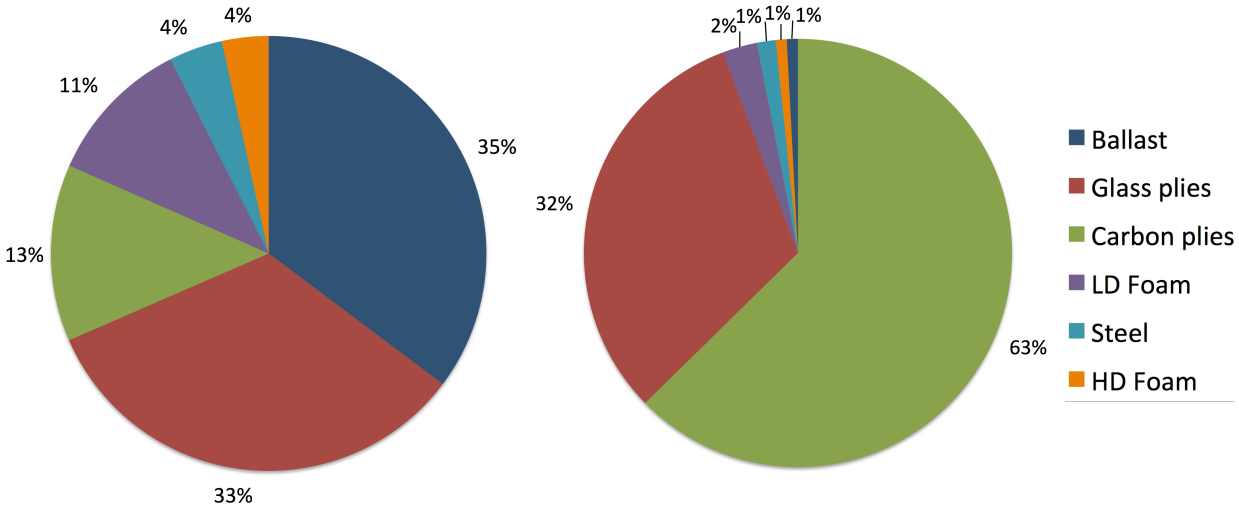

(a) Weight (b) Material-cost (c) Legend

Figure 9.4: *Breakdown of contribution to weight and material-cost from constituents*

9.3 Conclusion to research question

The conclusions from the literature- and case study have given answers to the sub-questions of the main research question, as posed in the introduction of this report (see section 1.4). The required information is gathered to give a comprehensive answer to the following main research question:

"Can fibre reinforced polymer composites be used to develop technically and economically feasible alternatives for the rehabilitation or replacement of existing, heavy-traffic, bascule bridges?"

The technical feasibility of composite heavy-traffic movable bridges had already been demonstrated by a number of reference projects. However, some specific challenges regarding the pivot system of a bascule bridge still had to be addressed. Solutions to these challenges have been presented and verified in this thesis, showing that it is technically possible to compose a heavy-traffic bascule bridge from fibre reinforced polymer material that complies with the requirements and conditions.

The economical feasibility of the composite alternative has mostly been evaluated qualitatively. It is likely that the material-cost for a composite structure will, for the time being, be higher than that of an equivalent structure of conventional materials. However, the lightweight and durable characteristics of the material allow for a reduction of maintenance- and operational expenses over the service-life of the structure. The benefits are in particular significant for rehabilitation and replacement projects, as the substructure can be reused, the operational system can be simpler and the counterweight can be smaller.

Considering the above, it is highly plausible that superstructures composed of fibre reinforced composites can offer both a technically- and economically feasible alternative for the replacement of existing heavy-traffic bascule bridges.

10 Further research

It is obvious that not every design aspect is considered in this thesis. In a further design stage, aspects like fatigue, fire-safety, vibrations and impact damage should be assessed. The following recommendations for further research however focus on more distinctive topics, which might eventually help to accelerate the adoption of composite material in the (bridge) construction industry.

10.1 Sustainability

There is an active debate on whether or not composite material can be considered sustainable. On the one hand, the material is extremely durable and therefore has a longer service-life than structures composed of conventional materials. On the other, the material in its current composition is not produced from renewable sources, and is practically not recyclable.

Advancements are being made in the replacement of synthetic fibres by natural fibres (biofibres), which are mostly derived from trees or plants such as jute, bamboo and hemp. Next to having the advantages of regular composite material, biofibre-reinforced composites are renewable, recyclable and biodegradable. Also the core material of sandwich structures can be composed of, or supplemented with material from renewable sources.

Regarding recyclability, the main problem is that the commonly used thermoset resins cannot be melted, but instead decomposes at a certain temperature. The used material can be ground to small particles and used as filler material, however this way of downgrading material is not considered to be sustainable. In contrast to the commonly used thermosetting resins, thermoplastic polymers can be remelted and reused in a similar way to the first use. The problem with thermoplastics is that the material is susceptible to creep, track forming under wheel loads, and softening under the influence of sun radiation.

Further research is necessary to address the challenges with biofibres and thermoplastic resins, and to identify which parts of the structure can be substituted by more sustainable composite material.

10.2 Manufacturing

With the exception of the pultrusion process, relatively much manual labour is required for the production of composite elements. Where metal parts can be rolled, cut or grinded into the desired shape, composite material cannot. Doing so would damage the continuous fibres and the brittle resin. Instead, a mould is used in which the uncured constituents are shaped into the desired geometry. This process is usually done manually, and therefore has a big impact on the production cost of composite elements. Next to that, one cannot assure a consistent quality of the produced parts.

Mainly for the latter consideration, the high-tech aerospace, automotive and wind-energy industries heavily invest in the automation of production processes. Nowadays, the bigger companies in the aircraft industry rely on automated fibre placement processes, in which a robot takes care of the lay-up process of the laminates. A second promising technique is 3D printing of laminates and honeycombs, which is becoming popular in the automotive industry.

The required automation equipment is becoming more affordable, and might some day be in reach for serial production in the construction industry. Further research on the implementation of these techniques can lower the production cost and increase the quality of the produced parts.

10.3 Connections

In the case study, it became clear that local stress concentrations govern the design at the tail-section of the bridge. Mainly at the intersection of the longitudinal stiffener panels and the face laminates, the plies in the transverse direction needed strengthening. The same holds for the surface of the traffic lane, where the structure must be able to resist impact loads. In these locations, one would rather use a material with more toughness and isotropic strength properties.

An effective solution could be integrating 3D fibre preforms at these locations, which offer greatly improved through-the-thickness properties and toughness. These fibre preforms can be produced by traditional textile procedures such as weaving, braiding, kitting and stitching. The preforms can be embedded between the continuous laminates, be placing them at the desired location before starting the impregnation process.

Further research is required to assess the feasibility of the application of 3D fibre preforms in the composite bridge industry.

10.4 Optimisation

Although structural analysis and optimisation on a global level is possible with conventional finite element packages, it may pay off to invest in more material-specific software. High-tech industries make use of software packages that are able to model details of a structure at fibre-level. The optimisation modules can extract information from a material database, and take the limitations of the manufacturing process into consideration. Using an optimisation algorithm, the software derives the most efficient laminate configurations and stacking sequence at every location of the structure.

Further research on the impact of material-specific software on the efficiency of the structure could be interesting and useful.

10.5 Lifecycle cost analysis

In this thesis, the assessment of the economical feasibility of the composite alternative was mostly done qualitatively. It was concluded that the initial investment for a composite structure is relatively high, but the cost over the service-life could approach that of a conventional design.

Further lifecycle cost analysis is required to substantiate this conclusion. Breaking down the expenses into individual cost will also give better insight in which aspects should deserve more attention in further optimisation.

Part IV

References and lists of figures/tables

References

AASHTO (2013). Aashto lrfd bridge design specifications. Technical report, American Association of State Highway and Transportation Officials.

Adams, R. and Maheri, M. (2003). Damping in advanced polymer-matrix composites. *Journal of Alloys and Compounds*.

Adams, W. (1987). State of the art hydraulic systems for movable bridges.

Aseff, G. V. (1987). Corrosion mechanisms in the deterioration of exposed bridge steel.

Bai, Y. and Keller, T. (2008). Modal parameter identification for a gfrp pedestrian bridge. *Composite Structures*.

Bakis, C., Nanni, A., Terosky, J., and Koehler, S. (2001). Self-monitoring, pseudo-ductile, hybrid frp reinforcement rods for concrete applications. *Composites Science and Technology*, 61.

Barefoot, G. (2007). Preserving history: Composites breathe new life into barbados landmark. *Composites Manufacturing*.

Campbell, F. (2010). *Structural Composite Materials*. ASM International.

Carlsson, L. and Kardomateas, G. (2011). *Structural and Failure Mechanics of Sandwich Composites*. Springer.

Centraal Bureau voor de Statistiek (2013). Motorvoertuigen; aantal voertuigen en autodichtheid per provincie.

Clarke, J. L. (1996). *Structural Design of Polymer Composites - EUROCOMP Design Code and Handbook*. E&FN Spon.

Coates, A. C. and Bluni, S. A. (2004). Movable bridge design. *STRUCTURE magazine*.

Componeering Inc. (2013). Esacomp material database.

Cragg, R. L. (1987). Trunnion bascule bridge static stabilizing systems.

Cragg, R. L. (2004). Energy absorbing live load shoes and anchorages for bascule bridges.

Creative Pultrusions Inc. (2004). *The Pultex Pultrusion Design Manual*. Creative Pultrusions.

CUR-96 (2003). *Vezelversterkte Kunststoffen in Civiele Draagconstructies*. Civieltechnisch Centrum Uitvoering Research en Regelgeving.

CUR-96+ (2012). *Vezelversterkte Kunststoffen in Civiele Draagconstructies - Concept version 2013*. Civieltechnisch Centrum Uitvoering Research en Regelgeving.

de Winter, S. (1999). *Vezelversterkte Kunststoffen in Constructieve Toepassingen*. Vereniging FME-CWM, Federatie NRK.

DIAB Group (1999). Diab sandwich handbook.

Dooley, S. (2004). *The Development of Material-Adapted Structural Form*. PhD thesis, Ecole Polytechnique Federale de Lausanne.

Douglas, E. (2006). Backgound on fiber reinforced polymers for civil infrastructure.

Fiberline (2013). Case stories: Footbridges and cycle bridges.

Granor Rubber & Engineering (2014). Elastomeric bearings.

Gürtler, H. W. (2004). *Composite Action of FRP Bridge Decks Adhesively Bonded to Steel Main Girders*. PhD thesis, Ecole Polytechnique Federale de Lausanne.

Halpin, J. and Kardos, J. (1976). The halpin-tsai equations: A review. *Polymer Engineering and Science*, 16.

HCB Company (2013). Hybrid composite beam brochure.

Karbhari, V. M., Wang, D., and Gao, Y. (2001). Processing and performance of bridge deck subcomponents using two schemes of resin infusion. *Composite Structures*, 51.

Kaw, A. K. (2006). *Mechanics of Composite Materials 2nd Edition*. Taylor & Francis Group.

Keller, T. (2003). *Use of Fibre Reinforced Polymers in Bridge Construction*. International Association for Bridge and Structural Engineering.

Kindinger, J. (2001). *Lightweight Structural Cores*. ASM International.

Koglin, T. (2003). *Movable Bridge Engineering*. Wiley.

Kolstein, M. (2008). *Fibre Reinforced Polymer (FRP) Structures*. Technische Universiteit Delft.

Matthews, F., Davies, G., Hitchings, D., and Soutis, C. (2000). *Finite Element Modelling of Composite Materials and Structures*. Woodhead Publishing Ltd.

Mazumdar, S. K. (2002). *Composite Manufacturing - Materials, Product and Process Engineering*. CRC Press.

Meunier, M. and Knibbs, S. (2007). *Design Tools for Fibre Reinforced Polymer Structures*. National Composites Network.

Mosallam, A. S. (2011). *Design Guide for FRP Composite Connections*. Americal Society of Civil Engineers.

Mottram, J. T. and Turvey, G. J. (1998). *State of the Art Review on Design, Testing, Analysis and Applications of Polymeric Composite Connections*. European Commission.

National Association of Corrosion Engineers (1994). Corrosion control and treatment manual.

NauticExpo (2014). The online boating and maritime exhibition.

NEN 6786 (2001). *Voorschriften voor het ontwerp van beweegbare bruggen*. Nederlands Normalisatie-instituut.

NEN-EN 1990 (2002). *Basis of Structural Design*. Comité Européen de Normalisation.

NEN-EN 1990/A1 (2006). *Basis of Structural Design*. Comité Européen de Normalisation.

NEN-EN 1990/NB (2011). *Basis of Structural Design - Dutch National Annex*. Comité Européen de Normalisation.

NEN-EN 1991-1-1 (2011). *Actions on structures - General actions - Densities, self-weight, imposed loads for buildings*. Comité Européen de Normalisation.

NEN-EN 1991-1-4 (2005). *Actions on structures - General actions - Wind actions*. Comité Européen de Normalisation.

NEN-EN 1991-1-4/NB (2011). *Actions on structures - General actions - Wind actions - Dutch national annex*. Comité Européen de Normalisation.

NEN-EN 1991-1-5 (2011). *Actions on structures - General actions - Thermal actions*. Comité Européen de Normalisation.

NEN-EN 1991-1-5/NB (2011). *Actions on structures - General actions - Thermal actions - Dutch National Annex*. Comité Européen de Normalisation.

NEN-EN 1991-1-7 (2006). *Actions on structures - General actions - Accidental actions*. Comité Européen de Normalisation.

NEN-EN 1991-2 (2003). *Actions on structures - Traffic loads on bridges*. Comité Européen de Normalisation.

NEN-EN 1991-2/NB (2011). *Actions on structures - Traffic loads on bridges - Dutch National Annex*. Comité Européen de Normalisation.

NEN-EN 1993-2/NB (2011). *Design of Steel Structures - Steel Bridges - Dutch National Annex*. Comité Européen de Normalisation.

NEN-EN 1995-2/NB (2011). *Design of Timber Structures - Bridges*. Comité Européen de Normalisation.

Nijhof, A. (2004). *Vezelversterkte Kunststoffen - Mechanica en Ontwerp*. VSSD.

O'Connor, J. (2013). Current practices in frp composites technology.

O'Connor, J. S. and Hooks, J. M. (2006). Usa's experience using fiber reinforced polymer composite bridge decks to extend bridge service life.

Oosterhoff, J. and Coelman, B. (1999). *Bruggen in Nederland 1800-1940*. Nederlandse Bruggen Stichting.

Parke, G. and Hewson, N. (2008). *ICE Manual of Bridge Engineering 2nd Edition*. Thomas Telford Ltd.

Peeters, J. H. A. (2011). Sandwich panel and method for producing such a panel. Technical report, Fibercore Europe B.V.

Provinsje Fryslan (2010). Vervanging hoofdbrug oosterwolde.

Qian, Z. and Abruzzese, D. (2009). Fatigue failure of welded connections at ortotropic bridges. *Frattura ed Integrità Strutturale*.

Rijkswaterstaat (2007). Inventarisatie kunstwerken. Technical report, Ministerie van Verkeer en Waterstaat.

Rijkswaterstaat (2013a). Richtijnen beoordeling kunstwerken. Technical report.

Rijkswaterstaat (2013b). Richtlijnen ontwerpen kunstwerken. Technical report, Rijkswaterstaat.

Romeijn, A. (2006). *Steel Bridges Lecture Notes CIE5125*. TU Delft.

Ryan, T. W., Hartle, R. A., Mann, J. E., and Danovich, L. J. (2006). *Bridge Inspector's Reference Manual*. Federal Highway Administration (FHWA).

Soden, P., Hinton, M., and Kaddour, A. (1998). Lamina properties, lay-up configurations and loading conditions for a range of fibre-reinforced composite laminates. *Composites Science and Technology*, 58:1011–1022.

Souren, W. (1999). Ontwerp kunststof klapbrug te andel. *Demonstratie composiet-bruggen*.

Stichting CROW (2012). *ASVV Aanbevelingen voor Verkeersvoorzieningen Binnen de Bebouwde Kom*.

Strong, A. B. (2008). *Fundamentals of Composites Manufacturing - Materials, Methods and Applications*. Society of Manufacturing Engineers.

Strongwell (2013). Composolite fiberglass building panel system.

Tang, B. and Hooks, J. (2001). Frp composites technology is changing the american building industry.

Teng, J. (2001). *FRP composites in civil engineering*. Elsevier.

Teufelberger Composite (2014). T-igel composite-metal connection.

Timoshenko, S. (1959). *Theory of plates and shells*. McGraw-Hill.

Transportation Research Board (2006). Fifty years of interstate structures.

University of South Florida (2001). Design of trunnion-hub girder assemblies for bascule bridges.

Vassilopoulos, A. P. (2010). *Fatigue life prediction of composites and composite structures*. Woodhead Publishing Ltd.

Wikipedia (2014).

Wu, H.-C. and Yan, A. (2013). Durability simulation of frp bridge decks subject to weathering. *Composites*.

Zenkert, D. (1997). *The Handbook of Sandwich Construction*. EMAS Publishing.

Zhang, Y., Cai, C., Shi, X., and Wang, C. (2006). Vehicle-induced dynamic performance of frp versus concrete slab bridge. *Journal of Bridge Engineering*.

List of Figures

List of Tables

Part V

Appendices

A

Computer-aided design tools

A.1 Laminate design tools

Table A.1: *Non-exhaustive list of laminate design tools [Meunier and Knibbs, 2007]*

Software	Specification	Comments	Theories Used	Link
LPA	Online program	• Free software. • Ideal for-one off analysis.		http://www.ccm.udel.edu/Techsite/Pages/Simulations-Index.html
The Laminator Version 3.6	Independent simple laminate design tool	• Last released: April 2006. • Download online. • Good choice for quick laminate analysis. • Material library available. • Single licence valid for life.	• Micromechanics; • CLT; • Failure theories (Maximum stress, maximum strain, Tsai-Hill, Hoffman and Tsai-Wu)	http://www.thelaminator.net/
ESDU Composites Series	Consists of: ○ 40 'Data Items'; ○ 26 Fortran programs.	• Collection of Fortran codes and programs. • Volume 1 for laminated composites analysis and design • Volume 5 for failure criteria	Described in 'Data Item' associated with each program.	http://www.esdu.com
LAP Version 4.0	Independent laminate design tool	• Three modules available: ○ Basic module; ○ Non-linear module; ○ Additional failure criteria; ○ Design module. • Easy to use, efficient and robust solver.	• CLT; • Failure theories (Maximum stress, maximum strain, Tsai-Hill, Hoffman and Tsai-Wu and custom); • FPF and UPF.	http://www.anagleph.co.uk
CoDA Version 3.3	Analysis/Design software Can complement LAP	• Experimentally validated; • Extensive testing allowed integration of optional correlation factors which aim to provide more reliable predictions. • Parametric option. • Progressive formation of cracks (PREDICT module); • Moisture diffusion module; • Heat conductivity module; • Fatigue life prediction module.	• Micromechanics/Material synthesiser; • CLT • Failure theory: Tsai-Wu (only available for in-plane loading) • Full ply failure sequence (in-plane load only)	http://www.npl.co.uk/cog/index.html http://www.anagleph.co.uk
Kolibri Version 3	Analysis software	• Laminate solver feature; • Design features available: ○ Ply analysis; ○ Laminate analysis.	• CLT; • Failure theories (Maximum stress, maximum strain, Tsai-Hill, Hoffman and Tsai-Wu).	http://www.lightweight-structures.com/
ESAComp Version 3.5	Analysis/Design software	• Laminate solver feature; • Constant and variable load option; • Database available. • Design features available: ○ Laminate evaluation; ○ Laminate creation. • Moisture diffusion module; • Last released: February 2006; • Next release schedule for February 2007.	• Micromechanics (rule-of-mixture and user defined capability); • CLT; • Failure theories (Maximum stress, maximum strain, Tsai-Hill, Hoffman, Tsai-Wu, Puck 2D, Puck 3D, Hashin 2D, Hashin 3D and user defined capability); • FPF and UPF.	http://www.componeering.com/esacomp/
Composite Star Version 2.0	Analysis/Design software	• Laminate solver feature; • Database available. • Constant and variable load option.	• Micromechanics (rule-of-mixture and cylinder model); • CLT and Netting analysis; • Failure theories (Maximum stress, maximum strain, Tsai-Hill, Hoffman, Tsai-Wu, Simple Puck, Modified Puck, Hashin and Puck's action plane criterion); • FPF and UPF.	http://www.material.be/products/composite_star.html
Composite Pro Version 3.0	Analysis/Design software	• Laminate solver feature; • Last update: February 2006. • New release available soon. • Database available. • Utility module (volume fraction converter, filament winding calculator, textile converter, radius of curvature and fabric builder).	• Micromechanics (rule-of-mixture, cylinder model and Chammis method); • CLT; • Failure theories (Maximum stress, maximum strain and Quadratic) • FPF and UPF.	http://www.compositepro.com/
Think Composites	Selections of software packages	• Progressive failure of laminate; • Hygrothermal stress analysis; • Design module.	• Micromechanics; • CLT; • Failure theories (Maximum stress, maximum strain, Tsai-Hill, Hoffman, Tsai-Wu, Hashin and Dassault);	http://www.thinkcomposites.com

A.2 Analytical design tools

Table A.2: *Non-exhaustive list of analytical design tools [Meunier and Knibbs, 2007]*

		Software						
		ESDU Composites Series	CoDA Version 3.3	Kolibri Version 3	ESAComp Version 3.5	Composite Star Version 2.0	Composite Pro Version 3.0	Think Composites
Capability	Homogeneous and laminated plates	✓	✓	✓	✓	✓	✓	
	Plate buckling			✓	✓	✓	✓	
	Natural frequency of plates	✓			✓	✓	✓	
	Sandwich plates (skin wrinkling)	✓	✓	✓	✓		✓	✓
	Sandwich plates (shear deformation)			✓	✓		✓	✓
	Sandwich plates (core shear)				✓		✓	
	Stiffened plates	✓	✓		✓			
	Curved plates	✓						
	Beams (bending)		✓	✓	✓	✓	✓	✓
	Beams (buckling)		✓	✓	✓	✓	✓	
	Beams (twisting)		✓	✓			✓	
	Natural frequencies of beams				✓	✓	✓	
	Flange or curved beams		✓					
	Tube (column stability)						✓	
	Cylindrical shell / pressure vessel				Under development		✓	
	Bonded joints		✓		✓			
	Bolted joints		✓		✓			
	Damping/response to acoustic loading	✓						
	FE export		✓		✓	✓		
	FE import				✓	✓		

A.3 Finite element software

Table A.3: *Non-exhaustive list of FEA software with composite features [Meunier and Knibbs, 2007]*

Product	Composite version	Website	Composite Features	Notes
Abaqus	VCCT	http://www.abaqus.com/vcct/	Delamination, debonding and non linear.	Also has extension for wound filament
ANSYS		http://www.ansys.com/solutions/solid-mechanics-composites.asp		
LUSAS	Composite	http://www.lusas.com/products/composite.html	Ply lay-up definition, delamination, non-linear and composite elements.	
Nastran	Composites	http://www.nenastran.com/newnoran/composite	Ply lay-up definition, non-linear and composite elements.	Version integrated to Solidworks.
Cosmos	Advanced Professional	http://www.solidworks.com/pages/products/cosmos/cosmosworks/cosmosworks_adv.html?PID=41	Functionality to define composite mesh.	Solidworks integrated and Standalone.
Algor		http://www.algor.com/default.aspx		
genoa		http://www.alphastarcorp.com/right/genoa.html		
Mecano		http://www.samcef.com/en/pss.php?ID=24&W=products		
NISA	composite	http://www.nisasoftware.com/products/nisa-composite.html	Edge effects, delamination and temperature dependant material	
Pro/ENGINEER Advanced Mechanica	Advanced	http://www.ptc.com/appserver/mkt/products/home.jsp?k=1182		
SOLVIA		http://www.solvia.com/index.html		
STRAND7		http://www.strand7.com/		
ESI	Sysply	http://www.esi-group.com/SimulationSoftware/Design_composite/	Full suite of tools designed for composite analysis.	Can simulate filament winding and draping.
Mathmatica		http://www.wolfram.com/products/		
Extensive list of FEA codes		http://homepage.usask.ca/~ijm451/finite/fe_resources/fe_resources.html#CHILD_LINKS		

B

Design input

B.1 Geometrical boundary conditions

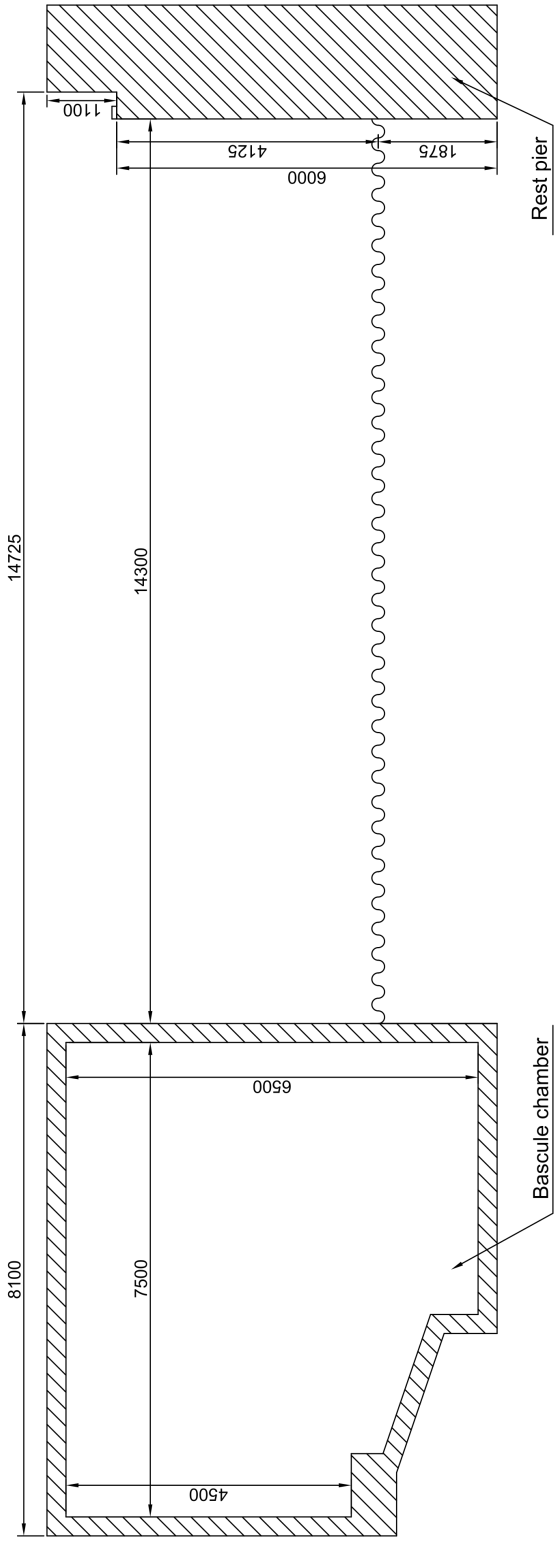

Figure B.1: *Geometrical boundary conditions for the reference bridge*

B.2 Traffic load models

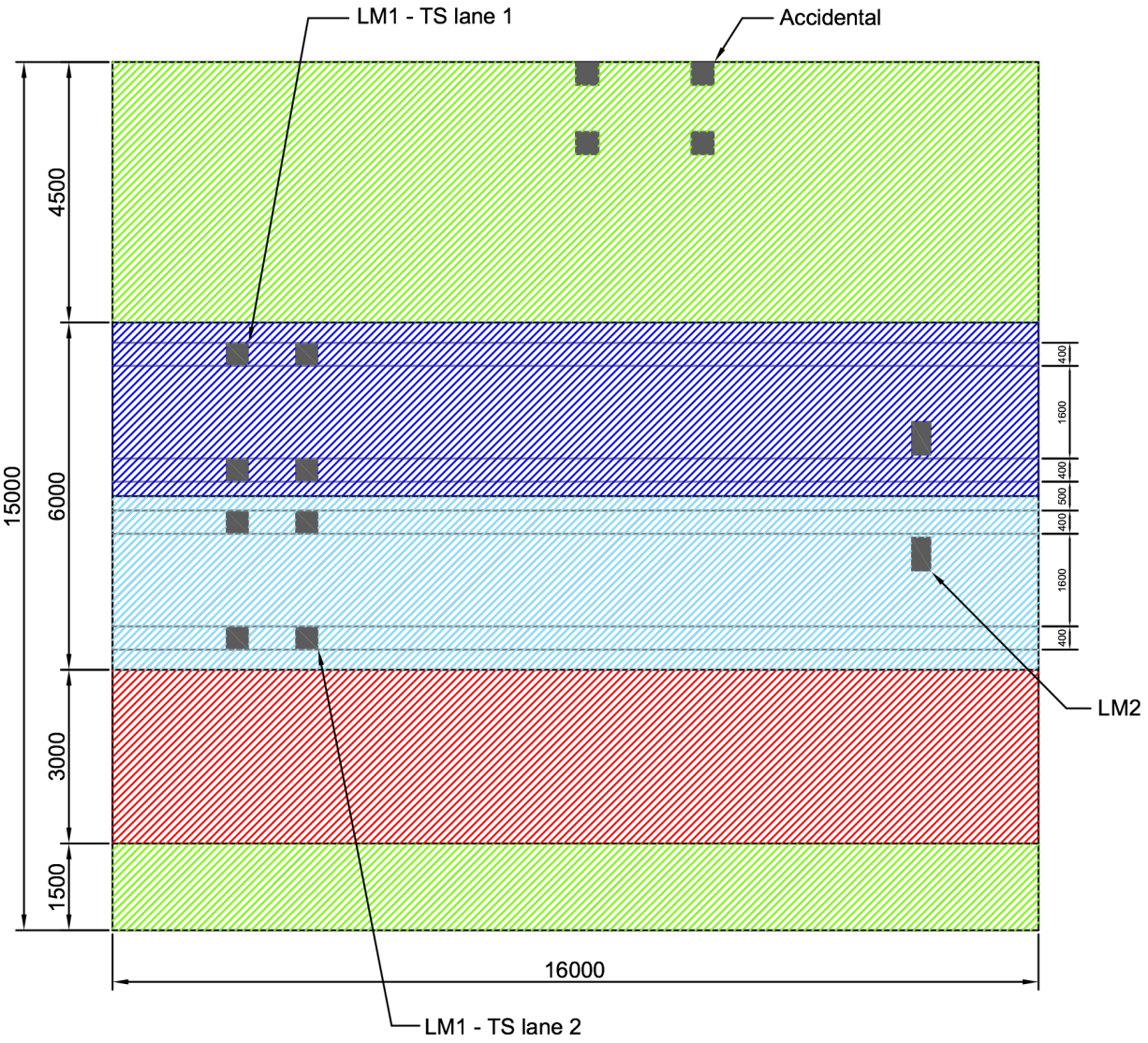

Figure B.2: *Traffic load models projected on reference bridge - green: pedestrian load, red: cyclist load, dark blue: UDL of LM1 on lane 1, light blue: UDL of LM1 on lane 2*

C

Hand calculation sheet

```
> restart; unprotect(D) : unprotect(gamma) :
> #Material properties

#Glass-fibre properties [GPa]
E_gls,1,k := 48.2 :
E_gls,2,k := 17.0 :
G_gls,k := 5.2 :
ν_gls := 0.256 :

#Carbon-fibre properties [GPa]
E_crb,1,k := 135.5 :
E_crb,2,k := 8.8 :
G_crb,k := 4.4 :
ν_crb := 0.256 :

#Core properties [GPa]
E_c,high,k := 0.282 :
G_c,high,k := 0.095 :
E_c,low,k := 0.115 :
G_c,low,k := 0.04 :

#Densities [kg m-3]
ρ_low := 100 :
ρ_high := 250 :
ρ_gls := 2040 :
ρ_crb := 1560 :

#Safety factors
γ_m,f := 1.38 :
γ_m,c := 1.3 :
γ_c,sls := 1.5 :
γ_c,uls := 1.21 :
γ_Q := 1.35 :
γ_G := 1.30 :

#Estimation of laminate properties [GPa]
p_gls := 1 − p_crb :
E_f := 0.55·(p_gls·E_gls,1,k + p_crb·E_crb,1,k) + 0.3·0.5·(E_gls,1,k + E_gls,2,k) + 0.15·E_gls,2,k :

E_f,eff := 1/(γ_m,f·γ_c,sls)·E_f :

E_f,eff,gls := subs(p_crb = 0, E_f,eff);
E_f,eff,crb := subs(p_crb = 1, E_f,eff);

#ESAComp laminate properties [GPa]
E_gls,1,d := 16.50 :
E_gls,2,d := 10.80 :
G_gls,d := 3.78 :
ν_gls := 0.299 :

E_crb,1,d := 39.25 :
E_crb,2,d := 9.03 :
G_crb,d := 3.57 :
ν_crb := 0.309 :

E_c,high,d := 0.2169 :
G_c,high,d := 0.0731 :
ν_c,high := 0.484 :

E_c,low,d := 0.0885 :
G_c,low,d := 0.0308 :
ν_c,low := 0.437 :

                                E_f,eff,gls := 18.76328503
                                E_f,eff,crb := 41.95893721   (1)

> #Geometry [mm]

L := 16000 :
B := 15000 :
c := H − 2 t :
d := H − t :
B_traffic := 6100 :
B_foot := 4500 :

> #Calculation of bending stiffness [GPa mm4]
```

$$EI_y := E_{f,1}\cdot\left(\frac{B\cdot t^3}{6}\right) + E_{f,1}\cdot\left(\frac{B\cdot t\cdot d^2}{2}\right) + E_c\cdot\left(\frac{B\cdot c^3}{12}\right) :$$

$EI_{y,A} := subs\left(E_{f,1} = E_{gls,1,d}, E_c = E_{c,low,d}, EI_y\right) :$
$EI_{y,B} := subs\left(E_{f,1} = E_{gls,1,d}, E_c = E_{c,high,d}, EI_y\right) :$
$EI_{y,C} := subs\left(E_{f,1} = E_{crb,1,d}, E_c = E_{c,low,d}, EI_y\right) :$
$EI_{y,D} := subs\left(E_{f,1} = E_{crb,1,d}, E_c = E_{c,high,d}, EI_y\right) :$

> **#Caculation of shear stiffness [GPa mm2]**

$GA_z := B\cdot d\cdot G_c :$

$GA_{z,A} := subs\left(G_c = G_{c,low,d}, GA_z\right) :$

$GA_{z,B} := subs\left(G_c = G_{c,high,d}, GA_z\right) :$

$GA_{z,C} := GA_{z,A} :$
$GA_{z,D} := GA_{z,B} :$

> **#Loads [kN, mm]**

$Q_k := 600 :$
$q_{LMI} := 10.35 :$
$q_{fk} := 4.6 :$
$q_r := 2.88 :$
$q_k := \left(B_{traffic}\cdot q_{LMI} + B_{foot}\cdot q_{fk} + \left(\mathrm{B} - B_{traffic} - B_{foot}\right)\cdot q_r\right)\cdot 10^{-6} :$
$Q_d := Q_k\cdot\gamma_Q :$
$q_d := q_k\cdot\gamma_Q :$

$$Q_d := 810.00$$

$$q_d := 0.1302844500 \qquad \textbf{(2)}$$

> **#Deformations q-load**

$$w_{q,b} := \frac{5}{384}\cdot\frac{q\cdot L^4}{EI} :$$

$$w_{q,s} := \frac{1}{8}\cdot\frac{q\cdot L^2}{GA} :$$

#ENABLE TO COMPARE WITH ESACOMP RESULTS
#H:= 1100:

#t:= 60:

 # Bending
$w_{A,q,b} := subs\left(q = \left(q_d\right), EI = EI_{y,A}, w_{q,b}\right) :$
$w_{B,q,b} := subs\left(q = \left(q_d\right), EI = EI_{y,B}, w_{q,b}\right) :$
$w_{C,q,b} := subs\left(q = \left(q_d\right), EI = EI_{y,C}, w_{q,b}\right) :$
$w_{D,q,b} := subs\left(q = \left(q_d\right), EI = EI_{y,D}, w_{q,b}\right) :$

 # Shear
$w_{A,q,s} := subs\left(q = \left(q_d\right), GA = GA_{z,A}, w_{q,s}\right) :$
$w_{B,q,s} := subs\left(q = \left(q_d\right), GA = GA_{z,B}, w_{q,s}\right) :$
$w_{C,q,s} := subs\left(q = \left(q_d\right), GA = GA_{z,C}, w_{q,s}\right) :$
$w_{D,q,s} := subs\left(q = \left(q_d\right), GA = GA_{z,D}, w_{q,s}\right) :$

#total
$w_{A,q} := w_{A,q,b} + w_{A,q,s} :$
$w_{B,q} := w_{B,q,b} + w_{B,q,s} :$
$w_{C,q} := w_{C,q,b} + w_{C,q,s} :$
$w_{D,q} := w_{D,q,b} + w_{D,q,s} :$

> **#Deformations Q-load**

$$w_{Q,b} := \frac{1}{48}\cdot\frac{Q_d\cdot L^3}{EI} :$$

$$w_{Q,s} := \frac{1}{4}\cdot\frac{Q_d\cdot L}{GA} :$$

 # Bending
$w_{A,Q,b} := subs\left(EI = EI_{y,A}, w_{Q,b}\right) :$
$w_{B,Q,b} := subs\left(EI = EI_{y,B}, w_{Q,b}\right) :$
$w_{C,Q,b} := subs\left(EI = EI_{y,C}, w_{Q,b}\right) :$
$w_{D,Q,b} := subs\left(EI = EI_{y,D}, w_{Q,b}\right) :$

 # Shear
$w_{A,Q,s} := subs\left(GA = GA_{z,A}, w_{Q,s}\right) :$
$w_{B,Q,s} := subs\left(GA = GA_{z,B}, w_{Q,s}\right) :$
$w_{C,Q,s} := subs\left(GA = GA_{z,C}, w_{Q,s}\right) :$
$w_{D,Q,s} := subs\left(GA = GA_{z,D}, w_{Q,s}\right) :$

#total
$w_{A,Q} := w_{A,Q,b} + w_{A,Q,s} :$

$w_{B,Q} := w_{B,Q,b} + w_{B,Q,s}$:
$w_{C,Q} := w_{C,Q,b} + w_{C,Q,s}$:
$w_{D,Q} := w_{D,Q,b} + w_{D,Q,s}$:

> **#Investigate effects of skin thickness for H=1100**

with(*plots*) :
p1 := *plot*(*subs*($H = 1100$, $(w_{A,q,b} + w_{A,Q,b})$), $t = 0..110$, *color* = *blue*, *legend* = "bending 0% carbon") :
p2 := *plot*(*subs*($H = 1100$, $(w_{C,q,b} + w_{C,Q,b})$), $t = 0..110$, *color* = *red*, *legend* = "bending 100% carbon") :
p3 := *plot*(*subs*($H = 1100$, $(w_{A,q,s} + w_{A,Q,s})$), $t = 0..110$, *color* = *green*, *legend* = "shear HD") :
p4 := *plot*(*subs*($H = 1100$, $(w_{B,q,s} + w_{B,Q,s})$), $t = 0..110$, *color* = *purple*, *legend* = "shear MD") :

p5 := *plot*(*subs*($H = 1100$, $(w_{A,q} + w_{A,Q})$), $t = 0..110$, *color* = *blue*, *legend* = "Panel A") :
p6 := *plot*(*subs*($H = 1100$, $(w_{B,q} + w_{B,Q})$), $t = 0..110$, *color* = *red*, *legend* = "Panel B") :
p7 := *plot*(*subs*($H = 1100$, $(w_{C,q} + w_{C,Q})$), $t = 0..110$, *color* = *green*, *legend* = "Panel C") :
p8 := *plot*(*subs*($H = 1100$, $(w_{D,q} + w_{D,Q})$), $t = 0..110$, *color* = *purple*, *legend* = "Panel D") :
p9 := *plot*((40), $t = 0..150$, *color* = *black*, *linestyle* = 2, *legend* = "L/400") :

display({*p1*, *p2*, *p3*, *p4*}, *labels* = ["Skin thickness: t [*mm*]","*Partial deflection* : *w* [*mm*]"], *labeldirections* = [*horizontal*, *vertical*], *view* = [0..110, 0..60]);
display({*p5*, *p6*, *p7*, *p8*, *p9*}, *labels* = ["Skin thickness: t [*mm*]","*Deflection* : *w* [*mm*]"], *labeldirections* = [*horizontal*, *vertical*], *view* = [0..110, 0..60]);

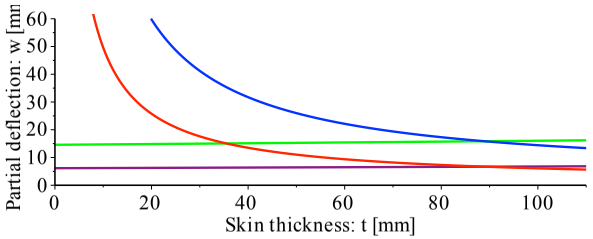

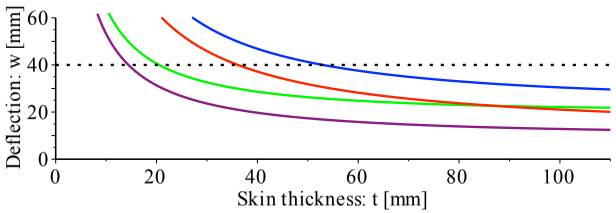

> **#Investigate core and skin thickness for w=40 mm**

$w_A := w_{A,q} + w_{A,Q} = \frac{L}{400}$:
$w_B := w_{B,q} + w_{B,Q} = \frac{L}{400}$:
$w_C := w_{C,q} + w_{C,Q} = \frac{L}{400}$:
$w_D := w_{D,q} + w_{D,Q} = \frac{L}{400}$:
p19 := *plot*(*solve*(w_A, t), $H = 600..1100$, *color* = *blue*, *legend* = "Panel A") :
p20 := *plot*(*solve*(w_B, t), $H = 600..1100$, *color* = *red*, *legend* = "Panel B") :
p21 := *plot*(*solve*(w_C, t), $H = 600..1100$, *color* = *green*, *legend* = "Panel C") :
p22 := *plot*(*solve*(w_D, t), $H = 600..1100$, *color* = *purple*, *legend* = "Panel D") :

display({*p19*, *p20*, *p21*, *p22*}, *labels* = ["Structural height: H [*mm*]","*Skin thickness* : *t* [*mm*]"], *labeldirections* = [*horizontal*, *vertical*], *view* = [600..1100, 0..110]);

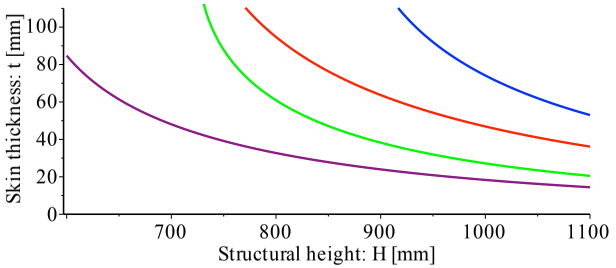

> **#Investigate self-weight for w=40 mm**

#Self−weight [kg·m-2]
$G_A := (2 \cdot t \cdot \rho_{gls} + c \cdot \rho_{low}) \cdot 10^{-3}$:
$G_B := (2 \cdot t \cdot \rho_{gls} + c \cdot \rho_{high}) \cdot 10^{-3}$:

$G_C := \left(2 \cdot t \cdot \left(0.55 \cdot \rho_{crb} + 0.45 \cdot \rho_{gls}\right) + c \cdot \rho_{low}\right) \cdot 10^{-3}$:
$G_D := \left(2 \cdot t \cdot \left(0.55 \cdot \rho_{crb} + 0.45 \cdot \rho_{gls}\right) + c \cdot \rho_{high}\right) \cdot 10^{-3}$:

$p23 := plot\left(subs\left(t = solve\left(w_A, t\right), G_A\right), H = 600..1100, color = blue, legend = \text{"Panel A"}\right)$:
$p24 := plot\left(subs\left(t = solve\left(w_B, t\right), G_B\right), H = 600..1100, color = red, legend = \text{"Panel B"}\right)$:
$p25 := plot\left(subs\left(t = solve\left(w_C, t\right), G_C\right), H = 600..1100, color = green, legend = \text{"Panel C"}\right)$:
$p26 := plot\left(subs\left(t = solve\left(w_D, t\right), G_D\right), H = 600..1100, color = purple, legend = \text{"Panel D"}\right)$:
$p27 := plot\left(\left(\frac{61000}{15 \cdot 16}\right), H = 600..1100, color = black, linestyle = 2, legend = \text{"Current structure"}\right)$:

$display(\{p23, p24, p25, p26, p27\}, labels = [\text{"Structural height: H [mm]"}, \text{"Self-weight [kg·m-2]"}], labeldirections = [horizontal, vertical], view = [600..1100, 0..800])$;

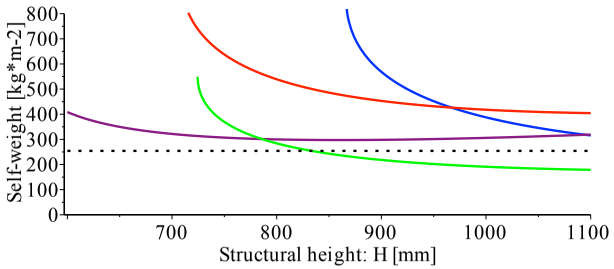

> **#Investigate material cost for w=40 mm**

#Unit cost [EUR kg-1]
$UC_{pvc} := 1$:
$UC_{gls} := 4$:
$UC_{crb} := 20$:

#Sandwich panel prices [EUR]
$P_A := \left(2 \cdot t \cdot UC_{gls} \cdot \rho_{gls} + c \cdot UC_{pvc} \cdot \rho_{low}\right) \cdot B \cdot L \cdot 10^{-9}$:
$P_B := \left(2 \cdot t \cdot UC_{gls} \cdot \rho_{gls} + c \cdot UC_{pvc} \cdot \rho_{high}\right) \cdot B \cdot L \cdot 10^{-9}$:
$P_C := \left(2 \cdot t \cdot \left(0.55 \cdot UC_{crb} \cdot \rho_{crb} + 0.45 \cdot UC_{gls} \cdot \rho_{gls}\right) + c \cdot UC_{pvc} \cdot \rho_{low}\right) \cdot B \cdot L \cdot 10^{-9}$:
$P_D := \left(2 \cdot t \cdot \left(0.55 \cdot UC_{crb} \cdot \rho_{crb} + 0.45 \cdot UC_{gls} \cdot \rho_{gls}\right) + c \cdot UC_{pvc} \cdot \rho_{high}\right) \cdot B \cdot L \cdot 10^{-9}$:

$p28 := plot\left(subs\left(t = solve\left(w_A, t\right), P_A\right), H = 600..1100, color = blue, legend = \text{"Panel A"}\right)$:
$p29 := plot\left(subs\left(t = solve\left(w_B, t\right), P_B\right), H = 600..1100, color = red, legend = \text{"Panel B"}\right)$:
$p30 := plot\left(subs\left(t = solve\left(w_C, t\right), P_C\right), H = 600..1100, color = green, legend = \text{"Panel C"}\right)$:
$p31 := plot\left(subs\left(t = solve\left(w_D, t\right), P_D\right), H = 600..1100, color = purple, legend = \text{"Panel D"}\right)$:
$display(\{p28, p28, p30, p31\}, labels = [\text{"Structural height [mm]"}, \text{"Material cost [EUR]"}], labeldirections = [horizontal, vertical], view = [600..1100, 0..750000])$;

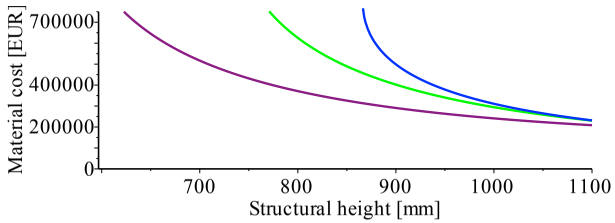

> **#Investigate stresses for w=40 mm**

$M_{max} := \frac{1}{8} \cdot q_d \cdot L^2 + \frac{1}{4} \cdot Q_d \cdot L$;
$V_{max} := \frac{1}{2} \cdot q_d \cdot L + Q_d$;

$\sigma_f := \frac{M_{max} \cdot \left(\frac{1}{2} \cdot H\right)}{EI} \cdot E_{f,1}$:
$\tau_c := \frac{V_{max}}{B \cdot d}$:

$\sigma_{f,A} := subs\left(EI = EI_{y,A}, E_{f,1} = E_{gls,1,d}, \sigma_f\right)$:
$\sigma_{f,B} := subs\left(EI = EI_{y,B}, E_{f,1} = E_{gls,1,d}, \sigma_f\right)$:
$\sigma_{f,C} := subs\left(EI = EI_{y,C}, E_{f,1} = E_{crb,1,d}, \sigma_f\right)$:
$\sigma_{f,D} := subs\left(EI = EI_{y,D}, E_{f,1} = E_{crb,1,d}, \sigma_f\right)$:

$p32 := plot\left(subs\left(t = solve\left(w_A, t\right), 1000 \cdot \sigma_{f,A}\right), H = 600..1100, color = blue, legend = \text{"Panel A"}\right)$:
$p33 := plot\left(subs\left(t = solve\left(w_B, t\right), 1000 \cdot \sigma_{f,B}\right), H = 600..1100, color = red, legend = \text{"Panel B"}\right)$:
$p34 := plot\left(subs\left(t = solve\left(w_C, t\right), 1000 \cdot \sigma_{f,C}\right), H = 600..1100, color = green, legend = \text{"Panel C"}\right)$:

$p35 := plot\left(subs\left(t = solve\left(w_D, t\right), 1000 \cdot \sigma_{f,D}\right), H = 600..1100, color = purple, legend = \text{"Panel D"}\right):$

$p36 := plot\left(subs\left(t = solve\left(w_A, t\right), 1000 \cdot \tau_c\right), H = 600..1100, color = blue, legend = \text{"Panel A"}\right):$

$p37 := plot\left(subs\left(t = solve\left(w_B, t\right), 1000 \cdot \tau_c\right), H = 600..1100, color = red, legend = \text{"Panel B"}\right):$

$p38 := plot\left(subs\left(t = solve\left(w_C, t\right), 1000 \cdot \tau_c\right), H = 600..1100, color = green, legend = \text{"Panel C"}\right):$

$p39 := plot\left(subs\left(t = solve\left(w_D, t\right), 1000 \cdot \tau_c\right), H = 600..1100, color = purple, legend = \text{"Panel D"}\right):$

$display(\{p32, p33, p34, p35\}, labels = [\text{"Structural height [mm]"}, \text{"Average flexural stress [MPa]"}], labeldirections = [horizontal, vertical], view = [600..1100, 0..30]);$

$display(\{p36, p37, p38, p39\}, labels = [\text{"Structural height [mm]"}, \text{"Shear stress [MPa]"}], labeldirections = [horizontal, vertical], view = [600..1100, 0.1..0.25]);$

$M_{max} := 7.409102400\ 10^6$

$V_{max} := 1852.275600$

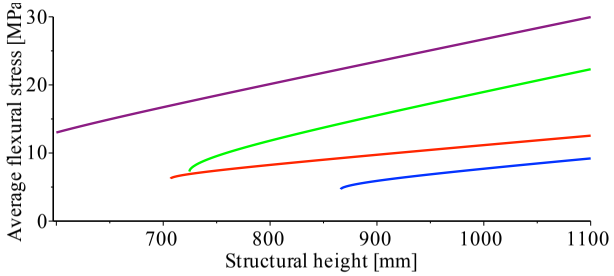

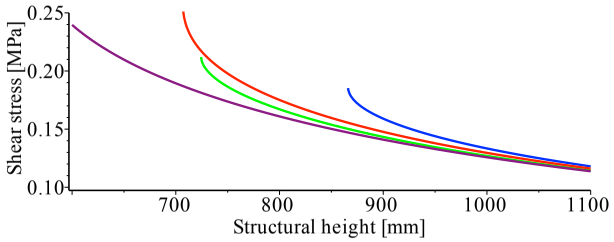

> ***#Investigate reserve factor for w=40 mm***

#core shear failure [MPa]

$\tau_{cr1} := \frac{1}{\gamma_{m,c}} \cdot S_c:$

$\tau_{cr1,MD} := \text{subs}\left(S_c = 1.7, \tau_{cr1}\right):$

$\tau_{cr1,HD} := subs\left(S_c = 4.7, \tau_{cr1}\right):$

$p40 := plot\left(subs\left(t = solve\left(w_A, t\right), \frac{\tau_{cr1,MD}}{1000 \cdot \tau_c}\right), H = 600..1100, color = blue, legend = \text{"Panel A"}\right):$

$p41 := plot\left(subs\left(t = solve\left(w_B, t\right), \frac{\tau_{cr1,HD}}{1000 \cdot \tau_c}\right), H = 600..1100, color = red, legend = \text{"Panel B"}\right):$

$p42 := plot\left(subs\left(t = solve\left(w_C, t\right), \frac{\tau_{cr1,MD}}{1000 \cdot \tau_c}\right), H = 600..1100, color = green, legend = \text{"Panel C"}\right):$

$p43 := plot\left(subs\left(t = solve\left(w_D, t\right), \frac{\tau_{cr1,HD}}{1000 \cdot \tau_c}\right), H = 600..1100, color = purple, legend = \text{"Panel D"}\right):$

$display(\{p40, p41, p42, p43\}, labels = [\text{"Structural height [mm]"}, \text{"Reserve factor : RF [-]"}], labeldirections = [horizontal, vertical], view = [600..1100, 0..35]);$

#core crimping [MPa]

$\tau_{cr2} := \frac{G_c \cdot d}{2 \cdot t}:$

$\tau_{cr2,MD} := subs\left(G_c = G_{c,low,d}, \tau_{cr2}\right):$

$\tau_{cr2,HD} := subs\left(G_c = G_{c,high,d}, \tau_{cr2}\right):$

$p44 := plot\left(subs\left(t = solve\left(w_A, t\right), \frac{\tau_{cr2,MD}}{1000 \cdot \tau_c}\right), H = 600..1100, color = blue, legend\right.$

D

Verification parametric analysis with ESAComp

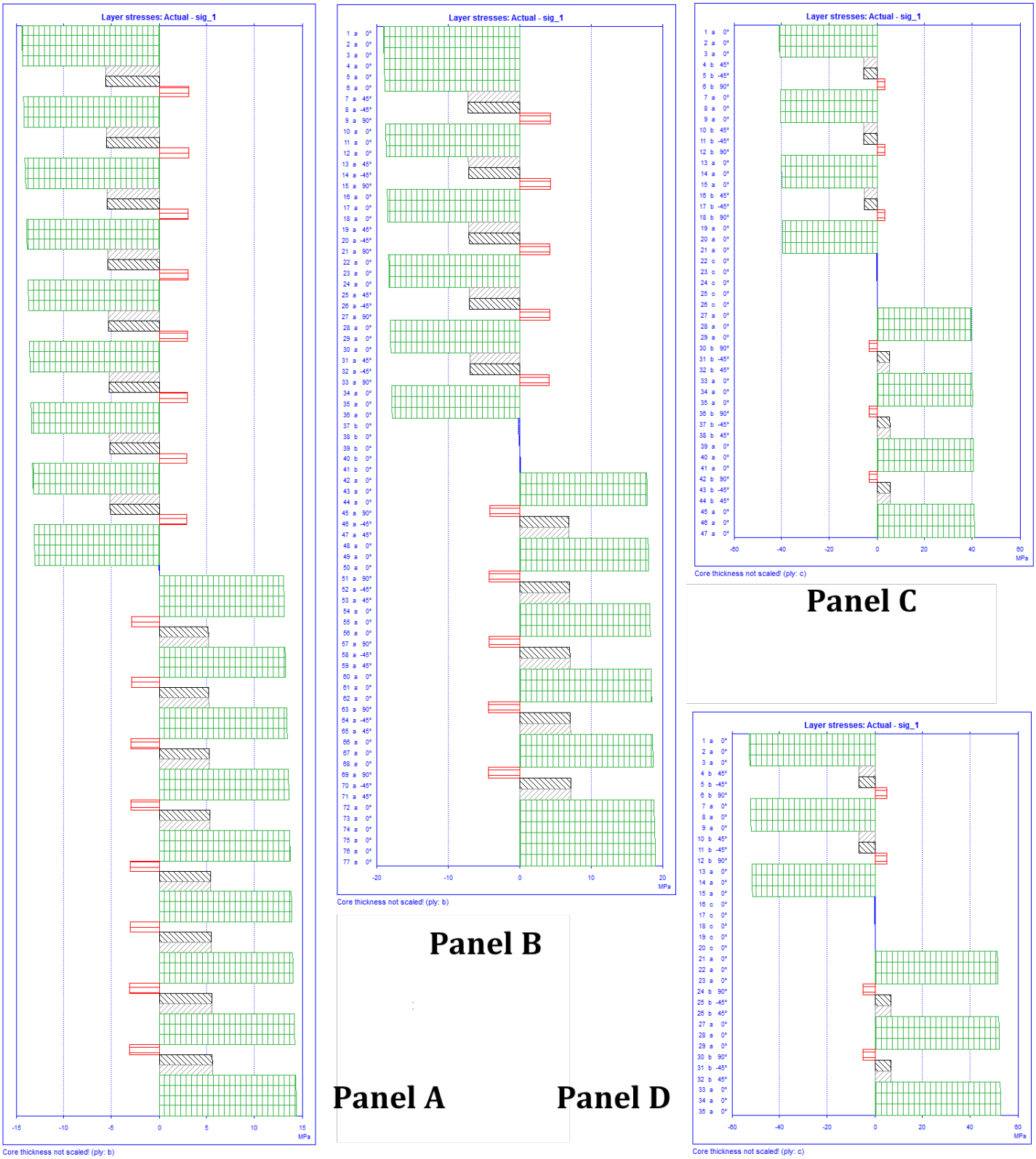

Figure D.1: *Effective laminate stresses* ($\sigma_{f,1}$) *for panels subjected to* M_{max} *(see section 6.1.2.5)*

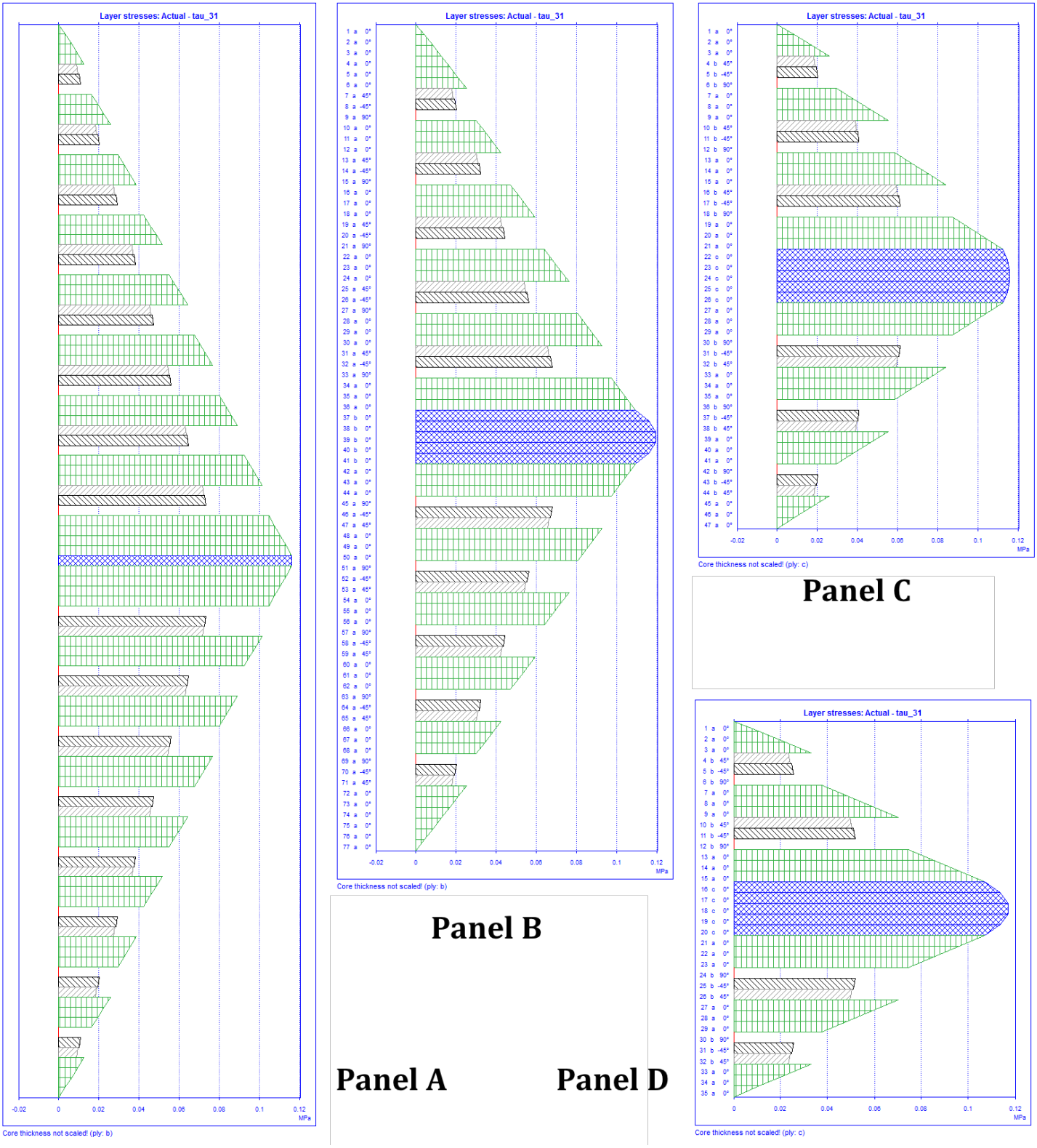

Figure D.2: *Shear stresses* (τ_c) *for panels subjected to* V_{max} *(see section 6.1.2.5)*

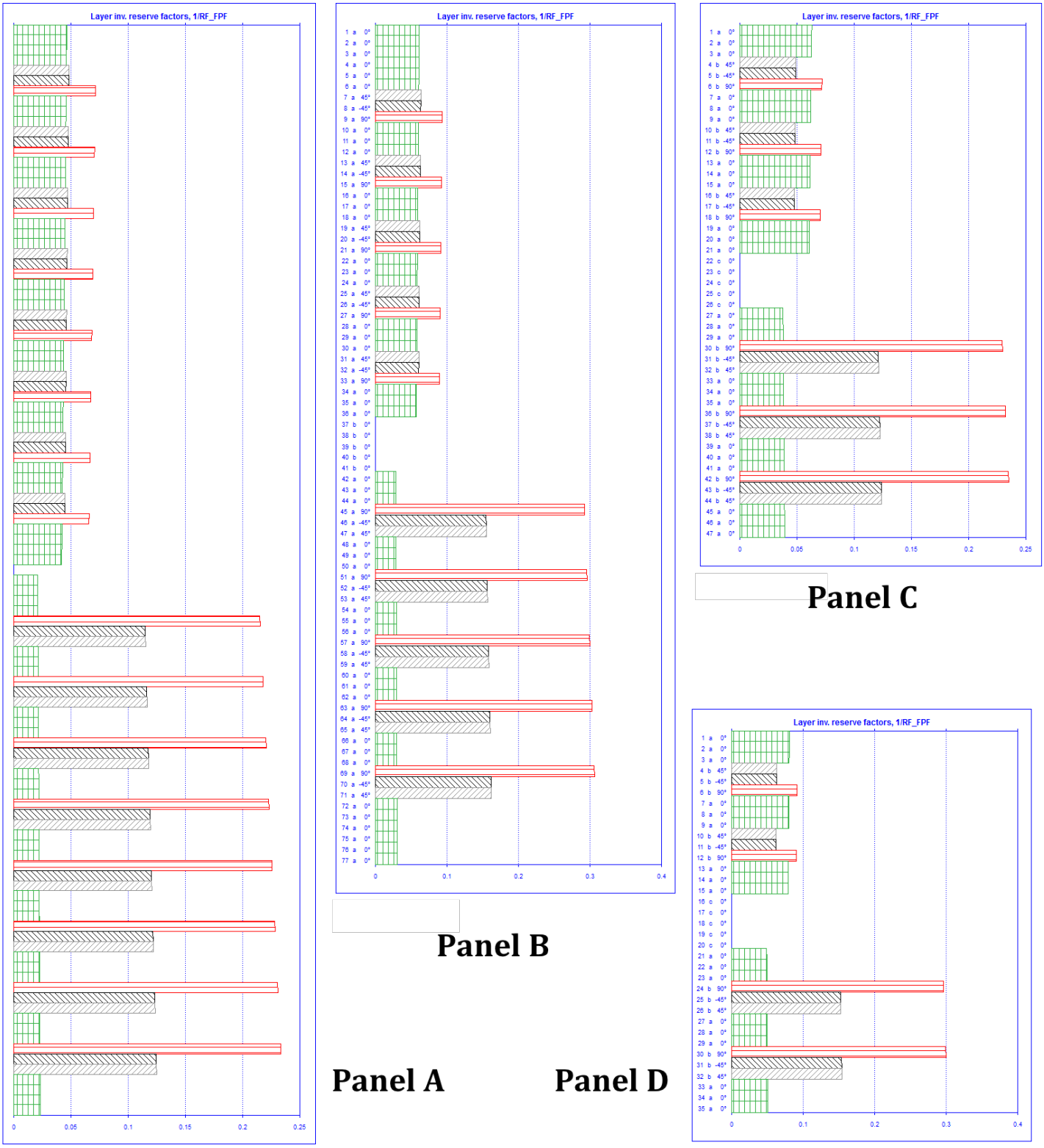

Figure D.3: *First-ply-failure inversed reserve factors* (RF^{-1}) *for panels subjected to* M_{max} *(see section 6.1.2.5)*

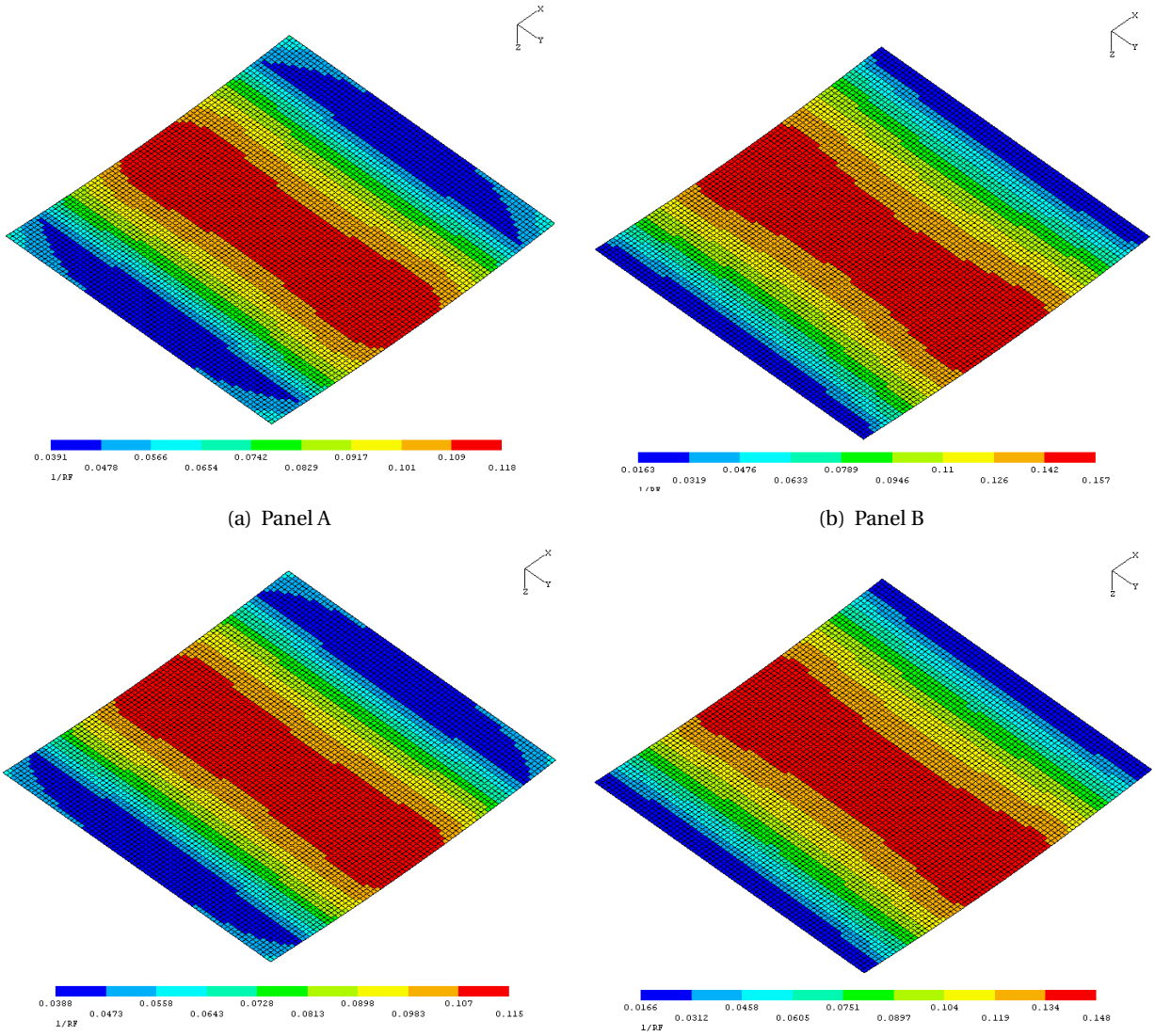

(a) Panel A

(b) Panel B

(c) Panel C

(d) Panel D

Figure D.4: *First-ply-failure inversed reserve factor* (RF^{-1}) *for panels subjected to* q_d

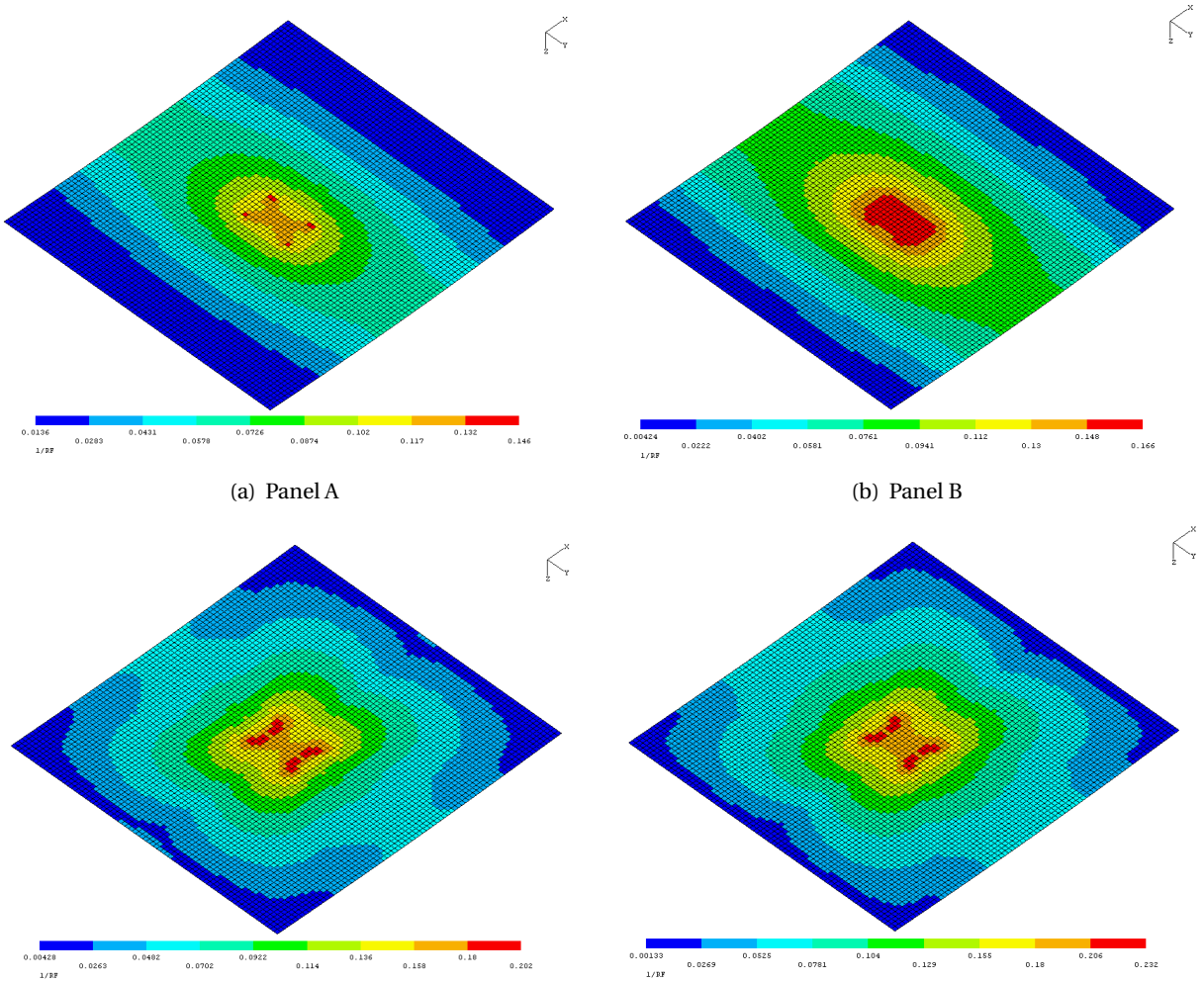

(a) Panel A

(b) Panel B

(c) Panel C

(d) Panel D

Figure D.5: *First-ply-failure inversed reserve factor* (RF^{-1}) *for panels subjected to* Q_a*, distributed as a double-axle tandem system*

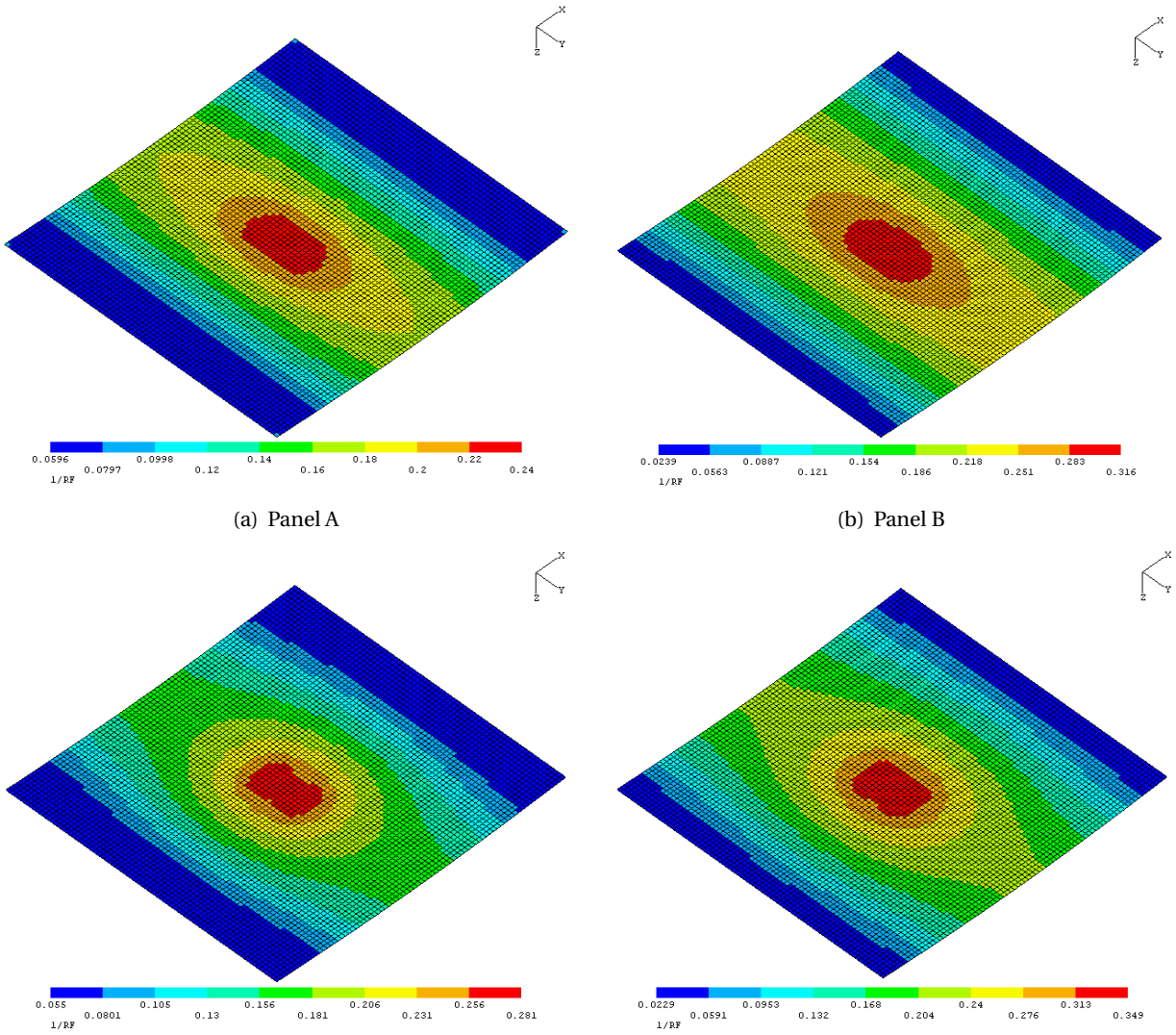

(a) Panel A

(b) Panel B

(c) Panel C

(d) Panel D

Figure D.6: *First-ply-failure inversed reserve factor* (RF^{-1}) *for panels subjected to* $q_d + Q_d$

E

Pivot alternatives

E.1 Trunnion pivot system

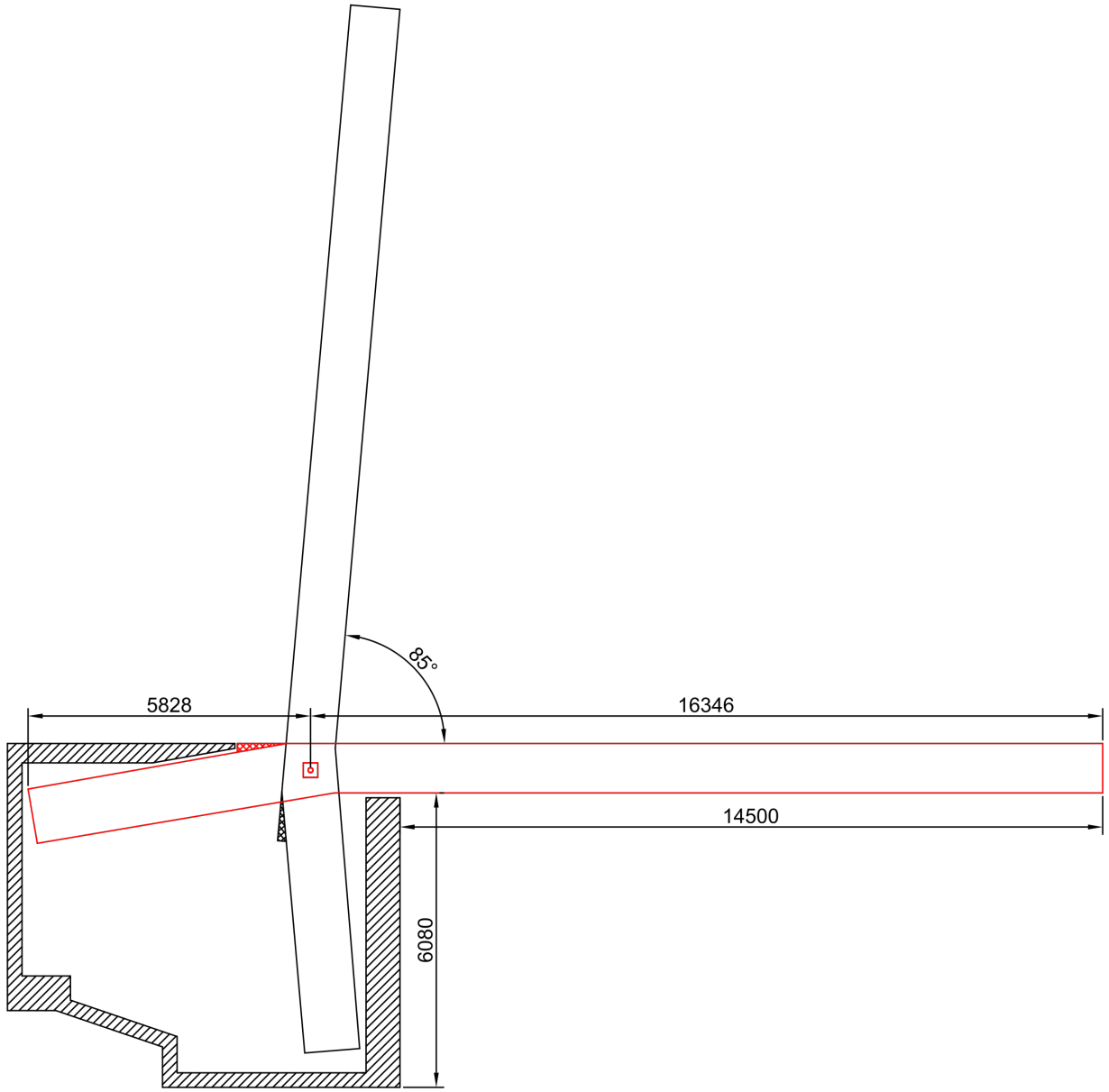

Figure E.1: *Implementation of trunnion bascule structure in geometrical boundaries of reference bridge*

E.2 Rolling pivot system

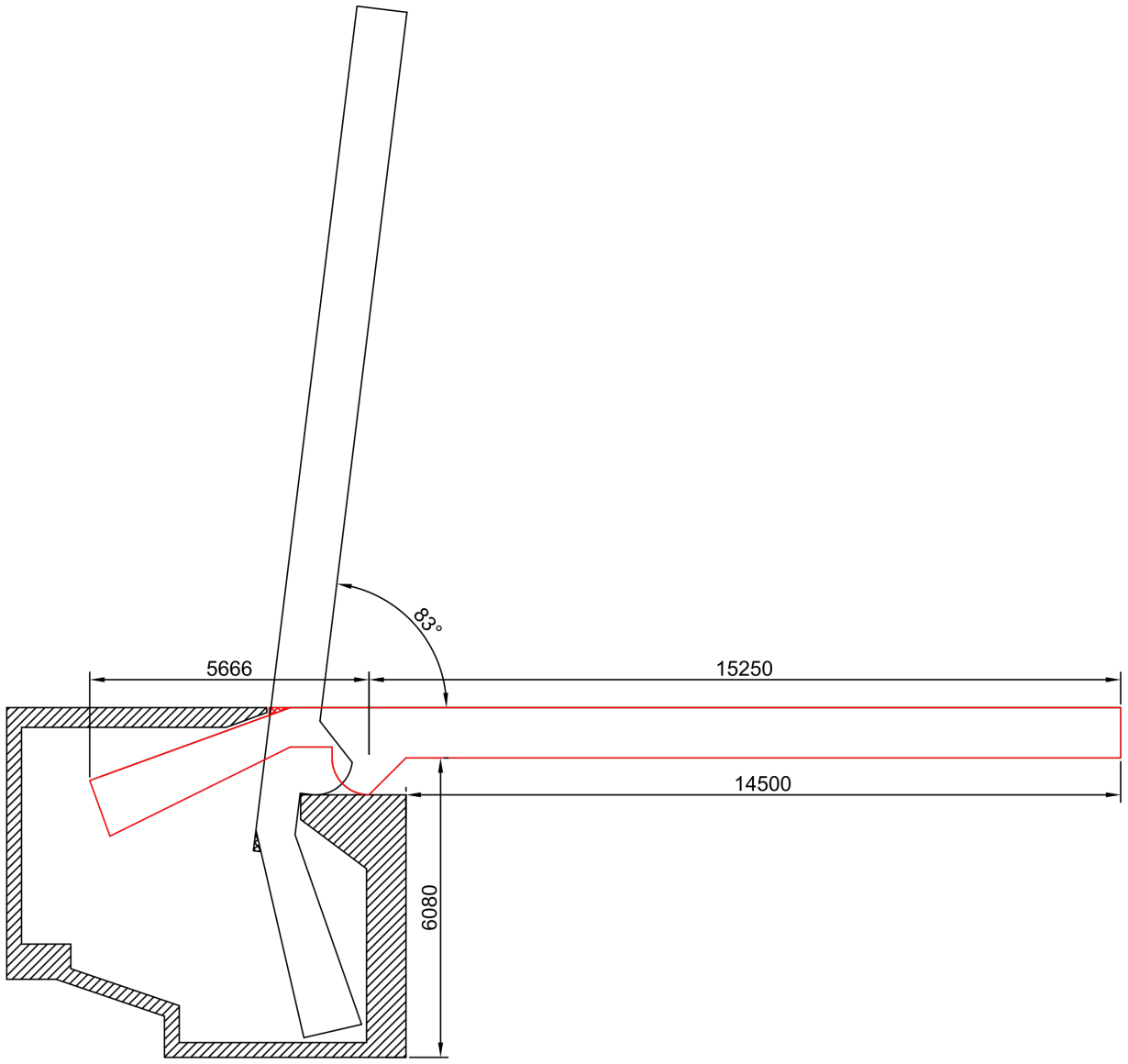

Figure E.2: *Implementation of rolling bascule structure in geometrical boundaries of reference bridge*

F

Laminate configurations final design

F.1 Top laminates

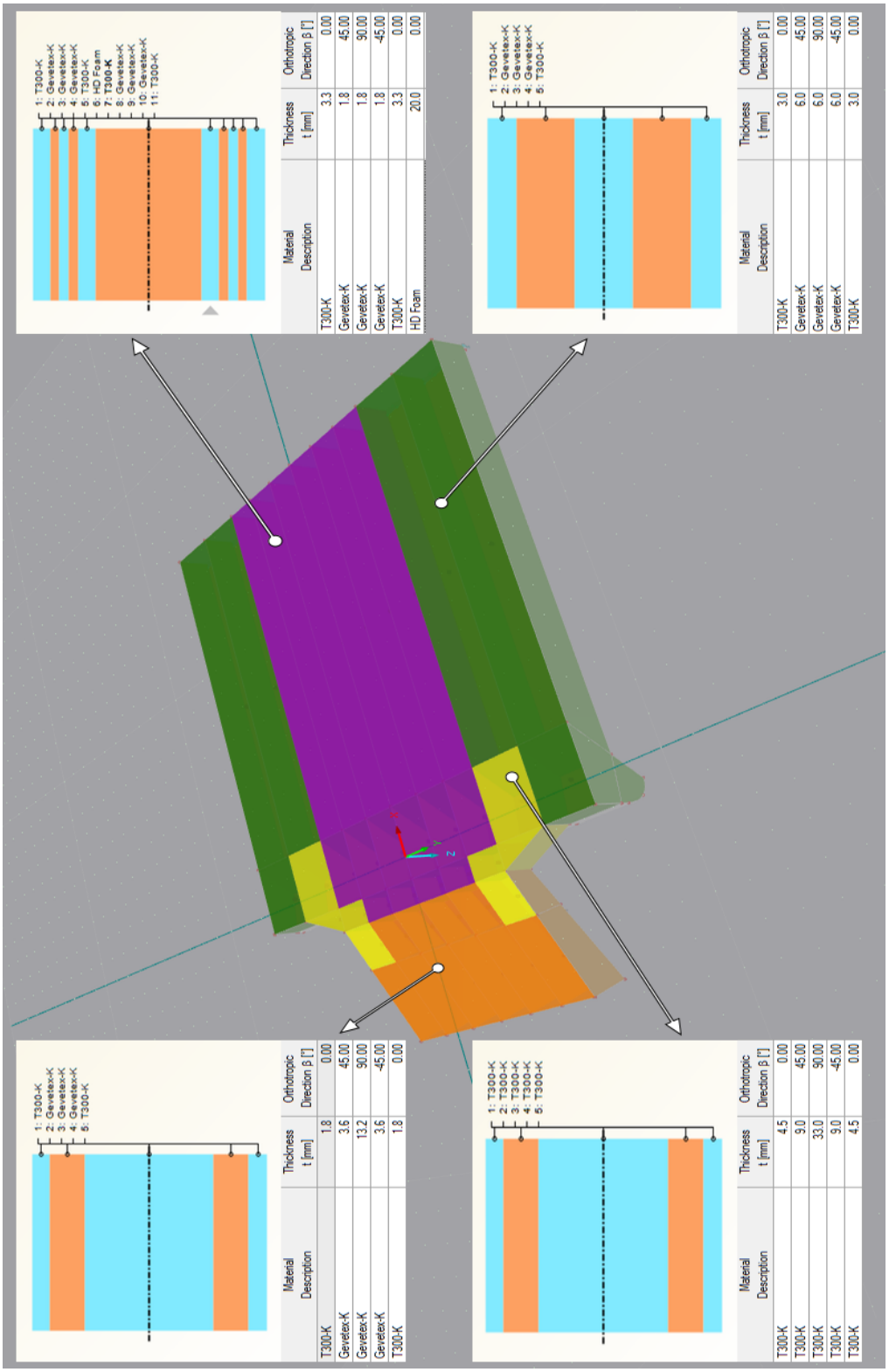

Figure F.1: *Top laminate configurations of final design*

F.2 Bottom laminates

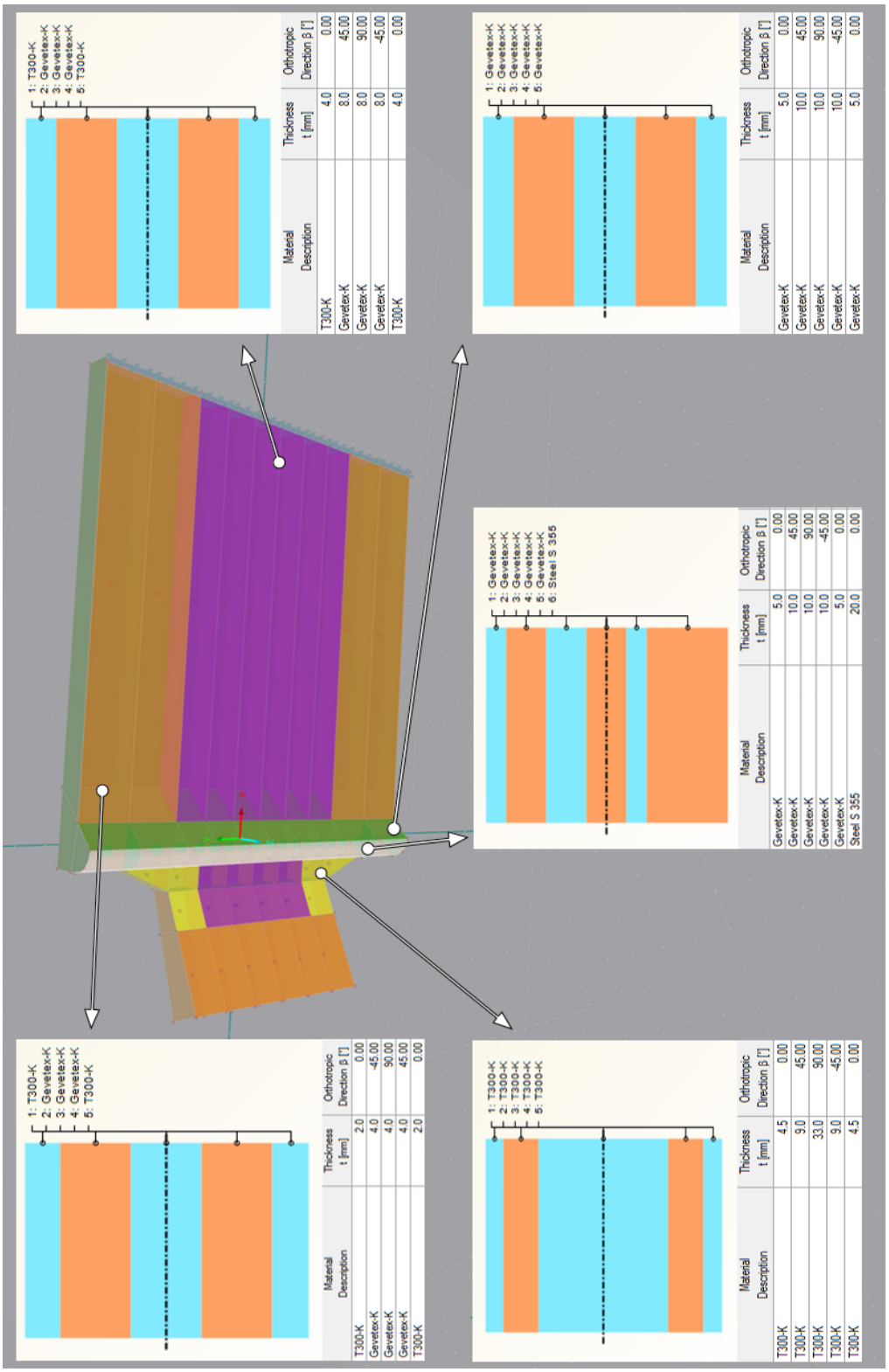

Figure F.2: *Bottom laminate configurations of final design*

F.3 Longitudinal stiffener laminates

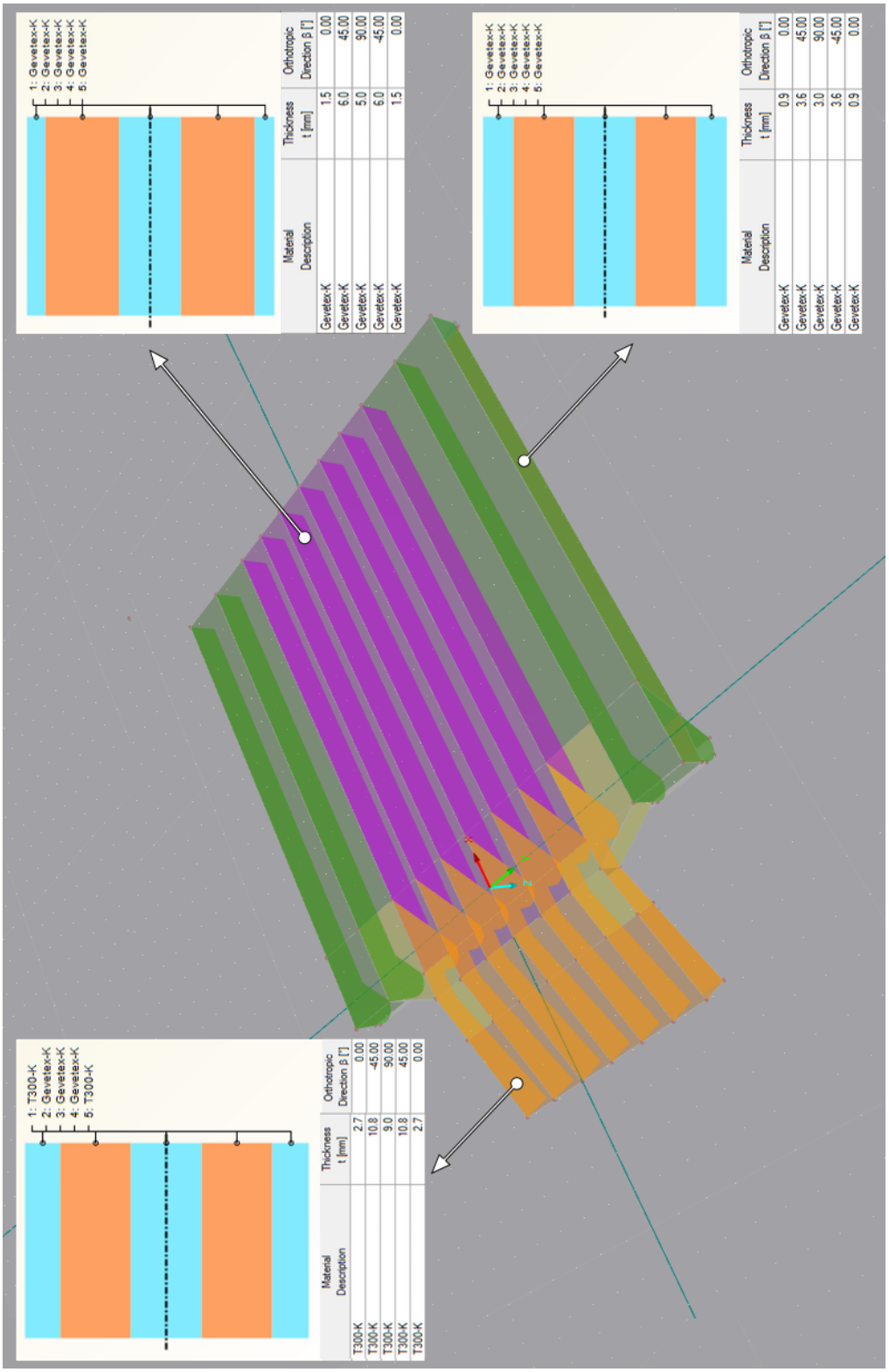

Figure F.3: *Longitudinal stiffener laminate configurations of final design*